UNIVERSITÀ
DEGLI STUDI
DI PALERMO

PhD in Information and Communication Technologies
Dipartimento di Ingegneria

Indistinguishability of identical particles as a genuine quantum resource for quantum information processing

Candidate: Matteo Piccolini

Supervisor: Prof. Rosario Lo Franco
Coordinator: Prof. Ilenia Tinnirello

CYCLE - XXXVI
ACADEMIC YEAR 2022/2023

To the indescribable beauty of this journey

All'indescrivibile bellezza di questo viaggio

Contents

List of Publications

Papers featured in this thesis:

1. M. Piccolini, F. Nosrati, G. Compagno, P. Livreri, R. Morandotti, and R. Lo Franco, "Entanglement robustness via spatial deformation of identical particle wave functions," *Entropy*, vol. 23, p. 708, 2021.

2. Y. Wang, M. Piccolini, Z.-Y. Hao, Z.-H. Liu, K. Sun, J.-S. Xu, C.-F. Li, G.-C. Guo, R. Morandotti, G. Compagno, et al., "Proof-of-principle direct measurement of particle statistical phase," *Phys. Rev. Appl.*, vol. 18, no. 6, p. 064024, 2022.

3. M. Piccolini, F. Nosrati, G. Adesso, R. Morandotti, and R. Lo Franco, "Generating indistinguishability within identical particle systems: spatial deformations as quantum resource activators," *Phil. Trans. R. Soc. A*, vol. 381, no. 2255, p. 20220104, 2023.

4. M. Piccolini, V. Giovannetti, and R. Lo Franco, "Robust engineering of maximally entangled states by identical particle interferometry," *Adv. Quantum Technol.*, vol. 6, no. 9, p. 2300146, 2023.

5. M. Piccolini, M. Karczewski, A. Winter, and R. Lo Franco, "Robust generation of N-partite N-level singlet states by identical particle interferometry," *arXiv preprint arXiv:2312.17184*, 2023.

6. M. Piccolini, V. Giovannetti, and R. Lo Franco, "Asymptotically deterministic robust preparation of maximally entangled bosonic states," *Phys. Rev. Res.*, vol. 6, no. 1, p. 013073, 2024.

Papers not included in this thesis:

7. M. Piccolini, F. Nosrati, R. Morandotti, and R. Lo Franco, "Indistinguishability-enhanced entanglement recovery by spatially localized operations and classical communication," *Open Syst. Inf. Dyn.*, vol. 28, no. 04, p. 2150020, 2021.

Others:

- M. Piccolini, V. Giovannetti, and R. Lo Franco, "Back cover: Robust engineering of maximally entangled states by identical particle interferometry (adv. quantum technol. 9/2023)," Adv. Quantum Technol., vol. 6, no. 9, p. 2370094, 2023

List of Figures

Abstract

This thesis is dedicated to the study of identical particles and to the exploitation of their indistinguishability as a useful quantum resource for quantum information protocols.

We begin by reviewing the main implications of dealing with systems of identical particles (Chapter 1). In particular, we recall the standard, label-based first quantization approach to identical particles, we highlight the issues it raises in evaluating the quantum correlations between them, and we discuss alternative approaches providing different solutions. The notion of spatial indistinguishability is here introduced together with the related spatially localized operations and classical communication framework, in relation to the concepts of no which-particle, no which-way, and no which-spin information. We proceed with the presentation of the main manuscripts published during my PhD studies at Università degli Studi di Palermo. These include a review and generalization to the many-body scenario of the above mentioned tools (Chapter 2), a theoretical design and experimental implementation of an optical setup exploiting spatial indistinguishability of identical constituents to directly measure their exchange phase (Chapter 3), the analysis of spatial indistinguishability as a resource to protect entanglement between identical qubits from the detrimental action of local noise (Chapter 4), the development of a protocol for the robust distillation of entangled states exploiting interferometric effects between two identical bosonic qubits (Chapter 6), its extension to fermionic qubits (Chapter 7), and a generalization of this scheme for the robust generation of generalized bosonic singlet states (Chapter 8). Also, an original chapter (Chapter 5) tackles an issue emerging with the previously introduced notion of spatial indistinguishability, sets it in relation with the occurrence of interferometric effects, and propose a solution which overcomes the problem and opens the way for new investigations. Chapter 5 shall be useful to better understand the physics underlying the results of the successive Chapters 6-8.

Indistinguishability of identical particles as a genuine quantum resource for quantum information processing

Chapter 1

Introductory remarks

In the first chapter of this thesis we introduce the main concepts about identical particles which will provide the main building blocks of the following work. In particular, in Section 1.1 we present the notion of identical particles and the problem of the exchange degeneracy affecting them, discussing the nature and the range of applicability of the symmetrization postulate introduced to fix it. In Section 1.2 we show how the symmetrization postulate leads to problems when trying to assess the entanglement of identical particles using the same tools employed for nonidentical ones, and discuss different approaches proposed in the literature to solve the issue. While doing so, we introduce the concept of spatially indistinguishable particles and the spatially localized operations and classical communication framework, which play a main role in the rest of this thesis. Finally, in Section 1.3 we present the notions of no which-particle information, no which-way information, and no which-spin information, and discuss how these can be exploited within the above framework to activate quantum resources exploitable in operational protocols.

The whole content of this chapter is an original review and reinterpretation of works published by other authors prior to the beginning of the PhD studies of the author of this thesis.

1.1 Exchange degeneracy and symmetrization postulate

In physics, particles are said to be identical if their intrinsic physical properties, such as mass, electric charge, and spin are the same [4, 5]. This is the case, for example, of subatomic particles like electrons, photons, and quarks, of atomic nuclei, and of atoms and molecules themselves. Particles identity is a cornerstone of both classical and quantum physics which provides the core of the inductive approach to the investigation of Nature's fundamental laws: the assumption that all the electrons in the universe possess the same electric charge, mass, spin, and so on, allows to conclude that some fundamental properties extrapolated from the behaviour of a sample of electrons observed in a laboratory also hold for all the other electrons in the universe. Note that this definition is independent of the experimental conditions: two particles are either identical or nonidentical regardless of the actions of an observer.

In classical physics, identical particles (IP) are treated on the same footage of nonidentical (NIP) ones. In the classical world, indeed, two physical systems, even when microscopic and identical, always occupy distinct positions in space at every fixed time,

thus being always individually addressable by following their trajectory [5]. However, in quantum mechanics things drastically change: the possibility for the wave functions of different particles to spatially overlap allows for a nonzero probability to find more than one constituent in the same spatial region. This peculiarity has strong consequences on the mathematical description of quantum systems. To illustrate this concept, let us consider an experiment where we measure the spin projection along an axis of two identical and independently prepared spin-1/2 particles (qubits). Suppose that we find the value $+\hbar/2$ for one spin and $-\hbar/2$ for the other, to which we associate the quantum states $|\uparrow\rangle$ and $|\downarrow\rangle$, respectively. To describe the system mathematically, the standard, first quantization approach (SA) to identical particles in quantum mechanics assigns to each constituent a label, which here we denote with A and B. After the spin measurement, two different mathematical kets can be associated with the same physical state: $|\uparrow\rangle_A \otimes |\downarrow\rangle_B$ and $|\downarrow\rangle_A \otimes |\uparrow\rangle_B$. This is because the two reported states are completely equivalent from the dynamical point of view, so that there is no physical distinction between the two scenarios: the assigned labels A, B are, in this sense, *unphysical*. The labelling choice thus has no physical consequences, with the resulting kets leading to the same predictions. However, $|\uparrow\rangle_A \otimes |\downarrow\rangle_B$ and $|\downarrow\rangle_A \otimes |\uparrow\rangle_B$ are orthogonal, and span a two-dimensional vector space whose normalized elements are of the form

$$|\Psi^{(2)}\rangle = \alpha\,|\uparrow\rangle_A \otimes |\downarrow\rangle_B + \beta\,|\downarrow\rangle_A \otimes |\uparrow\rangle_B\,, \quad |\alpha|^2 + |\beta|^2 = 1. \tag{1.1}$$

All the vectors in such a space can *a priori* represent the same physical state: this ambiguity, rooted in the freedom of the labelling choice, is called *exchange degeneracy* and leads to problematic consequences. For example, let us suppose that we are interested in computing the probability for the state $|\Psi^{(2)}\rangle$ in Eq. (1.1) to be found in a different state $|\Phi^{(2)}\rangle$. Such a probability will, in general, depend on the coefficients α, β, leading to physical predictions which depend on the specific ket chosen among others that equivalently describe the same physical situation. To solve this problem, the exchange degeneracy must be removed. The *symmetrization postulate* is introduced to this goal, stating that [4]

> When a system includes several identical particles, only certain kets of its state space can describe its physical states. Physical kets are, depending on the nature of the identical particles, either completely symmetric or completely antisymmetric with respect to permutation of these particles. Those particles for which the physical kets are symmetric are called bosons, and those for which they are antisymmetric, fermions.

The symmetrization postulate therefore eliminates the exchange degeneracy by associating one specific ket to the physical system, namely the one which is totally symmetric under every possible exchange of labels for bosons, and the totally antisymmetric one for fermions. In the scenario which led to Eq. (1.1), for example, the only physical state is ruled to be

$$|\Psi^{(2)}\rangle = \frac{1}{\sqrt{2}}\Big(\,|\uparrow\rangle_A \otimes |\downarrow\rangle_B + \eta\;|\downarrow\rangle_A \otimes |\uparrow\rangle_B\,\Big), \quad \text{with} \begin{cases} \eta = 1, & \text{for bosons} \\ \eta = -1, & \text{for fermions.} \end{cases} \tag{1.2}$$

The symmetrization postulate, which has been exemplified here for two identical particles, is straightforwardly generalizable to an arbitrary number of identical constituents. Finally, we point out the *Pauli exclusion principle* as one of its main consequences, stating that two identical fermions cannot be in the same individual state. Indeed, having

two or more particles in the same individual state lead, by construction, to a term in the global state which is invariant under the swapping of the associated labels, ruling out the possibility of constructing a multipartite state which is antisymmetric under the exchange of *any* pair of particles/labels.

1.1.1 Can we avoid the symmetrization postulate?

If the application of the symmetrization postulate were indispensable in every physical situation, the description of a system containing a restricted amount of identical particles should always involve all the other identical particles in the universe, as their states shoul participate to the symmetrization/antisymmetrization process. As we will discuss in Section 1.2, this would be not only deleterious from the point of view of the mathematical description, but would also lead to physical consequences which contrast with the experimental evidence. Luckily, this is not the case. To show why it is so, let us consider two identical spin-1/2 particles localized one on the spatial region $\mathcal{I}_1$ and the other on the spatial region $\mathcal{I}_2$. With this, we mean that the wave function ψ_1 of the first particle vanishes outside $\mathcal{I}_1$ (i.e., it has support in $\mathcal{I}_1$), and similarly the second particle's wave function ψ_2 vanishes outside $\mathcal{I}_2$. Denoting with σ_1, σ_2 their related spin, the symmetrization postulate rules the global bipartite state to be

$$|\Psi^{(2)}\rangle = \frac{1}{\sqrt{2}}\Big(|\psi_1\,\sigma_1\rangle_A \otimes |\psi_2\,\sigma_2\rangle_B + \eta\ |\psi_2\,\sigma_2\rangle_A \otimes |\psi_1\,\sigma_1\rangle_B \Big),$$

where $\eta = +1$ for bosons and $\eta = -1$ for fermions. We now measure the pseudospin projection along a preferred axis of the two particles with two detectors localized in the spatial regions $\mathcal{F}_1$ and $\mathcal{F}_2$ and compute the probability to find the individual state $|\phi_1\uparrow\rangle$ with the former detector and $|\phi_2\downarrow\rangle$ with the latter. Here, ϕ_1, ϕ_2 are wave functions localized on $\mathcal{F}_1$ and $\mathcal{F}_2$, respectively. The final bipartite state is given by the properly symmetrized state

$$|\Phi^{(2)}\rangle = \frac{1}{\sqrt{2}}\Big(|\phi_1\uparrow\rangle_A \otimes |\phi_2\downarrow\rangle_B + \eta\ |\phi_2\downarrow\rangle_A \otimes |\phi_1\uparrow\rangle_B \Big),$$

leading to the probability amplitude

$$\langle\Phi^{(2)}|\Psi^{(2)}\rangle = \langle\phi_1|\psi_1\rangle\,\langle\uparrow|\sigma_1\rangle\ \langle\phi_2|\psi_2\rangle\,\langle\downarrow|\sigma_2\rangle + \eta\Big(\ \langle\phi_2|\psi_1\rangle\,\langle\downarrow|\sigma_1\rangle\ \langle\phi_1|\psi_2\rangle\,\langle\uparrow|\sigma_2\rangle\ \Big). \quad (1.3)$$

The first term in the above summation is called *direct term*, whereas the second one is the *exchange term* [4]. The presence of both the direct and the exchange term is a direct consequence of the symmetrization postulate reflecting the ambiguity in the labelling choice of identical particles. It is thus reasonable to expect one of the two terms to disappear in those cases where a physical result can be related to a specific particle unambiguously, allowing to relate a physical meaning to its label and thus making the symmetrization postulate unnecessary. We can see that, in the above example, this happens when one of the following scenarios occurs:

1a. $\langle\phi_1|\psi_1\rangle = 0$ and/or $\langle\phi_2|\psi_2\rangle = 0$;

1b. $\langle\phi_2|\psi_1\rangle = 0$ and/or $\langle\phi_1|\psi_2\rangle = 0$;

2a. $\langle\uparrow|\sigma_1\rangle = 0$, and/or $\langle\downarrow|\sigma_2\rangle = 0$;

2b. $\langle\downarrow|\sigma_1\rangle = 0$, and/or $\langle\uparrow|\sigma_2\rangle = 0$.

Cases 1a, 1b describe the physical situation where *there is at least one detection region where it is impossible to find one of the two particles.* The contribution of such a particle to

the total probability amplitude is thus ruled out, with the result measured by the involved detector being uniquely ascribable to the other constituent. By exclusion, the first particle will be responsible of the result measured by the second detector, therefore eliminating any ambiguity. Cases 2a and 2b, instead, represent the physical situation where the spin of at least one constituent can be perfectly discriminated by the employed detectors: we can thus assign each measured result to a specific particle without ambiguity. What brings together all the described scenarios is the possibility to assign a *physical meaning* to the labels, such as "the only particle in that specific detection region" or "the only particle with that specific detected internal state". In these situations the symmetrization postulate is deemed to be unnecessary, meaning that we can obtain the same results for probability amplitudes by directly reasoning as if the labels denote particles of different natures. The irrelevance of the symmetrization postulate in computing probability amplitudes of particles measured in regions of space where it is impossible to find some of them individually is the reason why "the existence of identical particles does not prevent the separate study of restricted systems, composed of a small number of particles" [4], since "no quantum prediction, referring to an atom located in our laboratory, is affected by the mere presence of similar atoms in remote parts of the universe" [6]. However, we stress that this does not depend on the system's state alone, but on its relationship with the measurement (or set of measurements) that we want to implement. Consider, for example, two identical constituents with a nonzero probability of being individually found in a same region of space. The symmetrization postulate should be applied if we set the two detectors within that region, whereas it is unnecessary if at least one of them is placed outside of it (see Figure 1.1). The former scenario, where both constituents

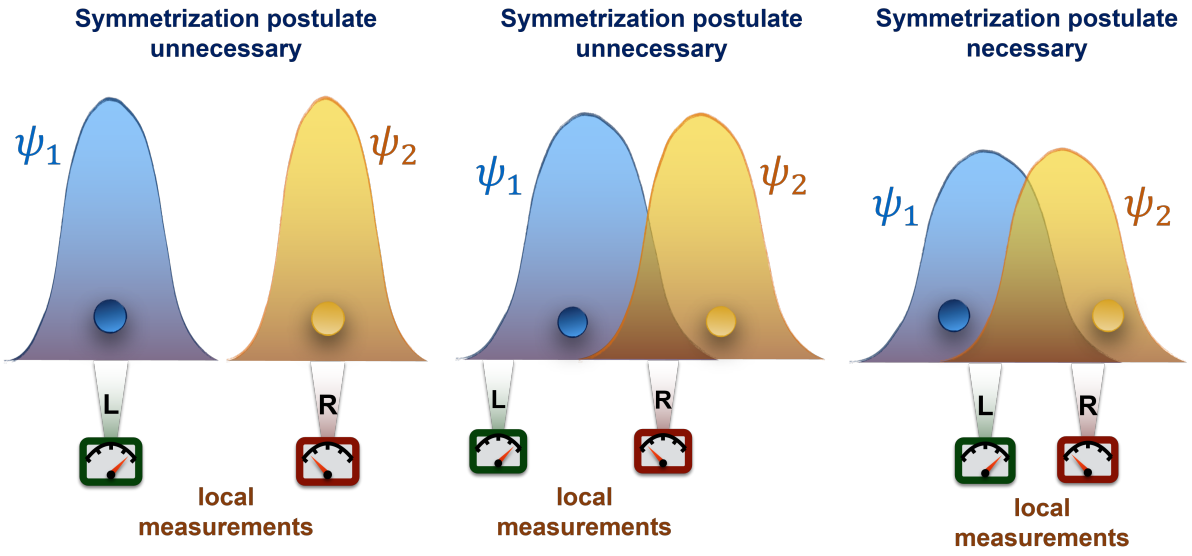

Figure 1.1: Different relations between wave functions' support and measurement devices' localization, deeming the application of the symmetrization postulate either necessary (left and central figures) or unnecessary (right figure).

can individually trigger each detector, is called *ambiguous*, while the latter is deemed *unambiguous* in contrast [7].

The relation between the spatial distribution of particles in a multipartite state and the involved detection regions gives rise to a plethora of concepts which will play a crucial role in the rest of this thesis, such as the *spatial indistinguishability* one, introduced in

the next section.

1.2 Consequences of the symmetrization postulate: evaluating the entanglement of IP

As discussed in Section 1.1, the symmetrization postulate rules the global state of IP to be symmetric or antisymmetric with respect to the exchange of labelled particles. In Subsection 1.1.1, we have shown that such labels assume a physical meaning in certain situations, as in unambiguous detection scenarios. Nonetheless, one could argue that the symmetrizzation postulate should always be applied *a priori*, to provide a mathematical description of a system's state which does not require to specify the measurement context. We will now show that such an approach leads to some problematic consequences when we try to evaluate the entanglement in systems of IP using the same tools employed for NIP, and illustrate some of the main techniques proposed in the literature to properly tackle them. These include measurement-independent methods defining new criteria for addressing quantum correlations in systems of IP, as well as approaches which rule out the possibility of evaluating entanglement in measurement-independent contexts and strictly bound its analysis to the operational measurement framework involved.

1.2.1 Addressing entanglement in NIP systems

Let us consider a bipartite system $\mathcal{S}$ composed of two nonidentical particles labelled A and B. Crucially, for NIP we can always assign a physical meaning to these labels, as they can be related to those properties which make the particles nonidentical (such as mass or charge). Let us now suppose that $\mathcal{S}$ is in the pure state $|\Psi^{(2)}\rangle \in \mathcal{H}$, where $\mathcal{H} = \mathcal{H}_A \otimes \mathcal{H}_B$ is the global Hilbert space given by the tensor product of the two single-particle Hilbert spaces $\mathcal{H}_A$ and $\mathcal{H}_B$. Then, there exist two orthonormal bases $\{|\varphi_i\rangle_A\} \in \mathcal{H}_A$ and $\{|\chi_i\rangle_B\} \in \mathcal{H}_B$ such that [4]

$$|\Psi^{(2)}\rangle = \sum_{i=0}^{r} \sqrt{\lambda_i}\, |\varphi_i\rangle_A \otimes |\chi_i\rangle_B \,, \tag{1.4}$$

where λ_i are real, non-negative coefficients satisfying $\sum_i \lambda_i^2 = 1$. Eq. (1.4) is called the *Schmidt decomposition* of $|\Psi^{(2)}\rangle$, with λ_i being the *Schmidt coefficients*. The number r of nonzero Schmidt coefficients in the above decomposition is named *Schmidt rank* and can be used to define entanglement for the system $\mathcal{S}$. In particular, $|\Psi^{(2)}\rangle$ is *entangled* if its Schmidt rank is $r > 1$, whereas it is *separable* if $r = 1$.

A separable state is always factorizable, meaning that it can always be rewritten as the $|\Psi^{(2)}\rangle = |\varphi\rangle_A \otimes |\chi\rangle_B$ for some $|\varphi\rangle_A \in \mathcal{H}_A$ and $|\chi\rangle_B \in \mathcal{H}_B$. This means that we can assign to each constituent a well-defined pure state which allows to compute any physical property of it without having to account for the other. In particular, measuring any observable on one subsystem has no effects on the other one. On the other hand, this does not hold for entangled particles, where the superposition principle makes it impossible to assign a unique state to each constituent. This leads to the purely nonclassical consequence that the physical predictions drawn for one subsystem are affected by the state of the other particles, with a measurement of the former influencing the latter.

Let us now consider the density matrix $\rho = |\Psi^{(2)}\rangle \langle\Psi^{(2)}|$ associated to the bipartite state in Eq. (1.4). We can describe the two subsystems A and B with the reduced density

operators obtained from ρ, namely

$$\rho_A := \mathrm{Tr}_B[\rho] = \sum_i \lambda_i \left|\varphi_i\right\rangle_A \left\langle\varphi_i\right|_A , \qquad \rho_B := \mathrm{Tr}_A[\rho] = \sum_i \lambda_i \left|\chi_i\right\rangle_B \left\langle\chi_i\right|_B . \tag{1.5}$$

When the composite system is in a pure state, the reduced density operators have the same eigenvalues, which coincides with the Schmidt coefficients of $|\Psi^{(2)}\rangle$. Notice, in particular, that when $|\Psi^{(2)}\rangle$ is separable the two subsystems are in a pure state, whereas they are in a mixed state if $|\Psi^{(2)}\rangle$ is entangled. This leads to a first method to quantify the entanglement $E(|\Psi^{(2)}\rangle)$ of composite systems in a pure state $|\Psi^{(2)}\rangle$: we define it as $E(|\Psi^{(2)}\rangle) = S(\rho_A) = S(\rho_B)$, where $S(\rho_A) = S(\rho_B)$ is the *von Neumann entropy* of the reduced density matrices

$$S(\rho_A) = S(\rho_B) := -\sum_i \lambda_i \log_2 \lambda_i. \tag{1.6}$$

When ρ_A and ρ_B are pure, $S(\rho_A) = S(\rho_B) = 0$ and ρ is separable. On the other hand, if ρ_A and ρ_B are mixed we have $0 < S(\rho_A) = S(\rho_B) \leq 1$ and ρ is entangled. The von Neumann entropy thus associates the entanglement of a composite state to the our ignorance about the state of the single subsystems. This connection between entanglement and ignorance will be crucial in the rest of this thesis.

Finally, we have previously discussed that for NIP the labels A and B have a physical meaning, as they denote the physical properties which make the two constituents nonidentical. Therefore, the trace operation in Eq. (1.6) can be given a physical interpretation, too: we are tracing out the particle with properties A or B. We thus conclude that we can always act *locally* on NIP within the paradigm of *local operations and classical communication* (LOCC) [8–10], where the term *local* refers to *particle locality*.

1.2.2 Addressing entanglement in IP systems: issues with the SA

We now try to evaluate the entanglement of IP systems using the criteria depicted in the previous section for NIP, adopting a measurement-independent point of view where the symmetrization postulate must always be applied. The entanglement which this approach tries to address only depends on the structure of the system's state and is called *a priori* entanglement [7].

Consider a bipartite system of two identical spinless particles, one in the state $|\varphi\rangle$ and the other one in the state $|\chi\rangle$. Similarly to Eq. (1.2), the global state is given by

$$|\Psi^{(2)}\rangle = \frac{1}{\sqrt{2}}\Big(\left|\varphi\right\rangle_A \otimes \left|\chi\right\rangle_B + \eta \left|\chi\right\rangle_A \otimes \left|\varphi\right\rangle_B \Big), \quad \text{with } \begin{cases} \eta = 1, & \text{for bosons} \\ \eta = -1, & \text{for fermions.} \end{cases} \tag{1.7}$$

We immediately notice that, unless we are dealing with identical bosons in the same single-particle state $|\varphi\rangle = |\chi\rangle$, *the symmetrization postulate makes a many-body state never separable and thus always formally entangled* according to the criteria developed for NIP. This can be easily confirmed by computing its von Neumann entropy. Indeed, we have

$$\rho_X = \frac{1}{2}\Big(\left|\varphi\right\rangle_X \left\langle\varphi\right|_X + \left|\chi\right\rangle_X \left\langle\chi\right|_X \Big), \quad X = A, B,$$

which implies $S(\rho_A) = S(\rho_B) = 1$. This raises, however, some problems. Consider for instance the scenario where the two constituents are spatially localized in distant

laboratories where they have been independently prepared. If we were to take the formal presence of entanglement in the state of Eq. (1.7) as signalling real physical correlations, we would be led to conclude that

> all identical particles are inherently correlated from the outset, regardless of how far apart their creation took place [11].

However, this result is in stark contrast with the empirical evidence that particles which have been independently generated in distant, spacelike-separated regions and which have never interacted before are intrinsically uncorrelated. This point of view is the most accepted within the scientific community, which deems the entanglement in the state of Eq. (1.7) to be only a formal mathematical consequence of the straightforward application to IP of the tools developed for the entanglement evaluation of NIP. Reconnecting with the interpretation of entanglement given at the end of Subsection 1.2.1, the presence of a nonzero von Neumann entropy in such a state is attributed to an ignorance about *the label* arbitrarily assigned to each constituent rather than about some physical property characterizing them, so that "the apparent correlations in the particle labels must not be accounted for as physical" [7] (see also [12]). Finally, an open question remains for IP which, after having been independently generated, are measured in ambiguous settings. In this situation where the symmetrization postulate cannot be avoided, is the entanglement appearing in $|\Psi^{(2)}\rangle$ physical or fictitious?

We are thus left with (at least) three possible ways to solve the problem of evaluating entanglement of IP:

1. preserving the SA (first quantization formalism), imposing the application of the symmetrization postulate regardless of the measurement setting, and providing a new a priori definition of *measurement-independent* entanglement for IP. The new definition must allow to filter out the contribution coming from the labels from the physical correlations, so that states like the one in Eq. (1.7) can be deemed unentangled;

2. preserving the SA (first quantization formalism) and addressing quantum correlations from an operational point of view as a physical resource exploitable in quantum information protocols. Adopting a *measurement-dependent* approach, the entanglement of IP in ambiguous settings can thus be defined in relation to the one exploitable by distinct parties. All the parties can only act on the constituents with LOCC operations in unambiguous settings, so that the application of the symmetrization postulate can now be avoided and the standard tools developed for NIP can be used to evaluate the entanglement of the resulting state;

3. giving up on the first quantization approach altogether, defining entanglement within a different formalism where the symmetrization postulate does not give rise to hindrances.

1.2.3 Redefining entanglement in the first quantization formalism: a measurement-independent approach

In Ref. [13], the authors introduce a criterion to evaluate the a priori entanglement of identical constituents. In particular, they define a bipartite system of two identical particles

as *non-entangled* when "both constituents possess a complete set of properties". This initially heuristic definition catches the physical meaning attributed to non-entangled states of NIP in Subsection 1.2.1, relating it to the possibility of computing any physical property of one constituent without having to account for the other. Notice that, however, in this case the absence of entanglement does not imply the separability of the global state (except for identical bosons in the same single-particle state), as the symmetrization postulate is always applied. The above condition is then formalized as follows: one constituent of a bipartite state $|\Psi^{(2)}\rangle$ possesses a complete set of properties if and only if *there exist a one-dimensional projector P, defined on the single-particle Hilbert space $\mathcal{H}^{(1)}$, such that:* [13]

$$\langle\Psi^{(2)}|\mathcal{E}_P(A,B)|\Psi^{(2)}\rangle = 1, \tag{1.8}$$

where

$$\mathcal{E}_P(A,B) := P_A \otimes [\mathbb{1}_B - P_B] + [\mathbb{1}_A - P_A] \otimes P_B + P^{(A)} \otimes P_B. \tag{1.9}$$

Here, the subscript denotes the label of the particle we are acting on. Eq. (1.8) gives the probability of finding at least one particle in the state associated with the projector P. It is subsequently shown that such a condition amounts to the following: *two identical fermions are non-entangled if and only if $|\Psi^{(2)}\rangle$ is obtained by antisymmetrizing a factorized state.* Similarly, *two identical bosons are non-entangled if and only if either $|\Psi^{(2)}\rangle$ is obtained by symmetrizing a factorized product of two orthogonal states or it is the product of the same state for the two particles.* Finally, a quantitative method to evaluate the entanglement condition is provided, similarly to the separability and von Neumann entropy criteria in the NIP scenario. To this aim, the Schmidt decomposition and rank are substituted with the *Slater decomposition* and *rank* [14, 15]. In particular, it can be shown that a properly antisymmetrized bipartite state $|\Psi^{(2)}_{fer}\rangle$ of two identical fermions with spin s is characterized by the Slater decomposition

$$|\Psi^{(2)}_{fer}\rangle = \sum_{i=1}^{(2s+1)/2} a_i \left(|2i-1\rangle_A \otimes |2i\rangle_B - |2i\rangle_A \otimes |2i-1\rangle_B \right)/\sqrt{2}, \tag{1.10}$$

where the states $\{|2i-1\rangle, |2i\rangle\}$ with $i = 1, \ldots, (2s+1)/2$ constitute an orthonormal basis of the two single-particle Hilbert spaces $\mathcal{H}_A$, $\mathcal{H}_B$, whereas the a_i are complex coefficients such that $\sum_i |a_i|^2 = 1$. Similarly, the Slater decomposition of a symmetrized state $|\Psi^{(2)}_{bos}\rangle$ of two spin s bosons is [14, 15]

$$|\Psi^{(2)}_{bos}\rangle = \sum_{i=1}^{(2s+1)/2} b_i \; |i\rangle_A \otimes |i\rangle_B \,, \tag{1.11}$$

where b_i with $i = 1, \ldots, (2s+1)/2$ are real coefficients satisfying $\sum_i b_i^2 = 1$. The amount of nonzero coefficients a_i and b_i provide the related fermionic and bosonic *Slater rank*. Differently from the NIP case where the Schmidt number and the von Neumann entropy provided two alternative, independent criteria to evaluate the entanglement of both fermionic and bosonic systems, the approach here developed for IP requires to consider both the Slater rank of the global state *and* the von Neumann entropy of the reduced density matrices, with results for fermions which differ from the ones for bosons. In particular, for a fermionic system it holds that [12, 13]:

f1. Slater rank of $|\Psi^{(2)}_{fer}\rangle = 1 \Leftrightarrow S(\rho_A) = S(\rho_B) = 1 \Leftrightarrow |\Psi^{(2)}_{fer}\rangle$ is non-entangled (the state is obtained by antisymmetrizing a factorized state);

f2. Slater rank of $|\Psi^{(2)}_{fer}\rangle > 1 \Leftrightarrow S(\rho_A) = S(\rho_B) > 1 \Leftrightarrow |\Psi^{(2)}_{fer}\rangle$ is entangled (the state is obtained by antisymmetrizing a sum of factorized states).

Scenario f1. is the analogous of the non-entangled situation for NIP, whereas scenario f2. corresponds to the entangled one. However, in contrast to NIP, the entropy of the reduced density matrix can here be greater than 1 and is bounded from below by unity instead of zero: the residual value reflects the unphysical entanglement originating from the uncertainty of the particle labels [12]. On the other hand, for bosonic systems the situation is more complex, and we have that:

b1. Slater rank of $|\Psi^{(2)}_{bos}\rangle = 1 \Leftrightarrow S(\rho_A) = S(\rho_B) = 0 \Rightarrow |\Psi^{(2)}_{bos}\rangle$ is non-entangled (both particles are in the same individual quantum state);

b2. Slater rank of $|\Psi^{(2)}_{bos}\rangle = 2$ and $S(\rho_A) = S(\rho_B) \in (0, 1) \Rightarrow |\Psi^{(2)}_{bos}\rangle$ is entangled (the state is obtained by symmetrizing a factorized state of non-orthogonal single-particle states);

b3. Slater rank of $|\Psi^{(2)}_{bos}\rangle = 2 \Leftrightarrow S(\rho_A) = S(\rho_B) = 1 \Rightarrow |\Psi^{(2)}_{bos}\rangle$ is non-entangled (the state is obtained by symmetrizing a factorized state of orthogonal single-particle states);

b4. Slater rank of $|\Psi^{(2)}_{bos}\rangle > 2 \Rightarrow |\Psi^{(2)}_{bos}\rangle$ is entangled (the state is obtained by symmetrizing a sum of factorized states).

Once again, the von Neumann entropy also accounts for the uncertainty originating from the labelling of the constituents. However, this time it can be smaller than 1, and cases b2 and b3 show that its value alone is not enough to determine the presence of entanglement in the state. Notice that scenarios b3 and b4 are the analogous of the non-entangled situation for NIP, whereas scenarios b1 and b2 has no counterpart for nonidentical constituents.

In conclusion, the method presented in this subsection allows to verify the presence of entanglement in bipartite systems of identical particles accounting only for the state structure (a priori entanglement). It requires the joint evaluation of the Slater rank and the von Neumann entropy of the reduced density matrices, leading to a categorization which differs between bosons and fermions.

1.2.4 Mode-entanglement in the second quantization formalism

We now briefly review how entanglement is approached in the second quantization formalism [12, 16–19]. Here, physical observables are given in terms of creation and annihilation operators acting on the single-particle Hilbert space $\mathcal{H}^{(1)}$ spanned by vector states called *modes* [16]. We denote the creation operator creating a particle in mode $|j\rangle \in \mathcal{H}^{(1)}$ as $a^\dagger_j$, and the related annihilation operator which annihilate a particle in the same mode as a_j. They satisfy the bosonic canonical commutation (CCR) or fermionic anticommutation (CAR) relations

$$[a_j, a^\dagger_k] = \langle j|k\rangle \quad \text{(CCR)}, \qquad \{a_j, a^\dagger_k\} = \langle j|k\rangle \quad \text{(CAR)}. \tag{1.12}$$

Polynomials in these operators act on the many-body Fock space $\mathcal{F}$ and construct the algebra $\mathcal{A}(\mathcal{F})$ of operators that are used to describe multipartite systems consisting of bosons and fermions [17]. Let us now consider a bipartition of $\mathcal{A}$ into two commuting subalgebras $\mathcal{A}_1, \mathcal{A}_2 \subset \mathcal{A}$ generated by a subset of the creation and annihilation operators

which generate $\mathcal{A}$. An operator $A \in \mathcal{A}$ is then said *local* with respect to the bipartition $(\mathcal{A}_1, \mathcal{A}_2)$ if it can be written as $A = A_1 A_2$ with $A_1 \in \mathcal{A}_1$ and $A_2 \in \mathcal{A}_2$. Notice that this concept, which we will refer to as *mode locality*, is inherently different from the meaning of *particle locality* employed for NIP in the LOCC framework, as it focuses on subgroups of single-particle states (modes) regardless of the number of constituents filling them rather than on individual particles. The definition of locality constitutes the main building block for the definition of entanglement, which is called *mode entanglement* within this framework: a state ρ is called *separable* with respect to the bipartition $(\mathcal{A}_1, \mathcal{A}_2)$ if the expectation value of any local operator $A = A_1 A_2$ can be decomposed into a convex combination of products of local expectation values as

$$\mathrm{Tr}\left[\rho A\right] = \sum_k \lambda_k \mathrm{Tr}\left[\rho_{1,k} A_1\right] \mathrm{Tr}\left[\rho_{2,k} A_2\right], \quad \lambda_k \geq 0, \quad \sum_k \lambda_k = 1, \tag{1.13}$$

where $\rho_{1,k}, \rho_{2,k}$ are many-body states living in the Hilbert subspaces associated to the subalgebras $\mathcal{A}_1, \mathcal{A}_2$. A state ρ is *entangled* if it's not separable.

To clarify this point, let us consider N bosons distributed over M orthogonal single-particle modes. The related annihilation and creator operators a_j, $a_j^\dagger$ with $j = 1, \ldots, M$ satisfy the CCR $[a_j, a_k^\dagger] = \delta_{jk}$. We consider a bipartition of the global algebra into the subalgebras $\mathcal{A}_1$ and $\mathcal{A}_2$ spanned by the operators $a_j, a_j^\dagger$ with, respectively, $j = 1, \ldots, m$ and $j = m+1, \ldots, M$. A pure state $|\Psi^{(N)}\rangle$ is mode separable with respect to this bipartition if and only if [16]

$$|\Psi^{(N)}\rangle = P(a_1^\dagger, \ldots, a_m^\dagger)\, Q(a_{m+1}^\dagger, \ldots, a_M^\dagger)\, |0\rangle, \tag{1.14}$$

where P and Q are polynomials in the creation operators and $|0\rangle$ is the vacuum state of the Fock space.

In conclusion, we emphasize that the entanglement of a state in the mode framework is not an a priori concept, as it depends on the specific bipartition chosen: the same state could be entangled with respect to one bipartition and separable with respect to another. We deem this approach as measurement-dependent, since a specific choice of a bipartition is typically reflected by a particular choice of a measurement framework where each employed detector is sensible only to the single particle states of a specific subalgebra.

1.2.5 Detector-level entanglement in the first quantization formalism: the sLOCC framework

A different solution to the problem of evaluating the entanglement of IP discussed in Subsection 1.2.2 is approaching entanglement as a property which can be exploited as a resource to realize quantum information protocols unachievable with only classical correlations. Crucially, any protocol of this kind involves a set of operations and measurements. We have seen in Subsection 1.1.1 that the symmetrization postulate can be avoided when such operations are realized in unambiguous settings. The bipartite state in Eq. (1.7) becomes factorized in this case, so that the standard tools developed for NIP can be employed to deem the state unentangled within the first quantization approach. In this scenario we thus recover the concept of *particle locality* characterizing the LOCC framework, since each particle can be individually addressed by means of the spatial location of the corresponding detector. However, this is impossible when ambiguous settings are

used to deal with IP: in this situation, the idea of particle locality must be abandoned. However, the detectors and the devices employed in operational protocols are typically designed to act on *local regions of space*, defined as *connected sets of* $\mathbf{R}^3$. Distinct detectors are then represented by mutually orthogonal projection operators which select a preferred orthonormal basis that we call *local in space*. The focus on particle locality characterizing the LOCC framework can thus be substituted with the idea of *spatial locality*, giving rise to the *spatially localized operations and classical communication* (sLOCC) framework [20]. Particles which have a nonzero probability to be individually found in a same local region are said to be *spatially overlapped* [20], otherwise they are *spatially separated*. Notice that, according to the previous definition, orthogonality does not imply spatial separation: for example, let us consider two single-particle states $|\psi_{\mathrm{L}}\rangle$ and $|\psi_{\mathrm{R}}\rangle$ localized on two spatially separated regions L and R. Two identical constituents in the single-particle states $|\psi_{\mathrm{D}}\rangle = (|\psi_{\mathrm{L}}\rangle + |\psi_{\mathrm{R}}\rangle)/\sqrt{2}$ and $|\psi_{\mathrm{A}}\rangle = (|\psi_{\mathrm{L}}\rangle - |\psi_{\mathrm{R}}\rangle)/\sqrt{2}$ are spatially delocalized and overlapped over the regions L and R, despite $\langle\psi_{\mathrm{L}}|\psi_{\mathrm{R}}\rangle = 0$. On the contrary, spatial separation always imply orthogonality. Finally, if the spatial overlap occurs over detection regions it is then impossible to associate a specific constituent to a detection event and we deem the particles to be *spatially indistinguishable to the eyes of the detectors*.

As for the mode-based approach in second quantization, the concept of locality provides the main building block to define entanglement. After the measurement, particles found by different detectors are spatially separated, acquiring orthogonal wave functions: in this sense, the detectors assign them an identity [7]. The entanglement of the resulting state can now be evaluated using the standard tools developed for the a priori entanglement of NIP, and it is defined to be the *detector-level entanglement of the state prior to the measurement with respect to the given set of detectors* (see Ref. [7] for a formal definition). Thus, the detector-level approach preserves the definition of entanglement given for NIP when the constituent are not spatially overlapped and the symmetrization postulate can be avoided, whereas it defines the entanglement of spatially overlapped particles (when labels are necessary) as the one "inferred by application of any entanglement measure on the detector-level density matrix, reconstructed by quantum state tomography in the local basis defined by the detectors" [7]. In this sense, detector-level entanglement provides an operational, measurement-dependent interpretation of the quantum correlations between spatially overlapped IP, relating it to the one extractable by suitable operations and measurements separating them within the sLOCC framework. We emphasize that in the scenario of local, unambiguous settings, the sLOCC framework coincides with the LOCC one.

1.2.6 sLOCC-based entanglement in the no-label formalism

The detector-level entanglement approach in the first quantization formalism solves the problem of the apparent entanglement between distant, independently prepared IP by avoiding to symmetrize/antisymmetrize the global state with respect to labels when unambiguous settings are involved. However, a different mathematical formalism has been developed to deal with IP without resorting to labels at all: the *no-label* approach [21,22].

We will start by considering bipartite systems to illustrate its main characteristics. Within this mathematical framework, many-body states are simply written as a list of the single-particle states composing it. For example, the global state in Eq. (1.7) of two constituents with orthogonal wave functions is here rewritten as $|\Psi^{(2)}\rangle = |\varphi, \chi\rangle$. The core of the no-label approach is provided by the rule to compute probability amplitudes:

given two bipartite states $|\psi_1, \psi_2\rangle$ and $|\psi_1', \psi_2'\rangle$, the two-particle probability amplitude $\langle\psi_1', \psi_2'|\psi_1, \psi_2\rangle$ is defined as a symmetrized inner product given by a linear combination with same weight of products of one-particle amplitudes [21]

$$\langle\psi_1', \psi_2'|\psi_1, \psi_2\rangle := \langle\psi_1'|\psi_1\rangle \langle\psi_2'|\psi_2\rangle + \eta \langle\psi_1'|\psi_2\rangle \langle\psi_2'|\psi_1\rangle . \tag{1.15}$$

We immediately notice that the exchange factor η, with $\eta = 1$ for bosons and $\eta = -1$ for fermions, is directly encoded in the above definition: in the no-label approach the symmetrization postulate does not intervene in the symmetrization/antisymmetrization of the global state with respect to unphysical labels but rather in the computation of multipartite probability amplitudes. The result is clearly the same as computed within the standard, label-based approach, with the two components in the right-hand side of Eq. (1.15) being the direct and exchange terms of Eq. (1.3). From Eq. (1.15) it directly follows that $\langle\psi_1', \psi_2'|\psi_1, \psi_2\rangle = \eta \langle\psi_1', \psi_2'|\psi_2, \psi_1\rangle$ for all ψ_1', ψ_2' in the no-label symmetric bipartite Hilbert space $\mathcal{H}^{(2)}$, so that

$$|\psi_1, \psi_2\rangle = \eta |\psi_2, \psi_1\rangle . \tag{1.16}$$

Notice that from Eq. (1.15) there follows linearity [17]: $\alpha |\psi_1, \psi_2\rangle = |\alpha \psi_1, \psi_2\rangle = |\psi_1, \alpha\psi_2\rangle$ for all $\alpha \in \mathbb{C}$.

The no-label approach encodes the dependence on the chosen measurement setting in the factorizability of the global state. Consider for example two particles in the single-particle states $|\psi_{\mathrm{L}}\rangle$ and $|\psi_{\mathrm{R}}\rangle$ localized on two spatially separated regions L and R, respectively, so that $\langle\psi_{\mathrm{L}}|\psi_{\mathrm{R}}\rangle = 0$. In the no-label approach, we denote such single-particle states with the shorthand notation $|L\rangle$, $|R\rangle$ and, by analogy with the second quantization formalism, we sometimes refer to L and R as *modes*. The global state $|\Psi^{(2)}\rangle$ is therefore given by $|\Psi^{(2)}\rangle = |L, R\rangle$ and is such that $|L, R\rangle = |L\rangle \otimes |R\rangle$ if and only if we are going to measure the two particles in an unambiguous setting within the sLOCC framework, that is, with detectors localized on L and R to which the particles are spatially distinguishable. This is a consequence of the fact that, denoting with $|D_{\mathrm{L}}\rangle$ and $|D_{\mathrm{R}}\rangle$ the states on which the two detectors project, the two-particle probability amplitude related to finding one constituent per spatial region is given by $\langle D_{\mathrm{L}}, D_{\mathrm{R}}|L, R\rangle = \langle D_{\mathrm{L}}|L\rangle \langle D_{\mathrm{R}}|R\rangle + \eta \cancel{\langle D_{\mathrm{L}}|R\rangle \langle D_{\mathrm{R}}|L\rangle}$, which is the same result that we would obtain for two NIP in the state $|L\rangle \otimes |R\rangle$ projected on the state $|D_{\mathrm{L}}\rangle \otimes |D_{\mathrm{R}}\rangle$: once again, the relation between NIP and spatially distinguishable IP is retrieved in the no-label approach. We conclude that the null contribution of the exchange term in the probability amplitude $\langle D_{\mathrm{L}}, D_{\mathrm{R}}|L, R\rangle$, which made unnecessary the application of the symmetrization postulate in the standard approach, makes the state factorizable in the no-label formalism. It follows that $|L, R\rangle \neq |L\rangle \otimes |R\rangle$ if and only if the particles are spatially indistinguishable.

We now highlight that a global state such as $|\Psi^{(2)}\rangle = |\psi_1, \psi_2\rangle$ is in general not normalized. Indeed, it holds that

$$\langle\psi_1, \psi_2|\psi_1, \psi_2\rangle = 1 + \eta |\langle\psi_1|\psi_2\rangle|^2 =: \mathcal{N}, \tag{1.17}$$

so that the properly normalized state is

$$|\Psi^{(2)}\rangle_N = \frac{|\psi_1, \psi_2\rangle}{\sqrt{\mathcal{N}}}. \tag{1.18}$$

In particular, $|\psi_1, \psi_2\rangle$ is normalized if and only if the wave functions of the two constituents are orthogonal.

Let us now consider a single-particle operator $O^{(1)}$ defined in the space of individual states, such as the momentum or the energy of a single particle. The total momentum or energy of a bipartite system is given by the action of the single-particle operator on the global state, which similarly to the label-based approach [4] is defined as

$$O^{(1)}\,|\psi_1,\psi_2\rangle := |O^{(1)}\psi_1,\psi_2\rangle + |\psi_1,O^{(1)}\psi_2\rangle\,. \tag{1.19}$$

We introduce an orthonormal basis $\mathcal{B}^{(1)} = \{|\varphi_k\rangle\}_k$ of the one-particle Hilbert space and consider the single-particle projector operator $P_{\varphi_k} = |\varphi_k\rangle\langle\varphi_k|$. From linearity and from Eq. (1.16) we have

$$P_{\varphi_k}\,|\psi_1,\psi_2\rangle = |\varphi_k, \langle\varphi_k|\psi_1\rangle\,\psi_2 + \eta\,\langle\varphi_k|\psi_2\rangle\,\psi_1\rangle\,. \tag{1.20}$$

This allows to define the following inner product between state spaces with different particle numbers:

$$\langle\varphi_k|\cdot|\psi_1,\psi_2\rangle := \langle\varphi_k|\psi_1\rangle\,|\psi_2\rangle + \eta\,\langle\varphi_k|\psi_2\rangle\,|\psi_1\rangle\,, \tag{1.21}$$

which amounts to projecting the bipartite state $|\Psi^{(2)}\rangle$ on $|\varphi_k\rangle$ (one-particle projective measurement). Projecting the normalized state $|\Psi^{(2)}\rangle_N$ gives an unnormalized one-particle pure state $|\phi_k\rangle = \langle\varphi_k|\cdot|\Psi^{(2)}\rangle_N$. The corresponding normalized one-particle state is

$$|\phi_k\rangle_N = \frac{|\phi_k\rangle}{\sqrt{\widetilde{\mathcal{N}_k}}}, \tag{1.22}$$

where

$$\widetilde{\mathcal{N}_k} := \frac{1}{\mathcal{N}}\Big[|\langle\varphi_k|\psi_1\rangle|^2 + |\langle\varphi_k|\psi_2\rangle|^2 + 2\eta\,\mathrm{Re}\big(\,\langle\psi_1|\varphi_k\rangle\,\langle\varphi_k|\psi_2\rangle\,\langle\psi_2|\psi_1\rangle\,\big)\Big]. \tag{1.23}$$

We can now introduce the one-particle partial trace $\mathrm{Tr}^{(1)}$ of a system, physically interpreted as the statistical ensemble of all the reduced states obtained after projective measurements on $\mathcal{B}^{(1)}$, which operationally corresponds to measure a subsystem particle without registering the outcomes [21]:

$$\mathrm{Tr}^{(1)}\left[|\Psi^{(2)}\rangle_N\,\langle\Psi^{(2)}|_N\right] := \sum_k \langle\varphi_k|\cdot|\Psi^{(2)}\rangle_N\,\langle\Psi^{(2)}|_N\cdot|\varphi_k\rangle\,, \tag{1.24}$$

that is,

$$\mathrm{Tr}^{(1)}\left[|\Psi^{(2)}\rangle_N\,\langle\Psi^{(2)}|_N\right] = \sum_k |\phi_k\rangle\,\langle\phi_k|\,.$$

From the partial trace we determine the one-particle density matrix

$$\rho^{(1)} = \mathrm{Tr}^{(1)}\Big[\,|\Psi^{(2)}\rangle_N\,\langle\Psi^{(2)}|_N\,\Big]/\widetilde{\widetilde{\mathcal{N}}}, \tag{1.25}$$

where the normalization factor $\widetilde{\widetilde{\mathcal{N}}}$ is such that $\mathrm{Tr}^{(1)}\rho^{(1)} = 1$. For the state $|\Psi^{(2)}\rangle$ in Eq. (1.18), this condition ultimately determines $\widetilde{\widetilde{\mathcal{N}}} = \sum_k \widetilde{\mathcal{N}_k} = 2$.

We highlight that the partial trace in Eq. (1.24) represents a physical operation on the system state based on effective projective measurements, in contrast with the partial trace performed on labels which are unphysical when ambiguous measurement settings are

involved. Furthermore, its introduction allows us to define the entanglement $E_{\mathrm{M}}(|\Psi^{(2)}\rangle)$ of a pure bipartite state $|\Psi^{(2)}\rangle$ with respect to a measurement performed on the region M. This is given by the von Neumann entropy of the one-particle reduced density matrix $\rho_{\mathrm{M}}^{(1)}$ obtained by the *localized partial trace* [20], which is given by Eq. (1.24) with the sum over the index k limited to the subset $\{k_{\mathrm{M}}\}$ corresponding to the subspace $\mathcal{B}_{\mathrm{M}}^{(1)}$ of one-particle basis states localized on M:

$$\rho_{\mathrm{M}}^{(1)} := \mathrm{Tr}_{\mathrm{M}}^{(1)}\Big[\, |\Psi^{(2)}\rangle_N \langle\Psi^{(2)}|_N \,\Big]/\mathcal{M}. \tag{1.26}$$

Here $\mathcal{M}$ is such that $\mathrm{Tr}^{(1)}\rho_{\mathrm{M}}^{(1)} = 1$. Therefore, we have

$$E_{\mathrm{M}}(|\Psi^{(2)}\rangle) := S(\rho_{\mathrm{M}}^{(1)}) = -\sum_j \lambda_j \log_2 \lambda_j, \tag{1.27}$$

where $S(\rho_{\mathrm{M}}^{(1)})$ is the von Neumann entropy of $\rho_{\mathrm{M}}^{(1)}$ and λ_j are its eigenvalues. We can understand the physical meaning of Eq. (1.27) by looking at the interpretation given for the entanglement entropy in the label-based approach (see Eq. (1.6)). In that case, we first traced over one specific particle of the bipartite system, as identified by either its physical properties which makes it distinguishable (as for NIP) or by its unphysical label (for IP). The outcome of this operation is physically interpreted as the state of the other particle after the traced out one has been measured without registering the outcome. For NIP, obtaining a pure state as result signals that the remaining particle is characterized by a specific state which does not depend on the traced out constituent, that is, it possesses a complete set of properties in the sense explained in Subsection 1.2.3, ruling out the presence of quantum correlations. If the resulting state is mixed, instead, there is an ignorance about the state of the remaining particle, which signals the presence of entanglement. The physical interpretation of Eq. (1.27) follows analogously, but this time we trace over a specific region of space rather than on a specific constituent, a change of point of view which clarifies the switching from the LOCC framework to the sLOCC one. Since more than one particle could be found in the interested region, the partial trace must account for the fact that the measured one could be any of them, as they cannot be specifically targeted by the measurement device due to their indistinguishability: this leads to the one-particle partial trace definition in Eq. (1.24). Obtaining a pure state finally means that the other constituent is in a perfectly determined state, showing no correlations with the traced out particle. Otherwise, the global state is entangled. The no-label approach thus allows to compute the entanglement of systems of two IP by using the same tool employed for systems of NIP, namely the von Neumann entropy of the reduced state, by suitably extending it to account for the indistinguishability of the different constituents to the eyes of the measurement setting and by overcoming the drawbacks of relying on unphysical labels.

Given the above definition of entanglement, we now stress that an entangled state of spatially separated IP written in the no-label formalism has always the form $a\,|\chi_1, \chi_2\rangle + b\,|\chi_1', \chi_2'\rangle$ for any $a, b \neq 0$ such that $|a|^2 + |b|^2 = 1$, as it happens for NIP in the standard approach (see the discussion about the Schmidt rank in Subsection 1.2.1). Here χ_j, χ_j', $j = 1, 2$ may also include an internal degree of freedom, as it is the case for the Bell singlet state of two spin-1/2 particles $|\Psi_-^{(2)}\rangle = (|\psi_1\uparrow, \psi_2\downarrow\rangle - |\psi_1\downarrow, \psi_2\uparrow\rangle)/\sqrt{2}$, where $|\psi_1\rangle$ and $|\psi_2\rangle$ are distinguishable spatial wave functions in the sLOCC sense. In contrast, the same state written in the standard, label-based approach requires four tensor product kets, as a consequence of the symmetrization postulate. This notational advantage is reported

in Figure 2.1, where the notation for writing bipartite states in the no-label formalism is summarized and compared with the standard approach. Notice, in particular, the possibility to factorize the spatial part from the spin one, so that $|\Psi_{\pm}^{(2)}\rangle = (|\psi_1\uparrow,\psi_2\downarrow\rangle \pm |\psi_1\downarrow,\psi_2\uparrow\rangle)/\sqrt{2}$ can be rewritten as $|\Psi_{\pm}^{(2)}\rangle = |\psi_1,\psi_2\rangle_{\pm\eta}\otimes|\uparrow,\downarrow\rangle_{\pm}$, where the subscript indicates the symmetry of the state: $|\alpha,\beta\rangle_{\pm} = \pm|\beta,\alpha\rangle$.

Finally, the generalization of the no-label formalism to the many-body scenario is straightforward: given N particles in the single-particle states $|\psi_j\rangle$, $j = 1,\ldots,N$, the unnormalized global state is written as $|\Psi^{(N)}\rangle = |\psi_1,\psi_2,\ldots,\psi_N\rangle$, which is properly normalized as $|\Psi^{(N)}\rangle_N = |\Psi^{(N)}\rangle/\sqrt{\langle\Psi^{(N)}|\Psi^{(N)}\rangle}$. Notice that $|\psi_1,\psi_2,\ldots,\psi_N\rangle \neq |\psi_1\rangle\otimes|\psi_2\rangle\otimes\cdots\otimes|\psi_N\rangle$ for spatially indistinguishable constituents. Further information about the generalization of the no-label approach to the many-body scenario, such as the general rule for computing many-body inner products and the multipartite partial trace, can be found, e.g., in Ref. [23].

In conclusion, the no-label approach to identical particles provides a midway formalism between the first and the second quantization. Its focus is on the individual constituents as for the former, rather than on modes as for the latter. However, the introduction of the inner product in Eq. (1.21) introduces a relation between states differing in the number of particles similarly to what is done with the creation and annihilation operators in the second quantization formalism, allowing to establish a rigorous connection between the two approaches [22]. The main advantage of the no-label approach is that it accounts for the indistinguishability of identical constituent without resorting to unphysical labels, allowing to evaluate entanglement with the same tools developed for NIP while treating bosons and fermions on the same footage. For these reasons, we will employ such a formalism in the rest of this thesis.

1.2.7 Discussion and comparison: entanglement of spatially overlapped particles

We will now compare the different approaches discussed in the previous subsections to evaluate the entanglement of peculiar states where identical particles are spatially overlapped in the sLOCC sense.

The first example that we consider is the pure state of two identical spinless bosons given by a balanced, coherent superposition of both the particles being in the same single-particle state $|\psi_{\mathrm{L}}\rangle$ and $|\psi_{\mathrm{R}}\rangle$. Here, $|\psi_{\mathrm{L}}\rangle$ and $|\psi_{\mathrm{R}}\rangle$ are localized on two nonoverlapping spatial regions L and R, so that $\langle\psi_{\mathrm{L}}|\psi_{\mathrm{R}}\rangle = 0$. The resulting bipartite state is written within the standard formalism as

$$|\Psi^{(2)}\rangle_a = \frac{1}{\sqrt{2}}\big(|\psi_{\mathrm{L}}\rangle_A|\psi_{\mathrm{L}}\rangle_B + e^{i\theta}|\psi_{\mathrm{R}}\rangle_A|\psi_{\mathrm{R}}\rangle_B\big), \tag{1.28}$$

where θ is a real phase. Let us now fix $\theta = \pi$. The a priori approach discussed in Subsection 1.2.3 deems $|\Psi^{(2)}\rangle_a$ to be non-entangled. Indeed, it can be obtained by symmetrizing the factorized product of the orthogonal delocalized single-particle states $|\psi_{\mathrm{D}}\rangle = (|\psi_{\mathrm{L}}\rangle + |\psi_{\mathrm{R}}\rangle)/\sqrt{2}$ and $|\psi_{\mathrm{A}}\rangle = (|\psi_{\mathrm{L}}\rangle - |\psi_{\mathrm{R}}\rangle)/\sqrt{2}$, that is,

$$|\Psi^{(2)}\rangle_a = \frac{1}{\sqrt{2}}\big(|\psi_{\mathrm{D}}\rangle_A|\psi_{\mathrm{A}}\rangle_B + |\psi_{\mathrm{A}}\rangle_A|\psi_{\mathrm{D}}\rangle_B\big), \tag{1.29}$$

where the terms $|\psi_{\mathrm{L}}\rangle_A|\psi_{\mathrm{R}}\rangle_B$ and $|\psi_{\mathrm{R}}\rangle_A|\psi_{\mathrm{L}}\rangle_B$ cancel out. Such an interference effect, which gives rise to the well-known Hong-Ou-Mandel effect [24], will play a central role in

this thesis and will be discussed in Chapter 5. Finally, we highlight that in the a priori approach there is no difference between the state in Eq. (1.29) and

$$|\Phi^{(2)}\rangle = \frac{1}{\sqrt{2}}\big(|\psi_{\rm L}\rangle_A |\psi_{\rm R}\rangle_B + |\psi_{\rm R}\rangle_A |\psi_{\rm L}\rangle_B \big) \tag{1.30}$$

since $\langle\psi_{\rm L}|\psi_{\rm R}\rangle = \langle\psi_{\rm D}|\psi_{\rm A}\rangle = 0$, so that they are equivalent under the algebraic point of view. Such an approach thus makes no difference between spatially overlapped and spatially separated particles, ignoring the eventual role played by indistinguishability to the detection setup. In the second quantization formalism, instead, we can define $|\psi_{\rm L}\rangle$ and $|\psi_{\rm R}\rangle$ as the two modes of our system. The state in Eq. (1.28) is then written as

$$|\Psi^{(2)}\rangle_a = \frac{1}{\sqrt{2}}\big(|2,0\rangle + e^{i\theta} |0,2\rangle \big). \tag{1.31}$$

This state is not separable with respect to the bipartition given by the two modes for every real θ and is thus mode entangled according to the second quantization approach. Since a generalization of $|\Psi^{(2)}\rangle_a$ to an N-particle system takes the form

$$|\Psi^{(N)}\rangle = \frac{1}{\sqrt{2}}\Big(|N,0\rangle + e^{i\theta} |0,N\rangle \Big), \tag{1.32}$$

$|\Psi^{(2)}\rangle_a$ is called a *NOON state* [25, 26], with $N = 2$. NOON states allow for enhanced performances in quantum estimation protocols which cannot be achieved using classical probes [27, 28]. We will meet again NOON states in Chapter 6 and Chapter 7. Finally, the state in Eq. (1.28) is written as

$$|\Psi^{(2)}\rangle_a = \frac{1}{2}\Big(|L,L\rangle + e^{i\theta} |R,R\rangle \Big) \tag{1.33}$$

in the no-label formalism, which becomes $|\Psi^{(2)}\rangle_a = |D,A\rangle$ for $\theta = \pi$ and $|D\rangle = (|L\rangle + |R\rangle)/\sqrt{2}$, $|A\rangle = (|L\rangle - |R\rangle)/\sqrt{2}$. We now compute the one-particle reduced density matrix localized on region L as in Eq. (1.26), obtaining

$$\rho_{\rm L}^{(1)} = |L\rangle\langle L| . \tag{1.34}$$

It follows that $S(|\Psi^{(2)}\rangle_a) = 0$: NOON states are non-entangled according to the sLOCC approach. This reflects the fact that after a particle is found in L the state of the other constituent is uniquely determined as $|L\rangle$.

As a second example, let us consider a bipartite state of two spin-1/2 particles localized in the same spatial region L with opposite spin. In the standard approach, the global state is written as

$$|\Psi^{(2)}\rangle_b = \frac{1}{\sqrt{2}}\Big(|\psi_{\rm L}\uparrow\rangle_A |\psi_{\rm L}\downarrow\rangle_B + \eta\, |\psi_{\rm L}\downarrow\rangle_A |\psi_{\rm L}\uparrow\rangle_B \Big) \tag{1.35}$$

and deemed non-entangled by the a priori criterion as obtained by symmetrizing the factorized product of the orthogonal states $|\psi_{\rm L}\uparrow\rangle$ and $|\psi_{\rm L}\downarrow\rangle$. Considering the two modes associated to these two single-particle states, $|\Psi^{(2)}\rangle_b$ is non-entangled also according to the second quantization approach, where it is written as $|\Psi^{(2)}\rangle_b = |1,1\rangle$. On the contrary, in the no-label approach we have $|\Psi^{(2)}\rangle = |L\uparrow, L\downarrow\rangle$, leading to the one-particle reduced density matrix localized on L

$$\rho_{\rm L}^{(1)} = \Big(|L\uparrow\rangle\langle L\uparrow| + |L\downarrow\rangle\langle L\downarrow| \Big)/2, \tag{1.36}$$

giving $S(\rho^{(1)}) = 1$: two identical particles in the same site with opposite spin are entangled according to the no-label approach. Indeed, after the detection of one particle on region L, the state of the other constituent can be either $|L\uparrow\rangle$ or $|L\downarrow\rangle$. This uncertainty gives rise to spin entanglement between the constituents, as a consequence of the intrinsic spatial and internal configuration [21]. This claim provides theoretical support of the experimental observations reported in Ref. [29]. Notice that this would not hold if the two particles had the same spin, that is, for $|\Psi^{(2)}\rangle_c = |L\uparrow, L\uparrow\rangle$: after the measurement of one particle the state of the remaining constituent is unavoidably identified as $|L\uparrow\rangle$: the global state is deemed non-entangled by all the approaches considered.

1.3 Activating quantum resources in the sLOCC operational framework

We will now show how it is possible to activate quantum resources in an operational framework which exploits the spatial indistinguishability of identical constituents in different spin states detected by devices which are not sensible to such a degree of freedom.

1.3.1 No which-particle, no which-way, and no which-spin information

Consider different spatially indistinguishable identical particles in an ambiguous setting. We have previously discussed how in such a framework the detectors are unable to determine which particle they have detected, a fact which makes the symmetrization postulate fundamental in the standard approach: in this sense, there is a lack of *which-particle* information. We now introduce a dynamical point of view on the situation, assuming that each constituent in the measured state was generated from a different source. It is therefore possible to associate each particle to an origin in space, so that the words *which-particle* can be rephrased as *which-way*: the ambiguity arising at the detector level as a consequence of the spatial overlap thus generates the so-called *no which-way information*. We highlight that the lack of which-particle and which-way information hold regardless of the different degrees of freedom characterizing the particles, as long as the detectors are not sensible to them (otherwise the constituents could be distinguished as in scenarios 2a. and 2b. of Subsection 1.1.1): *the which-particle and which-way information are related to the individuality of a particle, rather than to its physical properties*. However, let us now endow the two above particles with pure, linearly independent spin states, so that they can be factored out of the global state. If the detectors are not able to probe the spin, the no which-way information leads to an ambiguity about the internal degree of freedom of the detected constituents: we term this ignorance *no which-spin information*.

We will further see in Chapter 5 how entanglement and interference effects between identical particles complicate the relation between no which-way and no which-spin information, allowing for situations where the presence of the former is not due to the latter. Finally, we report in Fig. 1.2 a pictorial representation of scenarios where no which-particle, no which-way, and no which-spin information occur, highlighting the relation between the three concepts.

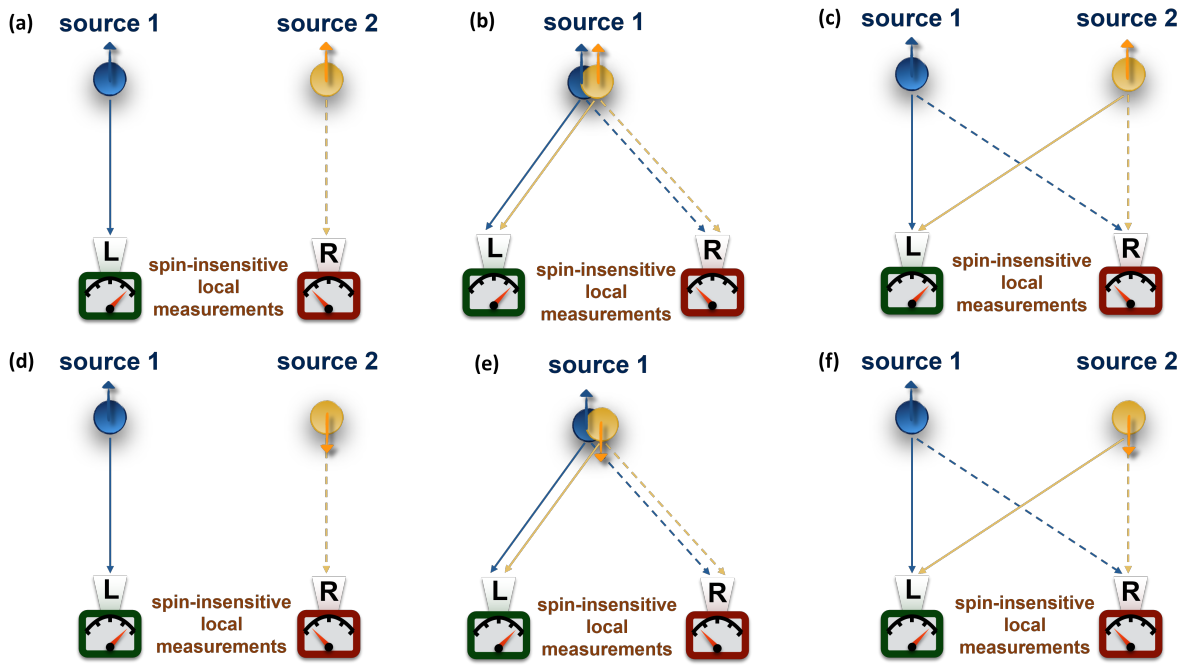

Figure 1.2: Different relations between particles source, their spin, and their overlap over detection regions lead to different types of missing information. **(a)**,**(d)** Unambiguous setting: all the information are known. **(b)** Ambiguous setting: no which-particle information, source and spin known. **(c)** Ambiguous setting: no which-particle and no which-way information, spin known. **(e)** Ambiguous setting: no which-particle and no which-spin information, source known. **(f)** Ambiguous setting: no which-particle, no which-way, and no which-spin information.

1.3.2 Generating entanglement

Consider two identical qubits initially localized in two spatially separated modes A and B corresponding to the single-particle states $|A\rangle, |B\rangle$, with $\langle A|B\rangle = 0$. We assume the two constituents to be in the initial state $|\Psi^{(2)}\rangle_{\text{in}} = |A\uparrow, B\downarrow\rangle$. Notice that $|\Psi^{(2)}\rangle_{\text{in}}$ is normalized and non-entangled according to all the criterion presented in the previous section. We now act on the wave function of the two particles to make them spatially overlap over two distinct detection regions L and R, corresponding to the single-particle states $|L\rangle, |R\rangle$ with $\langle L|R\rangle = 0$ (see Fig. 1.3). To do so, we introduce an operation D, called *spatial deformation*, such that

$$\begin{aligned} |A\rangle &\xrightarrow{D} |\psi\rangle = l\,|L\rangle + r\,|R\rangle \\ |B\rangle &\xrightarrow{D} |\psi'\rangle = l'\,|L\rangle + r'\,|R\rangle\,, \end{aligned} \tag{1.37}$$

where l, l', r, r' are complex coefficients and $|l|^2 + |r|^2 = |l'|^2 + |r'|^2 = 1$. Deformations will be discussed in depth in Chapter 2. At the moment, we limit to notice that D, which is in general non-unitary, acts on the initial state as $|\Psi^{(2)}\rangle_{\text{in}} \xrightarrow{D} |\Psi^{(2)}\rangle_D = |\psi\uparrow, \psi'\downarrow\rangle$, where

$$|\psi\uparrow, \psi'\downarrow\rangle = ll'\,|L\uparrow, L\downarrow\rangle + rr'\,|R\uparrow, R\downarrow\rangle + lr'\,|L\uparrow, R\downarrow\rangle + l'r\,|R\uparrow, L\downarrow\rangle\,, \tag{1.38}$$

and $|\Psi^{(2)}\rangle_D$ is already normalized. Crucially, D maps the spatially distinguishable particles into indistinguishable ones, creating no which-particle and no which-way information

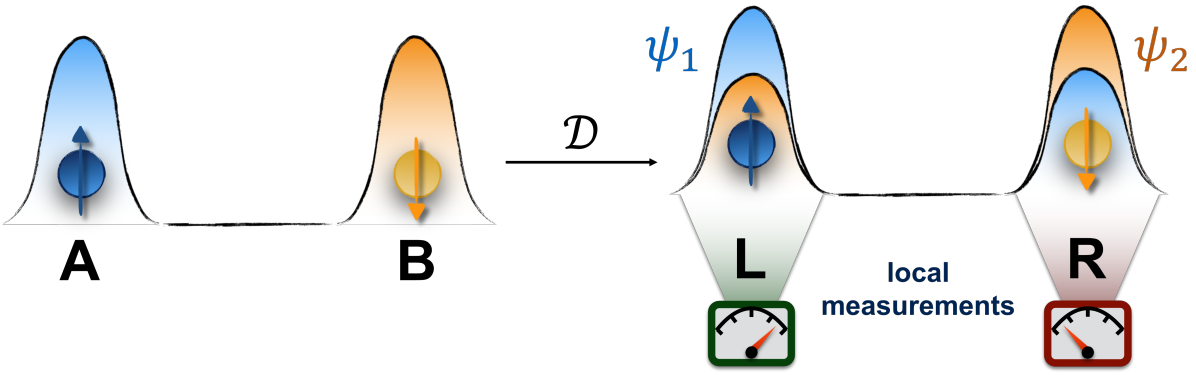

Figure 1.3: Deformation process: the spatial wave functions of two identical particles, initially localized on two distinct spatial modes A and B, are modified and made to overlap over two distinct detection regions L and R.

with respect to the spin-insensitive detectors set on L and R. Notice that, from the initial internal configuration, we also have no which-spin information, here ascribable to the deformation D. In the scenario where the initial modes coincides with the final ones, i.e., $|A\rangle = |L\rangle$, $|B\rangle = |R\rangle$, the deformation in Eq. (1.37) can represent, for example, the physical situation of particles tunneling to a neighboring site in systems such as Bose-Einstein condensates or double-quantum dots.

We are now interested in evaluating the entanglement of $|\Psi^{(2)}\rangle_D$. Using the tools provided by the no-label approach, we compute the one-particle reduced density matrix of $\rho_D = |\Psi^{(2)}\rangle_D \langle\Psi^{(2)}|_D$, tracing over the (arbitrarily chosen) region L (see Eq. (1.26)):

$$\begin{aligned}\rho_{\mathrm{L}}^{(1)} = &\Big[P_{\mathrm{L}}P'_{\mathrm{L}}\,|L\downarrow\rangle\langle L\downarrow| + P_{\mathrm{L}}P'_{\mathrm{R}}\,|R\downarrow\rangle\langle R\downarrow| + P_{\mathrm{L}}\,l'r'^{*}\,|L\downarrow\rangle\langle R\downarrow| + P_{\mathrm{L}}\,r'l'^{*}\,|R\downarrow\rangle\langle L\downarrow| \\ &+ P_{\mathrm{L}}P'_{\mathrm{L}}\,|L\uparrow\rangle\langle L\uparrow| + P_{\mathrm{R}}P'_{\mathrm{L}}\,|R\uparrow\rangle\langle R\uparrow| + P'_{\mathrm{L}}\,lr^{*}\,|L\uparrow\rangle\langle R\uparrow| + P'_{\mathrm{L}}\,rl^{*}\,|R\uparrow\rangle\langle L\uparrow|\Big] \\ &/\Big[P_{\mathrm{L}} + P'_{\mathrm{L}}\Big],\end{aligned} \tag{1.39}$$

where $P_{\mathrm{L}} := |l|^2 = |\langle L|\psi\rangle|^2$, $P'_{\mathrm{L}} := |l'|^2 = |\langle L|\psi'\rangle|^2$, $P_{\mathrm{R}} := |r|^2 = |\langle R|\psi\rangle|^2$, $P'_{\mathrm{R}} := |r'|^2 = |\langle R|\psi'\rangle|^2$, and $P_{\mathrm{L}} + P_{\mathrm{R}} = P'_{\mathrm{L}} + P'_{\mathrm{R}} = 1$. Notice that $\rho_{\mathrm{L}}^{(1)}$ is not defined when $P_{\mathrm{L}} = P'_{\mathrm{L}} = 0$, that is, when we are tracing over a region where none of the particles can be found, indicating that no single constituent is being measured. Using Eq. (1.27) we compute the related von Neumann entropy to evaluate the amount of entanglement $E_{\mathrm{L}}(|\Psi^{(2)}\rangle_D)$, getting

$$E_{\mathrm{L}}(|\Psi^{(2)}\rangle_D) = S(\rho_{\mathrm{L}}^{(1)}) = -\frac{P'_{\mathrm{L}}}{P_{\mathrm{L}}+P'_{\mathrm{L}}}\log_2\frac{P'_{\mathrm{L}}}{P_{\mathrm{L}}+P'_{\mathrm{L}}} - \frac{P_{\mathrm{L}}}{P_{\mathrm{L}}+P'_{\mathrm{L}}}\log_2\frac{P_{\mathrm{L}}}{P_{\mathrm{L}}+P'_{\mathrm{L}}}. \tag{1.40}$$

We thus see that $|\psi\uparrow, \psi'\downarrow\rangle$ is entangled as long as P_{L} and P'_{L} are both nonzero. The physical interpretation is as follows: from Eq. (1.38) we see that if $P_{\mathrm{L}} = 0$ (that is, $l = 0$), the state of the particle detected by a measurement on the region L will be uniquely determined as $|L\downarrow\rangle$, whereas it will be $|L\uparrow\rangle$ if $P'_{\mathrm{L}} = 0$, with the absence of uncertainty proving the two constituents to be non-entangled. Notice that this observation is similar to the one carried out for the state $|L\uparrow, L\downarrow\rangle$ in Subsection 1.2.7.

The no-label approach thus allows to probe the entanglement between the indistinguishable particles in $|\Psi^{(2)}\rangle_D$. However, it does not tell us *how to exploit it in an operational framework*, where two distinct parties need to perform tasks on individual particles

in remote, spatially separated regions. Indeed, the two constituents in the state $|\Psi^{(2)}\rangle$ of Eq. (1.38) can still be found in the same spatial mode, so that they must be somehow separated in order for their correlations to be used in practical protocols. Notice that this consideration also holds for the entanglement of the state $|L\uparrow, L\downarrow\rangle$, evaluated in Subsection 1.2.7. We have seen in Subsection 1.2.5 that the concept of detector-level entanglement developed within the sLOCC framework suits for this practical task. We thus proceed by performing a coincidence measurement, consisting in measuring the system with the two detectors set on L and R without probing the internal degree of freedom, and by postselecting only the results where one particle per region is found. This amounts to projecting $|\Psi^{(2)}\rangle_D$ on the two-particle basis

$$\mathcal{B}_{\rm LR} = \{|L\uparrow, R\uparrow\rangle, |L\uparrow, R\downarrow\rangle, |L\downarrow, R\uparrow\rangle, |L\downarrow, R\downarrow\rangle\} \tag{1.41}$$

via the projection operator

$$\Pi_{\rm LR} = \sum_{\sigma,\tau=\uparrow,\downarrow} |L\sigma, R\tau\rangle \langle L\sigma, R\tau|, \tag{1.42}$$

obtaining, after proper normalization,

$$|\Psi^{(2)}\rangle_{\rm LR} = \frac{\Pi_{\rm LR}|\Psi^{(2)}\rangle_{\rm LR}}{\sqrt{\langle\Psi^{(2)}|_D \Pi_{\rm LR}|\Psi^{(2)}\rangle_D}} = \frac{lr'|L\uparrow, R\downarrow\rangle + \eta\, l'r|L\downarrow, R\uparrow\rangle}{\sqrt{|lr'|^2 + |l'r|^2}}, \tag{1.43}$$

with $\eta = 1$ for bosons and $\eta = -1$ for fermions. Since we are rejecting the results where both qubits are found in the same spatial region, such a state is postselected with probability

$$P_{\rm LR} = \langle\Psi^{(2)}|_D \Pi_{\rm LR}|\Psi^{(2)}\rangle_D = |lr'|^2 + |l'r|^2 = P_{\rm L}P'_{\rm R} + P'_{\rm L}P_{\rm R}. \tag{1.44}$$

The two constituents in state $|\Psi^{(2)}\rangle_{\rm LR}$ are now spatially distinguishable with respect to regions L, R, so that their entanglement can be evaluated with the standard tools developed for NIP or for spatially separated IP, where labels can be given a physical meaning and the symmetrization postulate can be avoided. For example, let us label with L, R the particle on the respective region: tracing out particle L from $|\Psi^{(2)}\rangle_{\rm LR}$ and normalizing, we get the reduced density matrix

$$\rho_R = \Big[P_{\rm L}P'_{\rm R}|R\downarrow\rangle\langle R\downarrow| + P'_{\rm L}P_{\rm R}|R\uparrow\rangle\langle R\uparrow|\Big]/P_{\rm LR}, \tag{1.45}$$

leading to the von Neumann entropy [20]

$$S(\rho_R) = -\frac{P_{\rm L}P'_{\rm R}}{P_{\rm LR}}\log_2\frac{P_{\rm L}P'_{\rm R}}{P_{\rm LR}} - \frac{P'_{\rm L}P_{\rm R}}{P_{\rm LR}}\log_2\frac{P'_{\rm L}P_{\rm R}}{P_{\rm LR}}. \tag{1.46}$$

The amount of operative, detector-level entanglement $E_{\rm dl}\big(|\Psi^{(2)}\rangle_D\big) = S(\rho_R)$ extractable from state $|\Psi^{(2)}\rangle_D = |\psi\uparrow, \psi'\downarrow\rangle$ thus depends on the spatial overlap between the constituents and, accordingly, on their indistinguishability. In particular, it holds that

- $E_{\rm dl}\big(|\Psi^{(2)}\rangle_D\big) = 0$ if at least one of $P_{\rm L}, P'_{\rm L}, P_{\rm R}, P'_{\rm R}$ is equal to 0 or to 1. In this case, at least one particle is perfectly localized on one of the two spatial modes: the detection of the second particle on the other region thus allows to uniquely determine the state of both qubits. For example, if $P'_{\rm L} = 0$ (i.e., $l' = 0$) the postselected state in Eq. (1.43) becomes the manifestly non-entangled state $|\Psi^{(2)}\rangle_{\rm LR} = e^{i\theta}|L\uparrow, R\downarrow\rangle$, where θ is a phase which depends on l, r'.

- $E_{\rm dl}\big(\,|\Psi^{(2)}\rangle_D\,\big) = 1$ if $P_{\rm L} = P'_{\rm L}$, which implies $P_{\rm R} = P'_{\rm R}$. In this scenario, the two constituents are delocalized over the two detection regions with the same weights, leading to maximum entanglement.

It is now interesting to look for the relation between the intrinsic entanglement $E_{\rm L}\big(\,|\Psi^{(2)}\rangle_D\,\big)$ computed with respect to region L in the no-label approach and the operational one $E_{\rm dl}\big(\,|\Psi^{(2)}\rangle_D\,\big)$ computed in the detector-level approach. To this aim, we notice that the one-particle reduced density matrix $\rho_{\rm L}^{(1)}$ in Eq. (1.39) becomes equal to the reduced density matrix ρ_R in Eq. (1.45) when projected over region R and properly normalized, that is,

$$\rho_{\rm L\to R}^{(1)} := \Pi_{\rm R}\,\rho_{\rm L}^{(1)}\,\Pi_{\rm R} = \rho_R, \tag{1.47}$$

where $\Pi_{\rm R} = \sum_{\sigma=\uparrow,\downarrow} |R\sigma\rangle\,\langle R\sigma|$. It follows that

$$S\big(\rho_{\rm L\to R}^{(1)}\big) = S(\rho_R), \tag{1.48}$$

establishing a connection between the two approaches. Indeed, the projection of $\rho_{\rm L}^{(1)}$ over region R eliminates the possibility of finding the second particle in the same detection region L of the former, which is what the no-label approach needs to become operational. This is more evident for the state $|L\uparrow, L\downarrow\rangle$ discussed in Subsection 1.2.7: although deemed entangled by the no-label approach, the two particles must be spatially separated in order to be used in practical tasks.

In conclusion, we have presented an operational protocol to generate entanglement between identical particles within the sLOCC framework starting from non-entangled states. The procedure is composed of a deformation of the spatial wave function of the constituents followed by a postselected projection over distinct detection regions. The physical explanation of the process stands in the deformation creating no which-way information at the detector level: we don't know if the particle detected in regions L,R is coming from A or from B. Since the constituents are in well-determined, orthogonal pseudo-spin states, such a no which-way information gives rise to a no which-spin information: we do not know if the particle detected in regions L,R has pseudospin $\uparrow$ or $\downarrow$. This ignorance ultimately manifests as entanglement in the internal degree of freedom of the projected state. The physical nature of the emerging quantum correlations has been verified by experimentally performing a quantum teleportation protocol with the entangled qubits in the state $|\Psi^{(2)}\rangle_{\rm LR}$ of Eq. (1.43) [1]. Fig. 1.4 depicts the all-optical setup employed to achieve this goal, with part **(a)** implementing the deformation + sLOCC projection step and part **(b)** implementing the quantum teleportation protocol.

1.3.3 Enhancing coherence

Following Ref. [30], we now recall how the deformation + sLOCC projection protocol can be employed to generate coherence exploitable in quantum metrology tasks.

We start with two identical, spatially separated qubits localized on two spatial regions A and B and assume their initial state to be the incoherent mixture

$$\rho_{\rm in} = \sum_{\sigma,\tau=\uparrow,\downarrow} p_{\sigma\tau}\,|A\sigma, B\tau\rangle\,\langle A\sigma, B\tau|\,, \tag{1.49}$$

where the coefficients $p_{\sigma\tau}$ are such that $\mathrm{Tr}\,[\rho_{\rm in}] = 1$. Notice that, since the two particles are spatially separated, the above density matrix factorizes as

$$\rho_{\rm in} = \sum_{\sigma,\tau=\uparrow,\downarrow} p_{\sigma\tau}\big(\,|A\sigma\rangle\,\langle A\sigma| \otimes |B\tau\rangle\,\langle B\tau|\,\big).$$

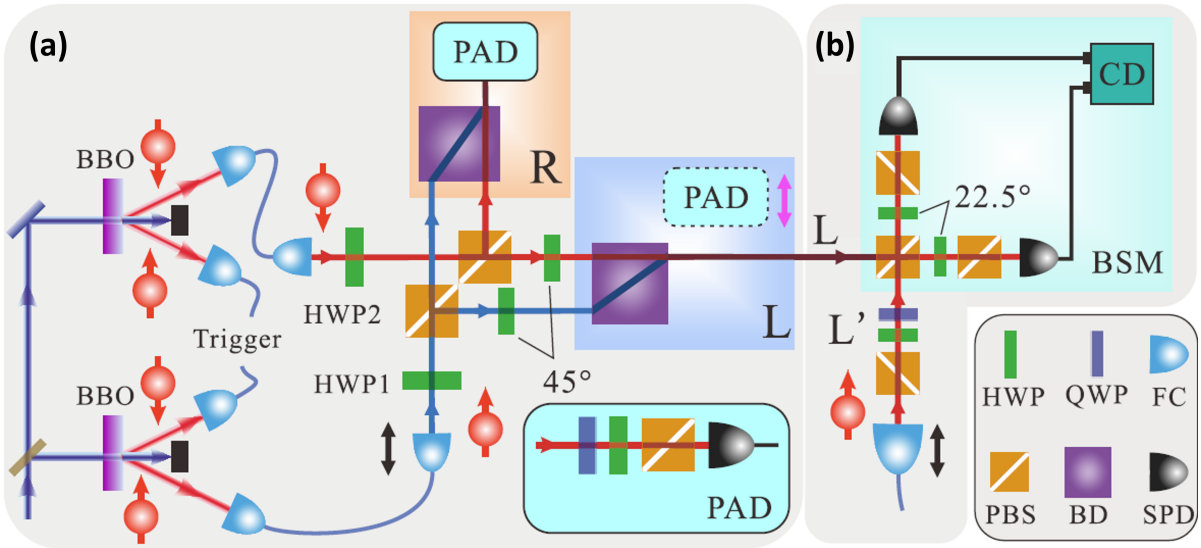

Figure 1.4: Schematic representation of the optical setup employed to implement the deformation + sLOCC projection and quantum teleportation protocol in Ref. [1]. **(a)** Using fiber couplers (FCs), half-wave plates (HWPs) and polarized beam splitters (PBSs), two oppositely-polarized independent photons generated from two BBO crystals go to the separated regions L and R, where a beam displacer (BD) makes the photon paths meet at detectors. The inset displays the unit of polarization analysis detection (PAD), including a quarter-wave plate (QWP) and a single-photon detector (SPD). **(b)** Teleportation part. PAD is removed and the photons in L proceed to a Bell state measurement (BSM) with coincidence device (CD). The photon state to be teleported is generated in L'. Figure taken from Ref. [1].

We now act on the system with the spatial deformation D in Eq. (1.37), obtaining the density matrix

$$\rho_D = \sum_{\sigma,\tau=\uparrow,\downarrow} p_{\sigma\tau} \left|\psi\sigma, \psi'\tau\right\rangle \left\langle\psi\sigma, \psi'\tau\right| . \tag{1.50}$$

Performing the coincidence measurement implementing the sLOCC projection on the two-particle basis in Eq. (1.41) via the projection operator Π_{LR} in Eq. (1.42), we get

$$\begin{aligned}\rho_{\mathrm{LR}} = \frac{\Pi_{\mathrm{LR}}\,\rho_D\,\Pi_{\mathrm{LR}}}{\mathrm{Tr}\left[\Pi_{\mathrm{LR}}\,\rho_D\right]} = \frac{1}{\mathcal{M}} \sum_{\sigma,\tau=\uparrow,\downarrow} p_{\sigma\tau}\big(P_{\mathrm{L}}P'_{\mathrm{R}} \left|L\sigma, R\tau\right\rangle \left\langle L\sigma, R\tau\right| + \eta\, P'_{\mathrm{L}}P_{\mathrm{R}} \left|L\tau, R\sigma\right\rangle \left\langle L\tau, R\sigma\right| \\ + \eta\, lr'l'^{*}r^{*} \left|L\sigma, R\tau\right\rangle \left\langle L\tau, R\sigma\right| + \eta\, l'rl^{*}r'^{*} \left|L\tau, R\sigma\right\rangle \left\langle L\sigma, R\tau\right|\big),\end{aligned} \tag{1.51}$$

where $\mathcal{M} = \sum_{\sigma,\tau=\uparrow,\downarrow} p_{\sigma\tau}\big(P_{\mathrm{L}}P'_{\mathrm{R}} \left|L\sigma, R\tau\right\rangle \left\langle L\sigma, R\tau\right| + \eta\, P'_{\mathrm{L}}P_{\mathrm{R}} \left|L\tau, R\sigma\right\rangle \left\langle L\tau, R\sigma\right|\big)$. We therefore notice that the resulting state ρ_{LR} presents coherence terms initially absent in ρ_{in}, provided by the second line in Eq. (1.51). For instance, these vanish when at least one of the coefficients l, l', r, r' is equal to zero, implying that at least one of the probabilities $P_{\mathrm{L}}, P'_{\mathrm{L}}, P_{\mathrm{R}}, P'_{\mathrm{R}}$ is null. Indeed, the vanishing of the probability amplitude of one constituent over a detection region allows to uniquely identify the particle detected in that spatial mode, erasing the no which-way and thus the no which-spin information responsible for the coherence. However, in this situation coherence vanishes also when $p_{\uparrow,\downarrow} = p_{\downarrow,\uparrow} = 0$: in this case, the initial state ρ_{in} is a classical mixture of two spatially separated particles in the same spin state, whether it be $\uparrow$ or $\downarrow$. This leads to a scenario where the state of

the two qubits after the detection can be uniquely determined, being either $|L\uparrow, R\uparrow\rangle$ or $|L\downarrow, R\downarrow\rangle$, with the density matrix ρ_{LR} given by an incoherent mixture of the two. We are thus in a situation where there is which-spin information despite the presence of no which-way information (see Fig. 1.2**(c)**), motivating the absence of coherence. On the contrary, this does not hold when $p_{\uparrow,\downarrow} \neq 0$ or/and $p_{\downarrow,\uparrow} \neq 0$, as these terms lead to a no which-spin information in the final state ρ_{LR} which manifests in the presence of coherence.

Finally, in Ref. [30] the authors show that the coherence generated by the deformation + sLOCC projection protocol provides an operational advantage in quantum phase discrimination tasks.

1.3.4 Recovering correlations

In this last subsection we report the main results of Ref. [2], where the authors show how the deformation + sLOCC projection procedure can be employed to recover the quantum correlations initially present in a state of two identical qubits and later spoiled by the noisy interaction with local environments.

We start once again with two particles initially localized on two spatially separated regions A and B, prepared in either the maximally entangled Bell triplet state $|1_+\rangle_{\mathrm{AB}}$ or singlet state $|1_-\rangle_{\mathrm{AB}}$, where

$$|1_\pm\rangle_{\mathrm{AB}} := \frac{1}{\sqrt{2}}\Big(|A\uparrow, B\downarrow\rangle \pm |A\downarrow, B\uparrow\rangle \Big). \tag{1.52}$$

We now account for the presence of white noise locally affecting both particles during the preparation of $|1_\pm\rangle_{\mathrm{AB}}$. This can be modeled as the noise introduced by the local interaction between the constituents and depolarizing environments, which leads to the formation of a Werner state $W^{\pm}_{\mathrm{AB}}$ [31,32]. Werner state is defined as a mixture of the pure target state, here represented by the Bell triplet or singlet, and of the maximally mixed state accounting for the white noise:

$$W^{\pm}_{\mathrm{AB}} := \Big(1-p\Big)\, |1_\pm\rangle_{\mathrm{AB}} \langle 1_\pm|_{\mathrm{AB}} + \frac{1}{4}\, p\, \mathbb{1}, \tag{1.53}$$

where p is the noise probability accounting for the amount of white noise which affected the system, whereas $\mathbb{1}$ is the 4 x 4 identity matrix. We now implement the deformation D defined in Eq. (1.37) delocalizing the two constituents over two distinct spatial regions L and R, here recalled:

$$\begin{aligned} |A\rangle &\xrightarrow{D} |\psi\rangle = l\,|L\rangle + r\,|R\rangle \\ |B\rangle &\xrightarrow{D} |\psi'\rangle = l'\,|L\rangle + r'\,|R\rangle\,. \end{aligned} \tag{1.54}$$

The resulting state is

$$W^{\pm}_{\mathrm{AB}} \xrightarrow{D} W^{\pm}_{D} := \Big(1-p\Big)\, |1_\pm\rangle_D \langle 1_\pm|_D + \frac{1}{4}\, p\, \mathbb{1}_D, \tag{1.55}$$

where $\mathbb{1}_D = \sum_{|v\rangle\in\mathcal{B}_{\mathrm{D}}} |v\rangle\langle v|$ is given in terms of the elements of the deformed Bell state basis $\mathcal{B}_D = \{|1_+\rangle_D, |1_-\rangle_D, |2_+\rangle_D, |2_-\rangle_D\}$, with

$$\begin{aligned} |1_\pm\rangle_D &:= \frac{1}{\sqrt{2}}\Big(|\psi\uparrow, \psi'\downarrow\rangle \pm |\psi\downarrow, \psi'\uparrow\rangle \Big), \\ |2_\pm\rangle_D &:= \frac{1}{\sqrt{2}}\Big(|\psi\uparrow, \psi'\uparrow\rangle \pm |\psi\downarrow, \psi'\downarrow\rangle \Big). \end{aligned} \tag{1.56}$$

Notice that the elements of the deformed Bell basis are orthogonal but not normalized. However, this is not an issue since we are interested in evaluating the detector-level entanglement of the normalized state obtained after projection on the detection regions.

The authors of Ref. [2] introduce a measure of the generated spatial indistinguishability, which is aimed to quantify the no which-way information induced by the deformation D. The introduced quantity is entropic-like and is defined as

$$\mathcal{I} := -\frac{P_{\rm L}P'_{\rm R}}{P_{\rm L}P'_{\rm R}+P'_{\rm L}P_{\rm R}}\log_2\frac{P_{\rm L}P'_{\rm R}}{P_{\rm L}P'_{\rm R}+P'_{\rm L}P_{\rm R}}-\frac{P'_{\rm L}P_{\rm R}}{P_{\rm L}P'_{\rm R}+P'_{\rm L}P_{\rm R}}\log_2\frac{P'_{\rm L}P_{\rm R}}{P_{\rm L}P'_{\rm R}+P'_{\rm L}P_{\rm R}}, \tag{1.57}$$

where we recall that $P_{\rm L}=|\langle L|\psi\rangle|^2$, $P'_{\rm L}=|\langle L|\psi'\rangle|^2$, $P_{\rm R}=|\langle R|\psi\rangle|^2, P'_{\rm R}=|\langle R|\psi'\rangle|^2$, and $P_{\rm L}+P_{\rm R}=P'_{\rm L}+P'_{\rm R}=1$. Notice that such entropic measure of spatial indistinguishability is defined as the detector-level entanglement $E_{\rm dl}(|\Psi^{(2)}\rangle_D)$ of the bipartite state $|\Psi^{(2)}\rangle_D = |\psi\uparrow,\psi'\downarrow\rangle$ obtained by deforming $|A\uparrow,B\downarrow\rangle$ with the deformation D, as computed in Eq. (1.46). In particular, it is minimum $\mathcal{I}=0$ when at least one of $P_{\rm L},P'_{\rm L},P_{\rm R},P'_{\rm R}$ is equal to 0 or to 1 (spatially distinguishable particles), while it is maximum $\mathcal{I}=1$ when $P_{\rm L}=P'_{\rm L}$, implying $P_{\rm R}=P'_{\rm R}=1/2$ (maximally indistinguishable particles).

We proceed by performing the sLOCC projection over the regions L and R via the sLOCC projector $\Pi_{\rm LR}$ defined in Eq. (1.42), obtaining the properly normalized state

$$W^{\pm}_{\rm LR}=\frac{\Pi_{\rm LR}\,W^{\pm}_D\,\Pi_{\rm LR}}{{\rm Tr}\left[\Pi_{\rm LR}\,W^{\pm}_D\right]} \tag{1.58}$$

with probability $P_{\rm LR}={\rm Tr}\left[\Pi_{\rm LR}\,W^{\pm}_D\right]$. To evaluate the entanglement of $W^{\pm}_{\rm LR}$, the authors of Ref. [2] analyze its *Wootters concurrence*, as the von Neumann entropy is defined for pure states only. Given a bipartite state $\rho_{\rm LR}$ of spatially separated particles localized on two separated regions L and R, its concurrence is defined as [33]

$$C(\rho_{\rm LR})=\max\{0,\sqrt{\lambda_4}-\sqrt{\lambda_3}-\sqrt{\lambda_2}-\sqrt{\lambda_1}\}, \tag{1.59}$$

where λ_i are the eigenvalues in decreasing order of the matrix $\xi=\rho_{\rm LR}\,\widetilde{\rho}_{\rm LR}$, with $\widetilde{\rho}_{\rm LR}:=(\sigma_y^{\rm L}\otimes\sigma_y^{\rm R})\,\rho^*_{\rm LR}\,(\sigma_y^{\rm L}\otimes\sigma_y^{\rm R})$ and $\sigma_y^{\rm L}$, $\sigma_y^{\rm R}$ being the usual Pauli matrix σ_y localized, respectively, on the particle in L and in R. The resulting $C(W^{\pm}_{\rm LR})$ depends on the noise probability p, on the particles bosonic or fermionic nature, and on the coefficients l,l',r,r' determining the spatial overlap of the constituents and their indistinguishability $\mathcal{I}$. Results for relevant parameters are reported in Fig. 1.5. It is crucial to compare the obtained outcomes with the entanglement of the state $W^{\pm}_{\rm LR}$ in Eq. (1.53) prior to the application of the deformation + sLOCC projection protocol. It is known that the concurrence of such a state is $C(W^{\pm}_{\rm AB})=1-3p/2$ when $0\leq p\leq 2/3$, being zero otherwise [34] (see the black dot-dashed line of Fig. 1.5**(a)**). In particular, let us focus on the situation $l=l'\Rightarrow P_{\rm L}=P'_{\rm L}$ which guarantees a maximum amount of indistinguishability $\mathcal{I}=1$ between the particles. We further assume the coefficients l,l',r to be real and nonzero, whereas $r'=e^{i\theta}\,|r'|$. When the target state is the singlet $|1_-\rangle_{\rm AB}$, it can be shown that the state in Eq. (1.58) resulting from the sLOCC projection for identical bosons with $\theta=\pi$ or fermions with $\theta=0$ is $W^{-}_{\rm LR}=|1_-\rangle_{\rm LR}\langle 1_-|_{\rm LR}$, that is, in these scenarios the sLOCC operational protocol returns the target singlet state regardless of the noise parameter p. This occurs with probability $P^b_{\rm LR}=2l^2(1-l^2)$ for bosons with $\theta=\pi$, and $P^f_{\rm LR}=2l^2(1-l^2)(4-3p)/[2-(1-2l^2)^2(2-3p)]$ for fermions with $\theta=\pi$. Since $|1_-\rangle_{\rm LR}$ is a maximally entangled state ($C(|1_-\rangle_{\rm LR})=1$), we have thus *recovered the quantum correlations spoiled by the white noise affecting the initial state* $W^{-}_{\rm AB}$. Finally, the results for nonidentical particles are retrieved when $\mathcal{I}=0$,

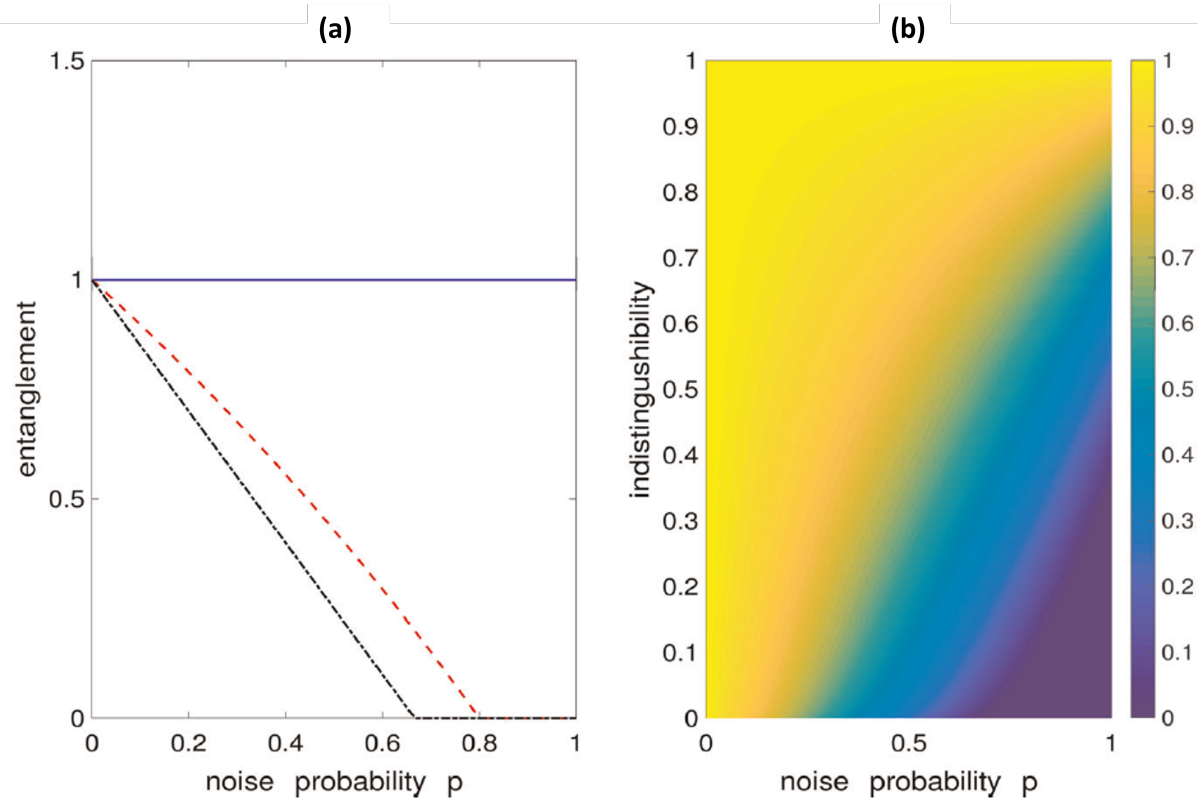

Figure 1.5: **(a)** Entanglement $C(W_{\rm LR}^{\pm})$ as a function of the noise probability p for different degrees of spatial indistinguishability $\mathcal{I}$ and system parameters: the blue solid line refers to the target state $|1_{-}\rangle_{\rm LR}$ of two maximally indistinguishable ($\mathcal{I}=1$, with $l=l'$) identical bosons with $\theta=\pi$ or fermions with $\theta=0$; the red dashed line refers to the target state $|1_{+}\rangle_{\rm LR}$ of two maximally indistinguishable ($\mathcal{I}=1$, with $l=l'$) identical bosons with $\theta=0$ or fermions with $\theta=\pi$; the black dot-dashed line refers to distinguishable qubits ($\mathcal{I}=0$, with $l=1$ and $l'=0$ or vice versa). **(b)** Contour plot of the entanglement $C(W_{\rm LR}^{-})$ as a function of the noise parameter p and the spatial indistinguishability $\mathcal{I}$ for the target state $|1_{-}\rangle_{\rm LR}$ of two identical bosons with $\theta=\pi$ or fermions with $\theta=0$, fixing $l=r'$. Figure taken from Ref. [2].

obtained, e.g., by setting $l=r'=1$ or $l=r'=0$. A more detailed analysis involving the choice of $|1_{+}\rangle_{\rm AB}$ as target state and intermediate values $0<\mathcal{I}<1$ can be found in Ref. [2].

In conclusion, we remark that an extension of the results discussed in this subsection can be found in the paper reported in Chapter 4, where different types of local noisy environments are considered. Furthermore, in Chapter 5 we highlight an issue affecting the spatial indistinguishability measure of Eq. (1.57) when employed to quantify the indistinguishability of states such as $|1_{\pm}\rangle_{D}$ obtained by the deformation of $|1_{\pm}\rangle_{\rm AB}$. We shall discuss the origin of the problem and propose a possible solution.

Chapter 2

Generating indistinguishability within identical particle systems: spatial deformations as quantum resource activators

Abstract

Identical quantum subsystems can possess a property which does not have any classical counterpart: indistinguishability. As a long-debated phenomenon, identical particles' indistinguishability has been shown to be at the heart of various fundamental physical results. When concerned with the spatial degree of freedom, identical constituents can be made indistinguishable by overlapping their spatial wave functions via appropriately defined *spatial deformations*. By the laws of quantum mechanics, any measurement designed to resolve a quantity which depends on the spatial degree of freedom only and performed on the regions of overlap is not able to assign the measured outcome to one specific particle within the system. The result is an entangled state where the measured property is *shared* between the identical constituents. In this work, we present a coherent formalization of the concept of deformation in a general N-particle scenario, together with a suitable measure of the degree of indistinguishability. We highlight the basic differences with nonidentical particles scenarios and discuss the inherent role of spatial deformations as entanglement activators within the *spatially localized operations and classical communication* operational framework.

This chapter reports the results of our manuscript of Ref. [23].

2.1 Introduction: identity and indistinguishability

In physics, particles are said to be *identical* if their intrinsic physical properties, such as mass, electric charge, and (total) spin, are the same [4,5]. This is the case, for example, of subatomic particles such as electrons, photons, quarks, of atomic nuclei, and of atoms and molecules themselves. Particles identity is a cornerstone of both classical and quantum physics which provides the core of the inductive approach to the investigation of Nature's fundamental laws: the assumption that all the electrons in the universe possess the same electric charge, mass, spin, etc., allows to conclude that some fundamental properties

extrapolated from the behaviour of a sample of electrons observed in a laboratory also hold for all the other electrons in the universe.

Despite being frequently used as synonyms, particles identity is not the same as particles *indistinguishability*. Being a purely quantum phenomenon, the latter is more strictly related to the concept of *individual addressability* [7,21]. Identical particles can indeed still be distinguished one from the other when their extrinsic properties, such as their position or the projection of their angular momentum along an axis, are different. This is clear in the classical world where two physical systems, even when microscopic and identical, always occupy distinct positions in space at a fixed time, thus always being potentially individually addressed by following their trajectory [5]. On the contrary, this is not always true in quantum mechanics, where the wave-like and probabilistic description of physical systems allows different particles wave functions to be spatially overlapped, thus having a nonzero probability of simultaneously occupying the same region of space. When this situation occurs, any measurement of quantities depending only on the particles position performed on the region of overlap does not allow the observer to understand to which specific particle the measured outcome belongs to. This is the case, for example, of two synchronized photon sources A and B emitting single photons impinging, with a certain probability, on a restricted detecting spatial region. If a single photon detector in that region clicks, we now have no way of knowing from which source the detected photon is coming from: in this situation, we say that there is *no which-way information* and the particles of interest are said to be *indistinguishable* [4, 21].

The difference between identity and indistinguishability is particularly evident in the everyday experience. It is indeed this difference which allows one to relate observed results to specific samples in an experiment: for example, we can talk about the characterization of a specific laser source carried out in a laboratory in Buenos Aires only because the photons emitted by such a source are very well distinguishable (not spatially overlapped, in this case) from the ones emitted by a neon sign in Tokyo, despite all the photons being identical [6, 7, 12, 35]. Still, the laser must be very well isolated from other light sources to be sure that the characterized device is the laser and not a street lamp nearby. Thus, differently from particle identity, particle indistinguishability depends on the variable degrees of freedom involved. As a crucial consequence, indistinguishability is a meaningful concept only when related to the discrimination capability of the measurement device employed to probe those degrees of freedom.

To better clarify this point, let us recover the above mentioned example of two synchronized single photon emitters and let us now assume that source A is known to emit photons with horizontal polarization, while source B produces only vertically polarized ones. Furthermore, let us suppose that the polarization is not changed by the dynamics. If the single photon detector placed on the region of spatial overlap is designed to discriminate also the photon polarization, we now have a way to understand whether the origin of the particle causing the click is source A or B. In other words, the two photons can now be individually addressed and are not indistinguishable anymore despite being identical and spatially overlapped. Similarly, if we now further assume the polarization of the two photons to be the same, we could employ a measurement device capable of detecting their energy to discriminate among them. Even the emission time can be used to discriminate between the two particles if we know one source to emit before the other. Finally, the number of detectors can be set to distinguish the two particles, too. For example, let us consider that a photon emitted from source A can only reach regions L and C while a photon emitted from source B can impinge only on C and R, with L, C, and R distinct: a

single-photon detector placed in region C would be unable to distinguish the two particles, while the addition of a second detector on L would be enough to reconstruct the origin of every click.

Summing up, particles are always assumed, often implicitly, to be (or not to be) indistinguishable *to the eyes of the employed measurement devices*, while they are universally identical or nonidentical. From the experimental point of view, the actual generation of indistinguishable photons is actually a hard operation of fine tuning and synchronization. From now on, we will always implicitly refer to *spatial indistinguishability* when not otherwise specified, i.e. to the indistinguishability of particles spatially overlapped in relation to detectors for which no which-way information exists.

In this paper we characterize the degree of indistinguishability in a general N-particle quantum system. This is achieved by formalizing and extending the idea of *deformation* operations. Firstly introduced in Ref. [36] and later exploited in Refs. [37, 38] in the particular scenario of bipartite systems, deformations provide a mathematical framework suitable to describe the manipulation of identical constituents when particles' indistinguishability is involved. They account for processes where indistinguishability is generated starting from identical, yet distinguishable particles, and vice versa. Remarkably, they play a fundamental role in devising a coherent extension of the traditional *local operations and classical communication* (LOCC) framework to systems of indistinguishable constituents, whereas the latter fails due to resorting on particles' individuality. After a short summary of the no-label approach to identical particles [21,22] in Section 2.2, we introduce, formalize, and generalize deformations in Section 2.3. In Section 2.4, we retrieve the definition of an entropic measure of spatial indistinguishability firstly introduced in Ref. [2], extending it to the multipartite scenario and to a general amount of degrees of freedom. Finally, in Section 2.5, we review and employ the *spatially localized operation and classical communication* (sLOCC) operational framework, which highlights the importance of spatial deformations as a fundamental tool for the manipulation of identical constituents in many practical applications, as confirmed by recent experiments. To help the reader to grasp the main aspects of the manuscript, we conclude each Section with a brief summary of the discussed arguments.

2.2 The no-label formalism

As is well known, particles living in a 3-dimensional space can be divided into two macro groups: bosons, with integer spin, and fermions, with semi-integer spin. According to the symmetrization postulate, the global state describing an ensemble of identical bosons must remain the same when the role of any pair of particles is exchanged: bosonic states are symmetric under particles swapping. On the contrary, fermionic states are ruled to be anti-symmetric under analogous particles exchange [6]. The existence of such a postulate is at the heart of the Pauli exclusion principle and sets the ground for fundamental results in modern physics, from models to analyze Bose-Einstein condensates to the description of the behaviour of neutron stars.

To deal with these conditions, the standard approach to identical particles assigns unphysical (unobservable) labels to each constituent, ensuring that the global state exhibits the correct symmetry when any two labels are switched [4]. For example, let us consider two non-entangled particles with spatial wave functions ψ_1, ψ_2. If the two particles are nonidentical, their global state is simply given by the tensor product $|\Psi^{(2)}\rangle = |\psi_1\rangle_A \otimes |\psi_2\rangle_B$, where the labels A and B encompass all the other physical degrees of freedom as well as

the properties which makes the two constituents different. Differently, if the two particles are identical and indistinguishable, labels A and B becomes simply fictitious names without any physical meaning and the global state must be written as [6]

$$|\Psi^{(2)}\rangle = \frac{1}{\sqrt{2}} \left(|\psi_1\rangle_A \otimes |\psi_2\rangle_B + \eta \, |\psi_2\rangle_A \otimes |\psi_1\rangle_B \right), \tag{2.1}$$

in order to satisfy the symmetrization postulate, where $\eta = 1$ for bosons and $\eta = -1$ for fermions.

The approach leading to Eq. (2.1), despite being the most frequently used even in didactic textbooks, is know to be affected by some formal problems [12,13]. For example, the necessity to symmetrize/antisymmetrize states by hand as in Eq. (2.1) leads to the emergence of fictitious entanglement when this is evaluated using standard tools such as the von Neumann entropy of the reduced density matrix. This is tackled by adopting ad hoc treatments to probe the existence of quantum correlations among identical particles systems. In addition, such methods require to treat bosons and fermions differently. In order to overcome these problems, a plethora of alternative approaches to deal with identical particles has been proposed over time [7, 13, 20–22, 39–51].

Among these methods, the *no-label approach* recognizes the origin of the problem in the unphysical labels A and B appearing in Eq. (2.1), removing them from the formalism [21, 22]. In this way, global states are simply given by a list of the single particle states: considering once again the example of two constituents with single spatial wave functions ψ_1 and ψ_2, the global state is written as $|\Psi^{(2)}\rangle := |\psi_1, \psi_2\rangle$. If the two particles are distinguishable, e.g. not spatially overlapped, the global state is still a product state. Nonetheless, when they are not perfectly distinguishable, the global state cannot be written as a tensor product anymore: $|\Psi^{(2)}\rangle \neq |\psi_1\rangle \otimes |\psi_2\rangle$. Similarly, the global Hilbert space $\mathcal{H}^{(2)}$ is generally not the tensor product of the single particle Hilbert spaces $\mathcal{H}_1^{(1)}$ and $\mathcal{H}_2^{(1)}$: $\mathcal{H}^{(2)} \neq \mathcal{H}_1^{(1)} \otimes \mathcal{H}_2^{(1)}$. The formalism easily accounts for other single particle degrees of freedom. For example, let us consider a bipartite state of two identical qubits, one with spatial wave function ψ_1 and pseudospin $\uparrow$ and the other one analogously characterized by ψ_2 and $\downarrow$. Within the standard approach, such a state is given by $|\Psi^{(2)}\rangle = \frac{1}{\sqrt{2}} \left(|\psi_1 \uparrow\rangle_A \otimes |\psi_2 \downarrow\rangle_B + \eta \, |\psi_2 \downarrow\rangle_A \otimes |\psi_1 \uparrow\rangle_B \right)$, analogously to Eq. (2.1). In the no-label approach, instead, the same situation is simply described by the state $|\Psi^{(2)}\rangle = |\psi_1 \uparrow, \psi_2 \downarrow\rangle$, with $|\Psi^{(2)}\rangle = |\psi_1 \uparrow\rangle \otimes |\psi_2 \downarrow\rangle$ if ψ_1 and ψ_2 do not overlap (distinguishable particles) and $|\Psi^{(2)}\rangle \neq |\psi_1 \uparrow\rangle \otimes |\psi_2 \downarrow\rangle$ otherwise (indistinguishable particles). The advantages of the no-label formalism emerge even more clearly when dealing with more complicated scenarios: consider, for example, the previously mentioned situation, where this time we don't know whether the particle with spatial wave function ψ_1 is characterized by the pseudospin $\uparrow$ and the one with ψ_2 by $\downarrow$ or vice versa. When such an uncertainty is maximum, two possible states for the bipartite system are the Bell triplet (+) and singlet (-) maximally entangled states, which the symmetrization postulate in the standard formalism rules to be written as

$$|\Psi^{(2)}\rangle = \frac{|\psi_1 \uparrow\rangle_A \otimes |\psi_2 \downarrow\rangle_B \pm |\psi_1 \downarrow\rangle_A \otimes |\psi_2 \uparrow\rangle_B + \eta \big(|\psi_2 \downarrow\rangle_A \otimes |\psi_1 \uparrow\rangle_B \pm |\psi_2 \uparrow\rangle_A \otimes |\psi_1 \downarrow\rangle_B \big)}{2}. \tag{2.2}$$

The no-label approach noticeably simplifies the notation, allowing to rewrite the same state as $|\Psi^{(2)}\rangle = |\psi_1 \uparrow, \psi_2 \downarrow\rangle \pm |\psi_1 \downarrow, \psi_2 \uparrow\rangle$, or equivalently [22] as $|\Psi^{(2)}\rangle = |\psi_1, \psi_2\rangle_{\pm\eta} \otimes |\uparrow, \downarrow\rangle_{\pm}$, where the subscript indicates the symmetry of the state: $|\alpha, \beta\rangle_{\pm} = \pm |\beta, \alpha\rangle$. Finally, the generalization to the N-particle scenario is straightforward, with the global

STANDARD VERSUS NO-LABEL APPROACH CONVERSION TABLE FOR TWO-PARTICLE STATES

$\sigma \neq \tau$		STANDARD APPROACH	NO-LABEL APPROACH
DIFFERENT PSEUDOSPIN. PSEUDOSPIN KNOWN	NONIDENTICAL	$\|\Psi\rangle = \|\psi_1\sigma\rangle_A \|\psi_2\tau\rangle_B$	$\|\Psi\rangle = \|\psi_1\sigma, \psi_2\tau\rangle = \|\psi_1\sigma\rangle \otimes \|\psi_2\tau\rangle$
	IDENTICAL	$\|\Psi\rangle = \|\psi_1\sigma\rangle_A \|\psi_2\tau\rangle_B + \eta \, \|\psi_2\tau\rangle_A \|\psi_1\sigma\rangle_B$	$\|\Psi\rangle = \|\psi_1\sigma, \psi_2\tau\rangle$ $= \|\psi_1\sigma\rangle \otimes \|\psi_2\tau\rangle$ if distinguishable, $\neq \|\psi_1\sigma\rangle \otimes \|\psi_2\tau\rangle$ if not
DIFFERENT PSEUDOSPIN. PSEUDOSPIN UNKNOWN (MAXIMALLY ENTANGLED STATE)	NONIDENTICAL	$\|\Psi\rangle = (\|\psi_1\rangle_A \|\psi_2\rangle_B) \otimes (\|\sigma\rangle_A \|\tau\rangle_B \pm \|\tau\rangle_A \|\sigma\rangle_B)$ $= \|\psi_1\sigma\rangle_A \|\psi_2\tau\rangle_B \pm \|\psi_1\tau\rangle_A \|\psi_2\sigma\rangle_B$	$\|\Psi\rangle = \|\psi_1\sigma, \psi_2\tau\rangle \pm \|\psi_1\tau, \psi_2\sigma\rangle$ $= \|\psi_1, \psi_2\rangle \otimes \|\sigma, \tau\rangle_\pm$
	IDENTICAL	$\|\Psi\rangle = (\|\psi_1\rangle_A \|\psi_2\rangle_B \pm \eta \, \|\psi_2\rangle_A \|\psi_1\rangle_B) \otimes (\|\sigma\rangle_A \|\tau\rangle_B \pm \|\tau\rangle_A \|\sigma\rangle_B)$ $= \|\psi_1\sigma\rangle_A \|\psi_2\tau\rangle_B \pm \|\psi_1\tau\rangle_A \|\psi_2\sigma\rangle_B + \eta \, (\|\psi_2\tau\rangle_A \|\psi_1\sigma\rangle_B \pm \|\psi_2\sigma\rangle_A \|\psi_1\tau\rangle_B)$	$\|\Psi\rangle = \|\psi_1\sigma, \psi_2\tau\rangle \pm \|\psi_1\tau, \psi_2\sigma\rangle$ $= \|\psi_1, \psi_2\rangle_{\pm\eta} \otimes \|\sigma, \tau\rangle_\pm$
SAME PSEUDOSPIN. PSEUDOSPIN KNOWN	NONIDENTICAL	$\|\Psi\rangle = \|\psi_1\sigma\rangle_A \|\psi_2\sigma\rangle_B$	$\|\Psi\rangle = \|\psi_1\sigma, \psi_2, \sigma\rangle = \|\psi_1\sigma\rangle \otimes \|\psi_2\sigma\rangle$
	IDENTICAL	$\|\Psi\rangle = \|\psi_1\sigma\rangle_A \|\psi_2\sigma\rangle_B + \eta \, \|\psi_2\sigma\rangle_A \|\psi_1\sigma\rangle_B$	$\|\Psi\rangle = \|\psi_1\sigma, \psi_2\sigma\rangle$ $= \|\psi_1\sigma\rangle \otimes \|\psi_2\sigma\rangle$ if distinguishable, $\neq \|\psi_1\sigma\rangle \otimes \|\psi_2\sigma\rangle$ if not
SAME PSEUDOSPIN. PSEUDOSPIN UNKNOWN (MAXIMALLY ENTANGLED STATE)	NONIDENTICAL	$\|\Psi\rangle = (\|\psi_1\rangle_A \|\psi_2\rangle_B) \otimes (\|\sigma\rangle_A \|\sigma\rangle_B \pm \|\tau\rangle_A \|\tau\rangle_B)$ $= \|\psi_1\sigma\rangle_A \|\psi_2\sigma\rangle_B \pm \|\psi_1\tau\rangle_A \|\psi_2\tau\rangle_B$	$\|\Psi\rangle = \|\psi_1\sigma, \psi_2\sigma\rangle \pm \|\psi_1\tau, \psi_2\tau\rangle$ $= \|\psi_1, \psi_2\rangle \otimes (\|\sigma, \sigma\rangle \pm \|\tau, \tau\rangle)$
	IDENTICAL	$\|\Psi\rangle = (\|\psi_1\rangle_A \|\psi_2\rangle_B + \eta \, \|\psi_2\rangle_A \|\psi_1\rangle_B) \otimes (\|\sigma\rangle_A \|\sigma\rangle_B \pm \|\tau\rangle_A \|\tau\rangle_B)$ $= \|\psi_1\sigma\rangle_A \|\psi_2\sigma\rangle_B \pm \|\psi_1\tau\rangle_A \|\psi_2\tau\rangle_B + \eta \, (\|\psi_2\sigma\rangle_A \|\psi_1\sigma\rangle_B \pm \|\psi_2\tau\rangle_A \|\psi_1\tau\rangle_B)$	$\|\Psi\rangle = \|\psi_1\sigma, \psi_2\sigma\rangle \pm \|\psi_1\tau, \psi_2\tau\rangle$ $= \|\psi_1, \psi_2\rangle_\eta \otimes (\|\sigma, \sigma\rangle \pm \|\tau, \tau\rangle)$

NOTES: for global states of identical particles in the no-label approach, it holds that $|\psi_1\sigma, \psi_2\tau\rangle = \eta \, |\psi_2\tau, \psi_2\sigma\rangle$.
This does not hold for the spatial and the pseudospin parts separately: $|\psi_1, \psi_2\rangle_{\pm\eta} \otimes |\sigma, \tau\rangle_\pm \neq (\eta \, |\psi_2, \psi_1\rangle_{\pm\eta}) \otimes |\sigma, \tau\rangle_\pm \neq |\psi_1, \psi_2\rangle_{\pm\eta} \otimes (\eta \, |\tau, \sigma\rangle_\pm)$. In the standard approach, $|\cdot\rangle_A \, |\cdot\rangle_B \equiv |\cdot\rangle_A \otimes |\cdot\rangle_B$.
Pseudospin known means that there is certainty about which pseudospin is associated to which spatial wave function; pseudospin unknown means that there is no such a certainty.

Figure 2.1: **Table 1.** Conversion table for two-particle states between the standard formalism and the no-label approach. ψ_1 and ψ_2 are the two single particle spatial wave functions, while σ and τ ($\sigma \neq \tau$) are the pseudospin projection along a preferred axis. Notation is reported for both nonidentical and identical particles states: for the first ones, labels used in the standard approach have a physical meaning, identifying physical, measurable properties; for the latter, no physical meaning can be assigned to labels when the described particles are indistinguishable. The no-label approach overcomes this problem by avoiding to resort on labels. Normalization coefficients are omitted to avoid cluttering.

state $|\Psi^{(N)}\rangle := |\psi_1, \psi_2, \ldots, \psi_N\rangle$ generally satisfying $|\Psi^{(N)}\rangle \neq |\psi_1\rangle \otimes |\psi_2\rangle \otimes \cdots \otimes |\psi_N\rangle$. For a more exhaustive review of how the most common two-particle states are written within the no-label approach, compared to their expressions in the standard approach with fictitious labels, see Table 2.1.

Given the two-particle state $|\psi_1, \psi_2\rangle$, the cornerstone of the no-label approach is provided by the definition of the probability amplitude related to finding the system in the state $|\varphi_1, \varphi_2\rangle$, which takes into account the eventual indistinguishability of the constituents. According to the meaning of indistinguishability discussed in Section 2.1, the impossibility to discriminate between the two particles should reasonably lead to both of them contributing with their probability amplitude of being found in φ_1 and φ_2. Thus, we define

$$\langle \varphi_1, \varphi_2 | \psi_1, \psi_2 \rangle := \langle \varphi_1 | \psi_1 \rangle \langle \varphi_2 | \psi_2 \rangle + \eta \langle \varphi_1 | \psi_2 \rangle \langle \varphi_2 | \psi_1 \rangle . \tag{2.3}$$

Remarkably, this definition directly encodes the statistical exchange phase η: within the no-label approach, the statistical information about the identical particles nature is encoded in the transition amplitudes, rather than in the symmetrization of the quantum state. Some important characteristics of the formalism can be directly derived from (2.3): comparing $\langle \varphi_1, \varphi_2 | \psi_1, \psi_2 \rangle$ with $\langle \varphi_1, \varphi_2 | \psi_2, \psi_1 \rangle$, it follows that

$$|\psi_2, \psi_1\rangle = \eta \, |\psi_1, \psi_2\rangle \tag{2.4}$$

(see the note at the bottom of Table 2.1). Furthermore, state $|\psi_1, \psi_2\rangle$ is not, in general, normalized: indeed, it can be easily checked that (assuming the single particle wave functions ψ_1, ψ_2 to be properly normalized)

$$\langle \psi_1, \psi_2 | \psi_1, \psi_2 \rangle = 1 + \eta \, |\langle \psi_1 | \psi_2 \rangle|^2 := C_+^2, \tag{2.5}$$

implying that the correctly normalized two particle state is

$$|\Psi^{(2)}\rangle_N = |\psi_1, \psi_2\rangle \, / C_+. \tag{2.6}$$

Notice that, when the spatial overlap is null (i.e. distinguishable particles), $\langle \psi_1 | \psi_2 \rangle = 0$ and the normalized two particle state simply reduces to $|\Psi^{(2)}\rangle_N = |\psi_1, \psi_2\rangle$. Eq. (2.3), Eq. (2.4), and Eq. (2.6) can be easily extended to the general N-particle scenario: given the states $|\psi_1, \psi_2, \ldots, \psi_N\rangle$ and $|\varphi_1, \varphi_2, \ldots, \varphi_N\rangle$, the related N-particle probability amplitude is given by

$$\langle \varphi_1, \varphi_2, \ldots, \varphi_N | \psi_1, \psi_2, \ldots, \psi_N \rangle = \sum_{\vec{\alpha}} \eta^{P_{\vec{\alpha}}} \langle \varphi_1 | \psi_{\alpha_1} \rangle \langle \varphi_2 | \psi_{\alpha_2} \rangle \ldots \langle \varphi_N | \psi_{\alpha_N} \rangle , \tag{2.7}$$

where $\vec{\alpha} = (\alpha_1, \alpha_2, \ldots, \alpha_N)$ is any arbitrary permutation of $(1, 2, \ldots, N)$, while $P_{\vec{\alpha}}$ is the parity of the permutation. Under particle swapping, the N-particle state behaves as

$$|\psi_{\alpha_1}, \psi_{\alpha_2}, \ldots, \psi_{\alpha_N}\rangle = \eta^{P_{\vec{\alpha}}} \, |\psi_1, \psi_2, \ldots, \psi_N\rangle , \tag{2.8}$$

while the properly normalized state is simply given by

$$|\Psi^{(N)}\rangle_N = |\psi_1, \ldots, \psi_N\rangle \, / \sqrt{\langle \psi_1, \ldots, \psi_N | \psi_1, \ldots, \psi_N \rangle}. \tag{2.9}$$

Notice that, if all the single particle wave functions are non-overlapping and individually normalized (distinguishable scenario), from Eq. (2.7) we have

$$\langle \psi_1, \ldots, \psi_N | \psi_1, \ldots, \psi_N \rangle = \langle \psi_1 | \psi_1 \rangle \ldots \langle \psi_N | \psi_N \rangle = 1 \tag{2.10}$$

and $|\Psi^{(N)}\rangle_N = |\psi_1, \psi_2, \ldots, \psi_N\rangle$.

When dealing with distinguishable particles, it is possible to resort to the *local operations and classical communication* framework to manipulate, quantify, and compare entanglement [34]. Here, *local* refers to the concept of *particle locality* and to the possibility of acting on the single constituents individually. Thus, such an approach is not applicable to systems of indistinguishable particles, where no individual constituent can be defined. In such a situation, one can instead rely on operations which are localized *in space*, rather than on single elements, leading to the *spatially localized operations and classical communication* (sLOCC) framework discussed further in Section 2.5 [1, 20]. Within this scenario, the action of a single particle operator $O_X^{(1)}$ localized on the spatial region X on the multipartite state $|\Psi^{(N)}\rangle$ is defined, according to the no-label approach, as

$$O_X^{(1)} \, |\Psi^{(N)}\rangle := \sum_i |\langle X | \psi_i \rangle| \, |\psi_1, \ldots, O_X^{(1)} \, \psi_i, \ldots, \psi_N\rangle , \tag{2.11}$$

where $|X\rangle$ denotes a generic state of a particle spatially localized on X, and the presence of at least one such constituent is assumed [36]. Remarkably, the operational necessity of focusing on a specific region of space rather than on individual particles is reflected, in Eq. (2.11), by the sum being weighted by the probability amplitudes associated to each

particle being in the region X. Notice that, when the region X is wide enough to enclose the whole spatial distribution of $|\Psi^{(N)}\rangle$, Eq. (2.11) reduces to

$$O_X^{(1)} |\Psi^{(N)}\rangle := \sum_i |\psi_1, \ldots, O_X^{(1)} \psi_i, \ldots, \psi_N\rangle \,, \tag{2.12}$$

which is the usual single particle operator acting on a state of N identical particles.

In this Section, we have briefly reviewed the no-label approach, an alternative formalism to deal with identical particles which avoid resorting on unphysical labels. We have shown its main features, with particular attention to the main advantages it provides over the standard, label-based, approach. Within this formalism, we have introduced the sLOCC framework as an operational method to deal with indistinguishable particles, postponing a more detailed discussion to Section 2.5. Finally, we remark the spreading which the no-label approach is undergoing to, having been used in different works such as, but not limited to, Refs [36, 51–56].

2.3 Deformations

In this Section, we discuss and formalize the concept of *deformation*, a tool of particular importance when applied to systems of identical particles.

In contrast to global unitary transformations where all the elements of a multipartite state are modified in the same way, deformations consist in transformations acting differently, but still unitarily, on each particle, thus changing the relative relations among the constituents. Given an N-partite state $|\Psi^{(N)}\rangle = |\psi_1, \psi_2, \ldots, \psi_N\rangle$ of either distinguishable or indistinguishable particles, the action of the deformation $D^{(N)}_{\vec{a},\vec{X}}$ is defined, within the no-label approach, as

$$\begin{aligned} D^{(N)}_{\vec{a},\vec{X}} |\Psi^{(N)}\rangle &:= \left(U^{(1)}_{a_1,X_1} \otimes U^{(1)}_{a_2,X_2} \otimes \cdots \otimes U^{(1)}_{a_N,X_N}\right) |\Psi^{(N)}\rangle \\ &= \sum_{\vec{\alpha}} |\langle X_1|\psi_{\alpha_1}\rangle \langle X_2|\psi_{\alpha_2}\rangle \ldots \langle X_N|\psi_{\alpha_N}\rangle| \; \eta^{P_{\vec{\alpha}}} \; |U^{(1)}_{a_1,X_1}\psi_{\alpha_1}, U^{(1)}_{a_2,X_2}\psi_{\alpha_2}, \ldots, U^{(1)}_{a_N,X_N}\psi_{\alpha_N}\rangle \,. \end{aligned} \tag{2.13}$$

Here, the elements a_j in $\vec{a} = (a_1, a_2, \ldots, a_N)$ identify the type of transformation represented by the single particle unitary operator $U^{(1)}_{a_j,X_j}$ and encode the set of parameters required to determine it, while $X_j \in \vec{X} = (X_1, X_2, \ldots, X_N)$ denotes its region of action. $\vec{\alpha}$ and $P_{\vec{\alpha}}$ are as in Eq. (2.7). In general, for a deformation $a_j \neq a_i$ for $j \neq i$. Eq. (2.13) holds when each operator acts on at least one particle, i.e. $\exists\, \vec{\alpha} : \forall\, i \,\exists\, j : \langle X_i|\psi_{\alpha_j}\rangle \neq 0$.

The probability amplitudes weighting the sum in Eq. (2.13) account, as in (2.11), for the spatially localized approach required when the constituents are indistinguishable. When they are distinguishable, either being identical or nonidentical, we can individually address each of them within the traditional LOCC framework and drop the subscript X, so that Eq. (2.13) becomes

$$D^{(N)}_{\vec{a}} |\Psi^{(N)}\rangle = |U^{(1)}_{a_1}\psi_1, U^{(1)}_{a_2}\psi_2, \ldots, U^{(1)}_{a_N}\psi_N\rangle \,. \tag{2.14}$$

Moreover, deformations are unitary when dealing with nonidentical particles. Indeed, in this case we are sure that the constituents are left distinguishable by the deformation. Thus, the right hand side of Eq. (2.14) reduces in this case to a tensor product, namely

$$D^{(N)}_{\vec{a}} |\Psi^{(N)}\rangle = |U^{(1)}_{a_1}\psi_1\rangle \otimes |U^{(1)}_{a_2}\psi_2\rangle \otimes \cdots \otimes |U^{(1)}_{a_N}\psi_N\rangle \,. \tag{2.15}$$

Hence, one has

$$\begin{aligned}\langle D^{(N)}_{\vec{a}}\Psi^{(N)}|D^{(N)}_{\vec{a}}\Psi^{(N)}\rangle &= \langle U^{(1)}_{a_1}\psi_1|U^{(1)}_{a_1}\psi_1\rangle\,\langle U^{(1)}_{a_2}\psi_2|U^{(1)}_{a_2}\psi_2\rangle\ldots\langle U^{(1)}_{a_N}\psi_N|U^{(1)}_{a_N}\psi_N\rangle\\ &= \langle\psi_1|\psi_1\rangle\,\langle\psi_2|\psi_2\rangle\ldots\langle\psi_N|\psi_N\rangle\,,\end{aligned}$$

which implies $\langle\Psi^{(N)}|\left[D^{(N)}_{\vec{a}}\right]^\dagger D^{(N)}_{\vec{a}}\,|\Psi^{(N)}\rangle = \langle\Psi^{(N)}|\Psi^{(N)}\rangle$, finally leading to

$$\left[D^{(N)}_{\vec{a}}\right]^\dagger D^{(N)}_{\vec{a}} = \mathbb{1}. \tag{2.16}$$

Remarkably, this is in general not true anymore for identical constituents, not even when initially distinguishable. From the physical point of view, this is so because the deformation can change the relative spatial overlap of particles, thus leading to the emergence of indistinguishability manifested in the cross-inner products appearing in the right hand side of Eq. (2.7). In order to explicitly show this, let us consider the scenario of $N = 2$ distinguishable but identical particles for simplicity. Before applying the deformation, from Eq. (2.10) we have

$$\langle\Psi^{(2)}|\Psi^{(2)}\rangle = \langle\psi_1,\psi_2|\psi_1,\psi_2\rangle = \langle\psi_1|\psi_1\rangle\,\langle\psi_2|\psi_2\rangle\,.$$

After the deformation, instead, from Eq. (2.7) it holds that

$$\begin{aligned}\langle D^{(2)}_{\vec{a}}\Psi^{(2)}|D^{(2)}_{\vec{a}}\Psi^{(2)}\rangle &= \langle U^{(1)}_{a_1}\psi_1, U^{(1)}_{a_2}\psi_2|U^{(1)}_{a_1}\psi_1, U^{(1)}_{a_2}\psi_2\rangle\\ &= \langle U^{(1)}_{a_1}\psi_1|U^{(1)}_{a_1}\psi_1\rangle\,\langle U^{(1)}_{a_2}\psi_2|U^{(1)}_{a_2}\psi_2\rangle + \eta\,|\langle U^{(1)}_{a_1}\psi_1|U^{(1)}_{a_2}\psi_2\rangle|^2\\ &= \langle\psi_1|\psi_1\rangle\,\langle\psi_2|\psi_2\rangle + \eta\,|\langle\psi_1|\left[U^{(1)}_{a_1}\right]^\dagger U^{(1)}_{a_2}|\psi_2\rangle|^2.\end{aligned}$$

Since, in general, $[U^{(1)}_i]^\dagger U^{(1)}_j \neq 0$, it follows that

$$\langle\Psi^{(2)}|\left[D^{(2)}_{\vec{a}}\right]^\dagger D^{(2)}_{\vec{a}}\,|\Psi^{(2)}\rangle \neq \langle\Psi^{(2)}|\Psi^{(2)}\rangle \Rightarrow \left[D^{(2)}_{\vec{a}}\right]^\dagger D^{(2)}_{\vec{a}} \neq \mathbb{1}. \tag{2.17}$$

We thus conclude that *deformations are unitary when applied to nonidentical particles and, in general, non-unitary for identical ones.* The latter situation is schematically represented in Figure 2.2(top), where we depict an example of deformation acting on three identical, nonetheless distinguishable, particles leading to the generation of spatial indistinguishability, thus being non-unitary. In Figure 2.2(bottom), instead, we report a pictorial representation of the particular scenario where three identical, distinguishable particles are manipulated via a deformation which does not generate indistinguishability, thus retaining unitarity.

Clearly, when normalization is important, states of indistinguishable particles obtained by a deformation can be straightforwardly normalized: given a system of N identical particles in a general mixed state ρ, the normalized state after the deformation is

$$\rho_N = \frac{D\rho D^\dagger}{\mathrm{Tr}\,[D^\dagger D\,\rho]}, \tag{2.18}$$

where we omit superscripts and subscripts of the deformation operator for simplicity.

In this Section, we have introduced and mathematically formalized deformations, namely transformations consisting in a set of unitary operations of particular relevance when dealing with identical particles. We have highlighted their crucial role as operational tools to generate indistinguishability among initially distinguishable, identical constituents, and their suitability to deal with them afterwards. Particular attention has been paid to their general non-unitarity, linking it to their physical interpretation and to the scenario of application.

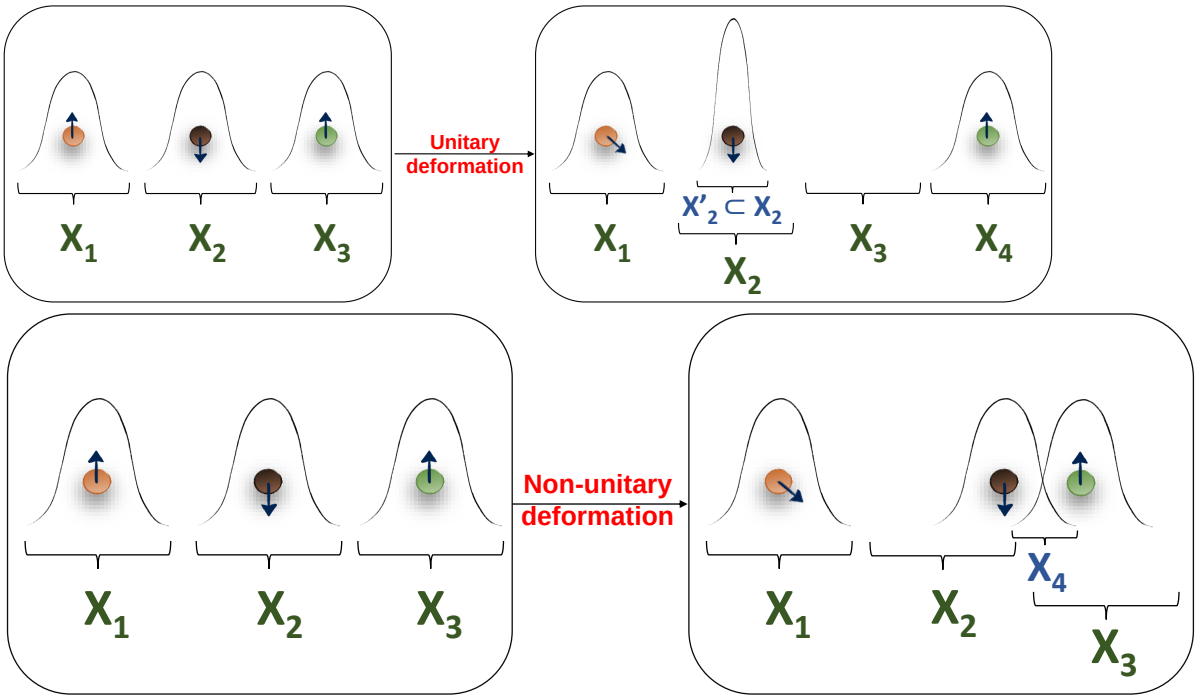

Figure 2.2: **Top.** Example of unitary deformation of three identical and distinguishable particles. The particle localized in region X_1 undergoes a spin rotation, the one in region X_2 sees a unitary restriction of its wave function support to a region $X'_2 \subset X_2$, while the particle in region X_3 gets spatially translated to X_4. No indistinguishability is generated by the process. **Bottom.** Example of non-unitary deformation of three identical and initially distinguishable particles. The particle localized in region X_1 undergoes a spin rotation, while the ones in regions X_2 and X_3 get spatially overlapped over region X_4, where spatial indistinguishability is generated.

2.4 Entropic measure of indistinguishability

As we shall discuss in the next Section, spatial indistinguishability provides an important quantum resource which can be accessed within the sLOCC operational framework for different goals. Within this picture, deformations generating indistinguishability from previously distinguishable constituents provide the key tool to activate such resources. In order to quantitatively demonstrate this, we need a way to quantify indistinguishability. To this aim, we now introduce an entropic measure of generalized indistinguishability, of which spatial indistinguishability is derived as a particular case.

Let us consider an elementary N-particle state $|\Psi^{(N)}\rangle = |\psi_1, \psi_2, \ldots, \psi_N\rangle$; here, each ψ_j encodes both the single particle spatial wave function χ_j and all the other relevant degrees of freedom given by the eigenvalues of a complete set of commuting observables and gathered in a vector $\vec{\sigma}_j$, so that $|\psi_j\rangle = |\chi_j\, \vec{\sigma}_j\rangle$. We now identify N regions of space S_1, S_2,...,S_N where we set N single particle detectors, corresponding to the spatial modes $|S_1\rangle, |S_2\rangle, \ldots, |S_N\rangle$. Since they represent detection regions, we require such spatial modes to be non-overlapping. Nonetheless, we allow for two or more detectors to be same, that is, $|S_i\rangle = |S_j\rangle$ for any $1 \leq i, j \leq N$. Typically, the detectors will be sensible to the spatial position of particles (by construction) and to a subset $\vec{\alpha}$ of the degrees of freedom encoded in $\vec{\sigma}$, while being unable to detect the remaining $\vec{\beta}$ (where $\vec{\sigma}_j = \vec{\alpha}_j \cup \vec{\beta}_j \, \forall \, j = 1, \ldots, N$). For example, each detector could be capable of

detecting the energy of a particle impinging on the spatial region where it is set, without having access to its spin. A single particle detection performed in the region S_k giving as outcomes the set of values $\vec{\alpha}_k$ is thus described by the projection operator $\Pi_k^{(1)} = \sum_{\vec{\beta}} |S_k\, \vec{\alpha}_k\, \vec{\beta}\rangle \langle S_k\, \vec{\alpha}_k\, \vec{\beta}|$, while the probability of such an outcome when detecting a particle whose state is $|\psi_j\rangle = |\chi_j\, \vec{\alpha}_j\, \vec{\beta}_j\rangle$ is given by

$$P_{k,j} = \langle \psi_j | \Pi_k^{(1)} | \psi_j \rangle = \sum_{\vec{\beta}} |\langle S_k\, \vec{\alpha}_k\, \vec{\beta} | \psi_j \rangle|^2 = |\langle S_k | \chi_j \rangle\, \langle \vec{\alpha}_k | \vec{\alpha}_j \rangle|^2. \tag{2.19}$$

A global simultaneous detection of the multipartite state giving as outcomes $\vec{\alpha}_1$ for the particle in the region S_1, $\vec{\alpha}_2$ for the one in S_2, and so on, is described by the action of the N-particle projection operator

$$\Pi^{(N)}_{\{S_k, \vec{\alpha}_k\}} = \bigotimes_{k=1}^{N} \Pi_k^{(1)}. \tag{2.20}$$

We now introduce the joint probability related to the projective measurement in Eq. (2.20) of detecting in the region S_1 with degrees of freedom $\vec{\alpha}_1$ the particle whose state is $|\psi_{j_1}\rangle$, in the region S_2 with degrees of freedom $\vec{\alpha}_2$ the one whose state is $|\psi_{j_2}\rangle$, and so on, that is

$$P^{j_1,\ldots,j_N}_{\{S_k, \vec{\alpha}_k\}} = \prod_{k=1}^{N} P_{k,j_k}. \tag{2.21}$$

With respect to the projective measurement in Eq. (2.20), we define the *degree of indistinguishability* of the N-particle state as

$$\mathcal{I}_{\{S_k, \vec{\alpha}_k\}} = - \sum_{\substack{j_1,\ldots,j_N=1 \\ j_1 \neq \ldots \neq j_N}}^{N} \frac{P^{j_1,\ldots,j_N}_{\{S_k, \vec{\alpha}_k\}}}{\mathcal{Z}} \log_2 \frac{P^{j_1,\ldots,j_N}_{\{S_k, \vec{\alpha}_k\}}}{\mathcal{Z}}, \tag{2.22}$$

where we have indicated the partition function

$$\mathcal{Z} = \sum_{\substack{j_1,\ldots,j_N=1 \\ j_1 \neq \ldots \neq j_N}}^{N} P^{j_1,\ldots,j_N}_{\{S_k, \vec{\alpha}_k\}}. \tag{2.23}$$

When all the particles are spatially separated, there is at most only one non-null joint probability contributing to Eq. (2.22). In particular, if they are perfectly localized on one region each and the values of their accessible degrees of freedom are $\{\vec{\alpha}_k\}_{k=1}^N$, such a probability is equal to 1 and $\mathcal{I}$ reaches its minimum $\mathcal{I}_{\{S_k, \vec{\alpha}_k\}} = 0$: particles are perfectly distinguishable with respect to the measurement given by Eq. (2.20). On the contrary, if all the constituents are equally distributed over all the N spatial regions and possess the same values $\vec{\alpha}_1 = \vec{\alpha}_2 = \cdots = \vec{\alpha}_N$, then all the joint probabilities contribute equally to Eq. (2.22): we have maximally indistinguishable particles and $\mathcal{I}$ takes its maximum value $\mathcal{I}_{\{S_k, \vec{\alpha}_k\}} = \log_2 N!$.

In what follows, we shall be interested in the scenario where the detectors are only sensible to the spatial degree of freedom. This situation is derived from the above described picture by setting $\vec{\alpha} = \{\emptyset\}$, so that Eq. (2.22) reduces to a measure of the degree of *spatial* indistinguishability, as described in the next Section.

In this Section, we have generalized the notion of spatial indistinguishability introduced in Ref. [2]. As we will discuss in the next Section, such a quantity allows to probe and further disclose the role of identical particles indistinguishability within quantum technology protocols involving the sLOCC operational framework.

2.5 Accessing quantum indistinguishability resources: the sLOCC operational framework

As discussed in Section 2.2, indistinguishable particles cannot be addressed with the traditional LOCC framework, since this relies on the possibility to individually manipulate, and thus distinguish, the single constituents. From an operational point of view, we thus resort to the sLOCC framework to access the quantum properties of an indistinguishable particles state [1, 20].

2.5.1 Presentation of the operational framework

For simplicity, we present the sLOCC framework within the simple scenario of two identical qubits with opposite pseudospin, initially distinguishable and localized in the distinct spatial regions A and B. Following the original formulation [20], we take the bipartite system to be in the initial elementary state $|\Psi\rangle_{\mathrm{AB}} = |A\uparrow, B\downarrow\rangle$. Notice that $|\Psi\rangle_{\mathrm{AB}}$ is normalized, since $\langle A|B\rangle = 0$. Applying the notions introduced in Section 2.3, we proceed by deforming such a state to make the two single particle wave functions spatially overlap over two distinct regions L and R corresponding to the normalized spatial modes $|L\rangle$, $|R\rangle$. This amount to performing the transformation

$$|\Psi\rangle_{\mathrm{AB}} = |A\uparrow, B\downarrow\rangle \xrightarrow{D} |\Psi\rangle_D = |\psi_1\uparrow, \psi_2\downarrow\rangle\,, \tag{2.24}$$

where $|\psi_1\rangle = l\,|L\rangle + r\,|R\rangle$ and $|\psi_2\rangle = l'\,|L\rangle + r'\,|R\rangle$. Here, the complex coefficients l, l', r, r' determine the different probabilities of finding each particle in each region and satisfy the relation $|l|^2 + |r|^2 = |l'|^2 + |r'|^2 = 1$. Following what discussed in Section 2.1 we highlight that, despite being spatially indistinguishable, the two qubits in state $|\Psi\rangle_D$ can still be discriminated by a device capable of detecting their spin direction, which has been left unchanged by the deformation. Finally, the deformation has left the state normalized: indeed, it holds that

$${}_D\langle\Psi|\Psi\rangle_D = \Big(\,\langle\psi_1|\psi_1\rangle\,\langle\uparrow|\uparrow\rangle\,\Big)\Big(\,\langle\psi_2|\psi_2\rangle\,\langle\downarrow|\downarrow\rangle\,\Big) + \eta\,|\langle\psi_1|\psi_2\rangle\,\langle\uparrow|\downarrow\rangle|^2 = 1.$$

We now set two single particle detectors on L and R respectively and perform a coincidence measurement, preserving the state if both of them detect a particle and discarding it otherwise. Crucially, the detectors are unable to access the spin direction, so that the two qubits are effectively indistinguishable to their eyes. Thus, this part of the process amounts to a postselected measurement where state $|\Psi\rangle_D$ is projected on the subspace spanned by the basis

$$\mathcal{B}_{\mathrm{LR}} = \{|L\uparrow, R\uparrow\rangle\,, |L\uparrow, R\downarrow\rangle\,, |L\downarrow, R\uparrow\rangle\,, |L\downarrow, R\downarrow\rangle\} \tag{2.25}$$

via the corresponding projection operator

$$\Pi_{\mathrm{LR}} = \sum_{\sigma,\tau=\uparrow,\downarrow} |L\sigma, R\tau\rangle\,\langle L\sigma, R\tau|\,. \tag{2.26}$$

After the proper normalization, the resulting state is given by

$$|\Psi\rangle_{\mathrm{LR}} = \frac{\Pi_{\mathrm{LR}}\,|\Psi\rangle_D}{\sqrt{{}_D\langle\Psi|\Pi_{\mathrm{LR}}|\Psi\rangle_D}} = \frac{lr'\,|L\uparrow, R\downarrow\rangle + \eta\,l'r\,|L\downarrow, R\uparrow\rangle}{\sqrt{|lr'|^2 + |l'r|^2}}, \tag{2.27}$$

postselected with probability

$$P_{\rm LR} = {}_D\langle\Psi|\Pi_{\rm LR}|\Psi\rangle_D = |lr'|^2 + |l'r|^2. \tag{2.28}$$

Notice that the two qubits in the final state $|\Psi\rangle_{\rm LR}$ of Eq. (2.27) are distinguishable, since one of them is now localized in region L while the other in region R.

2.5.2 Analysis and possible applications

The first aspect that emerges from Eq. (2.27) is that the final state $|\Psi\rangle_{\rm LR}$ is an entangled state, provided $l, l', r, r' \neq 0$. Since the initial state was non-entangled, we thus conclude that *the sLOCC protocol can be used to generate entanglement* [1, 20]. Remarkably, the superposition of states $|L\uparrow, R\downarrow\rangle$ and $|L\downarrow, R\uparrow\rangle$ is a direct consequence of the impossibility for the two detectors to understand which one of the two qubits they have detected, namely if the one with spin $\uparrow$ generated in A or the one with spin $\downarrow$ generated in B. In other words, *the origin of the quantum correlations* in the sLOCC-generated state of Eq. (2.27) is *the no-which-way information* discussed in Section 2.1 deriving from the achieved spatial indistinguishability. For this reason, we say that deformations leading to indistinguishability *activate* entanglement, while the sLOCC measurement allows to *access* it. To further stress this point, we remark that $|\Psi\rangle_{\rm LR}$ is non-entangled whenever at least one among l, l', r, r' is null; indeed, this amounts to the scenario where (at least) one of the qubits is perfectly localized either on L or on R, so that the coincidence click required by the sLOCC measurement allows to precisely track the origin of bothe the particles. This is the situation occurring, e.g., when no deformation is performed, so that $l = r' = 1$ and $l' = r = 0$: particles remain distinguishable and no entanglement is generated.

From Eq. (2.22) with $\vec{\alpha} = \{\emptyset\}$, $N = 2$, and $S_1 = L$, $S_2 = R$, the amount of spatial indistinguishability obtained with the deformation can be properly quantified by the entropic measure introduced in Section 2.4 [2]

$$\mathcal{I}_{\rm LR} = -\frac{|l|^2\,|r'|^2}{\mathcal{Z}}\log_2\frac{|l|^2\,|r'|^2}{\mathcal{Z}} - \frac{|l'|^2\,|r|^2}{\mathcal{Z}}\log_2\frac{|l'|^2\,|r|^2}{\mathcal{Z}}, \tag{2.29}$$

where $\mathcal{Z} = |l|^2\,|r'|^2 + |l'|^2\,|r|^2$. Such a quantity takes into account the no-which-way information, taking the minimum value $\mathcal{I} = 0$ when no overlap is present ($l = 1$, $r' = 1$ or $l' = 1$, $r = 1$: distinguishable particles) and the maximum one $\mathcal{I} = 1$ when the overlap is maximum ($l = l' = r = r' = 1/\sqrt{2}$: maximally indistinguishable particles).

The role of indistinguishability as a resource for quantum technologies within the sLOCC framework has been investigated by several recent experiments. Remarkably, in Ref. [1] the authors have experimentally implemented the deformation+sLOCC protocol with two photons initially prepared in the state $|\Psi\rangle_{\rm AB}$. They have performed quantum teleportation with the final state of Eq. (2.27), thus showing that the achieved entanglement is physical. Furthermore, by directly accessing the value of l, l', r, r' they fixed $l = r = 1/\sqrt{2}$ to make $\mathcal{I}$ a function of just one parameter and showed that *the amount of quantum correlations present in the state produced by the sLOCC protocol*, as quantified by the entanglement of formation [33], *is proportional to the degree of spatial indistinguishability achieved*. In particular, when $\mathcal{I} = 1$ we see from Eq. (2.27) that the sLOCC process generates the maximally entangled state $|\Psi\rangle_{\rm LR}^{\rm max} = (|L\uparrow, R\downarrow\rangle + \eta\,|L\downarrow, R\uparrow\rangle)/\sqrt{2}$.

In Refs. [2, 3, 36–38] the authors considered the more realistic scenario where the deformation+sLOCC protocol is applied to two qubits in different scenarios involving

local noisy environments. In the analyzed situations, which involve non-elementary states, the authors shown that the process can be employed to prepare entangled states. Thus, *the sLOCC operational framework can be used to achieve quantum correlations in a way which is robust under the detrimental action of local noise.*

Another relevant element emerging from the sLOCC-prepared state, as can be noticed from Eq. (2.27), is the factor $\eta := e^{i\theta}$ encoding the exchange phase θ, with $\theta = 0$ for bosons and $\theta = \pi$ for fermions being at the core of the symmetrization postulate discussed in Section 2.2. Although many decades have passed after the first formulation of the postulate, a first direct experimental measurement of the bosonic exchange phase has been only recently achieved with two photons in an all-optical setup [57, 58]. This is mainly due to the difficulty in designing a setup *manually* generating a superposition between a reference state and its physically permuted one, from which later extrapolating the relative exchange phase via interferometry. Thanks to its reliance on spatial indistinguishability, the sLOCC process allows to avoid such a difficulty by letting θ naturally emerge. Exploiting this effect, in Ref. [59] the authors designed and experimentally implemented a photonic setup capable of directly measuring the exchange phase of two real bosons and of simulated fermions and anyons by applying interferometry to the sLOCC-produced state of Eq. (2.27). Remarkably, the introduced theoretical setup is general and could be suitably adapted to directly measure the exchange phase of even real fermions and anyons.

Finally, spatial indistinguishability of identical particles undergoing the sLOCC measurement has been shown to provide a useful resource of quantum coherence yielding an advantage in quantum metrology [30, 60], whereas the endurance of quantum coherence within systems of indistinguishable particles in non-dissipative noisy quantum networks was demonstrated in Ref. [61].

It is interesting to highlight the connection between the deformation+sLOCC operational framework and the *entanglement extraction* protocol [50]. In the latter, a single-mode state of indistinguishable particles is splitted over distinct modes. The resulting particle number distribution is then measured along such modes, postselecting only those states which respect a desired partition. Being the resulting modes distinct, this allows to access the entanglement between groups of identical particles whose accessibility was previously ruled out by their single-mode indistinguishability. In relation to this framework, the mode splitting operation is a particular case of deformation acting on already indistinguishable particles. Furthermore, deformations such as mode merging operations can be seen themselves as the preparation step required to achieve the entanglement extraction single-mode starting point. Furthermore, the particles distribution postselected measurement and the sLOCC projection are clearly related, since they both make quantum correlations accessible by making an indistinguishable state distinguishable. Nonetheless, while entanglement extraction focuses on the splitting of an already indistinguishable state to show that quantum correlations inaccessible within identical systems are actually physically meaningful and constitute useful resources in their own right [43, 50], the sLOCC process presents itself as an alternative operational framework where indistinguishability is generated over previously arranged detection regions with the goal of generating, restoring, and/or manipulating entanglement in actual practical applications.

In this Section, we have discussed the sLOCC operational framework suitable to deal with indistinguishable particles. In contrast to the localized operations and classical communication approach traditionally employed when dealing with distinguishable con-

stituents, in the sLOCC framework different operations are localized in space rather than on specific particles, whose indistinguishability makes individually unaddressable. We have briefly commented on the main works reporting possible practical applications of deformations and the sLOCC protocol, where spatial indistinguishability of identical constituents is shown to provide an important resource to achieve quantum information tasks such as entanglement generation, entanglement restoration, coherence generation, and the direct measurement of particles' exchange phase. Finally, we have briefly compared the sLOCC operational framework to the entanglement extraction protocol.

2.6 Conclusion

In conclusion, we have discussed and elucidated the distinction between the concepts of particle identity and particle indistinguishability in quantum mechanics. We have presented a concise review of the no-label approach as a suitable tool to deal with indistinguishable constituents, as introduced in Ref. [21] and further deepened in Refs [22,36]. We have introduced a coherent formalization of deformations acting on either distinguishable or indistinguishable multipartite states, providing an extension of the indistinguishability entropic measure introduced in Ref. [36] to the general N-partite scenario. We have highlighted the relevance of deformations as operations exploitable to activate quantum correlations to be later accessed within the sLOCC operational framework. Finally, we have briefly discussed the relations between the sLOCC protocol and the entanglement extraction one as operational frameworks.

Given the results presented in this work, we believe that deformations, together with the sLOCC operational framework, have the potential to become a useful technique for many real-world applications exploiting quantum technologies. Indeed, identical particles constitute the main building blocks of platforms such as quantum networks, quantum computers, and quantum measurement systems. For instance, spatial indistinguishability of identical constituents generated by properly tuned deformations could be exploited to shield from noise the fundamental quantum correlation properties required for quantum cryptographic protocols, or the coherence of qubits used to run quantum algorithms. Furthermore, the entanglement-restoration characteristics of the presented techniques could be further investigated to preserve the super-sensitivity of states carrying information in quantum sensing and metrology protocols.

Chapter 3

Proof-of-Principle Direct Measurement of Particle Statistical Phase

Abstract

The symmetrization postulate in quantum mechanics is formally reflected in the appearance of an exchange phase ruling the symmetry of identical particle global states under particle swapping. Many indirect measurements of this fundamental phase have been reported thus far, but a direct observation has been only recently achieved for photons. Here, we propose a general scheme capable of directly measuring the exchange phase of any type of particle (bosons, fermions, or anyons), exploiting the operational framework of spatially localized operations and classical communication. We experimentally implement it on an all-optical platform, providing proof-of-principle for different simulated exchange phases. As a by-product, we supply a direct measurement of the real bosonic exchange phase of photons. Additionally, we analyze the performance of the proposed scheme when mixtures of particles of different natures are injected. Our results confirm the symmetrization tenet and provide a tool to explore it in various scenarios. Finally, we show that the proposed setup is suited to generate indistinguishability-driven N00N states useful for quantum-enhanced phase estimation.

This chapter reports the results of our manuscript of Ref. [59].

3.1 Introduction

The symmetrization postulate divides particles living in a three-dimensional space into two groups: bosons and fermions. This postulate forces the state of an ensemble of identical bosons (fermions) to be symmetric (antisymmetric) under the exchange of any pair of particles [6]. If we consider a system of two identical particles, its global state must then satisfy $|\psi(1,2)\rangle = e^{i\phi}|\psi(2,1)\rangle$, where 1 and 2 refer to the two constituents and the relative phase ϕ is the particle exchange phase (EP), with $\phi = 0$ for bosons and $\phi = \pi$ for fermions. Furthermore, the existence of particles called anyons, living in two-dimensional spaces with a fractional EP $\phi \in (0, 2\pi) \setminus (\pi)$ has been suggested [62, 63], and has attracted the attention of the scientific community in recent decades [64–66]. This fundamental phase has been indirectly measured in various experiments [67–72]. Despite the fundamental importance of the symmetrization postulate in both understanding the quantum world and practical applications, only the bosonic nature of photons has so far

been directly proven by use of a state transport protocol [57, 58]. Direct observation of fermionic and anyonic EPs is still missing, leaving the field open to the introduction of techniques capable of filling this gap.

In the standard approach to identical particles [6], the global state vector is symmetrized or antisymmetrized with respect to unphysical labels associated to each constituent. This approach is known to exhibit drawbacks when one is trying to assess real quantum correlations between constituents [12,13]. Given the key role played by entanglement in quantum technologies, several different methods have been developed to fix this issue [13, 20–22, 45, 47, 53, 73]. Among these, the no-label approach [21] has some advantages: it straightforwardly identifies physical entanglement and establishes its quantitative relation with the degree of spatial indistinguishability [2]; the latter is associated with the spatial overlap of particle wave functions. Importantly, in the no-label formalism, the role played by the particles' nature does not manifest itself in the (anti)symmetrization of the quantum state, but instead in the probability amplitudes of the global system [21, 22].

The no-label approach has been widely exploited in environments with spatially localized operations and classical communication (sLOCC) [1, 2, 20, 30, 36–38, 60, 74]. This procedure can be seen as a natural extension of the standard local operations and classical communication for distinguishable particles to the case of indistinguishable and individually unaddressable constituents. Operationally, sLOCC makes the global state of indistinguishable particles undergo a projective measurement over spatially separated regions, followed by postselection when one particle is found in each location. Consider a state of two independent identical qubits $|\psi_D\rangle = |\varphi_D \uparrow, \varphi'_D \downarrow\rangle$, where φ_D, φ'_D are spatial wave functions and $\uparrow, \downarrow$ are pseudospins. The result of applying sLOCC to $|\psi_D\rangle$ is [20]

$$|\psi_{\rm LR}\rangle = \frac{lr' \,|L \uparrow, R \downarrow\rangle + e^{i\phi} rl' \,|L \downarrow, R \uparrow\rangle}{\sqrt{|lr'|^2 + |rl'|^2}}, \tag{3.1}$$

where l, l' (r, r') are the probability amplitudes for each particle to be found in the region L (R), while ϕ is the exchange (statistical) phase; $|\psi_{\rm LR}\rangle$ is entangled only if the qubits spatially overlap, i.e., are spatially indistinguishable, in the regions L and R. Remarkably, the sLOCC process makes particle statistics emerge naturally in the final entangled state. The entanglement obtained is experimentally accessible [1, 74], and has been exploited for teleportation [1] and phase discrimination [60]. Also, sLOCC-based indistinguishability is useful for protecting entanglement against noise [2, 36–38].

Here we give further value to sLOCC by experimentally showing, in a quantum optical setup, that its theoretical framework enables a phase-estimation procedure to directly access the EPs of indistinguishable particles of any nature (Fig. 3.2(a)).

3.2 Theoretical framework

The conceptual procedure is depicted in Fig. 3.2(a). We take a pair of two-level identical particles, independently prepared and initially uncorrelated, whose spatial wave functions and pseudospins are φ, $\uparrow$ and φ', $\downarrow$, respectively. In the no-label formalism, we write this state as $|\psi_{\rm in}\rangle = |\varphi \uparrow, \varphi' \downarrow\rangle$. Then, a deformation operation $|\varphi\rangle \to |\varphi_D\rangle$, $|\varphi'\rangle \to |\varphi'_D\rangle$ is performed [2, 23, 37] to distribute the spatial wave functions over two distinct regions L and R in a controllable way, thus transforming $|\psi_{\rm in}\rangle$ into $|\psi_D\rangle = |\varphi_D \uparrow, \varphi'_D \downarrow\rangle$, where

$$|\varphi_D\rangle = l\,|{\rm L}\rangle + r\,|{\rm R}\rangle\,, \quad |\varphi'_D\rangle = l'\,|{\rm L}\rangle + r'\,|{\rm R}\rangle\,. \tag{3.2}$$

Here, the coefficients $l = \langle \mathrm{L}|\varphi_{\mathrm{D}}\rangle$, $l' = \langle \mathrm{L}|\varphi'_{\mathrm{D}}\rangle$, $r = \langle \mathrm{R}|\varphi_{\mathrm{D}}\rangle$ and $r' = \langle \mathrm{R}|\varphi'_{\mathrm{D}}\rangle$ are the tunable probability amplitudes of finding the particle whose spatial wave function is φ_D or φ'_D at the site L and R, respectively.

To implement the sLOCC measurement, we perform postselected detection of the states, where exactly one qubit per region is recorded. In total, this last step amounts to projecting the state $|\psi_D\rangle$ onto the two-particle basis $\mathcal{B}_{\mathrm{LR}} = \{|\mathrm{L}\uparrow, \mathrm{R}\uparrow\rangle, |\mathrm{L}\uparrow, \mathrm{R}\downarrow\rangle, |\mathrm{L}\downarrow, \mathrm{R}\uparrow\rangle, |\mathrm{L}\downarrow, \mathrm{R}\downarrow\rangle\}$ via the projection operator $\Pi_{\mathrm{LR}} = \sum_{\sigma,\tau=\uparrow,\downarrow} |\mathrm{L}\sigma, \mathrm{R}\tau\rangle \langle \mathrm{L}\sigma, \mathrm{R}\tau|$.

We recall that the two particles in the state $|\psi_D\rangle$ are indistinguishable to the eyes of the detectors. This means that it is not possible to know the region of space where each detected constituent comes from. This absence of which-way information is encoded in the result of the sLOCC operation, which is easily computed to be the (normalized) two-particle entangled state

$$|\psi_{\mathrm{LR}}\rangle = \frac{\Pi_{\mathrm{LR}}|\psi_D\rangle}{\sqrt{\langle\psi_D|\,\Pi_{\mathrm{LR}}\,|\psi_D\rangle}} = \frac{lr'\,|\mathrm{L}\uparrow, \mathrm{R}\downarrow\rangle + e^{i\phi} rl'\,|\mathrm{L}\downarrow, \mathrm{R}\uparrow\rangle}{\sqrt{|lr'|^2 + |rl'|^2}}, \tag{3.3}$$

generated with probability $P_{\mathrm{LR}} = |lr'|^2 + |rl'|^2$ [20]. The phase ϕ that emerges naturally in Eq. (3.3) is exactly the relative EP that we want to measure (Fig. 3.2(a)). In fact, it is fundamentally contained in the probability amplitudes $\langle \chi_{\mathrm{L}}, \chi_{\mathrm{R}}|\,\psi_D\rangle = \langle \chi_{\mathrm{L}}|\,\chi_D\rangle \langle \chi_{\mathrm{R}}|\,\chi'_D\rangle + \eta \langle \chi_{\mathrm{L}}|\,\chi'_D\rangle \langle \chi_{\mathrm{R}}|\,\chi_D\rangle$ [21], where $\chi_{\mathrm{L}} = \mathrm{L}\sigma$, $\chi_{\mathrm{R}} = \mathrm{R}\tau$, $\chi_D = \varphi_D\uparrow$, $\chi'_D = \varphi'_D\downarrow$, and $\eta = e^{i\phi}$ is the particle statistics parameter. It is worth highlighting that the state $|\psi_{\mathrm{LR}}\rangle$ resulting from the sLOCC process describes two particles occupying two distinct regions of space, which are thus now distinguishable and individually addressable. The spatial indistinguishability $\mathcal{I}$ under sLOCC associated with the state $|\psi_D\rangle$ and thus with the state $|\psi_{\mathrm{LR}}\rangle$ is given by [2]

$$\mathcal{I} = -\frac{|lr'|^2}{|lr'|^2 + |l'r|^2} \log_2 \frac{|lr'|^2}{|lr'|^2 + |l'r|^2} - \frac{|l'r|^2}{|lr'|^2 + |l'r|^2} \log_2 \frac{|l'r|^2}{|lr'|^2 + |l'r|^2}. \tag{3.4}$$

In general, the state in Eq. (3.3) represents a quantum superposition of two-particle states whose relative phase contains the EP of the particles. Notice that one of the major difficulties in directly measuring the particle statistical phase consists in creating quantum interference between a given state and its counterpart where particles have been physically exchanged [58]. A so-called state-dependent transport protocol has been engineered with this aim [75] and successively realized with photons [57]. On the other hand, in our scheme the fundamental EP appears straightforwardly as a natural consequence of spatial overlap in separated regions plus the sLOCC procedure, making it amenable to be directly measured via individual operations on the particles. We proceed by rotating the pseudospin of both qubits by $\pi/4$. Given the single-particle operator

$$M_X = \frac{1}{\sqrt{2}} \begin{pmatrix} 1 & -1 \\ 1 & 1 \end{pmatrix} \tag{3.5}$$

which performs this operation on the region X=L,R, the resulting state is given by $|\psi_f\rangle = M_{\mathrm{L}} \otimes M_{\mathrm{R}}\,|\psi_{\mathrm{LR}}\rangle$. Finally, a direct measurement of the pseudospin along the z axis in both of the regions L and R provides information about the EP. We find that

$$\langle \psi_f\,|\sigma^z_{\mathrm{L}} \otimes \sigma^z_{\mathrm{R}}|\,\psi_f\rangle = \frac{2lr'rl'}{|lr'|^2 + |rl'|^2} \cos\phi, \tag{3.6}$$

where we have taken the coefficients l, r, l', r' to be real, since we are able to directly control the distribution of the initial spatial wave functions over L and R during the preparation

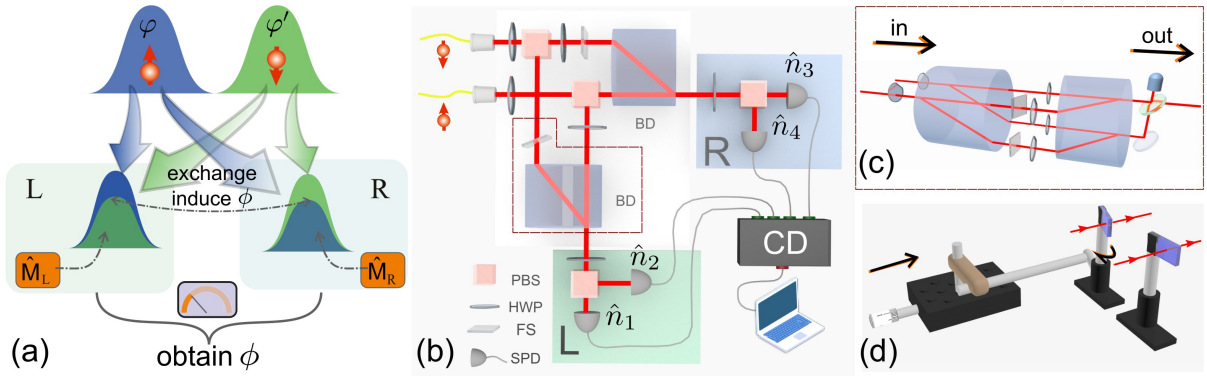

Figure 3.1: Theoretical scheme and experimental setup. (a) Conceptual procedure. The wave functions of two identical particles are distributed over two distinct regions L and R and adjusted to spatially overlap, generating spatial indistinguishability. A sLOCC measurement is used to directly observe the EP using a single-particle rotation M in the two regions. (b) Experimental setup. Two independently prepared photons with opposite polarizations are distributed to two distinct spatial regions L and R. In each region, a beam displacer (BD) is used to merge two beams, generating spatial indistinguishability between the two photons. The relative phase between the two spatial modes of the photons is tuned using a phase-adjustment device consisting of fused silicon (FS), shown in (d). The four outputs are individually directed towards four single-photon detectors (SPDs), where a coincidence device (CD) is used to deal with the signals. PBS: polarization beam splitter; HWP: half-wave plate. (c) Replacement setup for the framed area in (b). An unbalanced interferometer is used to prepare mixed states.

of the state $|\psi_D\rangle$. By knowing these amplitudes, it is thus possible to recover the value of the EP from repeated pseudospin measurements along the z axis.

Remarkably, the role of spatial indistinguishability $\mathcal{I}$ emerges clearly from Eq. (3.6): as its value varies from $\mathcal{I} = 1$ (maximum indistinguishability, which is obtained, e.g., when $l = r = l' = r' = 1/\sqrt{2}$) to $\mathcal{I} = 0$ (distinguishable particles, e.g., when $l = r' = 1$, $l' = r = 0$) [2], the values assumed by Eq. (3.6) change continuously from $\cos\phi$ to zero, correspondingly. It follows that spatial indistinguishability not only is an essential element for measuring the EP with our procedure, but it also acts as a sensitivity regulator that tunes our ability to access the value of ϕ.

3.3 Experimental details

Denoting with $|H\rangle$ and $|V\rangle$ the horizontal and vertical polarization, respectively, of a photon, we make the correspondence $|H\rangle \leftrightarrow |\uparrow\rangle$ and $|V\rangle \leftrightarrow |\downarrow\rangle$. A pulsed ultraviolet beam with wavelength of 400 nm is used to pump a type-II phase-matched β-barium borate (BBO) crystal to generate two uncorrelated photons ($|H\rangle \otimes |V\rangle$) via spontaneous parametric down-conversion. Hong-Ou-Mandel interference is performed to characterize the indistinguishability of the two photons, providing a visibility of 97.7% [1]. Single-mode fibers collect the photons via fiber couplers and direct them towards the effective experimental setup illustrated in Fig. 3.1(b). Here, the weights of their horizontal and vertical polarizations are tuned using a pair of half wave plates (HWPs) fixed at 22.5° and $-\beta/2$ (an adjustable angle), respectively. An additional pair of HWPs at 45° is placed on L to restore the original input polarizations. The result is the preparation of the state

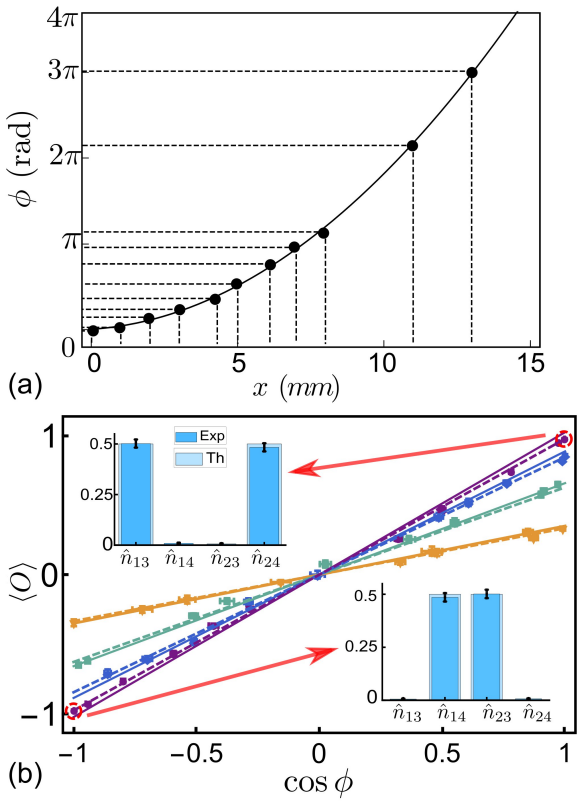

Figure 3.2: (a) Relation between the distance x of the movable plate from the place perpendicular to the beam and the generated relative phase ϕ. The black dots represent the experimental results, while the black curve is the theoretical prediction. The error bars are too small to be visible. (b) Relation between $\langle O \rangle$ and $\cos\phi$. Results are reported for different values of β, where the purple, blue, green, and brown colors represent $\beta = 45°$, $30°$, $20°$, and $10°$, respectively. The solid lines represent the ideal expected results, while the dashed lines show the predictions when noise is taken into consideration. The experimental values are represented by markers. The two insets show the coincidence counts n_{13}, n_{14}, n_{23}, and n_{24} for bosons and fermions.

$|\psi_D\rangle$, with $|\varphi_D\rangle = (|\mathrm{L}\rangle + |\mathrm{R}\rangle)/\sqrt{2}$, $|\varphi'_D\rangle = \sin\beta\,|\mathrm{L}\rangle + \cos\beta\,|\mathrm{R}\rangle$.

Using a home-made phase adjustment device composed of a thin plate of fused silicon (FS) fixed in R and another identical plate that is tilted and placed in L (Fig.3.2(b), (d)), an arbitrary relative phase ϕ_s is judiciously introduced between the components L and R of the photon state φ'_D, which becomes $|\varphi'_D\rangle = e^{i\phi_s}\sin\beta\,|\mathrm{L}\rangle + \cos\beta\,|\mathrm{R}\rangle$. As shown in Fig. 3.2(d), ϕ_s is tuned by directly adjusting the distance x (mm) of the movable plate from the place perpendicular to the beam. The relation between ϕ_s and x is displayed in Fig. 3.2(a) by experimental results (dots) and a theoretical prediction (solid line) for a plate thickness $d = 199.94 \pm 1.43$ μm and a rotation radius $r = 102.36 \pm 0.91$ mm (see Appendix A).

A beam displacer (BD) is used to make the two beams overlap in both regions. We proceed by setting an HWP at $22.5°$ after the BD in both L and R to implement the desired rotation, producing the final state $|\psi_f\rangle$. The pseudospin measurement $\hat{\sigma}_z^{(L)} \otimes \hat{\sigma}_z^{(R)}$ is then performed as a coincidence-counting measurement by placing each polarization beam splitter (PBS) in both of the regions L and R. Each output of the PBSs is individually

directed towards a single-photon detector. The corresponding measured observable is

$$\langle O\rangle = n_{13} + n_{24} - n_{14} - n_{23}, \tag{3.7}$$

where n_{ij} is the coincidence count between the outputs n_i and n_j, which are shown in Fig. 3.2(b). This spatially localized operation, implemented through local counting in L and R, and classical communication tools, realized via the coincidence device, create the state in Eq. (3.1) with $l = r = 1/\sqrt{2}$, $l' = \sin\beta$, $r' = \cos\beta$, i.e.,

$$|\psi_{\rm LR}\rangle = \cos\beta\,|{\rm L}H, {\rm R}V\rangle + e^{i\phi_s}\sin\beta\,|{\rm L}V, {\rm R}H\rangle\,, \tag{3.8}$$

before the final rotation transforms it into $|\psi_f\rangle$. Notice that the relative phase ϕ_s in Eq. (3.8) plays the exact same role as the real EP ϕ in Eq. (3.3) (which is set to zero here, since our experiment is run with bosons). Changing ϕ_s amounts to simulating the behaviour of identical particles with different natures. In other words, the ability of our setup to directly measure ϕ_s provides strong evidence that it can directly detect the EP of any type of particles. Renaming the simulated exchange phase as ϕ, we obtain

$$\langle O\rangle \equiv \langle\psi_f|\,O\,|\psi_f\rangle = \sin(2\beta)\cos\phi, \tag{3.9}$$

from which ϕ can be easily obtained.

We set $\beta = 45^\circ$ and $\phi = 0$ to prepare two maximally indistinguishable photons (bosons), generating a maximum entanglement $|\psi_{\rm LR}\rangle = (|{\rm L}H, {\rm R}V\rangle + |{\rm L}V, {\rm R}H\rangle)/\sqrt{2}$ with a fidelity of 0.99 ± 0.01. Unavoidable experimental errors prevent the achievement of the ideal maximum indistinguishability, which leads to a nonoptimal performance of the real setup. Following the method used in Ref. [57], we treat such errors as a constant factor affecting the final experimental results. We assume that the experimentally prepared state is the desired (ideal) one with probability F, while errors give rise to a spoiled state with probability $1 - F$. Within this model, the spoiled state does not contribute to the expectation value of O, leading to the experimentally measured expectation value $\langle O\rangle_e = F\langle O\rangle_i$, where $\langle O\rangle_i$ is the ideal prediction. By preparing several states of the type represented by Eq. (3.8) for different values of ϕ, we use quantum state tomography [76] to estimate the probability to be $F = 0.977$ (See Appendix B).

The two insets in Fig. 3.2(b) show the coincidence counts n_{13}, n_{14}, n_{23}, and n_{24} for the cases of (real) bosons and (simulated) fermions, with $\beta = 45^\circ$. Treating experimental errors in the manner introduced above, we obtain $\phi_b = 0.04 \pm 0.06$ for bosons and $\phi_f = 3.12 \pm 0.05$ for fermions, which match well with their expected EPs. Here, the error bars show the standard deviation, which is estimated based on the experimental data via a Monte Carlo method.

As shown in Fig. 3.2(b), by varying the angle β, we implement various spatial overlaps to provide deeper insights into the role played by spatial indistinguishability in our scheme, and adjust the EPs (including anyonic ones) with the homemade device. The detected values of $\langle O\rangle$ are given as a function of $\cos\phi$, where ϕ is obtained via tomographic measurements, for different degrees of spatial overlap and, hence, of the spatial indistinguishability $\mathcal{I} = -\sin^2\beta\log_2(\sin^2\beta) - \cos^2\beta\log_2(\cos^2\beta)$ [2]. The experimental results match quite well with the theoretical predictions. In particular, the case of $\beta = 45^\circ$ corresponds to the maximum spatial overlap ($\mathcal{I} = 1$), while $\beta = 30^\circ$, $\beta = 20^\circ$, and $\beta = 10^\circ$ are associated with partial spatial overlaps ($\mathcal{I} < 1$). Notice that when $\mathcal{I}$ decreases, the ranges of values of $\langle O\rangle$ decrease accordingly, leading to a lower sensitivity. Spatial indistinguishability acts as a sensitive regulator governing the range of measured values.

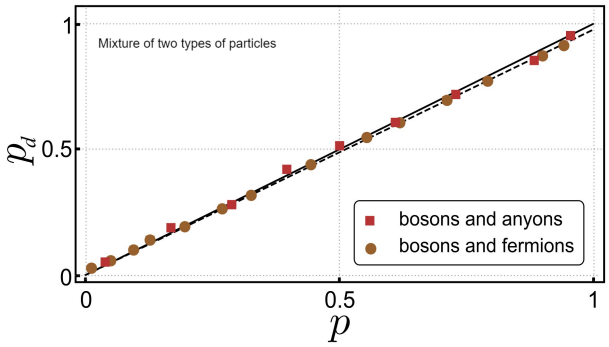

Figure 3.3: Probability distribution p_d for a mixture of two types of particles measured by our procedure versus the value p directly generated by rotating HWPs. Experimental results for a mixture of bosons and anyons with EP $\phi = \pi/2$ (red markers), and for a mixture of bosons and fermions (brown markers). The solid lines represent the ideal expected values, while the dashed lines are the theoretical predictions when noise is considered. The error bars are too small to be visible.

As an extension of our framework, we analyze the scenario where the input is a flux of particle pairs whose exchange phase is known to be either ϕ_1 with probability p or ϕ_2 with probability $1-p$. Each two-particle state is thus given by the classical mixture

$$\rho = p\,|\psi_1\rangle\,\langle\psi_1| + (1-p)\,|\psi_2\rangle\,\langle\psi_2|\,, \tag{3.10}$$

where $|\psi_1\rangle = \cos\beta\,|\mathrm{L}H,\mathrm{R}V\rangle + e^{i\phi_1}\sin\beta\,|\mathrm{L}V,\mathrm{R}H\rangle$ and $|\psi_2\rangle = \cos\beta\,|\mathrm{L}H,\mathrm{R}V\rangle + e^{i\phi_2}\sin\beta\,|\mathrm{L}V,\mathrm{R}H\rangle$. We now want to exploit our procedure to estimate the probability distribution p of the two types of particles by directly measuring their EPs.

To prepare ρ, we replace the framed area in Fig. 3.2(b) with the unbalanced interferometer shown in Fig. 3.2(c). Here, a BD equipped with two HWPs separately placed in each beam is used to split each beam into two vertical beams. The two upper arms are used to prepare a particle with EP ϕ_1, while two lower arms are used to prepare a particle with EP ϕ_2. By changing the angles of the two HWPs before the BD, the probability distribution p can be adjusted. As mentioned above, the EPs ϕ_1 and ϕ_2 are regulated with the corresponding homemade phase-adjustment devices. Then, another BD, together with several HWPs, combines two upper (lower) arms into one beam horizontally. Finally, the two beams are combined with a beam splitter, in which the desired classical mixed state of Eq. (3.10) is generated in one output and the other output is blocked.

The expectation value $\langle O\rangle = \mathrm{Tr}[\rho\,O] = p\,\langle\psi_1|\,O\,|\psi_1\rangle + (1-p)\,\langle\psi_2|\,O\,|\psi_2\rangle$ is measured following the same method as that introduced above. For simplicity, we assume that the values of ϕ_1 and ϕ_2 are provided as prior information, leading to a reduction in $\langle O\rangle$ as a linear function of p. Notice that, if this is not the case, the values of ϕ_1 and ϕ_2 can nonetheless be obtained by our procedure by directly measuring them on a sufficiently big sample of particles. We start with $\phi_1 = 0$ and $\phi_2 = \pi/2$ to investigate a classical mixture of bosons and anyons with $\beta = 45°$. We generate different probability distributions p by rotating the two HWPs before the first BD, as shown in Fig. 3.2(c). Also, we set $\phi_2 = \pi$ to investigate a mixture of bosons and fermions. The results are reported in Fig. 3.3, where the detected probability distributions p_d, obtained based on the measured values of $\langle O\rangle$, are shown versus the values of p directly generated by rotating the HWPs. Excellent agreement with the theoretical predictions is observed (see Appendix C). This last experiment demonstrates how our procedure can be used to obtain information about

the probability distribution p for a mixture of two known different types of particles. If the number of types of particles is increased or unknown, a complete characterization of the incoming flux can still be done by directly measuring the various EPs of particle pairs making up a sufficiently large sample.

3.4 Discussion

In summary, we show experimentally that the sLOCC framework is inherently amenable to direct measurement of the EP of indistinguishable particles. The particle statistics in the measured state are entirely due to the spatial indistinguishability achieved via the deformation of particle wave packets. The sLOCC process functions as a trigger that makes the EP directly accessible within the entanglement generated. For this reason, physical exchange of particles and the related geometric phase do not occur here, in contrast with the technique previously adopted [57] to measure the bosonic EP of photons. Our procedure works for bosons, fermions and anyons. We judiciously design the optical setup to simulate various particle statistics: differently from other methods used for this purpose in the context of photonic quantum walks [77, 78], we manually inject different EPs by accurately tuning a phase-adjustment device, always observing agreement between the measured values and predictions. Our apparatus confirms the real bosonic (symmetric) nature of photons, including the result of Ref. [57]. We also prove that repeated measurements of the EP permit us to reconstruct the probability distribution for statistical mixtures of states of particles of different nature. Our work provides a general scheme to directly explore the symmetrization principle and the role of particle statistics in various contexts, which should have extendable applications in other phase-measurement schemes [79–81].

In the future, it would be interesting to apply our setup on nonoptical platforms to achieve the direct measurement of real (not simulated) fermionic and anyonic EPs. In fact, our scheme can be translated to any platform that implements linear optics, such as platforms for electronic optics [82], where the degree of indistinguishability can be adjusted by use of quantum point contacts acting as electronic beam splitters [83]. Additionally, quantum dots appear promising for on-demand generation of single electrons [84], including their initialization and coherent control [85, 86], where the tunnel effect in double quantum dots could play the role of the deformation operation generating the indistinguishability [23, 87].

We also envisage possible practical applications of our protocol to measure the EP of anyons in topological quantum computers [64,88,89]. Furthermore, the proposed theoretical and experimental setup can be easily adapted to find application in a phase-estimation protocol aided by indistinguishability. Suppose that instead of postselecting the states where exactly one qubit per region is found in the sLOCC measurement, we discard these states by postselecting the complementary ones. This amounts to projecting the state $|\psi_D\rangle$ onto the two-particle basis $\mathcal{B}_{\mathrm{XX}} = \{|X\uparrow, X\uparrow\rangle, |X\uparrow, X\downarrow\rangle, |X\downarrow, X\downarrow\rangle\}$, with $X = L, R$. The resulting state is thus

$$|\psi_{\mathrm{XX}}\rangle = \frac{ll'\,|L\uparrow, L\downarrow\rangle + rr'\,|R\uparrow, R\downarrow\rangle}{\sqrt{|ll'|^2 + |rr'|^2}}, \tag{3.11}$$

which, as can be noticed by rewriting it in the Fock representation and disregarding the

pseudospin, is equivalent to

$$|\psi_{\mathrm{XX}}\rangle = \frac{ll'\,|2,0\rangle + rr'\,|0,2\rangle}{\sqrt{|ll'|^2 + |rr'|^2}}. \tag{3.12}$$

This is a NOON-like state exploitable for quantum-enhanced phase estimation [28,90,91]. By adjusting the values of the coefficients, one may obtain NOON states with various weights for the terms $|2,0\rangle$ and $|0,2\rangle$. Remarkably, since the only difference from the EP measurement scheme is in the postselection, this state can be experimentally generated with the same setup as that depicted in Fig. 3.2(b) (excluding the final measurement step).

Finally, we highlight that while the sLOCC operational framework is exploited here to achieve a result of fundamental interest, different practical applications have been designed and experimentally implemented in fields ranging from quantum communication to quantum metrology and sensing, including the generation of entanglement between identical constituents [1, 20], the protection of quantum correlations from detrimental external noise [2,36–38], and the generation of quantum coherence for metrological applications [30, 60].

A Introduction of phase adjustment

For a better and more intuitive understanding of subtle features of the adjustment of the EP ϕ, we aim here to derive an intuitive geometrical relationship between the distance x moved by the moving plate and the corresponding EP ϕ. This should help us to further connect the distance of movement x with the direct observable O, by exploiting our experimental setup's capability to obtain the exact value of the EP directly.

Here, the corresponding EP of the simulated identical particles ranges from 0 to π. The necessary experimental initialization starts from the adjustment to obtain $\phi = 0$ with two photons separately passing perpendicularly through two thin plates of fused silicon (both having the same thickness d), of which one is motionless and the other can be rotated by a small angle. This rotation is driven by a movable plate (MP). The thickness of d is about $200\,\mu$m, so that the moving part has no influence on the parts of the setup that follow. At each displacement, a tomography procedure is performed so as to construct the corresponding density matrix and, furthermore, to confirm the relative phase ϕ [76]. The experimental results are represented in Fig. 3.2(a), in which the associated error bars are too small to be seen.

Here, we determine the theoretical predictions based on our experimental setup. As shown in Fig. 3.4, the incident angle θ_i and the refraction angle θ_r satisfy the refraction law, where the refractive index of the glass sheet is $n = 1.5$ and the refractive index of air is $n_0 = 1$. We can assume $x = r\sin\theta_i$ for a small angle θ_i. The relationship between the distance of movement x and the phase ϕ is

$$\phi = \frac{2\pi}{\lambda} nd\left(\frac{1}{\sqrt{1-(\frac{\sin\theta_i n_0}{n})^2}} - 1\right) = \frac{2\pi}{\lambda} nd\left(\frac{1}{\sqrt{1-(\frac{x}{rn})^2}} - 1\right), \tag{A1}$$

where λ corresponds to the wavelength of the photon. Moreover, we find that the parameters d and r are $d = 199.94 \pm 1.43\,\mu$m and $r = 102.36 \pm 0.91$ mm. These numbers are in agreement with the measured values, and fit well with our experimental results presented

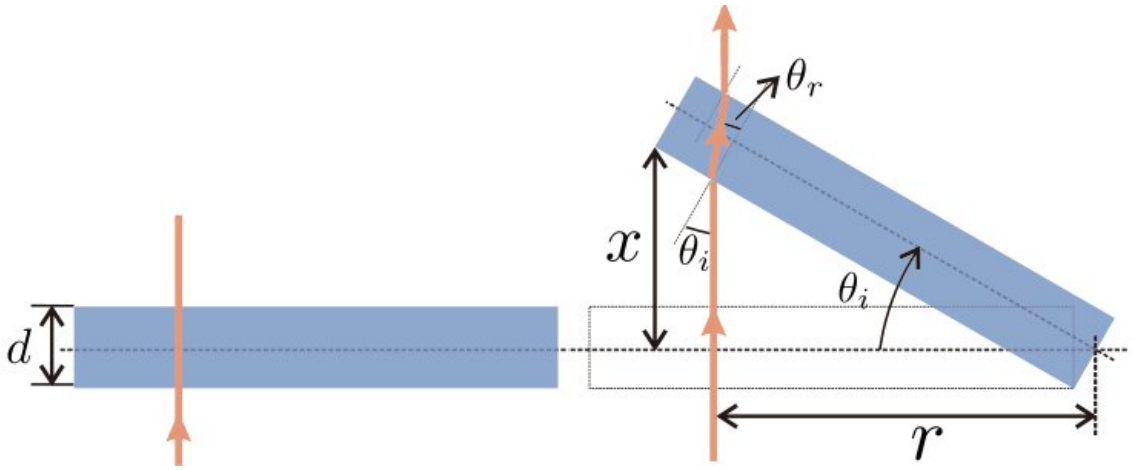

Figure 3.4: Sketch of the tilted experimental setup.

in Fig. 3.2(a). This means that we can straightforwardly obtain the EP ϕ through the displacement of MP x, which is a more intuitive quantity than ϕ. Also, we can exploit the direct measurement results between the observable O and x instead of between O and ϕ; see Fig. 3.4. Based on Eq. (A1), ϕ can be adjusted to be larger than π; however, considering its periodicity, it can be transformed to a value which is within the range $[0,\pi]$.

B Treatment of experimental errors and prediction of performance of the setup

The temporal indistinguishability characterizing the two photons in our setup is evaluated by measuring the Hong-Ou-Mandel interference dip, showing a visibility of 97.7%. This incomplete indistinguishability is the result of unavoidable environmental decoherence and of the somewhat limited performance of our experimental setup, e.g., the effects of white noise and dark counts, leading to the generation of states that deviate slightly from the ideal ones. Similarly to Ref. [57], we model these experimental errors as a constant factor and compute the estimated performance of our setup.

The ideal state we would like to prepare is

$$|\psi_{\mathrm{LR}}\rangle = \cos\beta\,|\mathrm{L}H,\mathrm{R}V\rangle + e^{i\phi}\sin\beta\,|\mathrm{L}V,\mathrm{R}H\rangle\,, \tag{B1}$$

where ϕ represents the simulated EP, while β characterizes the degree of spatial indistinguishability. Denoting by ρ_i the corresponding pure-state density matrix, i.e. $\rho_i = |\psi_{\mathrm{LR}}\rangle\langle\psi_{\mathrm{LR}}|$, we model the experimental errors as if they would lead to the generation of the ideal state ρ_i with probability F. If we use ρ_n to denote the noisy state otherwise achieved, obtained with probability $1-F$, the setup thus generates the mixed state

$$\rho_e = F\rho_i + (1-F)\rho_n. \tag{B2}$$

We consider the noisy part as composed of two contributions: a state ρ_{n1} accounting for white noise due to the accidental errors,

$$\begin{aligned}\rho_{n1} =& \frac{1}{4}(|\mathrm{L}H,\mathrm{R}H\rangle\langle\mathrm{L}H,\mathrm{R}H| + |\mathrm{L}H,\mathrm{R}V\rangle\langle\mathrm{L}H,\mathrm{R}V| \\ &+ |\mathrm{L}V,\mathrm{R}H\rangle\langle\mathrm{L}V,\mathrm{R}H| + |\mathrm{L}V,\mathrm{R}V\rangle\langle\mathrm{L}V,\mathrm{R}V|),\end{aligned} \tag{B3}$$

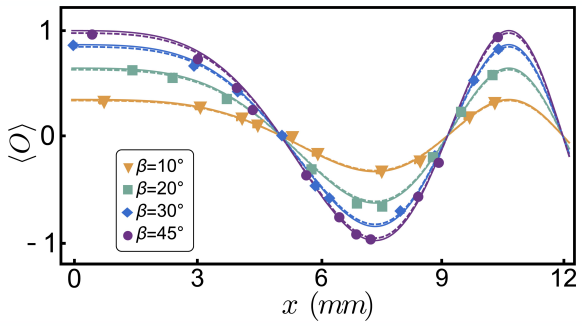

Figure 3.5: Experimental results for different simulated types of particles. Measured values of $\langle O \rangle$ versus the displacement x of the moving plate, generating a relative phase ϕ in the range from 0 to π. Results are reported for different values of β (different colors), corresponding to different degrees of spatial indistinguishability. The solid lines represent the theoretically expected results in the ideal (no-noise) scenario, while the dashed lines show the theoretical values when noise is taken into consideration. Experimentally measured values are represented by markers.

and a state ρ_{n2} accounting for decoherence effects,

$$\rho_{n2} = \frac{1}{2}(|\mathrm{L}H, \mathrm{R}V\rangle \langle \mathrm{L}H, \mathrm{R}V| + |\mathrm{L}V, \mathrm{R}H\rangle \langle \mathrm{L}V, \mathrm{R}H|). \tag{B4}$$

The complete noisy state generated is thus given by

$$\rho_n = a\rho_{n1} + b\rho_{n2},$$

where the coefficients a and b are such that $a + b = 1$.

It is now easy to show that, once it has been rotated as described in 3.3, the noisy component does not contribute to the expectation value of the observable $O = \sigma_{\mathrm{L}}^z \otimes \sigma_{\mathrm{R}}^z$ that we want to measure. As a consequence, the only relevant effect of the experimental errors within this model is to reduce the visibility of the two indistinguishable photons, meaning that the experimental results $\langle O \rangle_e$ are related to the ideal ones $\langle O \rangle_i$ by $\langle O \rangle_e = F \langle O \rangle_i$.

We now want to estimate the parameter F. To do so, we use quantum tomography to experimentally reconstruct ρ_e for different states generated while varying ϕ from 0 to π [76]. This allows us to compute ϕ and β, from which the ideal state in Eq. (B1) can be reconstructed. After preparing several experimental states and obtaining the corresponding groups of ϕ and β, we use (B2) to get $F = 0.977$. As for the noisy part ρ_n, composed of ρ_{n1} and ρ_{n2}, the values of a and b make little difference. Remarkably, we find that the parameter F is affected by fluctuations whose magnitude is of the order of 10^{-3}.

The treatment of the experimental errors presented above is exploited in the main text to perform direct measurement of the EP with a higher accuracy.

C Further experimental plots

By changing the angle β of the HWP, we measure various simulated phases (including anyonic ones) for different values of the spatial overlap in order to obtain further insights into the role played by spatial indistinguishability in our framework. The results are shown in Fig. 3.5. Here, the measured values of $\langle O \rangle$ are given directly as a function of

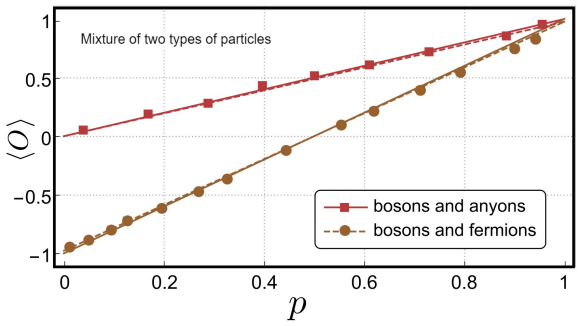

Figure 3.6: Relation between $\langle O \rangle$ and the simulated probability distribution p of a mixture of bosons and anyons with EP $\phi = \pi/2$ (red) and one of bosons and fermions (brown). The solid lines represent the ideal expected values, the dashed lines represent the theoretically expected values when noise is considered, and the markers represent the experimentally obtained results. The error bars are too small to be visible.

the movable plate's displacement for different degrees of spatial overlap and, thus, of the spatial indistinguishability $\mathcal{I}$. The latter is defined by an entropic expression in terms of the probabilities of finding each particle in a given region [2] and, in our experiment, reads $\mathcal{I} = -\sin^2\beta \log_2(\sin^2\beta) - \cos^2\beta \log_2(\cos^2\beta)$. We recall that $\beta = 45°$ corresponds to the maximum spatial overlap (i.e., the maximum spatial indistinguishability $\mathcal{I} = 1$), while $\beta = 30°$, $\beta = 20°$, and $\beta = 10°$ denote partial spatial overlap ($\mathcal{I} < 1$). The experimental results are reported by markers of different types, while the solid lines represent the ideal theoretically expected values $\langle O \rangle_i$. Finally, the dashed lines correspond to the values $\langle O \rangle_e$ expected when the experimental errors are taken into consideration. Notice that, as previously discussed, when the degree of spatial indistinguishability decreases, the ranges of values assumed by $\langle O \rangle$ decrease accordingly, thus leading to a lower sensitivity.

In performing the second experiment, for the classical mixture of two types of particles, we set $\beta = 45°$ for simplicity, as reported in Section 3.3. To begin with, we set $\phi_1 = 0$ and $\phi_2 = \pi/2$ to simulate a classical mixture of bosons and anyons. We simulate different probability distributions by rotating the two input HWPs shown in Fig. 3.1. The expectation value of O, given by

$$\langle O \rangle = \mathrm{Tr}[\rho\, O] = p \langle \psi_1 | O | \psi_1 \rangle + (1-p) \langle \psi_2 | O | \psi_2 \rangle , \tag{C1}$$

is measured as in the pure-state scenario. For simplicity, we assume that the values of ϕ_1 and ϕ_2 are given as prior information, allowing us to compute the expectation values $\langle \psi_j | O | \psi_j \rangle$, $j = 1, 2$, and reducing Eq. (C1) to one linear equation in p. Notice that if this is not the case, the values of ϕ_1 and ϕ_2 can nonetheless be obtained by exploiting our procedure to directly measure them on a sufficiently large sample of particle pairs.

The results obtained are represented by markers in Fig. 3.6, where $\langle O \rangle$ is plotted against the simulated probability p. Here, the efficacy of our setup is apparent when compared with the red solid line, representing the theoretically expected values of $\langle O \rangle$ computed using Eq. (C1). As before, the dashed line represents the theoretical values expected when the action of noise is considered, i.e., $\langle O \rangle_e = F \langle O \rangle$. Then, we set $\phi_2 = \pi$ to simulate a mixture of bosons and fermions and repeat the experiment. The results, displayed in Fig. 3.6 by brown markers and lines, are once again in good agreement with our theoretical predictions.

Chapter 4

Entanglement robustness via spatial deformation of identical particle wave functions

Abstract

We address the problem of entanglement protection against surrounding noise by a procedure suitably exploiting spatial indistinguishability of identical subsystems. To this purpose, we take two initially separated and entangled identical qubits interacting with two independent noisy environments. Three typical models of environments are considered: amplitude damping channel, phase damping channel and depolarizing channel. After the interaction, we deform the wave functions of the two qubits to make them spatially overlap before performing spatially localized operations and classical communication (sLOCC) and eventually computing the entanglement of the resulting state. This way, we show that spatial indistinguishability of identical qubits can be utilized within the sLOCC operational framework to partially recover the quantum correlations spoiled by the environment. A general behavior emerges: the higher the spatial indistinguishability achieved via deformation, the larger the amount of recovered entanglement.

This chapter reports the results of our manuscript of Ref. [37].

4.1 Introduction

It is well known that the environment of an open quantum system produces a detrimental noise which has to be dealt with during the implementation of many useful quantum information processing schemes [92, 93]. One of the main goals in the development of fault-tolerant enhanced quantum technologies is to provide a strategy to protect the entanglement from such degradation. This challenge has been addressed, e.g., by the seminal works on quantum error corrections [94–97], structured environments with memory effects [98–108], distillation protocols [109–111], decoherence-free subspaces [112,113], dynamical decoupling and control techniques [114–123].

It is not unusual to find identical particles (i.e., subsystems such as photons, atoms, nuclei, electrons or any artificial qubits of the same species) as building blocks of quantum information processing devices and quantum technologies [124, 125]. Nonetheless, the standard approach to identical particles based on unphysical labels is known to give

rise to formal problems when trying to asses the correlations between constituents with (partially or completely) overlapping spatial wave functions [12,13]. For this reason, many alternative approaches have been developed to deal with the formal aspects of the entanglement of identical particles [7, 13, 20–22, 39–49, 51, 126, 127]. Among these, the *no-label* approach [20–22] provides many advantages: for example, it allows to address the correlations between identical particles exploiting the same tools used for nonidentical ones (e.g., the von Neumann entropy of the reduced density matrix). Furthermore, it provides the known results for distinguishable particles in the limit of non-overlapping (spatially separated) wave functions. Treating the global multiparticle state as a whole, indivisible object, in the no-label approach entanglement strictly depends on both the spatial overlap of the wave functions and on spatially localized measurements. An entropic measure has been recently introduced [2] to quantify the degree of indistinguishability of identical particles arising from their spatial overlap. Furthermore, an operational framework based on spatially localized operations and classical communication (sLOCC), where the no-label approach finds its natural application, has been firstly theorized [20] and later experimentally implemented [1, 74] as a way of activating physical entanglement. Such framework has also been applied to fields such as the exploitation of the Hanbury Brown-Twiss effect with identical particles [55], quantum entanglement in one-dimensional systems of anyons [56], entanglement transfer in a quantum network [128], and quantum metrology [30, 60]. Moreover, in a recent paper [2] it has been shown that spatial indistinguishability, even partial, can be exploited to recover the entanglement spoiled from the preparation noise of a depolarizing channel.

In this work, we aim to extend the results of Ref. [2] to the wider scenario of different paradigmatic noise channels, namely amplitude damping, phase damping and depolarizing channels, under both Markovian and non-Markovian regimes. To do so, we introduce *spatial deformations*, i.e., transformations turning initially spatially separated (and thus distinguishable) particles into indistinguishable ones by making their wave functions spatially overlap. We then analyze the entanglement dynamics of two identical qubits interacting separately with their own environment, with the goal of showing that the application of the mentioned spatial deformation at a given time of the evolution, immediately followed by the sLOCC measurement, constitutes a procedure capable of recovering quantum correlations.

This paper is organized as follows: in Section 4.2 we introduce the general framework of the analyzed dynamics and the main tools used, namely the deformation operation and the sLOCC protocol. The main results follow in Section 4.3, where we describe the considered model and study the scenarios of an amplitude damping channel, a phase damping channel and a depolarizing channel. Finally, Section 4.4 summarizes and discusses the main results.

4.2 Materials and Methods

In this section we introduce the goal of this paper and the main tools used to achieve it.

Let us consider the following process, illustrated in Figure 4.1: at the beginning, two identical qubits in the entangled state $\rho_{\mathrm{AB}}(0)$ occupy two different regions of space A and B, thus being distinguishable and individually addressable. Here, they locally interact with two spatially separated and independent noisy environments which spoil the initial correlations. At time t, the two particles get decoupled from the environments and undergo a deformation which makes their wave functions spatially overlap into the state $\rho_D(t)$.

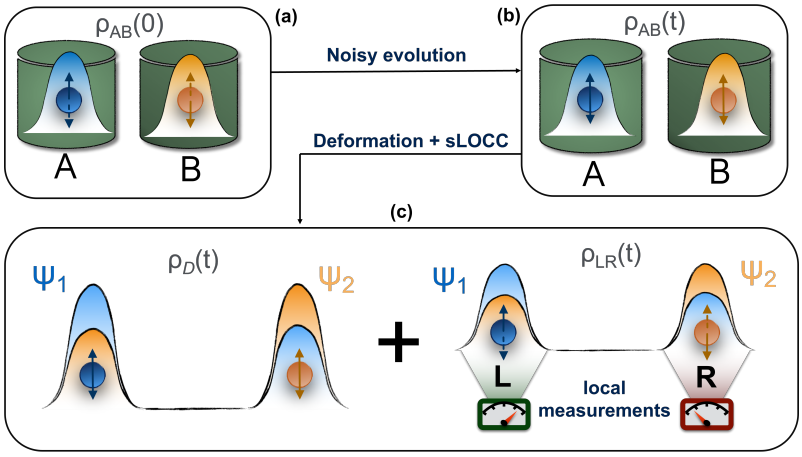

Figure 4.1: State evolution in the considered scenario. (**a**) The two qubits are initially prepared in the pure entangled state $\rho_{\mathrm{AB}}(0)$. (**b**) They are left to interact with a noisy environment, whose detrimental action produces the mixed state $\rho_{\mathrm{AB}}(t)$. (**c**) At time t a deformation of the two particles wave functions is performed, immediately followed by a sLOCC measurement.

Immediately after that, a sLOCC measurement is performed to generate the entangled state $\rho_{\mathrm{LR}}(t)$. In this work, we show that this procedure allows for the recovery of the entanglement spoiled by the previously introduced noise in an amount which depends on the degree of spatial indistinguishability achieved with the deformation. Three different models of environmental noise shall be considered: an amplitude damping channel, a phase damping channel and a depolarizing channel.

Notice that here the system-environment interaction occurs when the two particles are still distinguishable and no finite time interval separates the deformation from the immediately subsequent sLOCC operation. It will thus be interesting to compare the results of this work with those discussed in Ref. [36], where the interaction with the noisy channels happens instead during a finite time interval between the deformation and the sLOCC operation, that is when the qubits are indistinguishable in the frame of the localized environments.

The deformation process bringing two particles to spatially overlap shall be now briefly introduced, followed by a recall of the sLOCC operational framework.

4.2.1 Deformations of identical particle states

Given a multipartite quantum system, a quantum transformation acting differently on each subpart changing the relations among them is called a *deformation*. In this section we focus on the specific set of continuous deformations which modify the single spatial wave functions of identical particles. In what follows, the no-label formalism [21] is used.

Let us take a non-entangled state of two identical particles $|\Phi\rangle = |\phi_1;\phi_2\rangle$, where ϕ_i $(i = 1, 2)$ is identified by the values of a complete set of commuting observables describing a spatial wave function ψ_i and an internal degree of freedom τ_i. We suppose that the two particles are initially spatially separated, e.g., localized in two distinct regions A and B such that $|\psi_1^{(0)}\rangle = |A\rangle$, $|\psi_2^{(0)}\rangle = |B\rangle$ and $\langle A|B\rangle = 0$. We want to modify the spatial wave functions of the two particles in order to make them overlap. Thus, we introduce a

deformation D such that

$$|\phi_1;\phi_2\rangle = |A,\tau_1\rangle \otimes |B,\tau_2\rangle \xrightarrow{D} |\psi_1,\tau_1;\psi_2,\tau_2\rangle\,, \tag{4.1}$$

where ψ_1 and ψ_2 are now at least partially overlapped. Since the two spatially overlapping particles are also identical, they are now *indistinguishable*: their final global state cannot be written as the tensor product of single particle states anymore and must be considered as a whole, i.e. $|\psi_1,\tau_1;\psi_2,\tau_2\rangle \neq |\psi_1,\tau_1\rangle \otimes |\psi_2,\tau_2\rangle$.

A deformation operator acting on identical particles is not, in general, unitary, and its normalized action on a state ρ written in terms of a convex set of density matrices $\{\rho_i\}$, $\rho = \sum_i p_i\,\rho_i$ with $p_i \in [0,1]$ and $\sum_i p_i = 1$, is thus

$$D[\rho] = \frac{D\rho D^\dagger}{\mathrm{Tr}[DD^\dagger\rho]} = \sum_i \bar{p}_i D[\rho_i], \tag{4.2}$$

where

$$\bar{p}_i = \frac{\mathrm{Tr}[DD^\dagger\rho_i]}{\mathrm{Tr}[DD^\dagger\rho]}, \quad D[\rho_i] = \frac{D\rho_i D^\dagger}{\mathrm{Tr}[DD^\dagger\rho_i]}. \tag{4.3}$$

4.2.2 sLOCC, Spatial Indistinguishability and Concurrence

The natural extension of the standard local operation and classical communication framework (LOCC) for distinguishable particles to the scenario of indistinguishable (and thus individually unaddressable) particles is provided by the *spatially localized operations and classical communication* (sLOCC) environment [20]. Given a set of indistinguishable particles, sLOCC consist in a projective measurement of the global state over distinct spatially separated regions, followed by a post-selection of the outcomes where only one particle is found in each location. The result of this operation is an entangled state whose physical accessibility has been demonstrated in a quantum teleportation experiment [1].

Suppose we are given a state ρ of two identical and indistinguishable particles, e.g., obtained by the application (4.2) of the deformation (4.1), and assume they have pseudo-spin 1/2. The whole sLOCC operation (projection and post-selection) amounts to projecting the two qubits state on the subspace spanned by the basis

$$\mathcal{B}_{\mathrm{LR}} = \{|L\uparrow,R\uparrow\rangle\,,|L\uparrow,R\downarrow\rangle\,,|L\downarrow,R\uparrow\rangle\,,|L\downarrow,R\downarrow\rangle\}, \tag{4.4}$$

via the projection operator

$$\Pi_{\mathrm{LR}} = \sum_{\sigma,\tau=\uparrow,\downarrow} |L\sigma,R\tau\rangle\,\langle L\sigma,R\tau|\,. \tag{4.5}$$

Since the constituents are indistinguishable before the detection, it is impossible to know exactly which particle will be found in which region. The sLOCC operation generates the (normalized) two-particle entangled state

$$\rho_{\mathrm{LR}}(t) = \frac{\Pi_{\mathrm{LR}}\,\rho(t)\,\Pi_{\mathrm{LR}}}{\mathrm{Tr}\left[\Pi_{\mathrm{LR}}\,\rho\right]}, \tag{4.6}$$

with probability

$$P_{\mathrm{LR}} = \mathrm{Tr}\left[\Pi_{\mathrm{LR}}\,\rho\right]. \tag{4.7}$$

After the sLOCC measurement, the two qubits occupy two distinct regions of space and are thus now distinguishable and individually addressable. Furthermore, since in the no-label formalism the inner product between two-particle states is given by the rule [21]

$$\langle \phi_1'; \phi_2' | \phi_1; \phi_2 \rangle = \langle \phi_1' | \phi_1 \rangle \langle \phi_2' | \phi_2 \rangle + \eta \langle \phi_1' | \phi_2 \rangle \langle \phi_2' | \phi_1 \rangle , \tag{4.8}$$

with $\eta = 1$ for bosons and $\eta = -1$ for fermions, particle statistics naturally emerges within the sLOCC framework and is thus expected to play a role in the dynamics.

The sLOCC scenario also allows for the introduction of an entropic measure of the particles' indistinguishability after the deformation (2.13), which depends on the achieved spatial distribution of their wave functions ψ_1, ψ_2 over the two regions L and R where sLOCC measurement occurs. Given the probability $P_{X\psi_i}$ of finding the qubit having wave function ψ_i $(i = 1, 2)$ in the region X $(X = L, R)$, the spatial indistinguishability measure is given by [2]

$$\mathcal{I} = -\frac{P_{L\psi_1} P_{R\psi_2}}{\mathcal{Z}} \log_2 \frac{P_{L\psi_1} P_{R\psi_2}}{\mathcal{Z}} - \frac{P_{L\psi_2} P_{R\psi_1}}{\mathcal{Z}} \log_2 \frac{P_{L\psi_2} P_{R\psi_1}}{\mathcal{Z}}, \tag{4.9}$$

where $\mathcal{Z} = P_{L\psi_1} P_{R\psi_2} + P_{L\psi_2} P_{R\psi_1}$. Notice that (4.9) ranges from 0 for spatially separated (thus distinguishable) particles (e.g. when $P_{L\psi_1} = P_{R\psi_2} = 1$) to 1 for maximally indistinguishable particles ($P_{L\psi_1} = P_{L\psi_2}$, $P_{R\psi_1} = P_{R\psi_2}$). Hereafter, we assume for convenience that the spatial wave functions of the single indistinguishable particles after the deformation have the form

$$|\psi_1\rangle = l\,|L\rangle + r\,|R\rangle , \quad |\psi_2\rangle = l'\,|L\rangle + r'\,|R\rangle , \tag{4.10}$$

where

$$l = \langle L|\psi_1\rangle , \; r = \langle R|\psi_1\rangle , \; l' = \langle L|\psi_2\rangle , \; r' = \langle R|\psi_2\rangle \tag{4.11}$$

are complex coefficients such that $|l|^2 + |r|^2 = |l'|^2 + |r'|^2 = 1$. In the following analysis, we shall conveniently set $l = r'$ to assure that the sLOCC probability P_{LR} is different from zero.

As previously stated, the state ρ_{LR} obtained by the sLOCC measurement is entangled. Among the existing entanglement quantifiers [10, 129, 130], we address the quantification of the quantum correlations characterizing the bipartite quantum state ρ_{LR} of two distinguishable qubits via the Wootters concurrence for convenience, namely [2, 33]

$$C(\rho_{\mathrm{LR}}) = \max\{0, \sqrt{\lambda_4} - \sqrt{\lambda_3} - \sqrt{\lambda_2} - \sqrt{\lambda_1}\}, \tag{4.12}$$

where λ_i are the eigenvalues in decreasing order of the matrix $\xi = \rho_{\mathrm{LR}}\,\widetilde{\rho}_{\mathrm{LR}}$, with $\widetilde{\rho}_{\mathrm{LR}} = (\sigma_y^{\mathrm{L}} \otimes \sigma_y^{\mathrm{R}})\,\rho_{\mathrm{AB}}^{*}\,(\sigma_y^{\mathrm{L}} \otimes \sigma_y^{\mathrm{R}})$ and σ_y^{L}, σ_y^{R} being the usual Pauli matrix σ_y localized, respectively, on the particle in L and in R.

Finally, we consider the fidelity $F(\tau, \rho_{\mathrm{LR}}) = \left(\mathrm{Tr}\,\sqrt{\sqrt{\tau}\,\rho_{\mathrm{LR}}\,\sqrt{\tau}}\right)^2$ as a valid figure of merit to quantify the closeness between the state ρ_{LR} and the initial state τ. Notice that if the initial state is pure, i.e. $\tau = |\psi_0\rangle\langle\psi_0|$, then the fidelity takes the simple form

$$F(\tau, \rho_{\mathrm{LR}}) = \langle \psi_0 | \rho_{\mathrm{LR}} | \psi_0 \rangle . \tag{4.13}$$

4.3 Indistinguishability as a feature for recovering entanglement

In this section we report our main results. Each of the two independent environments is modeled as a bath of harmonic oscillators in the vacuum state except for one mode which is coupled to the qubit interacting with it. Considering a qubit-cavity model with just one excitation overall allows us to treat the reservoir as characterized by a Lorentzian spectral density [131, 132]

$$J(\omega) = \frac{\gamma}{2\pi} \frac{\lambda^2}{(\omega - \omega_0)^2 + \lambda^2}, \tag{4.14}$$

where ω_0 is the qubit transition frequency, γ is the microscopic system-environment coupling constant related to the decay of the excited state of the qubit in the Markovian limit of flat spectrum, and λ is the spectral width of the coupling quantifying the leakage of photons through the cavity walls. The relaxation time τ_R on which the state of the system changes is related to the coupling constant by the relation $\tau_R \approx \gamma^{-1}$, while the reservoir correlation time τ_B is connected to the spectral width of the coupling by $\tau_B \approx \lambda^{-1}$. These coefficients regulate the behavior of the system: when $\gamma < \lambda/2\,(\tau_R > 2\tau_B)$ the system is weakly coupled to the environment, the reservoir correlation time is shorter than the relaxation time and we are in a Markovian regime; when $\gamma > \lambda/2\,(\tau_R < 2\tau_B)$ instead, we are in the strong coupling scenario, where the relaxation time is shorter than the bath correlation time and the regime is non-Markovian. The way each qubit interacts with its own reservoir depends on the type of noise channel taken into account.

The action of the three noisy channels considered in this paper shall be computed within the usual Kraus operators formalism, or operator-sum representation [32]. The general expression of the single-qubit evolved density matrix is then given by $\rho(t) = \sum_i E_i \rho(0) E_i^\dagger$, where the E_i's are the time-dependent Kraus operators corresponding to the specific channel and depend on the disturbance probability (decoherence function) $p(t)$. Each channel in fact introduces a time-dependent disturbance on the system with a probability $p(t) = 1 - q(t)$ obtained by solving the differential equation [131, 133]

$$\dot{q}(t) = -\int_0^t dt_1\, f(t - t_1)\, q(t_1), \tag{4.15}$$

where the correlation function $f(t - t_1)$ is given by the Fourier transform of the spectral density $J(\omega)$ of the reservoir, namely

$$f(t - t_1) = \int d\omega\, J(\omega)\, e^{-i(\omega - \omega_0)(t - t_1)}. \tag{4.16}$$

Solving Eq. (4.15) for the spectral density (4.14), one obtains the disturbance (or error) probability [131]

$$p(t) = 1 - e^{-\lambda t} \left[\cos\left(\frac{d\,t}{2}\right) + \frac{\lambda}{d} \sin\left(\frac{d\,t}{2}\right) \right]^2, \tag{4.17}$$

with $d = \sqrt{2\gamma\lambda - \lambda^2}$. Notice that this solution encompasses both Markovian and non-Markovian regimes, depending on the ratio λ/γ. In particular, in the Markovian limit of flat spectrum which occurs for $\gamma/\lambda \ll 1$, it is straightforward to see that $p(t) = 1 - e^{-\gamma t/2}$, as expected [32]. In general, the error probability (4.17) is such that $p(0) = 0$ and $\lim_{t\to\infty} p(t) = 1$.

4.3.1 Amplitude Damping Channel

The amplitude damping channel is one of the most used models describing energy dissipation in quantum systems. This is mainly due to the wide range of physical phenomena that it encompasses, from the spontaneous emission of a photon by an atom [134–136] to processes involving spin chains [137], the scattering of a photon in cavity QED [32], superconducting qubits in circuit QED [138, 139], and high temperature spin systems relaxing to the equilibrium state with their environment [32]. Furthermore, it can be easily simulated using linear-optics devices, thus making it of experimental interest.

The action of the amplitude damping channel on a single qubit in the operator-sum representation is given by the Kraus operators [32]

$$\begin{aligned} E_0 &= |\uparrow\rangle\langle\uparrow| + \sqrt{1-p(t)}\;|\downarrow\rangle\langle\downarrow| = E_0^\dagger, \\ E_1 &= \sqrt{p(t)}\;|\uparrow\rangle\langle\downarrow|\,, \quad E_1^\dagger = \sqrt{p(t)}\;|\downarrow\rangle\langle\uparrow|\,. \end{aligned} \tag{4.18}$$

Consider two identical qubits initially prepared in the Bell singlet state

$$|1_-\rangle_{\mathrm{AB}} = \frac{1}{\sqrt{2}}\Big(\,|A\uparrow, B\downarrow\rangle - |A\downarrow, B\uparrow\rangle\,\Big), \tag{4.19}$$

with A and B being two distinct spatial regions ($\langle A|B\rangle = 0$). Thanks to the fact that the the two environmental interactions are independent, the state after the noisy interaction is given by

$$\begin{aligned} \rho_{\mathrm{AB}}(t) = &\left(E_0^A \otimes E_0^B\right)\rho_{\mathrm{AB}}(0)\left(E_0^A \otimes E_0^B\right) \\ &+ \left(E_1^A \otimes E_1^B\right)\rho_{\mathrm{AB}}(0)\left(E_1^{A\,\dagger} \otimes E_1^{B\,\dagger}\right) \\ &+ \left(E_0^A \otimes E_1^B\right)\rho_{\mathrm{AB}}(0)\left(E_0^A \otimes E_1^{B\,\dagger}\right) \\ &+ \left(E_1^A \otimes E_0^B\right)\rho_{\mathrm{AB}}(0)\left(E_1^{A\,\dagger} \otimes E_0^B\right), \end{aligned} \tag{4.20}$$

where E_i^X ($i = 1, 2$, $X = A, B$) denotes the i-th single particle Kraus operator of Eq. (4.18) acting on the qubit localized in region X, while $\rho_{\mathrm{AB}}(0) = |1_-\rangle_{\mathrm{AB}}\langle 1_-|_{\mathrm{AB}}$ is the initial density matrix. Using Eq. (4.18) in the above equation, one then finds

$$\rho_{\mathrm{AB}}(t) = \Big(1 - p(t)\Big)\,|1_-\rangle_{\mathrm{AB}}\langle 1_-|_{\mathrm{AB}} + p(t)\,|A\uparrow, B\uparrow\rangle\langle A\uparrow, B\uparrow|\,. \tag{4.21}$$

We now want to apply the deformation defined in Eq. (2.13) to the state (4.21) at time t. State $|1_-\rangle_{\mathrm{AB}}$ gets mapped to

$$|\bar{1}_-\rangle_D = \frac{1}{\sqrt{2}}\Big(\,|\psi_1\uparrow, \psi_2\downarrow\rangle - |\psi_1\downarrow, \psi_2\uparrow\rangle\,\Big), \tag{4.22}$$

which is not a normalized state since $\langle\psi_1|\psi_2\rangle \neq 0$. In order to write it in terms of a normalized state $|\bar{1}_-\rangle_N$, we compute

$$\langle\bar{1}_-|\bar{1}_-\rangle_D = C_1^2, \quad C_1 := \sqrt{1 - \eta|\langle\psi_1|\psi_2\rangle|^2}, \tag{4.23}$$

and write it as

$$|\bar{1}_-\rangle_D = C_1\,|\bar{1}_-\rangle_N\,. \tag{4.24}$$

The same is done for the deformation of $|A\uparrow, B\uparrow\rangle$, which gets mapped to

$$|\psi_1\uparrow, \psi_2\uparrow\rangle_D = C_2\,|\psi_1\uparrow, \psi_2\uparrow\rangle_{\mathrm{N}}\,, \quad C_2 := \sqrt{1 + \eta|\langle\psi_1|\psi_2\rangle|^2}, \tag{4.25}$$

where

$$\langle \psi_1 \uparrow, \psi_2 \uparrow | \psi_1 \uparrow, \psi_2 \uparrow \rangle_{\mathrm{N}} = 1. \tag{4.26}$$

The normalized state resulting from the spatial deformation (4.2) of the state (4.21) is thus

$$\rho_D(t) = \frac{\Big(1-p(t)\Big) C_1^2 \, |\bar{1}_-\rangle_N \, \langle \bar{1}_-|_N + p(t)\, C_2^2 \, |\psi_1 \uparrow, \psi_2 \uparrow\rangle_{\mathrm{N}} \, \langle \psi_1 \uparrow, \psi_2 \uparrow|_{\mathrm{N}}}{\Big(1-p(t)\Big) C_1^2 + p(t)\, C_2^2}. \tag{4.27}$$

Following the scheme shown in Figure 4.1, we perform the sLOCC measurement immediately after the deformation, applying the projection operator (4.5) onto the state (4.27), which finally gives

$$\rho_{\mathrm{LR}}(t) = \frac{\Big(1-p(t)\Big) |lr' - \eta\, l'r|^2 \, |1_-\rangle_{\mathrm{LR}} \, \langle 1_-|_{\mathrm{LR}} + p(t)\, |lr' + \eta\, l'r|^2 \, |L\uparrow, R\uparrow\rangle \, \langle L\uparrow, R\uparrow|}{\Big(1-p(t)\Big) |lr' - \eta\, l'r|^2 + p(t)\, |lr' + \eta\, l'r|^2} \tag{4.28}$$

where l, r, l', r' are the wave function coefficients defined in (4.11).

In order to study the entanglement evolution of the state $\rho_{\mathrm{LR}}(t)$ of Eq. (4.28), we calculate the concurrence defined in Eq. (4.12), which is

$$C\big(\rho_{\mathrm{LR}}(t)\big) = \frac{|lr' - \eta\, l'r|^2 \Big(1-p(t)\Big)}{|lr' - \eta\, l'r|^2 \Big(1-p(t)\Big) + |lr' + \eta\, l'r|^2\, p(t)}, \tag{4.29}$$

where the statistics parameter η explicitly appears, as expected. As a first consideration, we notice that the results about entanglement dynamics for bosons can be obtained from the ones for fermions (and vice versa) by simply changing sign to one of the coefficients l, r, l', r' (that is, by shifting the phase of one of them by π). Therefore, in order to fix a framework to analyze the concurrence, we assume we are dealing with fermions whose spatial wave functions are distributed over the regions L and R with positive real coefficients. This reasoning shall hold for the other noisy channels, so that the presented results are also valid for bosons. With this assumption, we get the concurrence as

$$C\big(\rho_{\mathrm{LR}}(t)\big) = \frac{\Big[(lr')^2 + (l'r)^2 + 2\, ll'rr'\Big]\Big(1-p(t)\Big)}{(lr')^2 + (l'r)^2 + 2\, ll'rr'\Big(1-2p(t)\Big)}. \tag{4.30}$$

We point out that when no deformation is performed and the particles remain distinguishable in two distinct regions ($\mathcal{I} = 0$), the sLOCC projector (4.5) is equivalent to the identity operator. This implies that when the particles are not brought to spatially overlap, our procedure gives the same entanglement we would have without performing the sLOCC operation. For this reason, we take the results for $\mathcal{I} = 0$ (black dashed lines in the following figures) as the term of comparison to quantify the entanglement gained due to the *deformation + sLOCC procedure*, i.e., $\Delta C(t) := C\big(\rho_{\mathrm{LR}}(t)\big) - C\big(\rho_{\mathrm{AB}}(t)\big)$. Figure 4.2 shows the concurrence (4.30) for both the Markovian and the non-Markovian regimes, while Figure 4.3 displays $\Delta C(t)$.

As can be seen in Figure 4.2, spatial indistinguishability (4.9) has a direct influence on the general behavior: when the particles are not perfectly indistinguishable ($\mathcal{I} \neq 1$),

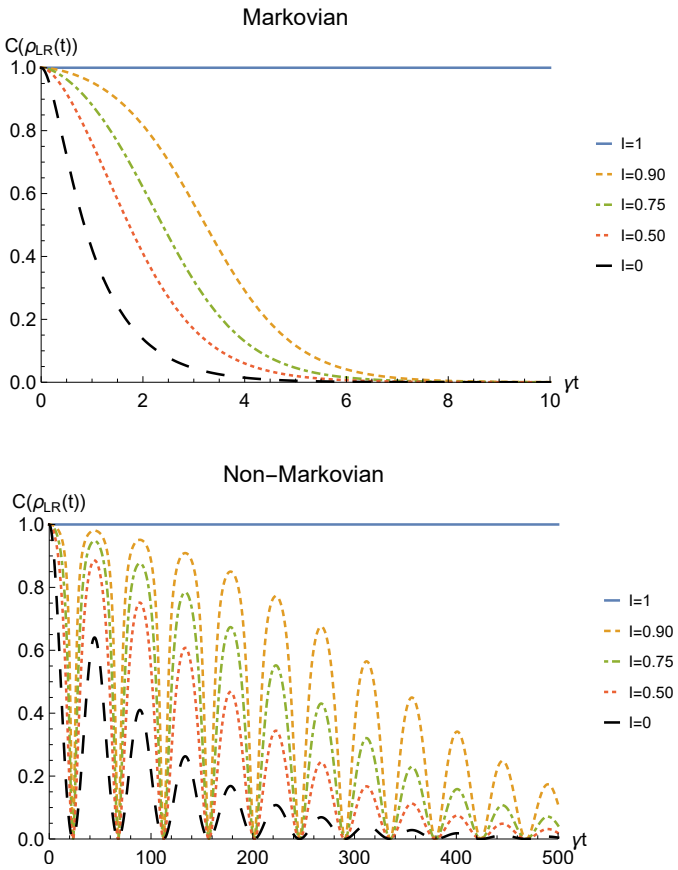

Figure 4.2: Concurrence of two identical qubits (fermions with real $l, l', r, r' > 0$, bosons with one of these four coefficients negative) in the initial state $|1_-\rangle_{\rm AB}$ subjected to localized amplitude damping channels, undergoing an instantaneous deformation+sLOCC operation at time t for different degrees of spatial indistinguishability $\mathcal{I}$ (with $|l| = |r'|$). Both the Markovian ($\lambda = 5\gamma$) (upper panel) and non-Markovian ($\lambda = 0.01\gamma$) (lower panel) regimes are reported.

the entanglement vanishes with a monotonic decay in the Markovian regime and with a periodic one in the non-Markovian regime. From Figure 4.3, we can see that when $\mathcal{I} \neq 1$ the deformation and sLOCC procedure becomes inefficient in recovering the correlations as time grows. Nonetheless, it is interesting to notice that it provides an initial effective advantage as a consequence of the fact that the decay rate shown in Figure 4.2 gets lower as the indistinguishability increases. However, when the particles wave functions maximally overlap ($\mathcal{I} = 1$, blue solid line), the entanglement remains stable at its initial maximum value, thus becoming unaffected by the noise. These results show that, in the scenario of the amplitude damping channel, we have provided an operational framework where spatial indistinguishability, even imperfect, of two identical qubits can be exploited as a scheme to recover quantum correlations spoiled by a short-time interaction with the noisy environment.

Finally, to check whether such procedure would be of any practical interest we have to analyze its theoretical probability of success. This strictly depends on the probability for the sLOCC projection (4.6) to produce a non-null result, physically representing a state which does not get discarded during the postselection. Such probability is defined in Eq. (4.7) and, for identical qubits undergoing a local interaction with an amplitude

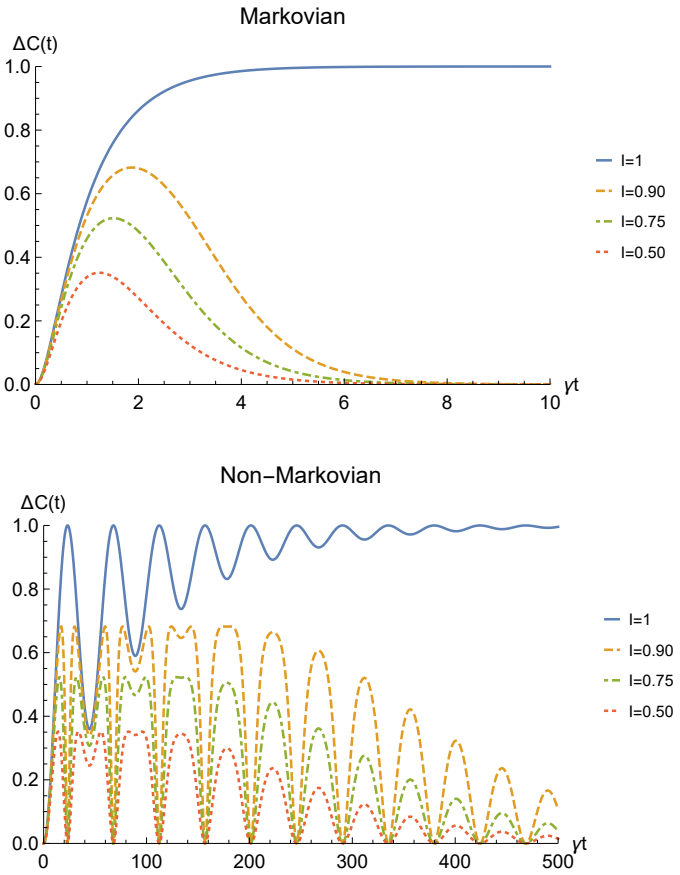

Figure 4.3: Net gain in the entanglement recovery of two identical qubits (fermions with real $l, l', r, r' > 0$, bosons with one of these four coefficients negative) in the initial state $|1_-\rangle_{\rm AB}$ under localized amplitude damping channels, thanks to the deformation+sLOCC operation performed at time t. Results are reported for different degrees of spatial indistinguishability $\mathcal{I}$ (with $|l| = |r'|$). Both the Markovian ($\lambda = 5\gamma$) (upper panel) and non-Markovian ($\lambda = 0.01\gamma$) (lower panel) regimes are shown.

damping channel, it is equal to

$$P_{\rm LR}(t) = \frac{(lr')^2 + (l'r)^2 - 2\eta\, ll'rr'\Big(1 - 2\,p(t)\Big)}{C_1^2\Big(1 - p(t)\Big) + C_2^2\,p(t)}. \tag{4.31}$$

Figure 4.4 shows the success probability (4.31) for different degrees of spatial indistinguishability in both the Markovian and non-Markovian regime in the case of fermions. As can be seen, when the indistinguishability is not maximum, the probability of success tends to 1 as time passes in both regimes, thus giving rise to a trade-off with the concurrence. The trade-off is confirmed by the probability being constant and equal to 1/2 when the concurrence is maximum, i.e. for $\mathcal{I} = 1$ (blue solid line). For bosons, the time-dependent success probability corresponding to $\mathcal{I} = 1$ (with the constraint $l = r' = l' = -r$) and to the concurrence plotted in Fig. 4.2 is $P_{\rm LR}(t) = 1 - p(t)$ (notice, however, that this success probability can be improved by differently setting the coefficients of the spatial wave functions).

We conclude the analysis of the amplitude damping channel by showing the fidelity (4.13) between the state (4.28) resulting from the sLOCC measurement and the initial state

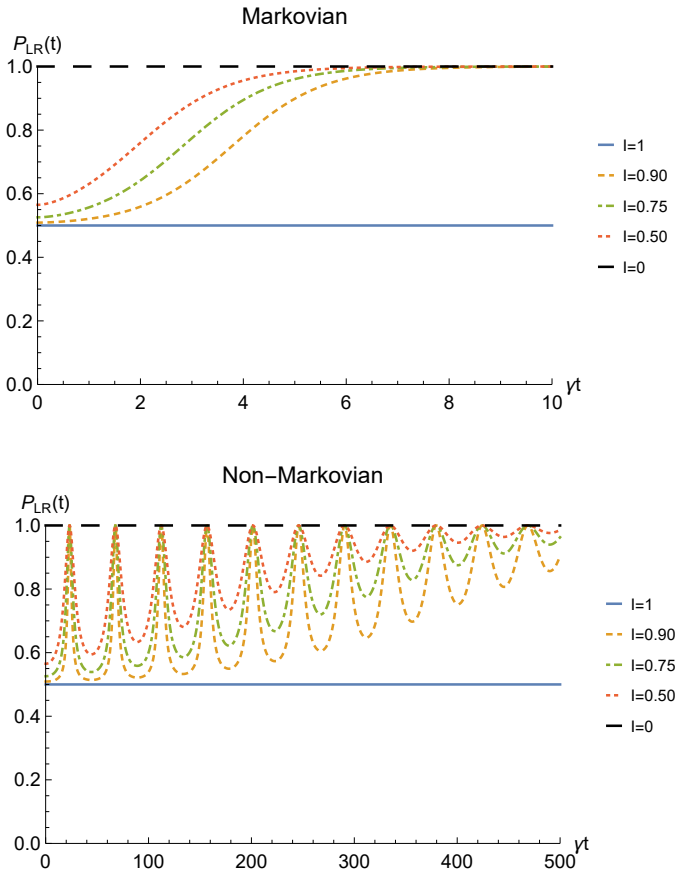

Figure 4.4: Success probability of obtaining a nonzero outcome from the sLOCC projection for fermions ($l, l', r, r' > 0$ and $l = r'$) interacting with localized amplitude damping channels. Different degrees of spatial indistinguishability are reported in both the Markovian ($\lambda = 5\gamma$) (upper panel) and non-Markovian ($\lambda = 0.01\gamma$) (lower panel) regimes.

where locations A and B are assumed to coincide with L and R, namely $\tau = |1_-\rangle_{\rm LR}\langle 1_-|_{\rm LR}$. This is reported for fermions with real and positive coefficients in Fig. 4.5 as a function of time and for different values of indistinguishability. Similarly to the concurrence, the fidelity decays to zero with time for $\mathcal{I} \neq 1$, with a decay rate which diminishes with the spatial indistinguishability. When the maximal spatial indistinguishability is achieved, instead, the fidelity maintain its maximum value $F = 1$ ($\mathcal{I} = 1$, solid blue line). This behaviour holds in both the Markovian and non-Markovian regimes.

4.3.2 Phase Damping channel

The phase damping channel is used to model the inherently quantum non-dissipative physical situation where a system undergoes a loss of coherence without losing energy. In this scenario, the energy eigenstates of the system are not changed by the dynamics, but they accumulate a phase which is responsible for the gradual degradation of the interference terms. Physical systems undergoing this phenomena are, e.g., random telegraph noise and phase noisy lasers [140–145], photons randomly scattering through a waveguide, and superconducting qubits under low-frequency noise.

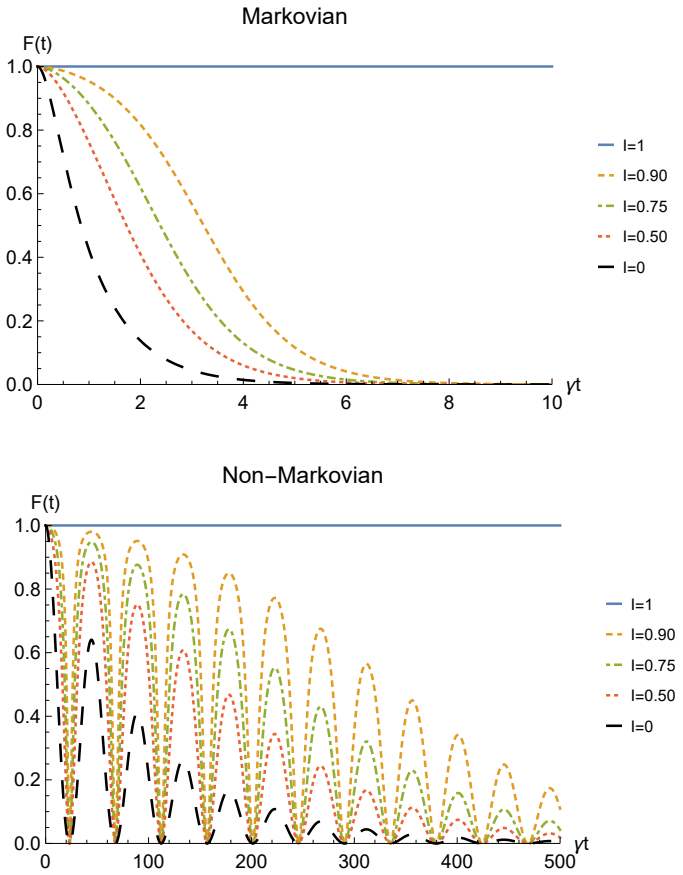

Figure 4.5: Fidelity of two identical qubits (fermions with real $l, l', r, r' > 0$) subjected to localized amplitude damping channels, computed between the initial state $|1_-\rangle_{\rm LR}\langle 1_-|_{\rm LR}$ and the state produced by an instantaneous deformation+sLOCC operation at time t for different degrees of spatial indistinguishability $\mathcal{I}$ (with $|l| = |r'|$). Both the Markovian ($\lambda = 5\gamma$) (upper panel) and non-Markovian ($\lambda = 0.01\gamma$) (lower panel) regimes are reported.

A phase damping channel acting on a single qubit is described by the Kraus operators

$$\begin{aligned} E_0 &= |\uparrow\rangle\langle\uparrow| + \sqrt{1-p(t)}\,|\downarrow\rangle\langle\downarrow| = E_0^\dagger, \\ E_1 &= \sqrt{p(t)}\,|\downarrow\rangle\langle\downarrow| = E_1^\dagger. \end{aligned} \tag{4.32}$$

Once again, we consider the Bell state $|1_-\rangle_{\rm AB}$ of two identical qubits defined in (4.19) as our initial state. The evolved state $\rho_{\rm AB}(t)$ after the interaction with the two independent environments is computed as in Eq. (4.20), which for the phase damping channel described by the above Kraus operators gives

$$\rho_{\rm AB}(t) = \left(1 - \frac{p(t)}{2}\right)|1_-\rangle_{\rm AB}\langle 1_-|_{\rm AB} + \frac{p(t)}{2}\,|1_+\rangle_{\rm AB}\langle 1_+|_{\rm AB}\,, \tag{4.33}$$

where $|1_+\rangle_{\rm AB}$ is the Bell state defined as

$$|1_+\rangle_{\rm AB} = \frac{1}{\sqrt{2}}\Big(|A\uparrow, B\downarrow\rangle + |A\downarrow, B\uparrow\rangle\Big). \tag{4.34}$$

At time t, deformation (2.13) is applied to the state (4.33) to make the two particles spatially overlap. Deformation of $|1_-\rangle_{\rm AB}$ gives the state (4.22), while $|1_+\rangle_{\rm AB}$ gets mapped

to

$$|\bar{1}_+\rangle_D = \frac{1}{\sqrt{2}}\Big(|\psi_1 \uparrow, \psi_2 \downarrow\rangle + |\psi_1 \downarrow, \psi_2 \uparrow\rangle \Big). \tag{4.35}$$

Once again, state $|\bar{1}_+\rangle_D$ is not normalized: it is indeed easy to show that

$$|\bar{1}_+\rangle_D = C_2\, |\bar{1}_+\rangle_N\,, \tag{4.36}$$

where $\langle\bar{1}_+|\bar{1}_+\rangle_N = 1$ and C_2 is defined in (4.25). Thus, the global normalized state after the deformation is

$$\rho_D(t) = \frac{\Big(1 - \frac{1}{2}\,p(t)\Big) C_1^2\ |\bar{1}_-\rangle_N \langle\bar{1}_-|_N + \frac{1}{2}\,p(t)\, C_2^2\ |\bar{1}_+\rangle_N \langle\bar{1}_+|_N}{\Big(1 - \frac{1}{2}\,p(t)\Big) C_1^2 + \frac{1}{2}\,p(t)\, C_2^2}. \tag{4.37}$$

Finally, the sLOCC operation is performed: the action of the projection operator (4.5) on the state (4.37), as defined in Eq. (4.6), gives

$$\rho_{\rm LR}(t) = \frac{\big(1 - \frac{1}{2}\,p(t)\big)\, |lr' - \eta\, l'r|^2\, |1_-\rangle_{\rm LR} \langle 1_-|_{\rm LR} + \frac{1}{2}\,p(t) |lr' + \eta\, l'r|^2\, |1_+\rangle_{\rm LR} \langle 1_+|_{\rm LR}}{\big(1 - \frac{1}{2}\,p(t)\big)\, |lr' - \eta\, l'r|^2 + \frac{1}{2}\,p(t) |lr' + \eta\, l'r|^2}. \tag{4.38}$$

We now study the entanglement evolution of such a state by the concurrence $C(\rho_{\rm LR}(t))$, which is readily found to be

$$\begin{gathered} C\big(\rho_{\rm LR}(t)\big) = \max\{0,\ \lambda_1(t) - \lambda_2(t)\}\,, \\ \lambda_1(t) := \max\{\lambda_A(t),\ \lambda_B(t)\}\,, \lambda_2(t) := \min\{\lambda_A(t), \quad \lambda_B(t)\}\,, \end{gathered} \tag{4.39}$$

with

$$\lambda_A(t) := \frac{\big(1 - \frac{1}{2}\,p(t)\big)\, |lr' - \eta\, l'r|^2}{\big(1 - \frac{1}{2}\,p(t)\big)\, |lr' - \eta\, l'r|^2 + \frac{1}{2}\,p(t) |lr' + \eta\, l'r|^2},$$

$$\lambda_B(t) := \frac{\frac{1}{2}\,p(t)\, |lr' + \eta\, l'r|^2}{\big(1 - \frac{1}{2}\,p(t)\big)\, |lr' - \eta\, l'r|^2 + \frac{1}{2}\,p(t) |lr' + \eta\, l'r|^2}.$$

Focusing the analysis once again on fermions with real and positive coefficients l, r, l', r' to fix a framework, concurrence (4.39) is then equal to

$$C\big(\rho_{\rm LR}(t)\big) = \frac{\Big(1 - p(t)\Big)\Big[(lr')^2 + (l'r)^2\Big] + 2ll'rr'}{(lr')^2 + (l'r)^2 + \Big(1 - p(t)\Big) 2ll'rr'}. \tag{4.40}$$

The time behavior of the concurrence of Eq. (4.40) is plotted in Figure 4.6 for both the Markovian and the non-Markovian regime, while the net gain due to the deformation and sLOCC operation is depicted in Figure 4.7. Once again, the entanglement recovered is found to decrease as the interaction time increases where the generated spatial indistinguishability is not maximum. As in the amplitude damping scenario, such dephasing is monotonic in the Markovian regime and periodic in the non-Markovian one, with a decay rate which decreases as particle indistinguishability increases. Nonetheless, differently from that case, the entanglement now does not vanish. Indeed, for $t \to \infty$ it reaches a constant value which, under the above assumptions, is given by

$$C_\infty = \frac{2ll'rr'}{(lr')^2 + (l'r)^2}. \tag{4.41}$$

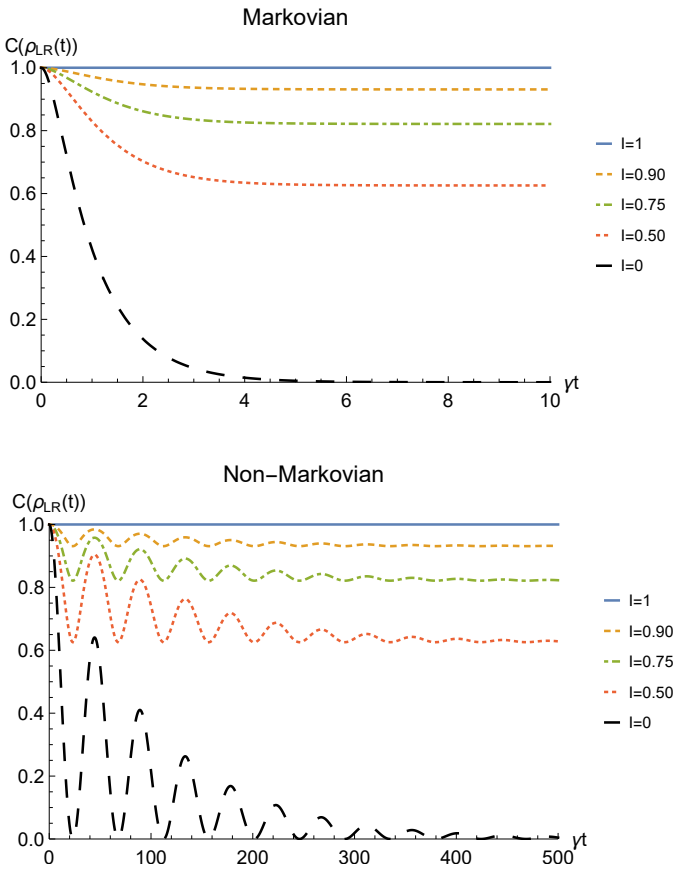

Figure 4.6: Concurrence of two identical qubits (fermions with real $l, l', r, r' > 0$, bosons with one of these four coefficients negative) in the initial state $|1_-\rangle_{\rm AB}$ interacting with localized phase damping channels, undergoing an instantaneous deformation+sLOCC operation at time t for different degrees of spatial indistinguishability $\mathcal{I}$ (with $|l| = |r'|$). Both the Markovian ($\lambda = 5\gamma$) (upper panel) and non-Markovian ($\lambda = 0.01\gamma$) (lower panel) regimes are reported.

Furthermore, when the indistinguishability is maximum ($\mathcal{I} = 1$, blue solid line) quantum correlations after the sLOCC measurement result to be completely immune to the action of the noisy environment and maintain their initial value. Is is important to highlight that the existence of such a steady value for the entanglement of identical particles is only due to the spatial indistinguishability of the qubits and to the procedure used to produce the entangled state, i.e. the sLOCC operation. This result clearly shows that spatial indistinguishability of identical qubits can be exploited to recover quantum correlations spoiled by the detrimental noise of a phase damping-like environment interacting independently with the constituents, as shown in Figure 4.7.

Finally, the success (sLOCC) probability of obtaining the outcome $\rho_{\rm LR}(t)$ for two identical qubits undergoing local phase damping channels is

$$P_{\rm LR}(t) = \frac{(lr')^2 + (l'r)^2 - 2\eta\, ll'rr'\Big(1 - p(t)\Big)}{\Big(1 - \frac{1}{2}p(t)\Big)C_1^2 + \frac{1}{2}p(t)C_2^2}. \tag{4.42}$$

Figure 4.8 depicts the behavior of the sLOCC probability of success (4.7) for fermions (with real and positive coefficients of the spatial wave functions) for different values of $\mathcal{I}$.

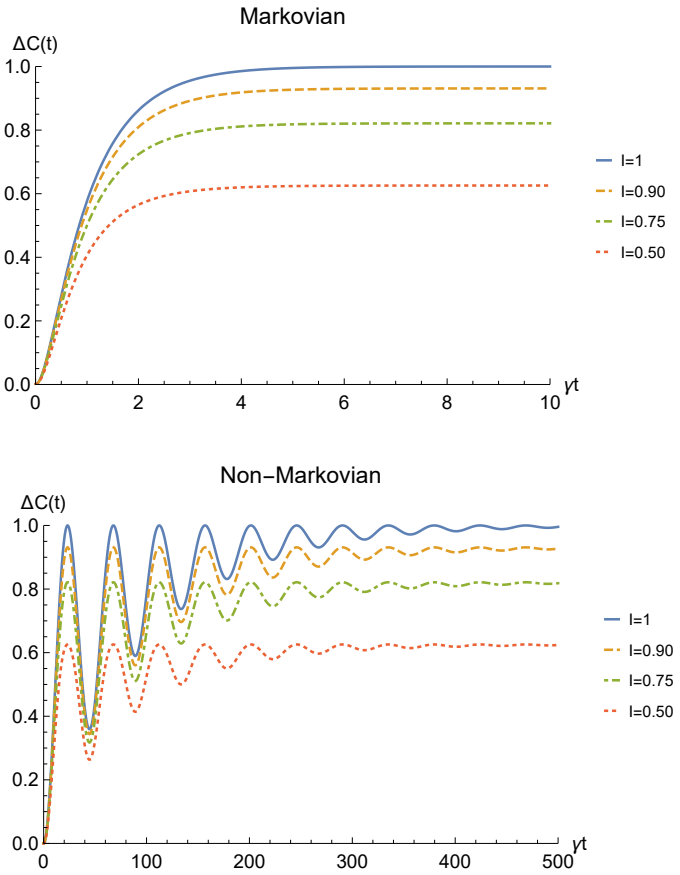

Figure 4.7: Net gain in the entanglement recovery of two identical qubits (fermions with real $l, l', r, r' > 0$, bosons with one of these four coefficients negative) in the initial state $|1_-\rangle_{\rm AB}$ under localized phase damping channels, thanks to the deformation+sLOCC operation performed at time t. Results are reported for different degrees of spatial indistinguishability $\mathcal{I}$ (with $|l| = |r'|$). Both the Markovian ($\lambda = 5\gamma$) (upper panel) and non-Markovian ($\lambda = 0.01\gamma$) (lower panel) regimes are shown.

Once again, there is a trade-off between the probability of success and the concurrence, with $P_{\rm LR}(t) = 1$ when the particles are distinguishable (black dashed line) and $P_{\rm LR} = 1/2$ for perfectly indistinguishable qubits (blue solid line). A similar general behavior is found for bosons (with the constraint $l = r' = l' = -r$), having $P_{\rm LR}(t) = 1 - p(t)/2$ in the case of maximal indistinguishability $\mathcal{I} = 1$.

The same general relation between concurrence and spatial indistinguishability is found also for the fidelity between the initial state $\tau = |1_-\rangle_{\rm LR}\langle 1_-|_{\rm LR}$ and the final one (4.38), displayed in Fig. 4.9 for both the Markovian and the non-Markovian regime.

Notice that, differently from the amplitude damping scenario, this time the fidelity does not vanish but it reaches an asymptotic value which increases with the indistinguishability, starting from $F = 1$ for distinguishable particles ($\mathcal{I} = 0$, black dashed line) and reaching the maximum value $F = 1$ when $\mathcal{I} = 1$ (solid blue line).

4.3.3 Depolarizing Channel

In this section we reconsider and expand the results on entanglement protection at the preparation stage presented in Ref. [2].

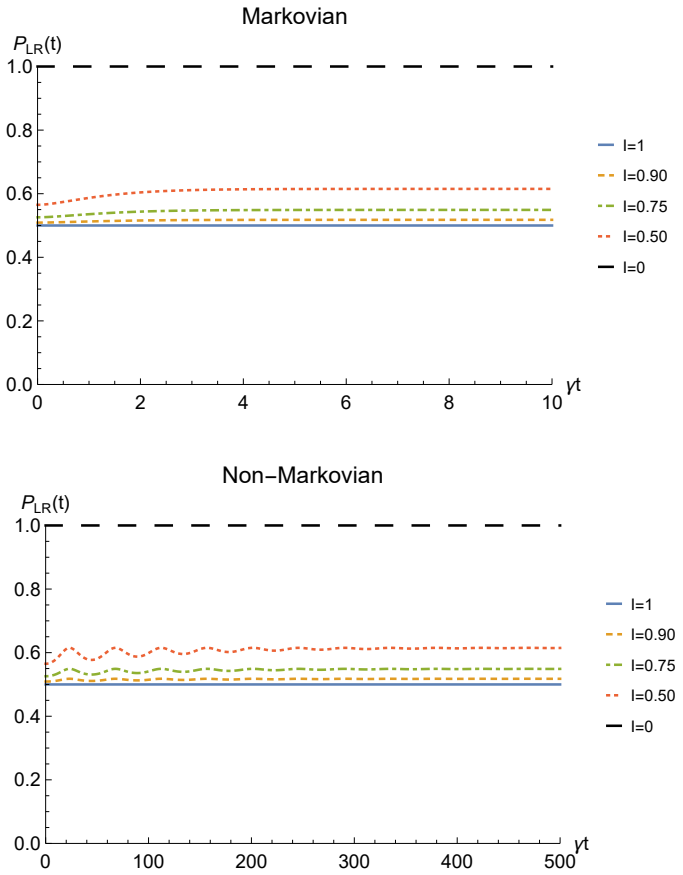

Figure 4.8: Probability of obtaining a non-zero outcome from the sLOCC projection for fermions (with real $l, l', r, r' > 0$ and $l = r'$) interacting with localized phase damping channels. Different degrees of spatial indistinguishability are reported in both the Markovian ($\lambda = 5\gamma$) (upper panel) and non-Markovian ($\lambda = 0.01\gamma$) (lower panel) regimes.

The depolarizing channel describes the process where a system undergoes a symmetric decoherence. This can occur, for example, during the scattering of randomly polarized photons, the isotropic interaction of qubits with their environment, or even in Bose-Einstein condensates.

A depolarizing channel acting on a system of two qubits has the effect of leaving it untouched with probability $1 - p(t)$ and of introducing a white noise which drives it into the maximally mixed state with probability $p(t)$. This is, for instance, a typical noise occurring when quantum states are initialized. Supposing once again that our system of two identical particles is initially in the Bell state $|1_-\rangle_{\rm AB}$, it is well known that this kind of noisy interaction produces the Werner state [32]

$$\rho_{\rm AB}(t) = W^{-}_{\rm AB}(t) := \Big(1 - p(t)\Big)\, |1_-\rangle_{\rm AB}\, \langle 1_-|_{\rm AB} + \frac{1}{4}\, p(t)\, \mathbb{1}, \tag{4.43}$$

where $\mathbb{1}$ is the 4×4 identity operator. Hereafter, we work for convenience on the Bell states basis

$$\mathcal{B}_B = \{|1_+\rangle_{\rm AB}\,, |1_-\rangle_{\rm AB}\,, |2_+\rangle_{\rm AB}\,, |2_-\rangle_{\rm AB}\},$$

where $|1_+\rangle_{\rm AB}\,, |1_-\rangle_{\rm AB}$ have been previously defined respectively in (4.19) and (4.34), while

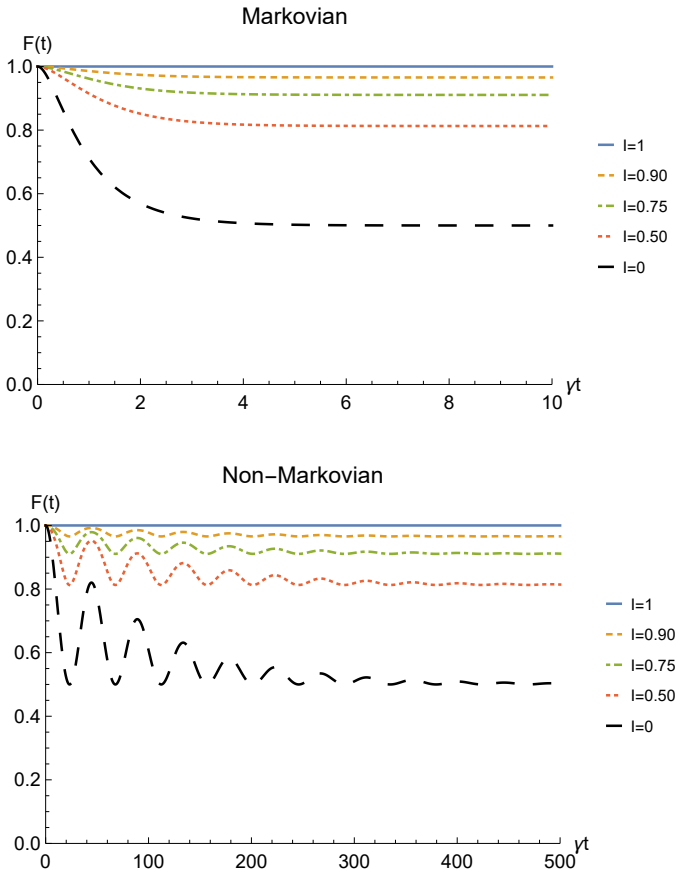

Figure 4.9: Fidelity of two identical qubits (fermions with real $l, l', r, r' > 0$) interacting with localized phase damping channels, computed between the initial state $|1_-\rangle_{\rm LR}\langle 1_-|_{\rm LR}$ and the state produced by an instantaneous deformation+sLOCC operation at time t for different degrees of spatial indistinguishability $\mathcal{I}$ (with $|l| = |r'|$). Both the Markovian ($\lambda = 5\gamma$) (upper panel) and non-Markovian ($\lambda = 0.01\gamma$) (lower panel) regimes are reported.

$|2_+\rangle_{\rm AB}$ and $|2_-\rangle_{\rm AB}$ are given by

$$\begin{aligned} |2_+\rangle_{\rm AB} &= \frac{1}{\sqrt{2}}\Big(|A\uparrow, B\uparrow\rangle + |A\downarrow, B\downarrow\rangle \Big), \\ |2_-\rangle_{\rm AB} &= \frac{1}{\sqrt{2}}\Big(|A\uparrow, B\uparrow\rangle - |A\downarrow, B\downarrow\rangle \Big). \end{aligned} \tag{4.44}$$

We recall that since such basis is orthonormal, the identity operator can be written as

$$\mathbb{1} = \sum_{\substack{j=1,2 \\ s=\uparrow,\downarrow}} |j_s\rangle_{\rm AB}\langle j_s|_{\rm AB}\,.$$

At time t we deform the two qubits wave functions. The deformation of states $|1_+\rangle_{\rm AB}$ and $|1_-\rangle_{\rm AB}$ has already been discussed in (4.35) and (4.22), while states $|2_+\rangle_{\rm AB}$ and $|2_-\rangle_{\rm AB}$ get mapped respectively to

$$|\bar{2}_+\rangle_D = C_2\,|\bar{2}_+\rangle_N\,, \quad |\bar{2}_-\rangle_D = C_2\,|\bar{2}_-\rangle_N\,, \tag{4.45}$$

where $\langle\bar{2}_+|\bar{2}_+\rangle_N = \langle\bar{2}_-|\bar{2}_-\rangle_N = 1$ and C_2 is defined in (4.25). The result of the deformation of state (4.43) is thus the deformed Werner state of two indistinguishable qubits $\rho_D(t) =$

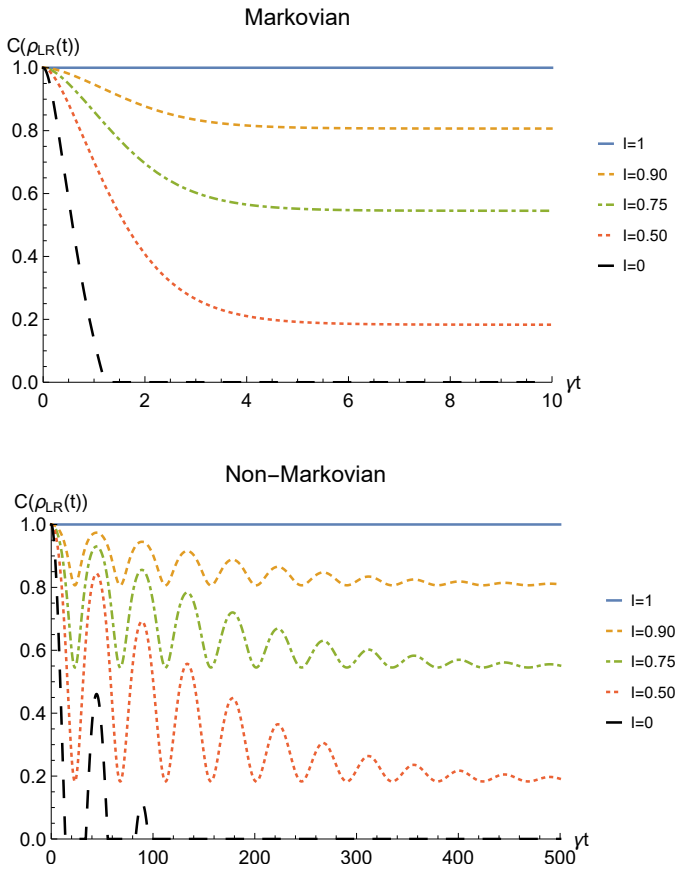

Figure 4.10: Concurrence of two identical qubits (fermions with real $l, l', r, r' > 0$, bosons with one of these four coefficients negative) in the initial state $|1_-\rangle_{\rm AB}$ subjected to localized depolarizing channels, undergoing an instantaneous deformation+sLOCC operation at time t for different degrees of spatial indistinguishability $\mathcal{I}$ (with $|l| = |r'|$). Both Markovian ($\lambda = 5\gamma$) (upper panel) and non-Markovian ($\lambda = 0.01\gamma$) (lower panel) regimes are reported.

$\bar{W}_D^-(t)$ [2], where

$$\begin{aligned}\bar{W}_D^-(t) := \Big[&\Big(1-\frac{3}{4}p(t)\Big)\,C_1^2\;|\bar{1}_-\rangle_N\,\langle\bar{1}_-|_N \\ &+ C_2^2\;\frac{1}{4}\,p(t)\,\Big(|\bar{1}_+\rangle_N\,\langle\bar{1}_+|_N + |\bar{2}_+\rangle_N\,\langle\bar{2}_+|_N + |\bar{2}_-\rangle_N\,\langle\bar{2}_-|_N\Big)\Big] \\ &/\Big[1-\eta\,|\langle\psi_1|\psi_2\rangle|^2\Big(1-\frac{3}{2}\,p(t)\Big)\Big]\,.\end{aligned} \tag{4.46}$$

To perform the final sLOCC measurement we assume that $|\psi_1\rangle\,,\,|\psi_2\rangle$ have the usual structure given in Eq. (4.10). Applying the projection operator on the state (4.46) as

defined in Eq. (4.6) we get

$$\begin{aligned}\rho_{\rm LR}(t) = \Bigg[&\Big(1-\frac{3}{4}\,p(t)\Big)\,|lr'-\eta\,l'r|^2\,|1_-\rangle_{\rm LR}\,\langle 1_-|_{\rm LR}\\ &+\frac{1}{4}\,p(t)\,|lr'+\eta\,l'r|^2\Big(\,|1_+\rangle_{\rm LR}\,\langle 1_+|_{\rm LR}+|2_+\rangle_{\rm LR}\,\langle 2_+|_{\rm LR}+|2_-\rangle_{\rm LR}\,\langle 2_-|_{\rm LR}\,\Big)\Bigg]\\ /&\left[\Big(1-\frac{3}{4}\,p(t)\Big)|lr'-\eta\,l'r|^2+\frac{3}{4}\,p(t)\,|lr'+\eta\,l'r|^2\right].\end{aligned}\tag{4.47}$$

Before computing the concurrence we notice that, as for the phase damping channel, the state of Eq. (4.47) is real and diagonal on the Bell states basis, thus being invariant under the localized action of the Pauli matrices $\sigma_y^L\otimes\sigma_y^R$. Therefore, the concurrence is evaluated in terms of the four eigenvalues of $\rho_{\rm LR}(t)$, namely

$$\begin{aligned}\lambda_A(t) &= \frac{\Big(1-\frac{3}{4}\,p(t)\Big)|lr'-\eta\,l'r|^2}{\Big(1-\frac{3}{4}\,p(t)\Big)|lr'-\eta\,l'r|^2+\frac{3}{4}\,p(t)\,|lr'+\eta\,l'r|^2},\\ \lambda_B(t)=\lambda_C(t)=\lambda_D(t) &= \frac{\frac{1}{4}\,p(t)\,|lr'+\eta\,l'r|^2}{\Big(1-\frac{3}{4}\,p(t)\Big)|lr'-\eta\,l'r|^2+\frac{3}{4}\,p(t)\,|lr'+\eta\,l'r|^2}.\end{aligned}$$

Considering once again fermions with real and positive coefficients l, r, l', r', the concurrence has the expression

$$C\big(\rho_{\rm LR}(t)\big) = \max\left\{0,\ \frac{\Big(1-\frac{3}{2}\,p(t)\Big)\Big[(lr')^2+(l'r)^2\Big]+2ll'rr'}{(lr')^2+(l'r)^2+\Big(1-\frac{3}{2}\,p(t)\Big)2ll'rr'}\right\}.\tag{4.48}$$

Figure 4.10 shows the time behavior of entanglement quantified by Eq. (4.48), while Figure 4.11 depicts $\Delta C(t)$. First of all, we emphasize that, differently from the amplitude damping channel and the phase damping channel, a sudden death phenomenon occurs when no deformation and sLOCC are performed: indeed, when $\mathcal{I}=0$ (black dashed line) the entanglement vanishes at the finite time $\widetilde{t}$ such that $p(\widetilde{t})=2/3$. However, when $0<\mathcal{I}<1$, the state emerging from the sLOCC procedure recovers an amount of entanglement which decreases monotonically with t in the Markovian regime and periodically in the non-Markovian regime. Nonetheless, as in the phase damping case, such decrease approaches a constant value given by

$$C_\infty = \max\left\{0,\ -\frac{(lr')^2+(l'r)^2-4\,ll'rr'}{2\big[(lr')^2+(l'r)^2-ll'rr'\big]}\right\}.\tag{4.49}$$

Furthermore, we notice once again that when the maximum spatial indistinguishability ($\mathcal{I}=1$, blue solid line) is achieved, our procedure allows for a complete entanglement recovery independently on t.

As a further quantity of interest we obtain the sLOCC probability of success, defined in Eq. (4.7), for two identical qubits whose correlations have been spoiled by a local depolarizing channel, that is

$$P_{\rm LR}(t) = \frac{(lr')^2+(l'r)^2-2\eta\,ll'rr'\Big(1-\frac{3}{2}\,p(t)\Big)}{1-\eta\Big[(ll')^2+(rr')^2+2ll'rr'\Big]\Big(1-\frac{3}{2}\,p(t)\Big)}.\tag{4.50}$$

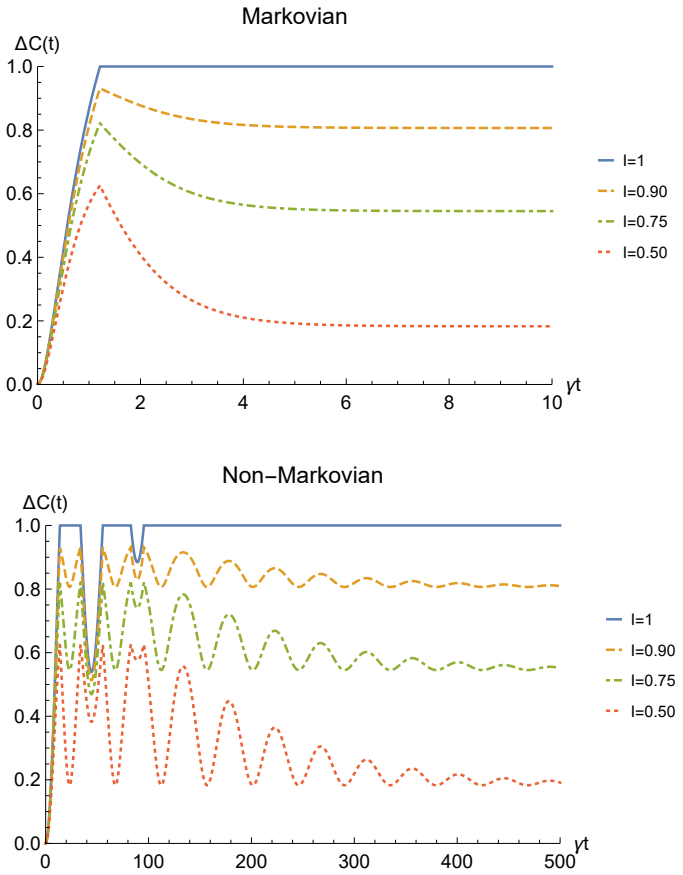

Figure 4.11: Net gain in the entanglement recovery of two identical qubits (fermions with real $l, l', r, r' > 0$, bosons with one of these four coefficients negative) in the initial state $|1_-\rangle_{\rm AB}$ interacting with a depolarizing channel, thanks to the deformation+sLOCC operation performed at time t. Results are reported for different degrees of spatial indistinguishability $\mathcal{I}$ (with $|l| = |r'|$). Both the Markovian ($\lambda = 5\gamma$) (upper panel) and non-Markovian ($\lambda = 0.01\gamma$) (lower panel) regimes are shown.

In Figure 4.12, $P_{\rm LR}(t)$ is plotted in the case of two fermions (with real and positive coefficients and $l = r'$) for different degrees of spatial indistinguishability. Again, as expected, a trade-off exists between the probability of success and the concurrence, with the higher probability achieved when the qubits are perfectly distinguishable. Nonetheless, as happens in the previous channels, such probability reaches a stationary value which decreases as the indistinguishability increases, with $P_{\rm LR} = 1/2$ as the minimum value when $\mathcal{I} = 1$ (blue solid line). For bosons, a similar behavior is found (with the constraint $l = r' = l' = -r$), having $P_{\rm LR}(t) = 1 - 3p(t)/4$ when $\mathcal{I} = 1$ [2].

Finally, we show in Fig. 4.13 the fidelity between the initial state $\tau = |1_-\rangle_{\rm LR}\langle 1_-|_{\rm LR}$ and the final one (4.47), for fermions with real and positive coefficients and different degrees of spatial indistinguishability. Once again, spatial indistinguishability is found to be directly influencing the fidelity, with a general behaviour identical to the one emerged for the phase damping channel (Fig.tilde4.9). Nonetheless, the asymptotic value reached for distinguishable particles in this scenario is $F = 1/4$ ($\mathcal{I} = 0$, black dashed line), thus placing between the two other channels considered in this work.

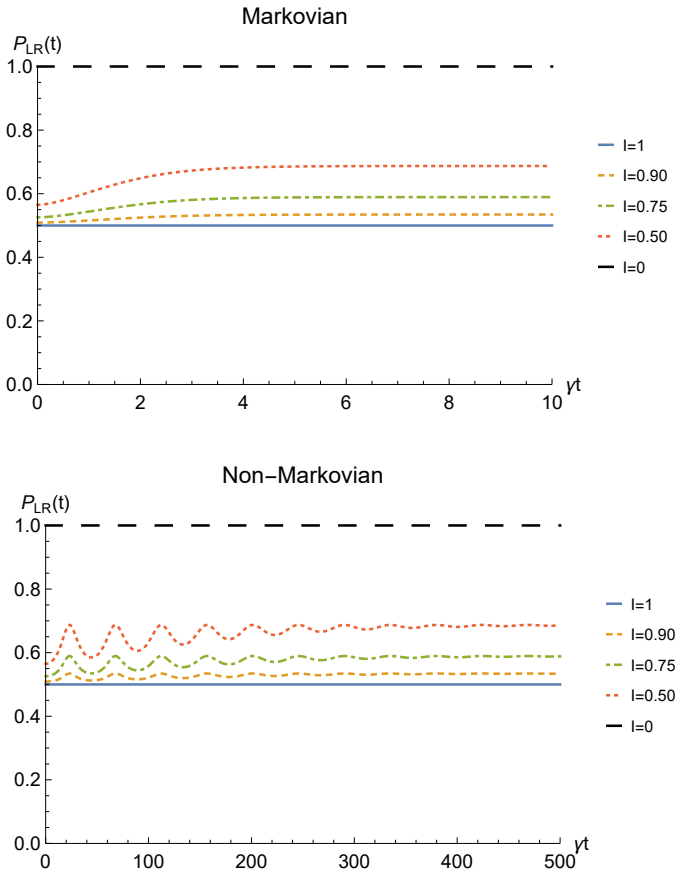

Figure 4.12: Probability of obtaining a nonzero outcome from the sLOCC projection for fermions with real and positive coefficients ($l = r'$) under a depolarizing channel. Different degrees of spatial indistinguishability $\mathcal{I}$ are reported in both Markovian ($\lambda = 5\gamma$) (upper panel) and non-Markovian ($\lambda = 0.01\gamma$) (lower panel) regimes.

4.4 Discussion

In this paper we have shown that spatially localized operations and classical communication (sLOCC) provide an operational framework to successfully recover the quantum correlations between two identical qubits spoiled by the independent interaction with two noisy environments. The performance of such procedure is found to be strictly dependent on the degree of spatial indistinguishability reached by the spatial deformation of the particles wave functions. A general behavior has emerged: the higher is the degree of spatial indistinguishability, the better is the efficacy of the protocol, quantified by the difference between the amount of entanglement present at time t with and without the application of our procedure. In particular, when the two particles are brought to perfectly overlap and the maximum degree of indistinguishability is achieved, the initial (maximum) amount of entanglement is completely recovered in all the considered scenarios, independently on how long the qubits have been interacting with the detrimental environment.

If the indistinguishability is not maximum, instead, our results show that for an amplitude damping channel-like environment the entanglement after the sLOCC drops to zero after a short interaction time; nonetheless, the interval of time where the amount of recovered entanglement is significant increases with the indistinguishability in both the Markovian and the non-Markovian regimes. When the environment acts as a phase

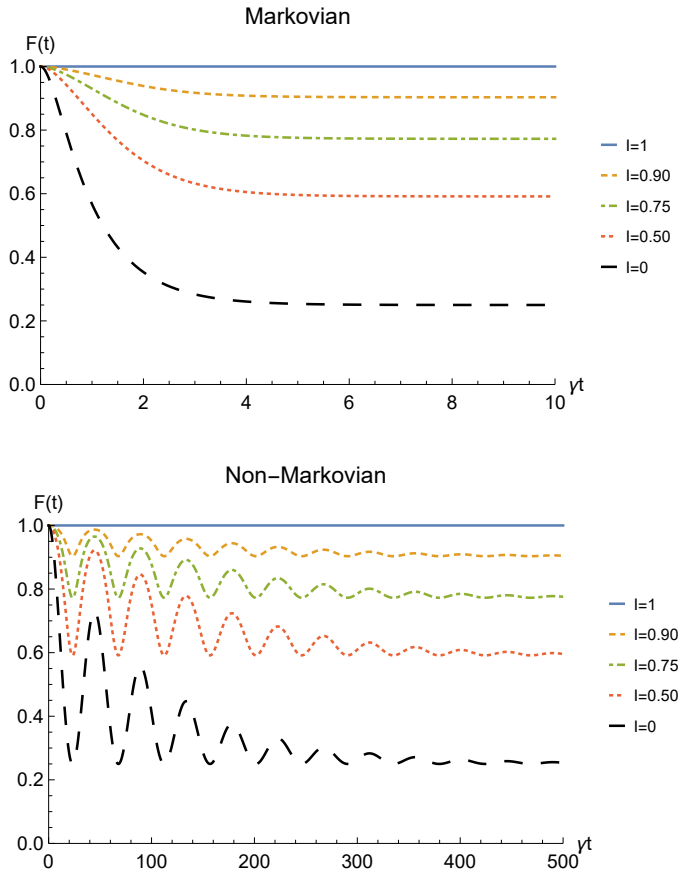

Figure 4.13: Fidelity of two identical qubits (fermions with real $l, l', r, r' > 0$) subjected to localized depolarizing channels, computed between the initial state $|1_-\rangle_{\rm LR}\langle 1_-|_{\rm LR}$ and the state produced by an instantaneous deformation+sLOCC operation at time t for different degrees of spatial indistinguishability $\mathcal{I}$ (with $|l| = |r'|$). Both the Markovian ($\lambda = 5\gamma$) (upper panel) and non-Markovian ($\lambda = 0.01\gamma$) (lower panel) regimes are reported.

damping channel, instead, the recovered correlations are always nonzero and our protocol provides an exploitable resource independently on the interaction time (stationary entanglement). This behavior also holds in the depolarizing channel scenario, where the *deformation+sLOCC protocol* achieves a special usefulness since it allows to recover quantum correlations destroyed at finite time by a sudden death phenomena.

Then same behaviour is found also for the fidelity between the initial pure state and the one produced by the *deformation+sLOCC protocol*: when the indistinguishability is maximum, such quantity maintains its maximum value constant. When $\mathcal{I} < 1$, instead, it drops to zero faster as the indistinguishability decreases for an amplitude damping-like environment, while it reaches a constant value which grows with the indistinguishability when a phase damping channel or a depolarizing channel are considered. Nonetheless, we want to stress that

We point out that the results reported in Figs. 4.2, 4.6, 4.10 show a similar behavior to the ones discussed in Ref. [36] (for a Markovian regime) where, in contrast to the present analysis, the system-environment interaction occurs between the deformation bringing the particles to spatially overlap and the final sLOCC measurements. Nonetheless, the decay rate is much larger in the situation considered here: the sLOCC operational framework for entanglement recovery performs better when the environment is not able to distin-

guish the particle it is interacting with, as happens in Ref. [36]. Despite this, our protocol deals with a different physical context: indeed, it expressly refers to the scenario where we are given a two identical particle entangled state which got spoiled by the environment in a situation where the particles remain distinguishable. Furthermore, in a real world application it is likely that the system-environment interaction will occur both before the (spatial) deformation and between the deformation and the sLOCC. Therefore, an interesting possible prospect of this work would be to investigate the general open quantum system framework provided in Ref. [36] when applied to noisy initial states such as those given in Eqs. (4.21), (4.33), and (4.43).

Our results can apply to all the physical systems undergoing the noisy interactions discussed in Section 4.3, e.g. Bose-Einstein condensates, cavity QED systems, and quantum photonics, once we are experimentally able to implement the deformation + sLOCC procedure. Among these scenarios, quantum photonics is most likely the best candidate for a first experimental verification of our results; indeed, in [1] the authors have managed to experimentally apply the deformation + sLOCC protocol to a pair of photons in a tunable way using a simple optical setup. We strongly believe that such setup could be used as a starting point to validate the results discussed in this paper, where the implementation of simulated noisy environments is a task which can be easily achieved using linear optics devices.

Our findings ultimately provide further insights about protection techniques of entangled states from the detrimental effects of surrounding environments by suitably manipulating the inherent indistinguishability of identical particle systems.

Chapter 5

Spatial indistinguishability and interference: unveiling the connection

In this original chapter, we discuss an issue arising when applying the definition of spatial indistinguishability and the related entropic measure to systems subjected to deformations giving rise to interferometric effects. After investigating the origin of the problem, we propose a solution which shifts the focus from the no which-way information to the no which-spin information introduced in Subsection 1.3.1.

5.1 Identifying the issue

We have seen in the previous chapters that we can generate spatial indistinguishability between initially distinguishable identical particles by acting on them with deformations taking their wave functions to spatially overlap over detection regions. In Chapters 1, 2, 3, 4, we have focused on a specific deformation D taking two particles localized in two distinct regions A and B to spatially overlap over two distinct regions L and R, that is,

$$\begin{aligned} |A\rangle &\xrightarrow{D} |\psi\rangle = l\,|L\rangle + r\,|R\rangle\,, \\ |B\rangle &\xrightarrow{D} |\psi'\rangle = l'\,|L\rangle + r'\,|R\rangle\,, \end{aligned} \tag{5.1}$$

where l, l', r, r' are complex coefficients such that $|l|^2 + |r|^2 = |l'|^2 + |r'|^2 = 1$. We have quantified the induced no which-way information by the entropic measure of indistinguishability

$$\mathcal{I} = -\frac{P_{\rm L}P'_{\rm R}}{P_{\rm L}P'_{\rm R} + P'_{\rm L}P_{\rm R}} \log_2 \frac{P_{\rm L}P'_{\rm R}}{P_{\rm L}P'_{\rm R} + P'_{\rm L}P_{\rm R}} - \frac{P'_{\rm L}P_{\rm R}}{P_{\rm L}P'_{\rm R} + P'_{\rm L}P_{\rm R}} \log_2 \frac{P'_{\rm L}P_{\rm R}}{P_{\rm L}P'_{\rm R} + P'_{\rm L}P_{\rm R}}, \tag{5.2}$$

where $P_{\rm L} = |l|^2 = |\langle L|\psi\rangle|^2$, $P'_{\rm L} = |l'|^2 = |\langle L|\psi'\rangle|^2$, $P_{\rm R} = |r|^2 = |\langle R|\psi\rangle|^2$, $P'_{\rm R} := |r'|^2 = |\langle R|\psi'\rangle|^2$, and $P_{\rm L} + P_{\rm R} = P'_{\rm L} + P'_{\rm R} = 1$. This quantity thus accounts for the individual probability amplitudes of the two constituents to be found in each region. However, the assessment of the no which-way information in terms of Eq. (5.2) is flawed. To see this, consider the singlet state of two spatially separated bosonic qubits localized on A and B, that is $|1_-\rangle_{\rm AB} = \frac{1}{\sqrt{2}}(|A\uparrow, B\downarrow\rangle - |A\downarrow, B\uparrow\rangle)$, and let us act on it with the deformation of Eq. (5.1). This scenario corresponds to the one considered in Refs. [2,37], discussed, respectively, in Subsection 1.3.4 and Chapter 4. Some terms in the resulting state $|\Psi^{(2)}\rangle_D = (|\psi\uparrow, \psi'\downarrow\rangle - |\psi\downarrow, \psi'\uparrow\rangle)/\sqrt{2}$ interfere destructively, finally returning the

state $|\Psi^{(2)}\rangle_{\rm LR} = (|L\uparrow, R\downarrow\rangle - |L\downarrow, R\uparrow\rangle)/\sqrt{2}$. Taking the input modes to coincide with the output ones A=L, B=R, we thus conclude that *the bosonic singlet state is invariant under the action of the deformation* D of Eq. (5.1):

$$|1_-\rangle_{\rm LR} \xrightarrow{D} |1_-\rangle_{\rm LR}\,. \tag{5.3}$$

This observation raises a problem: we assumed the two constituents to be spatially distinguishable ($\mathcal{I} = 0$) before the application of D, whereas they are deemed spatially indistinguishable afterwards by the definition given in Subsection 1.2.5 ($\mathcal{I} > 0$). However, the state is not changed by the deformation. The issue acquires more relevance when we notice that the invariance of the singlet state under D holds for any l, l', r, r', including the scenario $l = l' = r = -r' = 1/\sqrt{2}$ where the deformation D coincides with the unitary action of a balanced beam splitter generating the maximum degree of indistinguishability $\mathcal{I} = 1$ according to Eq. (5.2). Spatial indistinguishability as defined in Chapter 1 and the entropic measure of no which-way information of Eq. (5.2) are thus, in general, not state-dependent: given a bosonic singlet state without further information on its dynamical history, it is not possible to discriminate whether it describes two spatially localized and separated qubits or two delocalized, spatially overlapped ones after interference. As a consequence, it is not possible to evaluate the indistinguishability of the involved particles and the associated $\mathcal{I}$. Notice that the same problem holds for the fermionic state $|L\uparrow, R\uparrow\rangle$, which remains invariant under the action of a balanced beam splitter (fermionic anti-bunching). In contrast, no problem arises when dealing with the deformation of the state $|A\uparrow, B\downarrow\rangle$, which in Subsection 1.3.2 we shown to return

$$|\Psi^{(2)}\rangle_D = ll'\,|L\uparrow, L\downarrow\rangle + rr'\,|R\uparrow, R\downarrow\rangle + lr'\,|L\uparrow, R\downarrow\rangle + l'r\,|R\uparrow, L\downarrow\rangle\,.$$

$|\Psi^{(2)}\rangle_D$ is always different from the initial state as long as $\mathcal{I} \neq 0$, with its entanglement directly depending on the coefficients l, l', r, r' and thus on $\mathcal{I}$, found, e.g., in Refs. [20, 59] (see the discussion reported, respectively, in Subsection 1.3.2 and Chapter 3).

It is therefore crucial to investigate the origin of the problem in order to provide an interpretation of the indistinguishability of identical particles which is state-dependent, encompassing the distinction between the deformation of states such as the bosonic singlet $|1_-\rangle_{\rm AB}$, the fermionic $|A\uparrow, B\uparrow\rangle$, or the generic $|A\uparrow, B\downarrow\rangle$.

5.2 Origin of the problem

In Subsection 1.2.5 we have defined spatial indistinguishability as the property of identical particles to have a nonzero probability to be individually found in a same detection region. Here, the word *individually* is crucial and was introduced in reference to the no which-particle and no which-way information scenarios where the possibility for more than one constituent to individually trigger one detector does not allow to discriminate and assign an identity to the detected particle (see Subsection 1.3.1). However, what actually determines the outcomes of the detection process are not the single-particle probability amplitudes (as the ones encoded in the probabilities $P_{\rm L}$, $P_{\rm R}$, $P'_{\rm L}$, $P'_{\rm R}$ of Eq. (5.2)), but the *many-body probability amplitudes*. Interference effects peculiar of identical particles lead to the cancellation of terms in the global probability amplitude, eliminating the contribution of some of the products of the single-particle probability amplitudes. The result is that *the individuality of the single constituents can get lost* in the measurable collective effect: the two particles emerging from the deformation of Eq. (5.3) can be thought of as either the

same input particles delocalized on L and R or two new particles localized one on L and one on R. It is therefore evident how the problem stems from the particle interpretation of quantum mechanics provided by the first quantization approach, an issue which the second quantization approach tackles by allowing for particles to be created and annihilated. It follows that concepts which are strictly related to particles' individuality, such as no which-particle/way information, spatial indistinguishability, and entropic measure $\mathcal{I}$, become flawed in the presence of interference. Crucially, interference effects explain the difficulties in addressing the spatial indistinguishability of identical particles after the deformation of the bosonic state $|1_-\rangle_{\mathrm{AB}}$ and the fermionic state $|A\uparrow, B\uparrow\rangle$, whereas the same issue does not affect $|A\uparrow, B\downarrow\rangle$, whose deformation does not cause interference.

5.3 A possible solution: addressing no which-spin information

Given the issue discussed above, how can we interpret the concepts of spatial indistinguishability and the related entropic measure of no which-way information $\mathcal{I}$ previously introduced? Since they happen to be state-independent in interferometric scenarios, a natural conclusion is that *they must be meant as concepts related to the dynamical evolution of the system and thus characterizing the deformation D rather than the resulting state, about which they may or may not carry information.* However, the given definition of indistinguishability and the related entropic measure can be slightly modified to recover their heuristic meaning of *uncertainty at the detection stage* while making them state-dependent and relevant for the system evolution. To do so, we must avoid to associate indistinguishability to the identity of a particle, as the information about it can get lost in the interference. Instead, we should associate it to some specific measurement outcome, whose probability can always be retrieved by the state itself. Similarly, we must remove the dependence on ψ and ψ' from $\mathcal{I}$. We accomplish this goal by binding the particle detected on each region to its unmeasured internal degree of freedom: instead of expressing uncertainty about the single-particle spatial wave function of the detected constituent, we therefore express uncertainty about its spin state. Let us consider two identical qubits in the global state $|\Psi^{(2)}\rangle$ and the arbitrarily chosen spin basis $\mathcal{B}_{\uparrow,\downarrow} = \{|\uparrow\rangle, |\downarrow\rangle\}$. We introduce the state-dependent entropic measure of indistinguishability of the two particles with respect to two detectors localized or regions L and R and to basis $\mathcal{B}_{\uparrow,\downarrow}$ as

$$\widetilde{\mathcal{I}} = -\frac{P_{\mathrm{L}\uparrow\mathrm{R}\downarrow}}{P_{\mathrm{L}\uparrow\mathrm{R}\downarrow}+P_{\mathrm{L}\downarrow\mathrm{R}\uparrow}}\log_2\frac{P_{\mathrm{L}\uparrow\mathrm{R}\downarrow}}{P_{\mathrm{L}\uparrow\mathrm{R}\downarrow}+P_{\mathrm{L}\downarrow\mathrm{R}\uparrow}} - \frac{P_{\mathrm{L}\downarrow\mathrm{R}\uparrow}}{P_{\mathrm{L}\uparrow\mathrm{R}\downarrow}+P_{\mathrm{L}\downarrow\mathrm{R}\uparrow}}\log_2\frac{P_{\mathrm{L}\downarrow\mathrm{R}\uparrow}}{P_{\mathrm{L}\uparrow\mathrm{R}\downarrow}+P_{\mathrm{L}\downarrow\mathrm{R}\uparrow}}, \qquad (5.4)$$

where $P_{\mathrm{L}\sigma\mathrm{R}\tau} = |\langle L\sigma, R\tau|\Psi^{(2)}\rangle|^2$, $\sigma,\tau = \uparrow,\downarrow$. The probabilities $P_{\mathrm{L}\uparrow\mathrm{R}\downarrow}$, $P_{\mathrm{L}\downarrow\mathrm{R}\uparrow}$ are given by the squared modulus of two-particle probability amplitudes in the global state and are thus exempt from the problems affecting the definition based on an individual-particle viewpoint.

Recalling Subsection 1.3.1, we notice that $\widetilde{\mathcal{I}}$ *addresses the no which-spin information instead of the no which-particle/way information.* We have previously shown that no which-spin information can be induced by generating no which-particle information between constituents in definite, orthogonal spin states (Figs. 1.2**(e)**,**(f)**). This is the case emerging, for example, from the deformation of state $|A\uparrow, B\downarrow\rangle$. In this case, where no interference effect occurs, the new indistinguishability measure of Eq. (5.4) coincides with the old one of Eq. (5.2). However, let us consider the bosonic singlet state $|1_-\rangle_{\mathrm{AB}}$:

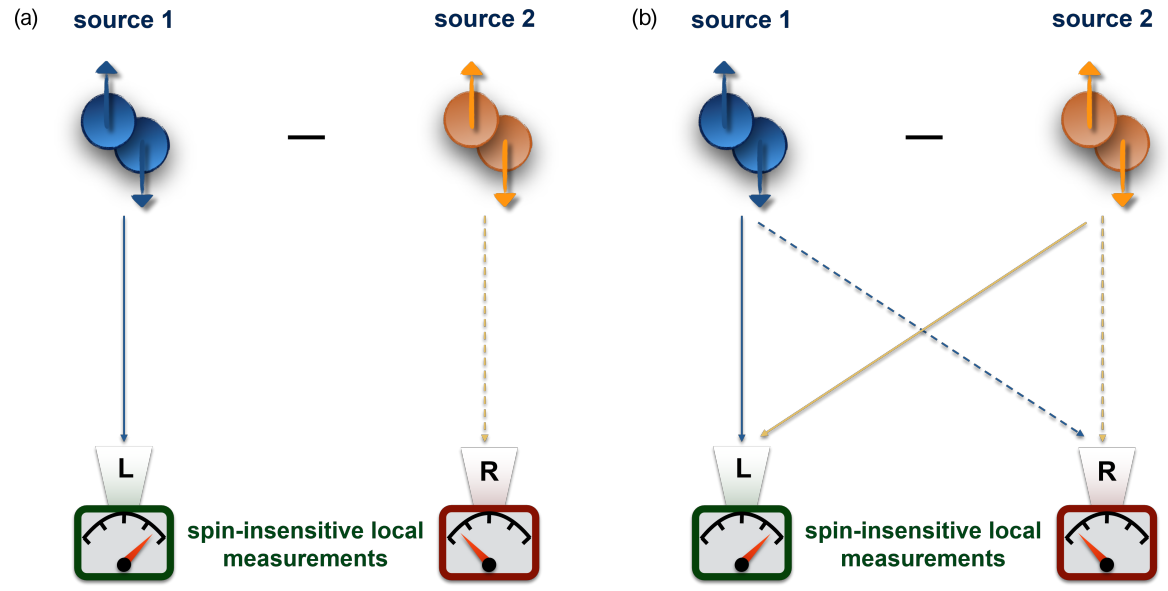

Figure 5.1: Detection of a bosonic singlet state $|1_-\rangle_{\mathrm{LR}}$ of **(a)** two spatially distinguishable qubits (absence of no which-particle and no which-way information), and of **(b)** two spatially indistinguishable ones (presence of no which-particle and no which-way information generated by a deformation). No which-spin information is present in both cases.

here the two constituents are in orthogonal but *undefined* spin states, as both can be in either $|\uparrow\rangle$ or $|\downarrow\rangle$, and the new indistinguishability measure returns $\widetilde{\mathcal{I}} = 1$. While the no which-particle/way information depend on the spatial overlap of the single-particle wave functions ψ, ψ', the no which-spin information in state $|1_-\rangle_{\mathrm{AB}}$ and the related ignorance probed by $\widetilde{\mathcal{I}}$ are here due to the entangled structure of the singlet state. We therefore conclude that there can be no which-spin information even in unambiguous settings where the detected particles and their origin can be uniquely identified, such as when two particles in a singlet state have been generated and confined in two distinct laboratories[1] (see Fig. 5.1**(a)**).

We now highlight the relation between the indistinguishability $\widetilde{\mathcal{I}}$ of two identical particles and their detector-level entanglement (see Section 1.2). The no which-spin information is responsible for the presence of entanglement in the state resulting from the sLOCC coincidence measurement, as the ignorance about the internal state of the particles probed by $\widetilde{\mathcal{I}}$ is reflected in the presence of quantum correlations in the postselected state. Notice that this point of view also clarifies why the deformation and sLOCC projection of particles prepared in the same known internal state does not lead to entangled states despite the presence of no which-way information, as the spin of the constituents remains perfectly determined after the detection (see Fig. 1.2**(b)**,**(c)**). Within this picture, the *generation of spatial overlap*, leading to ambiguous settings and creating no which-particle/way information, emerges clearly as *one possible way to establish no which-spin information and thus to activate quantum correlations within IP systems.*

As a possible future direction, it would be interesting to deeply investigate the relation between $\widetilde{\mathcal{I}}$ and detector-level entanglement. Furthermore, the indistinguishability measure

[1]Here we are assuming that the correlations between the two particles have been generated via some long-distance interaction which does not cause spatial overlap.

introduced in Eq. (5.4) could be generalized, as done for the old entropic measure $\mathcal{I}$ in Section 2.4, leading to a definition analogous to Eq. (2.22) in terms of many-body probability amplitudes.

5.4 Analysis of the previous results

In view of the above analysis, how can we explain the results reported in Ref. [2] (Subsection 1.3.4) and their extension in Ref. [37] (Chapter 4) about the recovery of quantum correlations between two qubits prepared in a singlet state $|1_-\rangle_{\rm AB}$ locally interacting with noisy environments? Looking at Eqs. (4.21), (4.33), (4.43), we notice that the state $\rho_{\rm AB}(t)$ of the system, after the two particles have independently interacted with the considered local environments, is given by: (i) a diagonal mixture of the original singlet state $|1_-\rangle_{\rm AB}$ and the remaining elements $|1_+\rangle_{\rm AB}$, $|2_+\rangle_{\rm AB}$, $|2_-\rangle_{\rm AB}$ of the Bell basis for the phase damping and depolarizing channels; (ii) a mixture of $|1_-\rangle_{\rm AB}$ and $|A\uparrow, B\uparrow\rangle$ for the amplitude damping channels. Let us now describe what happens to these states when we act on them with the deformation D of Eq. (5.1). For simplicity, we focus on the bosonic scenario and consider the action of a balanced beam splitter by fixing $l = l' = r = -r' = 1/\sqrt{2}$ ($\mathcal{I} = 1$). We have already commented that the singlet state is invariant under this operation. On the contrary, it can be easily shown that $|1_+\rangle_{\rm AB}$, $|2_+\rangle_{\rm AB}$, $|2_-\rangle_{\rm AB}$, and $|A\uparrow, B\uparrow\rangle$ are all transformed by D into states of two particles localized in the same spatial mode, due to the occurrence of interference effects. The resulting states are therefore discarded by the sLOCC coincidence measurement, which leads to the postselection of the remaining pure, maximally entangled singlet state $|1_-\rangle_{\rm LR}$ exhibiting concurrence $C(\rho_{\rm LR}) = 1$ when $\mathcal{I} = 1$.

This example shows that the recovery of quantum correlations reported in Refs. [2,37] is ultimately due to the occurrence of interference effects caused by the spatial overlap of the particles' wave functions during the deformation, and to the subsequent sLOCC postselection. With the constraint $|l| = |r'|$ considered in the mentioned references, a more balanced spatial redistribution results in a lower contamination of the singlet state $|1_-\rangle_{\rm LR}$ by states with one particle per spatial mode. Since these states are postselected by the coincidence measurement, a higher value of $\mathcal{I}$ ultimately results in a higher purity of the distilled singlet state. Despite the occurrence of interference effects hinders the physical interpretation and evaluation of the no which-way information, the generation of spatial overlap/indistinguishability acquires a fundamental role in the activation of those interference effects responsible for the recovery of quantum correlations.

In conclusion, the new interpretation of the phenomenon occurring within the sLOCC operational framework discussed in this chapter provides the main building block for the development of an operational scheme to distill maximally entangled states of identical particles. This is the central topic of the three manuscripts reported in the next three chapters, where we devise an optimization of the sLOCC protocol employed in Ref. [37] for both bosons and fermions, and provide a generalization to the multipartite scenario.

Chapter 6

Asymptotically-deterministic robust preparation of maximally entangled bosonic states

Abstract

We introduce a theoretical scheme to prepare a pure Bell singlet state of two bosonic qubits, in a way that is robust under the action of arbitrary local noise. Focusing on a photonic platform, the proposed procedure employs passive optical devices and a polarization-insensitive, non-absorbing, parity check detector in an iterative process which achieves determinism asymptotically with the number of repetitions. Distributing the photons over two distinct spatial modes, we further show that the elements of the related basis composed of maximally entangled states can be divided in two groups according to an equivalence based on passive optical transformations. We demonstrate that the parity check detector can be used to connect the two sets of states. We thus conclude that the proposed protocol can be employed to prepare any pure state of two bosons which are maximally entangled in either the internal degree of freedom (Bell states) or the spatial mode (NOON states).

This chapter reports the results of our manuscript of Ref. [3].

6.1 Introduction

Entanglement, the most exotic property of quantum mechanics, is at the heart of the enhancement provided by quantum protocols in many different fields of application [10], ranging from metrology and parameter estimation [28, 146], to computation [147], communication, and cryptography [148]. The ability to prepare entangled states with high reliability is thus crucial for the practical development of quantum technologies. Nonetheless, realistic preparations of entangled states are known to be hindered by the ubiquitous interaction with the surrounding environment, whose noisy action is detrimental for the quantum correlations within the system [10, 101, 131]. For this reason, many different techniques to circumvent the problem have been proposed over time [94–123, 149–153].

In this Letter, we first propose a protocol to distil a pure, maximally entangled Bell singlet state of two bosons from a completely depolarized one. We focus on a photonic implementation. The local action of depolarizing channels, which can be efficiently induced

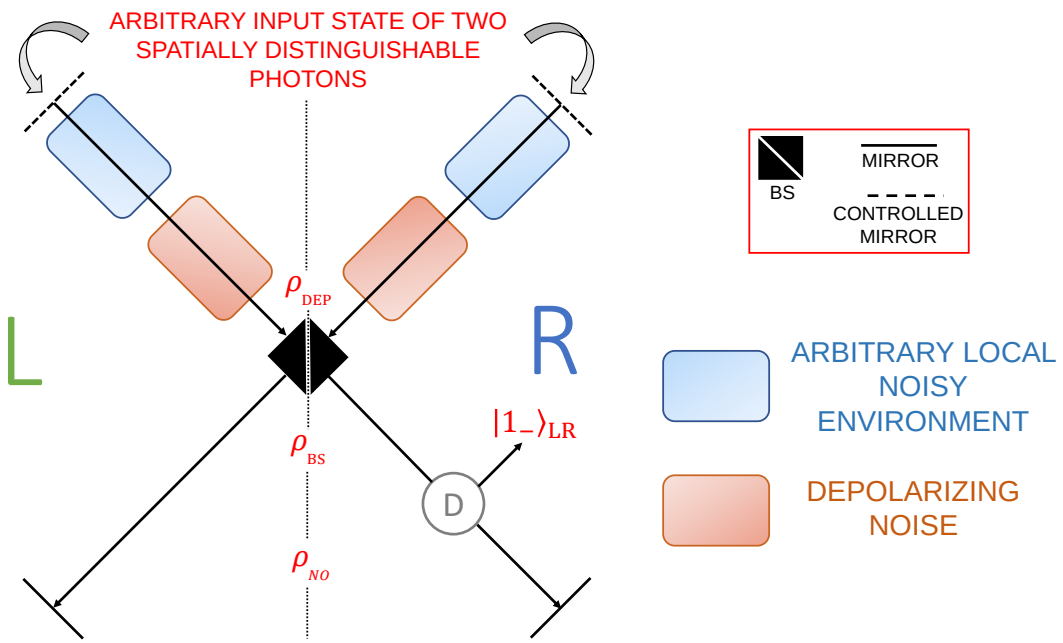

Figure 6.1: **Schematic representation of the setup.** The D element represents a polarization-insensitive, non-absorbing parity check detector. The depolarization noises in the red area (just before the BS) are assumed to be externally activated, while the noise sources in the blue area are environmentally induced.

by randomized local polarization rotators, transforms any arbitrary state of spatially distinguishable photons into a maximally mixed one. Thus, the proposed procedure can be applied to *any* arbitrary *initial state* of two spatially distinguishable photons, regardless of local noises affecting them before the depolarization. Our scheme employs passive optical (PO) devices and a polarization-insensitive, non-absorbing, parity check detector. The latter is a highly nonlinear transformation which performs a quantum nondemolition (QND) measurement capable to discriminate between states with even/odd number of photons. More precisely we only require the detector to distinguish between the cases where in a given location we have a single photon (corresponding to the successful generation of the Bell singlet), and those in which the total number of photons is either zero or equal to two (corresponding to a failure). The nondemolition character of the measurement ensures that in case of failure the whole protocol can be repeated by depolarizing the system once again, resetting it to the maximally mixed state. By doing so, the preparation of the Bell singlet is achieved with a probability scaling to 1 exponentially with the number of repetitions, thus being *asymptotically-deterministic*.

Differently from other entanglement distillation protocols [109, 149–151] allowing only for local operations and classical communication (LOCC), our scheme makes explicit use of the interference effects due to particle indistinguishability when non-locality is generated by a beam splitter (BS). In this sense, the proposed procedure extends the results obtained in Refs. [2, 37, 38], where the authors employed a technique based on *spatially localized operations and classical communication* (sLOCC) [1, 20, 23, 59, 60, 74, 154, 155] to achieve a probabilistic distillation of a Bell singlet state from a singlet subjected to the action of local noisy environments.

Finally, we introduce an equivalence between bosonic bipartite states based on PO transformations. We consider an orthonormal basis of the bipartite Hilbert space com-

posed of only maximally entangled states, and show that it can be divided in two sets of PO equivalent elements. We demonstrate that the two sets can be connected by means of the polarization-insensitive, non-absorbing, parity check detector previously discussed. As the Bell singlet state belongs to one of the two sets, we thus conclude that the proposed procedure allows for the preparation of *any* arbitrary *maximally entangled, pure bipartite state*. This comes with a trade-off in the difficult realization of the exotic detector required, whose crucial role for quantum information protocols emerges by the relevance of the reported results themselves.

Identical particles are treated via the *no-label approach* [20–22], a mathematical framework which allows to overcome some of the main issues affecting the standard label-based formalism [12, 13]. Also, it allows to write multiparticle states without having to explicitly symmetrize/antisymmetrize them as ruled by the symmetrization postulate [20–22], thus simplifying the notation

6.2 Notation

The Hilbert space of two bosonic qubits distributed over two distinct spatial regions L and R is 10-dimensional. We consider a basis $\mathcal{B} = \mathcal{B}_{\rm LR} \cup \mathcal{B}_{\rm NO}$ of maximally entangled states, where

$$\begin{aligned} \mathcal{B}_{\rm LR} &:= \Big\{ |1_\pm\rangle_{\rm LR} \,,\, |2_\pm\rangle_{\rm LR} \Big\}, \\ \mathcal{B}_{\rm NO} &:= \Big\{ |1_\pm\rangle_{\rm NO} \,,\, |U_\pm\rangle_{\rm NO} \,,\, |D_\pm\rangle_{\rm NO} \Big\}, \end{aligned} \tag{6.1}$$

and

$$\begin{aligned} |1_\pm\rangle_{\rm LR} &:= \frac{1}{\sqrt{2}}\Big(|L\uparrow, R\downarrow\rangle \pm |L\downarrow, R\uparrow\rangle \Big), \\ |2_\pm\rangle_{\rm LR} &:= \frac{1}{\sqrt{2}}\Big(|L\uparrow, R\uparrow\rangle \pm |L\downarrow, R\downarrow\rangle \Big), \\ |1_\pm\rangle_{\rm NO} &:= \frac{1}{\sqrt{2}}\Big(|L\uparrow, L\downarrow\rangle \pm |R\uparrow, R\downarrow\rangle \Big), \\ |U_\pm\rangle_{\rm NO} &:= \frac{1}{2}\Big(|L\uparrow, L\uparrow\rangle \pm |R\uparrow, R\uparrow\rangle \Big), \\ |D_\pm\rangle_{\rm NO} &:= \frac{1}{2}\Big(|L\downarrow, L\downarrow\rangle \pm |R\downarrow, R\downarrow\rangle \Big). \end{aligned} \tag{6.2}$$

Notice that the elements of basis $\mathcal{B}_{\rm LR}$ are Bell states entangled in the internal degree of freedom $|\uparrow\rangle$, $|\downarrow\rangle$, which, for the photonic implementation considered in the following paragraphs, can be identified with the polarization; instead, the basis $\mathcal{B}_{\rm NO}$ is composed of NOON states entangled in the spatial degree of freedom.

6.3 Procedure

The proposed scheme is depicted in Fig. 6.1. Let us take an arbitrary state of two photons localized in two distinct spatial modes L and R. If each photon is locally subjected to a depolarizing channel that induces a complete randomization of its polarization degree of freedom, such a state will be mapped into a maximally mixed configuration which can be expressed as a uniform mixture of the elements of the basis $\mathcal{B}_{\rm LR}$ introduced above, i.e., $\rho_{\rm dep} := \frac{1}{4}\,\Pi_{\rm LR}$, where $\Pi_{\rm LR} := \sum_{|v\rangle\in\mathcal{B}_{\rm LR}} |v\rangle\langle v|$ is the projector onto the subspace spanned by

the elements of the basis $\mathcal{B}_{\rm LR}$. We now let the two photons impinge on the two input ports of a balanced beam splitter (BS), which mixes the L and R regions inducing, at the level of single particle states, the mappings $|L\rangle \longrightarrow (|L\rangle + |R\rangle)/\sqrt{2}$ and $|R\rangle \longrightarrow (|L\rangle - |R\rangle)/\sqrt{2}$. Applied to the elements of the set $\mathcal{B}_{\rm LR}$, this achieves the transformations

$$\begin{cases} |1_-\rangle_{\rm LR} \longleftrightarrow -|1_-\rangle_{\rm LR}\,, \\ |1_+\rangle_{\rm LR} \longleftrightarrow |1_-\rangle_{\rm NO}\,, \\ |2_-\rangle_{\rm LR} \longleftrightarrow (|U_-\rangle_{\rm NO} - |D_-\rangle_{\rm NO})/\sqrt{2}, \\ |2_+\rangle_{\rm LR} \longleftrightarrow (|U_-\rangle_{\rm NO} + |D_-\rangle_{\rm NO})/\sqrt{2}. \end{cases} \tag{6.3}$$

As a result, the state $\rho_{\rm dep}$ introduced previously is mapped into

$$\rho_{\rm BS} = \frac{1}{4}\,|1_-\rangle_{\rm LR}\,\langle 1_-|_{\rm LR} + \frac{3}{4}\rho_{\rm NO}, \tag{6.4}$$

where

$$\rho_{\rm NO} := \frac{1}{3}\Big(\,|1_-\rangle_{\rm NO}\,\langle 1_-|_{\rm NO} + |U_-\rangle_{\rm NO}\,\langle U_-|_{\rm NO} + |D_-\rangle_{\rm NO}\,\langle D_-|_{\rm NO}\,\Big). \tag{6.5}$$

We highlight that $\rho_{\rm BS}$ in Eq. (6.4) is a classical mixture of the Bell singlet state $|1_-\rangle_{\rm LR}$ and of NOON states. Crucially, the former is characterized by an odd number of photons in each spatial mode, while an even number (0 or 2) characterizes the latter. This fact can be exploited to distil the singlet as follows. We employ a polarization-insensitive, non-absorbing, parity check detector D. By monitoring one of the two spatial modes, such a detector is capable to distinguish whether it contains an odd or an even number of photons. In the first case, $\rho_{\rm BS}$ is projected onto the subspace spanned by the Bell states composing $\mathcal{B}_{\rm LR}$ via the projection operator $\Pi_{\rm LR}$ previously introduced, giving the desired singlet $|1_-\rangle_{\rm LR}$. In this case, occurring with probability $p_{\rm LR} = {\rm Tr}\,[\Pi_{\rm LR}\rho_{\rm BS}] = 1/4$, we collect the state and conclude the process. If D registers an even number of photons, instead, $\rho_{\rm BS}$ is projected onto the subspace spanned by the NOON states in basis $\mathcal{B}_{\rm NO}$ via the projection operator $\Pi_{\rm NO} := \sum_{|k\rangle\in\mathcal{B}_{\rm NO}} |k\rangle\,\langle k|$. This scenario, which occurs with probability $p_{\rm NO} = {\rm Tr}\,[\Pi_{\rm NO}\rho_{\rm BS}] = 3/4$, leaves the system in the state $\rho_{\rm NO}$ of Eq. (6.5). In this case, we act on the system with another beam splitting operation, getting the state

$$\xi_{\rm LR} := \frac{1}{3}\Big(\,|1_+\rangle_{\rm LR}\,\langle 1_+|_{\rm LR} + |2_+\rangle_{\rm LR}\,\langle 2_+|_{\rm LR} + |2_-\rangle_{\rm LR}\,\langle 2_-|_{\rm LR}\,\Big). \tag{6.6}$$

The two photons are now subjected to local depolarizing channels once again, resetting the system to the completely depolarized state $\rho_{\rm dep}$ we started with. The process can thus be repeated a second time without having to inject new photons in the setup, leading to the generation of a Bell singlet state with total probability $p^{(2)}_{\rm LR} = 1/4 + (3/4)(1/4)$. Proceeding this way, the j-th iteration returns $|1_-\rangle_{\rm LR}$ with probability $p^{(j)}_{\rm LR} = \sum_{n=1}^{j}(1/4)(3/4)^{n-1}$, which converges exponentially to 1 for $j \to \infty$. We emphasize that such an iterated implementation can be achieved with the closed configuration depicted in Fig. 6.1. Here, two actively controlled mirrors close the input arms of the interferometer after the photons have been injected in the setup, while two other mirrors are set on the output modes after the detector. In this way, the two particles are reflected back into the same BS and noisy channels, allowing for the process to be repeated without requiring further resources.

6.4 Amplitude damping-based implementation

Here we propose an alternative implementation of our scheme which adopts two local amplitude damping channels instead of the depolarizing ones. In this case, the noisy

environments map two spatially separated qubits into the pure ground state $|L\downarrow, R\downarrow\rangle$. Placing a polarization rotator (PR) (see below) on the spatial mode L (to fix a framework), we get $|L\uparrow, R\downarrow\rangle = (|1_+\rangle_{\rm LR} + |1_-\rangle_{\rm LR})/\sqrt{2}$. From Eq. (6.3), we notice that the BS transforms this state into $(|1_-\rangle_{\rm NO} - |1_-\rangle_{\rm LR})/\sqrt{2}$. The detector D can now be employed to distill a Bell singlet state with probability $p_{\rm LR} = 1/2$. When the system is found in state $|1_-\rangle_{\rm NO}$, instead, the process is repeated analogously to the case where depolarizing channels are employed. At the j-th iteration, the singlet is distilled with probability $p_{\rm LR}^{(j)} = \sum_{n=1}^{j} 1/2^n$, which again converges to 1 exponentially when $j \to \infty$.

6.5 Passive optical equivalence

We introduce *PO operations* as the set of transformations which can be obtained by a proper sequence of BSs, polarization BSs (PBSs), polarization-dependent or -independent phase shifters (PDPSs/PIPSs), and local polarization rotators (PRs). We further define two states to be *PO equivalent* if they can be obtained one from the other by means of PO operations.

PO equivalence allows to divide basis $\mathcal{B}$ in Eq. (6.1) in two sets of equivalent states:

$$\begin{aligned} \mathcal{S}_1 &:= \Big\{ |1_\pm\rangle_{\rm LR}\,, |2_\pm\rangle_{\rm LR}\,, |1_\pm\rangle_{\rm NO} \Big\}, \\ \mathcal{S}_2 &:= \Big\{ |U_\pm\rangle_{\rm NO}\,, |D_\pm\rangle_{\rm NO} \Big\}. \end{aligned} \tag{6.7}$$

Focusing on $\mathcal{S}_1$, mappings $|1_-\rangle_{\rm LR} \leftrightarrow |1_+\rangle_{\rm LR}$ and $|2_-\rangle_{\rm LR} \leftrightarrow |2_+\rangle_{\rm LR}$ can be obtained by locally applying a π-PIPS to one of the two spatial modes, while a PIPS of $\pi/2$ achieves $|1_-\rangle_{\rm NO} \leftrightarrow |1_+\rangle_{\rm NO}$. Connections $|1_-\rangle_{\rm LR} \leftrightarrow |2_-\rangle_{\rm LR}$ and $|1_+\rangle_{\rm LR} \leftrightarrow |2_+\rangle_{\rm LR}$ can be obtained by means of a local PR performing the operation $|\uparrow\rangle \leftrightarrow |\downarrow\rangle$ on one mode. This set of local transformations relating Bell states were firstly introduced in Ref. [109]. We now extend them by noticing from Eq. (6.3) that the non-locality generated by a BS can be employed to achieve the transformation $|1_+\rangle_{\rm LR} \leftrightarrow |1_-\rangle_{\rm NO}$. Considering $\mathcal{S}_2$, instead, mappings $|U_-\rangle_{\rm NO} \leftrightarrow |U_+\rangle_{\rm NO}$ and $|D_-\rangle_{\rm NO} \leftrightarrow |D_+\rangle_{\rm NO}$ can be realized by a local $\pi/2$-PIPS on one spatial mode, while $|U_-\rangle_{\rm NO} \leftrightarrow |D_-\rangle_{\rm NO}$ and $|U_+\rangle_{\rm NO} \leftrightarrow |D_+\rangle_{\rm NO}$ can be obtained by applying a PR to both modes. Sets $\mathcal{S}_1$ and $\mathcal{S}_2$ and the related intra-set PO relations are depicted in Fig 6.2.

We now show that a link between the two sets can be established by employing the (non PO) detector D described above. To move from $\mathcal{S}_1$ to $\mathcal{S}_2$, we start from state $|2_+\rangle_{\rm LR} \in \mathcal{S}_1$. We apply a PBS on one arbitrary spatial mode, placing D at the output of one of its ports before recombining the outputs in another PBS. Notice that such a Mach-Zehnder-like setup behaves as a *polarization-sensitive*, non-absorbing, parity check detector. This allows to discriminate the component $|L\uparrow, R\uparrow\rangle$ of state $|2_+\rangle_{\rm LR}$ from the one $|L\downarrow, R\downarrow\rangle$. Combining the two spatial modes in a BS now leads to either state $|U_-\rangle_{\rm NO} \in \mathcal{S}_2$ or $|D_-\rangle_{\rm NO} \in \mathcal{S}_2$, respectively, as can be computed using Eq. (6.3) and recalling that $|L\uparrow, R\uparrow\rangle = |2_+\rangle_{\rm LR} + |2_-\rangle_{\rm LR}$, $|L\downarrow, R\downarrow\rangle = |2_+\rangle_{\rm LR} - |2_-\rangle_{\rm LR}$. To move from $\mathcal{S}_2$ to $\mathcal{S}_1$, instead, let us begin with $|U_-\rangle_{\rm NO} \in \mathcal{S}_2$. Acting on it with a beam splitting operation, we obtain $(|2_+\rangle_{\rm LR} + |2_-\rangle_{\rm LR})/\sqrt{2}$. A PR set on the R spatial mode gives $(|1_+\rangle_{\rm LR} + |1_-\rangle_{\rm LR})/\sqrt{2}$, which is transformed by a second BS into $(|1_-\rangle_{\rm NO} - |1_-\rangle_{\rm LR})/\sqrt{2}$. The detector D can now be employed to discriminate the odd component $(|1_-\rangle_{\rm LR})$ from the even one $(|1_-\rangle_{\rm NO})$, both belonging to $\mathcal{S}_1$. Given the intra-set connections discussed above, we have thus found a link

$$\mathcal{S}_1 \xleftrightarrow{PO+D} \mathcal{S}_2, \tag{6.8}$$

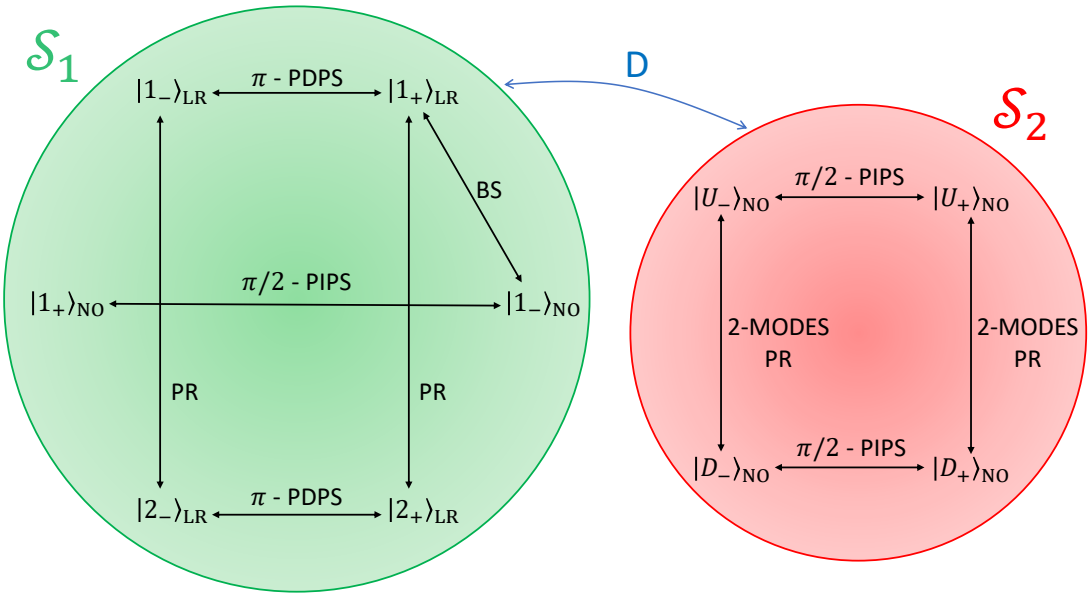

Figure 6.2: **Structure of passive optical equivalent maximally entangled states of two photons.** The figure shows two sets of PO equivalent maximally entangled states of two bosonic qubits distributed over two spatial modes. Examples of PO transformations connecting them are reported for each set. All the depicted PO transformations are assumed to occur on a single arbitrary spatial mode, except when 2-modes is stated. θ-PDPS/PIPS are polarization dependent/independent phase shifters inducing a phase θ on the spatial mode they are set on, PRs are 90° polarization rotators, and BSs are beam splitters. The two sets are linked by a polarization-insensitive, non-absorbing, parity check detector D (see main text).

which allows to transform any two arbitrary maximally entangled states in $\mathcal{B}$ one into the other. As these include the Bell singlet state, the proposed scheme can be employed to prepare any maximally entangled state of two photonic qubits.

6.6 Faulty parity check detector

We conclude our analysis by accounting for possible errors occurring during the parity check detection.

Errors may occur when the system state $|1_-\rangle_{LR}\langle 1_-|_{LR}$ is mistakenly detected as an even-parity state, and (or) when the system state ρ_{NO} in Eq. (6.5) is wrongly detected as an odd-parity state. Accounting for these events amounts to substituting the previously defined projectors Π_{LR} and Π_{NO} with $\Pi'_{LR} := (1-\epsilon)\,\Pi_{LR}+\epsilon'\,\Pi_{NO}$ and $\Pi'_{NO} := (1-\epsilon')\,\Pi_{NO}+\epsilon\,\Pi_{LR}$, respectively, where error probabilities ϵ, ϵ' are considered. Correspondingly, the system is projected into the states

$$\begin{aligned}\rho'_{LR} &= \frac{1}{4}\Big[(1-\epsilon)\;|1_-\rangle_{LR}\langle 1_-|_{LR} + 3\,\epsilon'\,\rho_{NO}\Big]/p'_{LR},\\ \rho'_{NO} &= \frac{1}{4}\Big[3\,(1-\epsilon')\,\rho_{NO} + \epsilon\;|1_-\rangle_{LR}\langle 1_-|_{LR}\Big]/p'_{NO},\end{aligned} \tag{6.9}$$

with respective probabilities $p'_{LR} = (1-\epsilon)/4 + 3\epsilon'/4$, $p'_{NO} = 3(1-\epsilon')/4 + \epsilon/4 = 1 - p'_{LR}$.

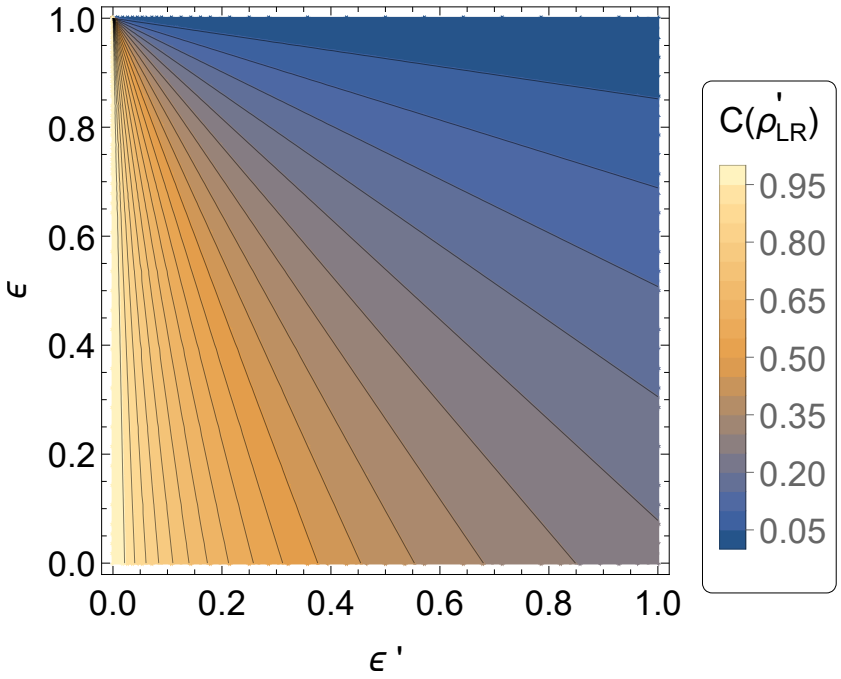

Figure 6.3: Concurrence of the prepared state $\rho'_{\rm LR}$, as a function of the error probabilities ϵ and ϵ' characterizing a faulty detection.

We now quantify the amount of quantum correlations present in the faulty state $\rho'_{\rm LR}$ we collect. Since when no errors occur we expect to get the singlet state $|1_-\rangle_{\rm LR}$, we focus on the entanglement in polarization. To do so, we calculate the concurrence [33], obtaining

$$C(\rho'_{\rm LR}) = \frac{1-\epsilon}{1-\epsilon+3\,\epsilon'}. \tag{6.10}$$

Notice that the amount of entanglement in $\rho'_{\rm LR}$ depends on both the error probabilities ϵ and ϵ', ranging from $C(\rho'_{\rm LR}) = 0$ (separable state) when $\epsilon = 1$, to $C(\rho'_{\rm LR}) = 1/(1+3\epsilon')$ when $\epsilon = 0$. Fig. 6.3 reports the concurrence $C(\rho'_{\rm LR})$ as a function of ϵ and ϵ'. We remark that, however, not all the scenarios are relevant. When $\epsilon' = 1$, for example, it is enough to collect the photons when the detector signals an even parity state to achieve a state with nonzero entanglement (unless $\epsilon = 0$, too).

6.7 Conclusions

In this work, we have presented a procedure to robustly prepare maximally entangled states of two photonic qubits undergoing arbitrary local noise. The protocol employs PO transformations and a polarization-insensitive, non-absorbing, parity check detector to distil a Bell singlet state from a completely depolarized one. As the local depolarization of spatially distinguishable photons leads to the maximally mixed state regardless of the previous dynamics, the proposed scheme transforms any arbitrary initial state into the Bell singlet. In this way, the preparation is robust to the action of any local noise affecting the photons before their state is reset by the depolarization. We highlight that, in case a photon is lost during a noisy interaction, a new depolarized photon can be injected to recover the process. Via a QND measurement, the protocol is iterative and prepares the

desired state with a probability which scales exponentially with the number of repetitions, thus being asymptotically-deterministic.

We have introduced a formal equivalence based on PO transformations, showing that it allows to divide maximally entangled states of two qubits distributed over two distinct spatial modes in two sets of PO equivalent states. A link between the two sets has been established through the polarization-insensitive, non-absorbing, parity check detector. Since the Bell singlet state belongs to one of the two sets, we conclude that the scheme enables a robust generation of any arbitrary maximally entangled state of two photonic qubits.

We emphasize that, to achieve the correct interference patterns, the PO transformations realized by BSs or PBSs require the two photons to be indistinguishable in all the degrees of freedom but the spatial one and, at most, the polarization. In light of this, the PO equivalence defined in this Letter can be ultimately interpreted as a connection between two synchronized sources of single photons satisfying the above requirement and the set of maximally entangled bipartite states. Our work provides clear insights on the role played by indistinguishability as a tool to achieve a generation of entanglement which is robust to environmental noise, whatever the noise. Moreover, the externally induced noise acts as an ally towards this goal, in contrast to standard protection techniques where noise constitutes a detrimental trait to be avoided. Notice that the low-dimensional basic scheme proposed here is strategical, since it allows to focus on the main underlying physical mechanisms and their interpretation.

In a real-world implementation of our setup, the required PO transformations, including the realization of the depolarizing channels, can be reliably produced with commercially available devices such as mirrors, beam splitters, and optical fibers. Given the resetting function of the depolarizing channels, possible errors introduced by the mirrors do not affect the performances of the setup as long as the photons are not lost. Moreover, we have not considered photon number-preserving errors introduced by the beam splitter as very highly-efficient beam splitters are currently employed in the labs. Therefore, the realization of the polarization-insensitive, non-absorbing, parity check detector constitutes the main obstacle to be tackled and motivates experimental developments in different platforms. We have analyzed the case when faulty detections are involved, quantifying the entanglement between the two resulting photons as a function of the errors due to the parity check detector. To this regard, we remark that the proposed scheme can still be used substituting such a detector with commercially available single photon detectors performing a coincidence measurement on the two output modes, achieving the preparation of the desired maximally entangled state with probability $p_{\mathrm{LR}} = 1/4$. In the latter case, where the photon is absorbed by the detector, deferred measurements can be employed after running the quantum protocol which exploits the desired resource state conditionally [1, 59, 60].

It is interesting to compare our scheme with the standard entanglement distillation protocol [34, 109, 156]. While the latter requires entangled states as input, the resetting action of the depolarization of both qubits in our procedure admits initially unentangled states. Also, the proposed method transforms a pair of qubits into a pure maximally entangled state, either Bell-like or NOON-like, with asymptotic certainty, while the standard distillation protocol requires n copies of a bipartite mixed state to probabilistically extract $k < n$ copies of Bell singlet states. On the other hand, our technique is well-suited for the preparation of entangled particles but not for their distribution to remote parties, as the extraction of the desired states occurs after the BS and no noise is assumed to

act afterwards. We thus envision a combined implementation of the two schemes: entangled qubits prepared with our scheme propagate through noisy channels towards distant parties, providing the initial entangled states required for the application of the standard distillation protocol.

We finally highlight that the reported results hold for any type of bosonic system, thus not being limited to photons. We foresee an extension of our procedure to fermions, clarifying the role of particle statistics in the preparation of entangled states. Moreover, we aim at widening the analysis of PO transformations to systems of $N > 2$ particles, looking for a suitable generalization of the protocol presented in this work to prepare multipartite entangled states.

Chapter 7

Robust engineering of maximally entangled states by identical particle interferometry

Abstract

We propose a procedure for the robust preparation of maximally entangled states of identical fermionic qubits, studying the role played by particle statistics in the process. The protocol exploits externally activated noisy channels to reset the system to a known state. The subsequent interference effects generated at a beam splitter result in a mixture of maximally entangled Bell states and NOON states. We also discuss how every maximally entangled state of two fermionic qubits distributed over two spatial modes can be obtained from one another by fermionic passive optical transformations. Using a pseudospin-insensitive, non-absorbing, parity check detector, the proposed technique is thus shown to deterministically prepare any arbitrary maximally entangled state of two identical fermions. These results extend recent findings related to bosonic qubits. Finally, we analyze the performance of the protocol for both bosons and fermions when the externally activated noisy channels are not used and the two qubits undergo standard types of noise. The results supply further insights towards viable strategies for noise-protected entanglement exploitable in quantum-enhanced technologies.

This chapter reports the results of our manuscript of Ref. [].

7.1 Introduction

With the advent of technologies based on quantum paradigms, entanglement has become the subject of a rapidly increasing amount of studies [10]. These include, but are not limited to, its generation, manipulation, and protection from detrimental noise. The latter, in particular, is a crucial step to be tackled as quantum correlations are known to decay rapidly in systems exposed to the action of environmental noise [101]. Since achieving a perfectly isolated system at the quantum level is practically unfeasible, different strategies have been proposed over time to deal with entanglement fragility. These ranges from structured environments with memory effects [98–100, 102–108], decoherence-free subspaces [112, 113], dynamical decoupling and control techniques [114–123], to quantum error corrections [94–97] and distillation protocols [109–111, 149–151]. Furthermore, a

recently developed research line investigates the possibility to exploit the indistinguishability of identical particles to generate and protect quantum correlations in open quantum systems [2, 3, 23, 37, 155].

A method has been recently proposed to distill pure maximally entangled states from two bosonic qubits subjected to arbitrary local noisy environments [3]. To do so, this scheme exploits artificially induced noise to affect the two constituents after they have been subjected to the environmental noise sources. Allowing the externally activated noisy interaction to act for a sufficiently long time, the system is reset to a known state regardless of the environmental noise which previously affected it. Referring to a photonic implementation for simplicity, the resulting photons are later subjected to the non-local action of a beam splitter (BS). As a consequence of the interference effects occurring due to particle indistinguishability, the result is found to be a classical mixture of a Bell singlet state and NOON states. Using a polarization insensitive, non-absorbing, parity-check detector D set on one of the two spatial modes, the former is filtered probabilistically, while the latter are reintroduced in the BS and subjected once again to depolarization. In this way, the process can be iterated until a singlet is obtained, with distillation probability which scales to 1 exponentially. It has been also shown that all the maximally entangled states of two bosonic qubits distributed over two spatial modes can be mapped one into the other via *passive optical* (PO) transformations and the action of the detector D [3], suggesting that the proposed procedure can be used to prepare any arbitrary maximally entangled state of two identical bosons. It is then important to study how a similar procedure can be applied to particles of different nature, such as fermions.

In this work, we first extend the procedure proposed in Ref. [3] to identical fermions, introducing the analogous PO equivalences between fermionic maximally entangled states. After that, we analyze for both bosons and fermions the scenario where the artificially activated noise is not applicable to the two qubits. In this situation, where the system is not reset to a fixed state anymore, the performance of the scheme depends on the type of noisy environment affecting the particles, on the system-environment interaction time, and on the initially prepared state. In particular, we focus on three standard types of local noisy channels (phase damping, depolarizing, amplitude damping), and on a set of initial states which includes both entangled and separable ones.

Multiparticle states are written in the *no-label approach* [20–22], an alternative formalism for identical particles which allows to simplify the notation by avoiding to explicitly symmetrize/antisymmetrize global states as required by the symmetrization postulate in the standard first-quantization framework.

7.2 Procedure

The considered protocol is schematically depicted in Fig. 7.1. Two identical qubits are initially localized on two distinct spatial modes L and R, prepared in an initial state $|\psi_0\rangle$. Two arbitrary environmental induced noises act locally on the two spatial modes for a time t. After that, local depolarization is is artificially induced on both qubits, leading to a maximally mixed state. The two particles are now let to impinge on the two input ports of a BS. A pseudospin-insensitive, non-absorbing, parity check detector D is employed on one of the output modes to discriminate the outcomes with one constituent per mode (odd parity) from the ones with two particles in the same spatial mode (even parity). When dealing with bosons, the state is collected in the former case, terminating the process. If an even-parity state is found, instead, the method is iterated by depolar-

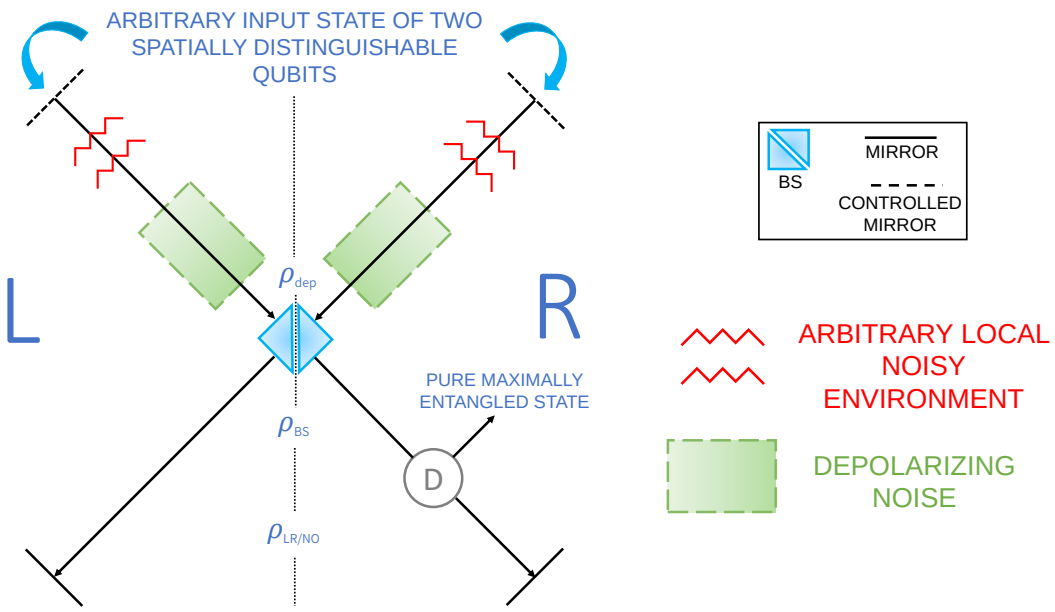

Figure 7.1: **Schematic representation of the setup**. The scheme uses externally activated depolarization noises, here represented by the green areas. The implementation with externally activated amplitude damping noises follows analogously, with the addition of a polarization rotator set on one spatial mode immediately before the BS. The red wavy lines represent environmentally-induced noise sources. The D element represents a pseudospin-insensitive, non-absorbing parity check detector. This setup is applicable to generic bosons and fermions by suitably adapting the represented photonic devices. The figure recalls Fig. 1 of Ref. [3].

izing the particles and detecting them again, until an odd-parity state is distilled. In an alternative implementation, two local amplitude damping channels are employed instead of the depolarizing ones. In this case, a pseudospin rotator, which maps the pseudospin $\uparrow$ of a qubit into $\downarrow$ and viceversa, is set on one spatial mode immediately before the BS. In Ref. [3], the authors showed that this procedure allows to distillate bosonic Bell singlet states, which can be afterward converted into arbitrary maximally entangled states via PO operations (see Subsection 7.3.1) and, if required, the action of the detector D.

We stress that, when the externally activated depolarizing (amplitude damping) channels are let to act on the qubits for a sufficiently long time, they lead to the maximally mixed state (ground state) independently on both the initial state $|\psi_0\rangle$, the interaction time t, and the type of environmental noise acting before them: in this sense, the artificially induced noises are used to reset the system to a fixed state. On the contrary, all the mentioned factors contribute to the final outcomes when such channels are not activated.

7.3 Fermionic implementation

We introduce the following notation for maximally entangled states of two qubits distributed over two distinct spatial modes L, R:

$$
\begin{aligned}
|1_\pm\rangle_{\rm LR} &:= \frac{1}{\sqrt{2}}\Big(|L\uparrow, R\downarrow\rangle \pm |L\downarrow, R\uparrow\rangle \Big),\\
|2_\pm\rangle_{\rm LR} &:= \frac{1}{\sqrt{2}}\Big(|L\uparrow, R\uparrow\rangle \pm |L\downarrow, R\downarrow\rangle \Big),\\
|1_\pm\rangle_{\rm NO} &:= \frac{1}{\sqrt{2}}\Big(|L\uparrow, L\downarrow\rangle \pm |R\uparrow, R\downarrow\rangle \Big),\\
|U_\pm\rangle_{\rm NO} &:= \frac{1}{2}\Big(|L\uparrow, L\uparrow\rangle \pm |R\uparrow, R\uparrow\rangle \Big),\\
|D_\pm\rangle_{\rm NO} &:= \frac{1}{2}\Big(|L\downarrow, L\downarrow\rangle \pm |R\downarrow, R\downarrow\rangle \Big).
\end{aligned}
\tag{7.1}
$$

Here, states with subscripts LR and NO are Bell states and NOON states, respectively. The two differ in the number of particles localized in one spatial mode, which is 1 for the former and 0 or 2 for the latter and can thus be discriminated by a parity measurement. States in Eq. (7.1) constitute a basis $\mathcal{B} := \mathcal{B}_{\rm LR} \cup \mathcal{B}_{\rm NO}$ of the 10-dimensional bosonic Hilbert space, where $\mathcal{B}_{\rm LR} := \Big\{ |1_\pm\rangle_{\rm LR}, |2_\pm\rangle_{\rm LR} \Big\}$ and $\mathcal{B}_{\rm NO} := \Big\{ |1_\pm\rangle_{\rm NO}, |U_\pm\rangle_{\rm NO}, |D_\pm\rangle_{\rm NO} \Big\}$. On the other hand, Pauli exclusion principle forbids the existence of states $|U_\pm\rangle_{\rm NO}$, $|D_\pm\rangle_{\rm NO}$ for identical fermions, restricting their Hilbert space to 6 dimensions spanned by the remaining vectors of $\mathcal{B}$.

7.3.1 Passive optical operations

Referring to a photonic implementation, *PO operations* are defined as the set of transformations which can be obtained by a proper sequence of BSs, polarization BSs (PBSs), polarization-dependent or -independent phase shifters (PDPSs/PIPSs), and local polarization rotators (PRs), with two states being *PO equivalent* if they can be obtained one from the other by means of PO operations [3]. Here, we extend PO operations to fermions by simply asking for the involved devices to act on the particle pseudospin rather than polarization, performing analogous transformations.

Fig. 7.2 reports the two sets of PO equivalent maximally entangled states of two bosons, with an example of PO transformations connecting them (see Ref. [3]). Similar relations can be found for fermions, as illustrated in Fig. 7.3. In particular, a PIPS introducing a phase π on one spatial mode links $|1_-\rangle_{\rm LR}$ to $|1_+\rangle_{\rm LR}$ and $|2_-\rangle_{\rm LR}$ to $|2_+\rangle_{\rm LR}$, while the introduction of a phase $\pi/2$ transforms $|1_-\rangle_{\rm NO}$ and $|1_+\rangle_{\rm NO}$ into each other. A PR mapping $\uparrow$ into $\downarrow$ and viceversa set on one spatial mode achieves the connections $|1_-\rangle_{\rm LR} \leftrightarrow |2_-\rangle_{\rm LR}$ and $|1_+\rangle_{\rm LR} \leftrightarrow |2_+\rangle_{\rm LR}$. Being inherently local, this net of PO equivalent states is the same for fermions and bosons (see Ref. [3]). On the contrary, a BS transforms two simultaneously impinging fermions differently from the bosonic situation, due to their different commutation/anticommutation rules. As a 50:50 BS transforms single particle states according to $|L\rangle \longrightarrow (|L\rangle + |R\rangle)/\sqrt{2}$ and $|R\rangle \longrightarrow (|L\rangle - |R\rangle)/\sqrt{2}$, we find its action

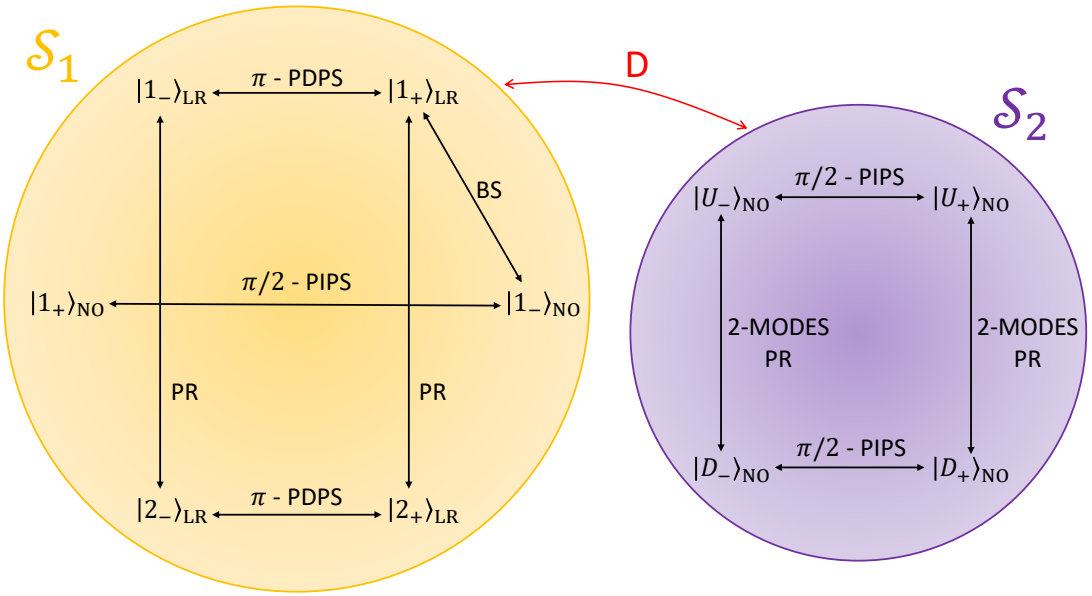

Figure 7.2: **Structure of passive optical equivalent maximally entangled states of two photons.** The figure shows two sets of PO equivalent maximally entangled states of two bosonic qubits distributed over two spatial modes. Examples of PO transformations connecting them are reported for each set. All the depicted PO transformations are assumed to occur on a single arbitrary spatial mode, except when "2-modes" is stated. θ-PDPS/PIPS are polarization dependent/independent phase shifter inducing a phase θ on the spatial mode they are set on, PRs are 90° polarization rotators, and BSs are beam splitters. The two sets are linked by a polarization-insensitive, non-absorbing, parity check detector D (see main text). The figure recalls Fig. 2 of Ref. [3].

on fermionic maximally entangled states to achieve the transformations

$$\text{fermionic BS:} \begin{cases} |1_-\rangle_{\rm LR} \longleftrightarrow |1_-\rangle_{\rm NO}\,, \\ |1_+\rangle_{\rm LR} \longleftrightarrow -|1_+\rangle_{\rm LR}\,, \\ |2_-\rangle_{\rm LR} \longleftrightarrow -|2_-\rangle_{\rm LR}\,, \\ |2_+\rangle_{\rm LR} \longleftrightarrow -|2_+\rangle_{\rm LR}\,, \end{cases} \tag{7.2}$$

whereas for bosons we have

$$\text{bosonic BS:} \begin{cases} |1_-\rangle_{\rm LR} \longleftrightarrow -|1_-\rangle_{\rm LR}\,, \\ |1_+\rangle_{\rm LR} \longleftrightarrow |1_-\rangle_{\rm NO}\,, \\ |2_-\rangle_{\rm LR} \longleftrightarrow (|U_-\rangle_{\rm NO} - |D_-\rangle_{\rm NO})/\sqrt{2}, \\ |2_+\rangle_{\rm LR} \longleftrightarrow (|U_-\rangle_{\rm NO} + |D_-\rangle_{\rm NO})/\sqrt{2}. \end{cases} \tag{7.3}$$

A 50:50 BS can thus be employed to connect the fermionic states $|1_-\rangle_{\rm LR}$ and $|1_-\rangle_{\rm NO}$. Since $|U_\pm\rangle_{\rm NO}$ and $|D_\pm\rangle_{\rm NO}$ are forbidden for identical fermions, we thus find that all the fermionic maximally entangled states are PO equivalent. The described situation is pictorially depicted in Fig. 7.3.

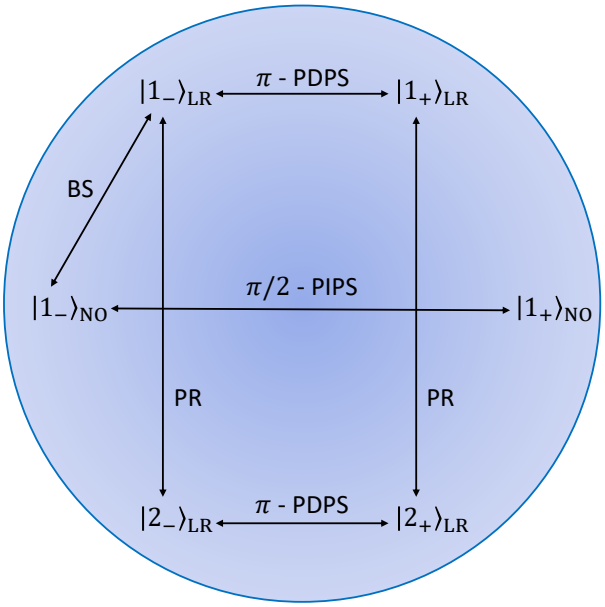

Figure 7.3: **Structure of passive optical equivalent maximally entangled states of two fermionic qubits.** The figure shows two sets of PO equivalent maximally entangled states of two fermionic qubits distributed over two spatial modes. Examples of PO transformations connecting them are reported. All the depicted PO transformations are assumed to occur on a single arbitrary spatial mode. θ-PDPS/PIPS, PRs, and BSs are devices acting on fermions performing operations analogous to their bosonic counterpart (see main text and Fig. 7.2).

7.3.2 Results for fermions

Let us consider the implementation of the protocol based on the artificially induced depolarization of the two qubits. Once the depolarization is complete, the system is left in a maximally mixed state $\rho_{\rm dep} := \frac{1}{4}\,\Pi_{\rm LR}$, where $\Pi_{\rm LR} := \sum_{|v\rangle\in\mathcal{B}_{\rm LR}} |v\rangle\langle v|$ is the projector onto the subspace spanned by the elements of the basis $\mathcal{B}_{\rm LR}$ introduced in Section 7.3. Under the action of a BS given in Eq. (7.2), state $\rho_{\rm dep}$ is transformed into

$$\rho_{\rm BS} = \frac{1}{4}\,|1_-\rangle_{\rm NO}\langle 1_-|_{\rm NO} + \frac{3}{4}\rho_{\rm LR}, \tag{7.4}$$

where

$$\rho_{\rm LR} := \frac{1}{3}\Big(\,|1_+\rangle_{\rm LR}\langle 1_+|_{\rm LR} + |2_+\rangle_{\rm LR}\langle 2_+|_{\rm LR} + |2_-\rangle_{\rm LR}\langle 2_-|_{\rm LR}\,\Big). \tag{7.5}$$

The previously discussed detector D can now be employed to discriminate the even-parity components of $\rho_{\rm BS}$ from the odd-parity ones. In the first case, $\rho_{\rm BS}$ is projected onto the subspace spanned by the elements of basis $\mathcal{B}_{\rm NO}$ via the projection operator $\Pi_{\rm NO} := \sum_{|k\rangle\in\mathcal{B}_{\rm NO}} |k\rangle\langle k|$, returning $|1_-\rangle_{\rm NO}\langle 1_-|_{\rm NO}$ with probability $p_{\rm NO} = {\rm Tr}\,[\Pi_{\rm NO}\rho_{\rm BS}] = 1/4$. We thus collect the qubits, and the process terminates. In the second case, instead, $\rho_{\rm BS}$ is projected onto the subspace spanned by the elements of basis $\mathcal{B}_{\rm LR}$ via $\Pi_{\rm LR}$, returning $\rho_{\rm LR}$ with probability $p_{\rm LR} = {\rm Tr}\,[\Pi_{\rm LR}\rho_{\rm BS}] = 3/4$. When this happens, the two qubits are artificially depolarized once again, re-obtaining $\rho_{\rm dep}$ and allowing for the process to be iterated. By repeating the procedure, we find the probability of distilling the state $|1_-\rangle_{\rm NO}\langle 1_-|_{\rm NO}$ at the j-th iteration to be $p^{(j)}_{\rm NO} = \sum_{n=1}^{j}(1/4)(3/4)^{n-1}$, which converges exponentially to 1 for $j\to\infty$. Given the PO transformations discussed in Subsection 7.3.1, we thus conclude

that the proposed scheme allows for the robust preparation of any maximally entangled state of two fermionic qubits in an asymptotically-deterministic way.

We now consider the implementation where the artificially induced noise is an amplitude damping locally acting on both particles, followed by a PR set on one spatial mode, which here we fix to be the L one for simplicity. When the damping is complete, the system is left in the ground state $|L\downarrow, R\downarrow\rangle$ regardless of the initial state $|\psi_0\rangle$, of the type of noise previously acting on the qubits, and of the interaction time t. The PR transforms it into $|L\uparrow, R\downarrow\rangle = (|1_-\rangle_{\rm LR} + |1_+\rangle_{\rm LR})/\sqrt{2}$, which is then transformed by a BS. From Eq. (7.2), the resulting state is easily found to be $(|1_-\rangle_{\rm NO} - |1_+\rangle_{\rm LR})/\sqrt{2}$. Once again, the detector D allows for discriminating the even component $|1_-\rangle_{\rm NO}$ from the odd one $|1_+\rangle_{\rm LR}$, both distilled with the same probability $p_{\rm NO} = p_{\rm LR} = 1/2$. Depending on whether we are interested in preparing a NOON state or a Bell state, we collect the particles when the corresponding parity is detected and repeat the process otherwise. In this way, the desired state is obtained at the j-th iteration with probability $p_{\rm NO}^{(j)} = p_{\rm LR}^{(j)} = \sum_{n=1}^{j} 1/2^n$, which for $j \to \infty$ converges to 1 exponentially. Nonetheless, differently from the depolarizing implementation, we stress that in this case both even and odd components are pure states, so that the desired state can always be obtained from the distilled one by means of the PO transformations previously discussed. Thus, we conclude that the implementation employing artificial amplitude damping channels enables the robust preparation of any maximally entangled state of two fermionic qubits in a way which is deterministic already in just one run of the protocol.

7.4 Implementation without externally activated noisy channels

In this Section, we analyze the situation where the artificial introduction of externally activated noise is not possible. Given its role of resetting the qubits to a determined state, dropping this assumption introduces new factors which ultimately determine the performances of the setup. In particular, the initial state $|\psi_0\rangle$, the type of environmental induced noise acting on the particles before the BS, and the interaction time t all affect the distilled state. In this work, we consider the pure initial state

$$|\psi_0\rangle = a\,|L\uparrow, R\downarrow\rangle + b\,e^{i\phi}\,|L\downarrow, R\uparrow\rangle\,. \tag{7.6}$$

Here, a is a real and positive number, $b := \sqrt{1-a^2}$, and $\phi \in [0, 2\pi)$. We highlight that the quantum correlations carried by $|\psi_0\rangle$ depend on the parameter a, ranging from separable states for $a = 0, 1$ to maximally entangled ones for $a = 1/\sqrt{2}$. Notice that, in the latter situation, we recover the Bell states $|1_+\rangle_{\rm LR}$, $|1_-\rangle_{\rm LR}$ in Eq. (7.1) when $\phi = 0, \pi$, respectively. We study three standard models of local noisy environments: phase damping channels, depolarizing channels, and amplitude damping channels. Within this framework, the results discussed in Ref. [3] for bosons and in the previous Section for fermions provide the limiting case of the two latter types of noise when $t \to \infty$, with the addition of a PR on one mode in the amplitude damping scenario. Particle statistics is taken into account, to highlight the different performances of bosons and fermions. Furthermore, we focus on a non-iterated version of the process.

7.4.1 Characterization of the noisy environments

We consider the two noisy environments to be of the same type and to independently act on one spatial mode each. We model them as baths of harmonic oscillators at zero temperature, the interaction with the particles being described by a qubit-cavity model where the coupling involves one single excited mode of the baths [131]. We assume the spectral density of the baths to be Lorentzian, i.e. [131, 132],

$$J(\omega) = \frac{\gamma}{2\pi} \frac{\lambda^2}{(\omega - \omega_0)^2 + \lambda^2}, \tag{7.7}$$

where γ is the coupling strength between the system and the related environment, λ is the spectral width of the coupling, and ω_0 is the qubit transition frequency. We compute the dynamics of the system using the operator-sum formalism [32, 131]. While the structure of the employed Kraus operators depends on the specific type of environment considered, they all encompass the time-dependent disturbance probability $p(t)$, which for the Lorentzian spectral density in Eq. (7.7) is given by [131, 133]

$$p(t) = 1 - e^{-\lambda t} \left[\cos\left(\frac{d\,t}{2}\right) + \frac{\lambda}{d} \sin\left(\frac{d\,t}{2}\right) \right]^2, \tag{7.8}$$

with $d := \sqrt{2\gamma\lambda - \lambda^2}$.

7.4.2 Phase damping channel

Under the action of two local phase damping channels, the initial state $\rho_0 = |\psi_0\rangle\langle\psi_0|$ evolves into

$$\begin{aligned} \rho_{\rm pd}(t) = & \Big(1 - p(t)\Big) |\psi_0\rangle\langle\psi_0| \\ & + \frac{p(t)}{2} \Big(|1_+\rangle_{\rm LR}\langle 1_+|_{\rm LR} + |1_-\rangle_{\rm LR}\langle 1_-|_{\rm LR} \Big) \\ & + \frac{p(t)}{2} (2a^2 - 1) \Big(|1_+\rangle_{\rm LR}\langle 1_-|_{\rm LR} + |1_-\rangle_{\rm LR}\langle 1_+|_{\rm LR} \Big). \end{aligned} \tag{7.9}$$

Bosons. Two identical bosons in the state $\rho_{\rm pd}(t)$ given in Eq. (7.9) impinging on the input ports of a 50:50 BS are transformed according to Eq. (7.3) into

$$\begin{aligned} \rho_{\rm BS}^{\rm bos}(t) = & \left[\frac{1}{2} + \Big(1 - p(t)\Big)\, a\, b\, \cos\phi\right] |1_-\rangle_{\rm NO}\langle 1_-|_{\rm NO} \\ & + \left[\frac{1}{2} - \Big(1 - p(t)\Big)\, a\, b\, \cos\phi\right] |1_-\rangle_{\rm LR}\langle 1_-|_{\rm LR} \\ & + \left[\frac{1}{2} - a^2 - i\,\Big(1 - p(t)\Big)\, a\, b\, \sin\phi\right] |1_-\rangle_{\rm NO}\langle 1_-|_{\rm LR} \\ & + \left[\frac{1}{2} - a^2 + i\,\Big(1 - p(t)\Big)\, a\, b\, \sin\phi\right] |1_-\rangle_{\rm LR}\langle 1_-|_{\rm NO}\,. \end{aligned} \tag{7.10}$$

We thus notice that, by employing the parity check detector D previously introduced, we can distill either the pure NOON state $\rho_{\rm NO}^{\rm bos} := |1_-\rangle_{\rm NO}\langle 1_-|_{\rm NO}$ with probability $p_{\rm NO}^{\rm bos}(t) = \frac{1}{2} + \big(1 - p(t)\big)\, a\, b\, \cos\phi$ or the pure Bell state $\rho_{\rm LR}^{\rm bos} = |1_-\rangle_{\rm LR}\langle 1_-|_{\rm LR}$ with probability $p_{\rm LR}^{\rm bos}(t) = \frac{1}{2} - \big(1 - p(t)\big)\, a\, b\, \cos\phi$. Fig. 7.4 depicts $p_{\rm LR}^{\rm bos}(t)$ as a function of a and of the interaction time t, for $\phi = 0,\, \pi$. We notice that, as $t \to \infty$, both $p_{\rm LR}^{\rm bos}(t) \to 1/2$ and $p_{\rm NO}^{\rm bos}(t) \to 1/2$ independently on a and ϕ, that is, on the initial state. When $|\psi_0\rangle$ is separable ($a = 0,\, 1$),

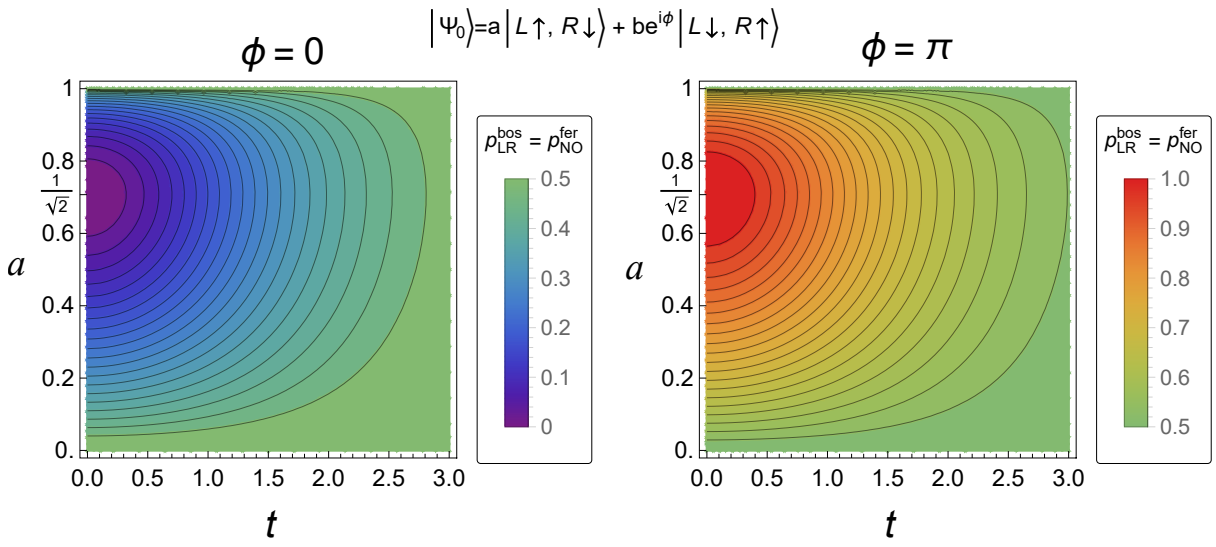

Figure 7.4: **Distillation probability** of the pure Bell state $\rho_{\rm LR}^{\rm bos}$ (NOON state $\rho_{\rm NO}^{\rm fer}$) of two bosonic (fermionic) qubits subjected to local **phase damping** for a time t. A Lorentzian spectral density is assumed (see Eq. (7.7)), with $\gamma = \lambda = 1$ (non-Markovian regime).

the detections of $\rho_{\rm LR}^{\rm bos}$ and $\rho_{\rm NO}^{\rm bos}$ are equiprobable, with $p_{\rm LR}^{\rm bos} = p_{\rm NO}^{\rm bos} = 1/2$ independently on the interaction time. Equiprobability is obtained also for $\phi = \pi/2,\, 3\pi/2$, independently on both a and t. When $|\psi_0\rangle$ is entangled and the relative phase is real, instead, it holds that $p_{\rm LR}^{\rm bos}(\phi = \pi) \geq p_{\rm LR}^{\rm bos}(\phi = 0)$ for any a and t, with the Bell singlet state ($a = 1/\sqrt{2}$, $\phi = \pi$) maximizing the probability of detecting $\rho_{\rm LR}^{\rm bos}$ at finite times. In particular, $p_{\rm LR}^{\rm bos}(t)$ increases with the interaction time for $\phi = 0$ and decreases when $\phi = \pi$. Nonetheless, we stress that both $\rho_{\rm LR}^{\rm bos}$ and $\rho_{\rm NO}^{\rm bos}$ are pure, maximally entangled states, either in the pseudospin or in the polarization, with related detection probabilities satisfying $p_{\rm NO}^{\rm bos}(t) + p_{\rm LR}^{\rm bos}(t) = 1$. Using the bosonic PO equivalences reported in Fig. 7.2, both the states can be transformed into any other maximally entangled state. Thus, we conclude that considering two bosons subjected to local phase damping, our method allows for the robust and deterministic preparation of any arbitrary pure and maximally entangled state, without the necessity to iterate the process.

Fermions. When the BS operation is applied to two identical fermionic qubits in the state given in Eq. (7.9), we get (see Eq. (7.2))

$$\begin{aligned}
\rho_{\rm BS}^{\rm fer}(t) = &\left[\frac{1}{2} + \big(1 - p(t)\big)\, a\, b\, \cos\phi\right] |1_+\rangle_{\rm LR}\, \langle 1_+|_{\rm LR} \\
&+ \left[\frac{1}{2} - \big(1 - p(t)\big)\, a\, b\, \cos\phi\right] |1_-\rangle_{\rm NO}\, \langle 1_-|_{\rm NO} \\
&+ \left[\frac{1}{2} - a^2 - i\,\big(1 - p(t)\big)\, a\, b\, \sin\phi\right] |1_+\rangle_{\rm LR}\, \langle 1_-|_{\rm NO} \\
&+ \left[\frac{1}{2} - a^2 + i\,\big(1 - p(t)\big)\, a\, b\, \sin\phi\right] |1_-\rangle_{\rm NO}\, \langle 1_+|_{\rm LR}\,.
\end{aligned} \tag{7.11}$$

As for the bosonic scenario, we notice that the parity check detector D allows to discriminate the even-parity component $\rho_{\rm NO}^{\rm fer} := |1_-\rangle_{\rm NO}\, \langle 1_-|_{\rm NO}$ of $\rho_{\rm BS}^{\rm fer}$ from the odd-parity one $\rho_{\rm LR}^{\rm fer} = |1_-\rangle_{\rm LR}\, \langle 1_-|_{\rm LR}$, detected with respective probabilities $p_{\rm NO}^{\rm fer}(t) = \frac{1}{2} - \big(1 - p(t)\big)\, a\, b\, \cos\phi$ and $p_{\rm LR}^{\rm fer}(t) = \frac{1}{2} + \big(1 - p(t)\big)\, a\, b\, \cos\phi$. Furthermore, as $p_{\rm NO}^{\rm fer}(t) = p_{\rm LR}^{\rm bos}(t)$ and $p_{\rm LR}^{\rm fer}(t) = p_{\rm NO}^{\rm bos}(t)$, the same considerations drawn for the odd-parity (even-parity) component in the bosonic

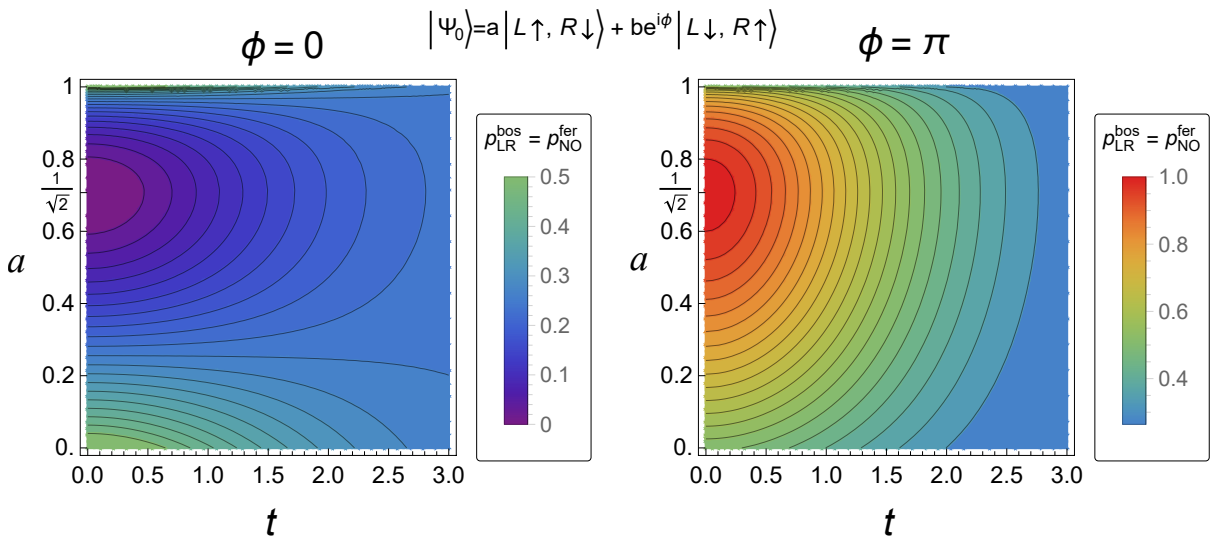

Figure 7.5: **Distillation probability** of the pure Bell state $\rho_{\rm LR}^{\rm bos}$ (NOON state $\rho_{\rm NO}^{\rm fer}$) of two bosonic (fermionic) qubits subjected to local **depolarization** for a time t. A Lorentzian spectral density is assumed (see Eq. (7.7)), with $\gamma = \lambda = 1$ (non-Markovian regime).

scenario hold for the even-parity (odd-parity) one for fermions, with $p_{\rm NO}^{\rm fer}(t)$ being reported in Fig. 7.4, too. Given the fermionic PO equivalences introduced in Subsection 7.3.1, we thus conclude that when applied to two fermions subjected to local phase damping, our method allows for the robust and deterministic preparation of any arbitrary pure and maximally entangled state, without having to iterate the process.

7.4.3 Depolarizing channel

Let us now consider the two qubits prepared in the initial state $\rho_0 = |\psi_0\rangle\langle\psi_0|$ to be subjected to the local action of a depolarizing channel each. Such an interaction leads to the Werner state

$$\rho_{\rm dep}(t) = \Big(1 - p(t)\Big)\,|\psi_0\rangle\langle\psi_0| + \frac{1}{4}\,p(t)\,\Pi_{\rm LR}, \tag{7.12}$$

with $\Pi_{\rm LR}$ defined in Subsection 7.3.2. As previously mentioned, the limit $t \to \infty$ provides the maximally mixed state studied in Ref. [3] (for bosons) and in Subsection 7.3.2 (for fermions).

Bosons. Two identical bosons in the state $\rho_{\rm dep}(t)$ given in Eq. (7.12) subjected to the BS operation in Eq. (7.3) are transformed into

$$\begin{aligned}
\rho_{\rm BS}^{\rm bos}(t) = &\Big[\frac{1}{2} - \frac{p(t)}{4} + \big(1-p(t)\big)\,a\,b\,\cos\phi\Big]\,|1_-\rangle_{\rm NO}\langle 1_-|_{\rm NO} \\
&+ \Big[\frac{1}{2} - \frac{p(t)}{4} - \big(1-p(t)\big)\,a\,b\,\cos\phi\Big]\,|1_-\rangle_{\rm LR}\langle 1_-|_{\rm LR} \\
&+ \Big(p(t)-1\Big)\big(a^2 - \frac{1}{2} + i\,a\,b\,\sin\phi\big)\,|1_-\rangle_{\rm NO}\langle 1_-|_{\rm LR} \\
&+ \Big(p(t)-1\Big)\big(a^2 - \frac{1}{2} - i\,a\,b\,\sin\phi\big)\,|1_-\rangle_{\rm LR}\langle 1_-|_{\rm NO} \\
&+ \frac{p(t)}{4}\big(\,|U_-\rangle_{\rm NO}\langle U_-|_{\rm NO} + |D_-\rangle_{\rm NO}\langle D_-|_{\rm NO}\,\big).
\end{aligned} \tag{7.13}$$

Once again, the parity check detector D can be employed to distill the pure Bell singlet state $\rho_{\rm LR}^{\rm bos} = |1_-\rangle_{\rm LR}\langle 1_-|_{\rm LR}$ with a probability $p_{\rm LR}^{\rm bos}(t) = \frac{1}{2} - \frac{p(t)}{4} - \big(1-p(t)\big)\, a\, b\, \cos\phi$. $p_{\rm LR}^{\rm bos}(t)$ is depicted in Fig. 7.5 as a function of a and t for $\phi = 0,\, \pi$.

First of all, $p_{\rm LR}^{\rm bos}(t) \to 1/4$ as $t \to \infty$ independently on a and ϕ, i.e., on the initial state $|\psi_0\rangle$, in agreement with the results reported in Ref. [3] when depolarization is used to reset the system to a maximally mixed state. Furthermore, it holds once again that $p_{\rm LR}^{\rm bos}(\phi = \pi) \geq p_{\rm LR}^{\rm bos}(\phi = 0)$ for any a and t. In particular, the Bell singlet state ($a = 1/\sqrt{2}$, $\phi = \pi$) is found to maximixe $p_{\rm LR}^{\rm bos}(t)$ at finite times. Nonetheless, differently from the phase damping scenario, the interaction time affects the probability of distilling $\rho_{\rm LR}^{\rm bos}$ even when the initial state is separable ($a = 0,\, 1$), ranging from $p_{\rm LR}^{\rm bos} = 1/2$ to $p_{\rm LR}^{\rm bos} = 1/4$ as $t \to \infty$. The same behaviour is obtained when $\phi = \pi/2,\, 3\pi/2$, regardless of a.

Fermions. When the two particles impinging on the BS are fermions, the state $\rho_{\rm dep}(t)$ in Eq. (7.12) is mapped into

$$\begin{aligned}
\rho_{\rm BS}^{\rm fer}(t) = &\left[\frac{1}{2} - \frac{p(t)}{4} + \big(1-p(t)\big)\, a\, b\, \cos\phi\right] |1_+\rangle_{\rm LR}\langle 1_+|_{\rm LR} \\
&+ \left[\frac{1}{2} - \frac{p(t)}{4} - \big(1-p(t)\big)\, a\, b\, \cos\phi\right] |1_-\rangle_{\rm NO}\langle 1_-|_{\rm NO} \\
&+ \Big(p(t)-1\Big)\Big(a^2 - \frac{1}{2} + i\, a\, b\, \sin\phi\Big)\, |1_+\rangle_{\rm LR}\langle 1_-|_{\rm NO} \\
&+ \Big(p(t)-1\Big)\Big(a^2 - \frac{1}{2} - i\, a\, b\, \sin\phi\Big)\, |1_-\rangle_{\rm NO}\langle 1_+|_{\rm LR} \\
&+ \frac{p(t)}{4}\big(\, |2_+\rangle_{\rm LR}\langle 2_+|_{\rm LR} + |2_-\rangle_{\rm LR}\langle 2_-|_{\rm LR}\,\big).
\end{aligned} \tag{7.14}$$

Analogously to the bosonic scenario and in agreement with the results discussed in Subsection 7.3.2, the parity check detector D can be used to distill the NOON state $\rho_{\rm NO}^{\rm fer} = |1_-\rangle_{\rm NO}\langle 1_-|_{\rm NO}$ with probability $p_{\rm NO}^{\rm fer}(t) = \frac{1}{2} - \frac{p(t)}{4} - \big(1-p(t)\big)\, a\, b\, \cos\phi$. Since $p_{\rm NO}^{\rm fer}(t) = p_{\rm LR}^{\rm bos}(t)$, Fig. 7.5 also reports $p_{\rm NO}^{\rm fer}(t)$ and the same considerations discussed for the distillation of the bosonic Bell singlet state can be drawn for the fermionic NOON state $|1_-\rangle_{\rm NO}$.

7.4.4 Amplitude damping channel

Finally, we study the performance of the proposed method when the two qubits are independently subjected to a local amplitude damping channel. In this situation, the initial state $\rho_0 = |\psi_0\rangle\langle\psi_0|$ evolves into

$$\rho_{\rm ad}(t) = \Big(1-p(t)\Big)\, |\psi_0\rangle\langle\psi_0| + p(t)\, |L\downarrow, R\downarrow\rangle\langle L\downarrow, R\downarrow|\,, \tag{7.15}$$

where $|L\downarrow, R\downarrow\rangle = (|2_+\rangle_{\rm LR} - |2_-\rangle_{\rm LR})/\sqrt{2}$ is the two-particle ground state. We highlight that, differently from the analogous scenario in Ref. [3] and in Section 7.3, here we do not assume the presence of a PR rotating the pseudospin of particles on one spatial mode before the BS operation.

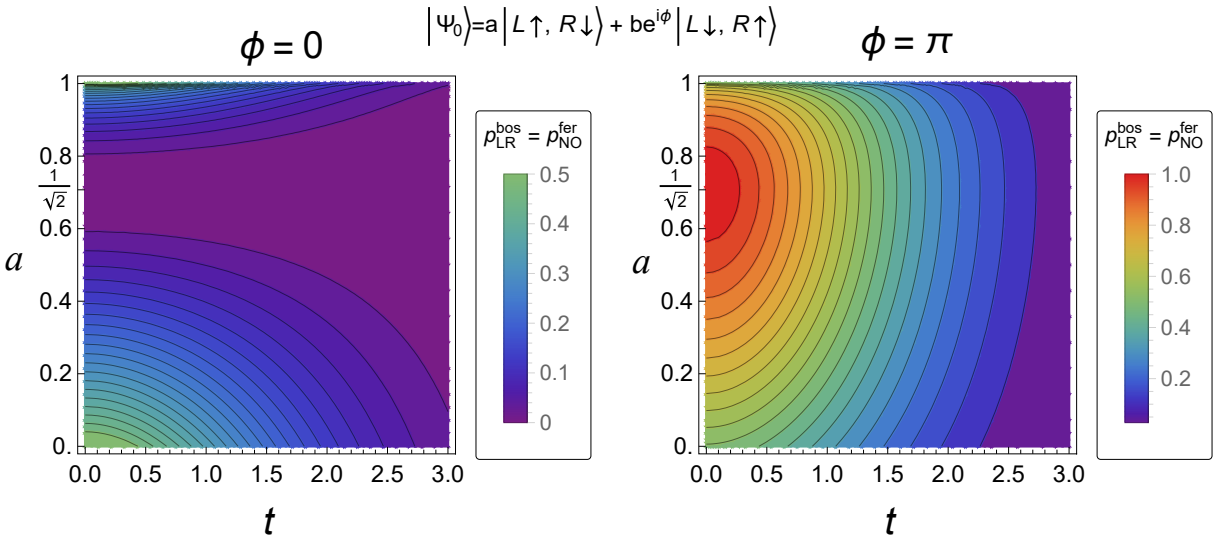

Figure 7.6: **Distillation probability** of the pure Bell state $\rho_{\rm LR}^{\rm bos}$ (NOON state $\rho_{\rm NO}^{\rm fer}$) of two bosonic (fermionic) qubits subjected to local **amplitude damping** for a time t. A Lorentzian spectral density is assumed (see Eq. (7.7)), with $\gamma = \lambda = 1$ (non-Markovian regime).

Bosons. The action of a BS on the bosonic state $\rho_{\rm ad}(t)$ given in Eq. (7.15) returns

$$\begin{aligned}\rho_{\rm BS}^{\rm bos}(t) = \Big(1-p(t)\Big)\Big[&\Big(\frac{1}{2}+a\,b\,\cos\phi\Big)\,|1_-\rangle_{\rm NO}\,\langle 1_-|_{\rm NO}\\ &+\Big(\frac{1}{2}-a\,b\,\cos\phi\Big)\,|1_-\rangle_{\rm LR}\,\langle 1_-|_{\rm LR}\\ &-\Big(a^2-\frac{1}{2}+i\,a\,b\,\sin\phi\Big)\,|1_-\rangle_{\rm NO}\,\langle 1_-|_{\rm LR}\\ &-\Big(a^2-\frac{1}{2}-i\,a\,b\,\sin\phi\Big)\,|1_-\rangle_{\rm LR}\,\langle 1_-|_{\rm NO}\Big]\\ &+p(t)\,|D_-\rangle_{\rm NO}\,\langle D_-|_{\rm NO}\,.\end{aligned} \tag{7.16}$$

The detector D allows to distill the pure Bell singlet state $\rho_{\rm LR}^{\rm bos} = |1_-\rangle_{\rm LR}\langle 1_-|_{\rm LR}$ with probability $p_{\rm LR}^{\rm bos}(t) = (1-p(t))(\frac{1}{2} - a\,b\,\cos\phi)$, depicted in Fig. 7.6.

As for the phase damping and the depolarizing channels, we notice that $p_{\rm LR}^{\rm bos}(\phi=\pi) \geq p_{\rm LR}^{\rm bos}(\phi=0)$ for every a, t. In particular, such a probability reaches its maximum at finite times when $|\psi_0\rangle$ is a Bell singlet state. However, this time $p_{\rm LR}^{\rm bos}(t)$ decays to 0 with the interaction time regardless of a and ϕ. As in this case $\rho_{\rm NO}^{\rm bos}(t)$ is not a pure state (similarly to the depolarizing scenario and in contrast with the phase damping one), at first sight such a decay could be interpreted as an inefficacy of the proposed technique to distill pure and maximally entangled states when the particles of interest have been subjected to the considered noise for too long. Nonetheless, we highlight that in the limit $t \to \infty$ the even parity state $\rho_{\rm NO}^{\rm bos}$ becomes the pure NOON state $|D_-\rangle_{\rm NO}$, and $p_{\rm NO}^{\rm bos}(t) = 1 - p_{\rm LR}^{\rm bos}(t) \to 1$. Thus, for sufficiently long interaction times we should collect the qubits when the detector D signals an even number of particles, achieving the distillation of a state which becomes pure as $t \to \infty$.

Fermions. When dealing with identical fermions, the state $\rho_{\rm ad}(t)$ in Eq. (7.12) is

transformed by a BS into

$$\begin{aligned}\rho_{\rm BS}^{\rm fer}(t) = \Big(1-p(t)\Big)\Big[&\Big(\frac{1}{2}+a\,b\,\cos\phi\Big)\,|1_+\rangle_{\rm LR}\,\langle 1_+|_{\rm LR}\\ &+\Big(\frac{1}{2}-a\,b\,\cos\phi\Big)\,|1_-\rangle_{\rm NO}\,\langle 1_-|_{\rm NO}\\ &-\Big(a^2-\frac{1}{2}+i\,a\,b\,\sin\phi\Big)\,|1_+\rangle_{\rm LR}\,\langle 1_-|_{\rm NO}\\ &-\Big(a^2-\frac{1}{2}-i\,a\,b\,\sin\phi\Big)\,|1_-\rangle_{\rm NO}\,\langle 1_+|_{\rm LR}\Big]\\ &+p(t)\,|L\downarrow,R\downarrow\rangle\,\langle L\downarrow,R\downarrow|\,.\end{aligned} \tag{7.17}$$

As in the other fermionic scenarios discussed, the detector D allows to distill the pure NOON state $\rho_{\rm NO}^{\rm fer} = |1_-\rangle_{\rm NO}\,\langle 1_-|_{\rm NO}$. The probability of such a detection is given by $p_{\rm NO}^{\rm fer}(t) = (1-p(t))(\frac{1}{2}-a\,b\,\cos\phi)$, which is reported in Fig. 7.6 as $p_{\rm NO}^{\rm fer}(t) = p_{\rm LR}^{\rm bos}(t)$. The considerations drawn for detection of the odd component in the bosonic situation are thus valid also for the detection of $\rho_{\rm NO}^{\rm fer}$. Nonetheless, an important difference emerges: in the limit $t\to\infty$ the fermionic odd-component, which is the only one distillable as $p_{\rm LR}^{\rm fer}(t) = p_{\rm NO}^{\rm bos}(t) \to 1$, is the pure state $\rho_{\rm LR}^{\rm fer} = |L\downarrow,R\downarrow\rangle\,\langle L\downarrow,R\downarrow|$ which is not entangled. Notice that the presence of this term in $\rho_{\rm BS}^{\rm fer}$ in contrast to $\rho_{\rm BS}^{\rm bos}$ is due to the anti-bunching effect characterizing identical fermions, which makes $|L\downarrow,R\downarrow\rangle$ in $\rho_{\rm ad}(t)$ invariant under the action of a BS whereas the bosonic bunching effect transforms it into the maximally entangled NOON state $|D_-\rangle_{\rm NO}$. Nonetheless, the fermionic state $|L\downarrow,R\downarrow\rangle$ can be transformed into a maximally entangled state by means of PO transformations and the detector D as discussed in Subsection 7.3.2, that is, by rotating the pseudospin of the qubit on one region, by applying a BS operation to the resulting state, and by finally distilling either the odd component $|1_+\rangle_{\rm LR}$ or the even one $|1_-\rangle_{\rm NO}$.

7.5 Conclusions

We have extended a theoretical procedure for the robust preparation of maximally entangled states introduced in Ref. [3] for bosons to the fermionic scenario. Considering two qubits set on two distinct spatial modes and subjected to local environmental noise, the protocol employs two externally activated local noisy channels to reset the bipartite state to a known one. A BS is then used to set the system in a mixture or a superposition of NOON states, entangled in the spatial mode, and Bell states, entangled in the internal degree of freedom. A non-absorbing, pseudospin-independent, parity check detector D set on one mode is later used to discriminate between the two components, distilling a maximally entangled state which is shown to be pure. Such a result is independent on the initial state of the system, on the characteristics of the environments, and on the interaction between the two besides requiring the latter to be local and particle-preserving, making the proposed preparation robust. We have analyzed two possible implementations of the protocol: one employing depolarizing channels as the externally activated noises, and one using amplitude damping channels as such. In both cases, the procedure can be iterated; by doing so, the implementation relying on externally activated depolarizing channels achieves determinism asymptotically with the number of iterations, while determinism can be reached either asymptotically or in a single run when employing externally activated amplitude damping channels.

It is worth to stress some main differences with previous works [2,37], where the authors present indistinguishability-based probabilistic preparation of Bell singlet states starting from noisy states which arise from unavoidable system-environment interactions. Here, we have extended such results by introducing the non-absorbing parity check detector, which allows to iterate the process achieving an asymptotically-deterministic preparation. Focusing on the indistinguishability of the two qubits at a beam splitter, we have also stressed the interplay between NOON states and Bell states, showing how pure NOON states can be distilled in the fermionic scenario. A further improvement comes from the insertion of this result in a wider preparation framework where noisy channels are suitably externally activated to reset the system to a desired state. Crucially, this solution leads to a protocol which is independent of the initial state and of any system-environment interaction occurring prior to the BS operation.

We have extended the bosonic PO equivalences introduced in Ref. [3] to fermions, showing that all the pure maximally entangled states of two fermionic qubits distributed on two spatial modes can be obtained one from another by means of transformations analogous to passive optical ones. Provided with such a set of transformations, the proposed framework can thus be employed to deterministically prepare any arbitrary maximally entangled state of two identical fermionic qubits.

The difficulty in realizing a polarization-insensitive, non-absorbing, parity check detector constitutes the main obstacle hindering an experimental implementation of the proposed scheme. Nonetheless, we emphasize that two commercially available single photon detectors can be used in its place to postselect the odd components by performing a coincidence measurement on the two spatial modes. In this way, the implementation employing amplitude damping channels can be used to achieve the probabilistic distillation of a pure fermionic Bell state with probability $p_{\mathrm{LR}} = 1/2$.

We have further studied the performances of our technique when the artificially induced noisy channels are not employed, analyzing both bosonic and fermionic qubits. In this case, the initial state, the characteristics of the environmental noise, and the system-environment interaction time all affect the result. We have taken the two particles to be initially prepared in a generic superposition of anti-parallel pseudospin states as given by Eq. (7.6). Such a set of states includes both entangled and separable ones, allowing the role of the initial quantum correlations to be assessed. The two environments acting locally on the qubits have been modeled as identical phase damping channels, depolarizing channels, and amplitude damping channels. Focusing on a single run of the protocol, we have shown that it allows to distillate pure and maximally entangled states deterministically when dealing with phase damping channels. When considering depolarizing channels, instead, a pure maximally entangled state can be prepared conditionally, with a distillation probability decaying to $1/4$ asymptotically with the interaction time regardless of the initial state. Nonetheless, preparing the system in a Bell singlet state increases the chances of success at finite interaction times. Finally, a pure maximally entangled state is probabilistically achieved when the two constituents are affected by amplitude damping noise for a finite time t, whereas a deterministic distillation is achievable as $t \to \infty$ regardless of the initial state. Remarkably, all the above results hold for both bosons and fermions.

We stress that the core of the proposed procedure lies in the bunching/antibunching interferometric effects characterizing identical particles under the action of a BS. In particular, we notice from Eqs. (7.2) and (7.3) that the singlet is the only Bell state whose number of particles on one spatial mode changes parity (for fermions) or preserves it

(for bosons) under a BS transformation. Thus, the parity-check detector ultimately discriminates the pure BS-transformed singlet component from the other ones, achieving the desired distillation. With a specific focus on coincidence measurements, i.e., on the detection of odd-parity terms, this mechanism is also at the heart of the technique employing the *spatially localized operations and classical communication* (sLOCC) operational framework [1, 20, 23, 59, 60, 74, 154] to recover the quantum correlations initially present in a Bell singlet state subjected to the local action of noisy environments [2, 37, 38].

Finally, we emphasize that in order that the discussed interference effects properly occur, the different 2-particle probability amplitudes must be indistinguishable when the qubits are collected. Crucially, as demonstrated in Ref. [157], this requirement is not equivalent to ask for the two particles to simultaneously impinge on the BS; an arbitrary time delay is indeed acceptable, provided it gets compensated after the BS. If a time delay occurs due, e.g., to the particle sources being desynchronized, the results of this paper can thus be restored, for example, by suitably arranging the lengths of the different paths after the BS or, referring to a photonic implementation, by inducing a proper dephasing on the particles with birefringent media prior to their collection [157, 158].

Chapter 8

Robust generation of N-partite N-level singlet states by identical particle interferometry

Abstract

We propose an interferometric scheme for generating the totally antisymmetric state of N identical bosons with N internal levels (generalized singlet). This state is a resource for various problems with dramatic quantum advantage. The procedure uses a sequence of Fourier multi-ports, combined with coincidence measurements filtering the results. Successful preparation of the generalized singlet is confirmed when the N particles of the input state stay separate (anti-bunch) on each multiport. The scheme is robust to local lossless noise and works even with a totally mixed input state.

This chapter reports the results of our manuscript of Ref. [159].

8.1 Introduction

Manipulation of entangled states is necessary to fully access the advantages of quantum technologies. For this reason, great attention has been dedicated to classes of entangled states proven to be useful for quantum information tasks, ranging from the simplest 2-qubit Bell states [32], to more complex classes of many-body systems such as W states [160], GHZ states [161, 162], NOON states [25], Dicke states [163], and many more [26].

Crucially, quantum correlations characterizing such states must be protected from the detrimental action of external noise to allow for their real-world exploitation. A plethora of techniques has been suggested to achieve this goal, including decoherence-free subspaces [112,113], structured environments with memory effects [98–100,102–108], quantum error correction codes [94–97], dynamical decoupling and control techniques [114–123], quantum repeaters [164–166], distillation protocols [109–111, 149–151], and interferometric effects in systems of identical particles [2, 3, 37, 38, 155, 167]. These techniques can be applied to physical systems featuring a wide range of inherent fragility to environmental noise. In particular, photons have a long coherence time, making them suitable for long-distance communications between remote parties [168,169]. However, there is a trade-off: as photons interact little with each other directly, entangling them requires alternative

methods such as nonlinear multiphoton generation techniques (such as SPDC [170] and four-wave mixing [171,172]), heralding processes [173–178], or postselected measurements of identical photons spatially overlapping over detection regions [1, 20, 60].

These techniques are typically employed in long-range communication scenarios, in which the resource states prepared by the sender require protection during their propagation through noisy environments. In Refs. [3, 167], the authors shift this viewpoint by proposing a protocol where the entangled resource is prepared by the receiver after the environmental noise has affected the system. To this end, they devise a scheme to prepare maximally entangled states of two identical qubits which probabilistically succeeds regardless of the initial state, that is, regardless of local particle-preserving noise previously acting on the system. This goal is achieved by locally injecting white noise on the two qubits, which resets the system to the maximally mixed state. The various components of the mixture interfere differently under the action of a beam splitter, with bosonic particles in the singlet state staying separate (anti-bunching) and the ones in symmetric states grouping together (bunching). This effect can then be exploited to postselect a pure Bell singlet state of two identical bosons with coincidence measurements.

In the present work, we extend this protocol to N identical bosons with N internal levels and devise a scheme to generate an N-partite singlet state from a maximally mixed state having one particle per mode. The multipartite singlet state, which is antisymmetric under the exchange of any pair of particles, can be exploited to solve communication tasks which have no known classical solution [179–181] and certify the non-projective character of measurements [182]. Furthermore, entangled states of spatially distinguishable particles can be used to simulate particle statistics of different types, a phenomenon which has been shown to obey monogamous relations: a totally antisymmetric state of N distinct bosons can thus provide a useful testing ground to study the properties of N spatially indistinguishable fermions [183]. Finally, generalized singlet states are invariant under global rotations of the internal levels and are characterized by a zero variance of the related pseudospin operator J^2. This property makes them potentially useful in quantum metrology, where they can be used to probe local fields with enhanced performances [184].

The usefulness of generalized singlet states is hindered by the difficulty of obtaining them. To achieve this, a method based on a sequence of quantum nondemolition (QND) measurements has been proposed in [185]. This technique, already implemented with both cold [186] and hot [187] atomic ensembles, involves postselection and allows for the preparation of a state approximating the generalized singlet. However, it does not lead to an exact, pure generalized singlet state, not even when endowed with a feedback mechanism implementing corrections between the measurements [188].

In contrast to this, the technique we propose here allows for the probabilistic preparation of exact multipartite singlet states. To do so, we relate the behavior of N identical particles injected in an N-port interferometer to their symmetries, as dictated by the general suppression law reported in Ref. [189]. Subsequently, we use the obtained insights to devise a scheme composed of a sequence of Fourier $2, \ldots, N-1, N$-port interferometers interlaced with QND coincidence measurements performed on the related output modes. As in Refs. [3, 167], the maximally mixed initial state guarantees that our procedure is robust under the action of local noise acting on the N particles. Finally, we propose an implementation that employs postselection and a specific initial state to prepare an $N = 3$ generalized singlet state without QND measurements.

8.2 Generalized singlet state

The goal of this work is to design an interferometric procedure to prepare the generalized singlet state of N spatially separated bosons with N internal levels

$$|A_N\rangle := \frac{1}{\sqrt{N!}} \sum_{\pi \in S_N} \prod_{i=1}^{N} \mathrm{sgn}\,(\pi)\, a^{\dagger}_{i,\pi(i)} \,|0\rangle\,, \tag{8.1}$$

where $\mathrm{sgn}\,(\pi)$ is the sign of the permutation π from symmetric group S_N, and $a^{\dagger}_{\ell,m}$ denotes the operator creating a particle with internal state m in spatial mode ℓ. For example, $|A_2\rangle = (|0,1\rangle - |1,0\rangle)/\sqrt{2}$ is the ordinary Bell singlet state of two qubits, whereas for three qutrits we have $|A_3\rangle = (|0,1,2\rangle - |0,2,1\rangle - |1,0,2\rangle + |1,2,0\rangle + |2,0,1\rangle - |2,1,0\rangle)/\sqrt{6}$. The interest in this class of states stems from their rotational invariance, leading to applications in quantum protocols [179], and total antisymmetry, which brings these bosonic states as close to fermionic properties as possible [183].

The systematic classification of the types of symmetries of N particles with d internal levels can be achieved with representation theory [190]. One of its basic results states that the space of totally antisymmetric states of N constituents with N internal levels is one-dimensional, that is, $|A_N\rangle$ is the unique totally antisymmetric state of the considered system.

8.3 Suppression law for anti-bunching

In order to prepare the generalized singlet state $|A_N\rangle$ given in Eq. (8.1), we consider the transformation of the input state under a Fourier N-port given by

$$b^{\dagger}_{k,m} = \sum_{\ell=1}^{N} (U_N)_{k,\ell}\, a^{\dagger}_{\ell,m}, \tag{8.2}$$

where $b^{\dagger}$ denotes the creation operator for the output mode and the matrix U_N is given by

$$U_N = \frac{1}{\sqrt{N}} \begin{pmatrix} 1 & 1 & 1 & \dots & 1 \\ 1 & \omega & \omega^2 & \dots & \omega^{N-1} \\ 1 & \omega^2 & \omega^4 & \dots & \omega^{2(N-1)} \\ \vdots & \vdots & \vdots & \vdots & \vdots \\ 1 & \omega^{N-1} & \omega^{2(N-1)} & \dots & \omega^{(N-1)(N-1)} \end{pmatrix} \tag{8.3}$$

for $\omega = e^{2\pi i/N}$. Since the state $|A_N\rangle$ has a single particle in each spatial mode, we would like to pin down the conditions that an N-particle input state must satisfy in order to anti-bunch on the Fourier N-port.

Conveniently, in Ref. [189] Dittel *et al.* provide a suppression law characterizing prohibited outcomes in interferometric experiments for a class of multiports including Fourier N-ports. Their results imply that the eigenstates $|\varphi\rangle$ of the cyclic permutation $\pi_{(1,2,\dots,N)}$ that can anti-bunch when transformed by U_N need to obey (see Appendix A)

$$\pi_{(1,2,\dots,N)}\,|\varphi\rangle = (-1)^{N-1}\,|\varphi\rangle\,. \tag{8.4}$$

To use this insight, let us note that a generic input state $|\psi_{\mathrm{in}}\rangle$ of N particles with N internal levels can always be decomposed in the N-particle eigenbasis of $\pi_{(1,2,\dots,N)}$. Then,

the condition Eq. (8.4) rules that $|\psi_{\rm in}\rangle$ can anti-bunch when transformed by U_N only if its projection onto the $(-1)^{N-1}$-eigenspace of $\pi_{(1,2,\ldots,N)}$ is nonzero. We denote this eigenspace $E_{(-1)^{N-1}}(\pi_{(1,2,\ldots,N)})$ and define the related projection operator

$$P_{E_{(-1)^{N-1}}(\pi_{(1,2,\ldots,N)})} := \frac{1}{N}\sum_{k=1}^{N}\left[(-1)^{N-1}\,\pi_{(1,2,\ldots,N)}\right]^k. \tag{8.5}$$

It is clear now that *a necessary condition for a generic N-boson input state $\rho_{\rm in}$ to anti-bunch on a Fourier N-port reads*

$$\mathrm{Tr}\left[\rho_{\rm in}P_{E_{(-1)^{N-1}}(\pi_{(1,2,\ldots,N)})}\right] \neq 0. \tag{8.6}$$

8.4 Implementing the eigenspace projector

Condition given by Eq. (8.6) can also be interpreted as an operational recipe for implementing a projection into the eigenspace $E_{(-1)^{N-1}}(\pi_{(1,2,\ldots,N)})$. It consists in casting an input state composed of N particles, one in each spatial mode, on a Fourier N-port followed by performing a coincidence measurement on the output modes. In particular, this measurement can be realized by means of N quantum non-demolition single particle detectors filtering out non-coincident detections, effectively implementing the operator $C_N = \sum_{\sigma_1,\ldots,\sigma_N=0}^{N-1}|\sigma_1,\ldots,\sigma_N\rangle\langle\sigma_1,\ldots,\sigma_N|$. This constitutes the basic step of our protocol.

8.5 Extracting the singlet

Let us now consider a sequence of the above steps with the size of the Fourier multiport increasing from 2 to N, defining $M_k := \prod_{j=k}^{2} C_jU_j$ (notice that the index in the product decreases to reflect the order of the operations). We are going to show that for an input state with a single d-level particle in each of N modes we have

$$M_N = e^{i\phi_N}\prod_{j=N}^{2} P_{E_{((-1)^{j-1})}(\pi_{(1,\ldots,j)})}, \tag{8.7}$$

where ϕ_N is an irrelevant global phase. By direct calculation one can verify that Eq. (8.7) is satisfied for $N = 2$. Suppose now that it holds for any $k < N$, with $N > 2$. Since Eq. (8.6) provides a necessary condition for anti-bunching, we have $\mathrm{supp}(C_NU_N) \subseteq \mathrm{Im}(P_{E_{(-1)^{N-1}}(\pi_{(1,2,\ldots,N)})})$. Thus we have

$$M_N = C_NU_NP_{E_{((-1)^{N-1})}(\pi_{(1,\ldots,N)})}\prod_{j=N-1}^{2} C_jU_j = e^{i\phi_{N-1}}C_NU_N\prod_{j=N}^{2} P_{E_{((-1)^{j-1})}(\pi_{(1,\ldots,j)})}. \tag{8.8}$$

But it can be shown (see Appendix B) that

$$\prod_{j=N}^{2} P_{E_{((-1)^{j-1})}(\pi_{(1,\ldots,j)})} = \frac{1}{N!}\sum_{\pi\in S_N}\mathrm{sgn}(\pi)\,\pi = P_{A_N^d}, \tag{8.9}$$

where $P_{A_N^d}$ is the projector onto the totally antisymmetric subspace of N particles with d internal levels. Therefore $M_N = e^{i\phi_{N-1}}C_NU_NP_{A_N^d}$. It remains to be shown that any state

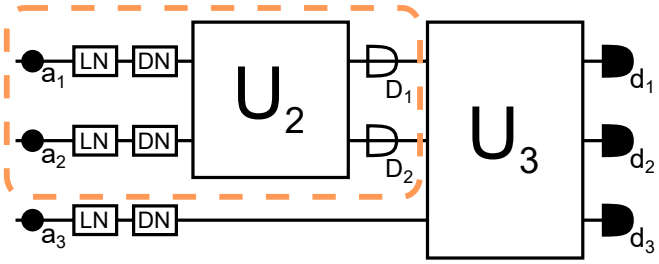

Figure 8.1: Procedure for the preparation of the $N = 3$ bosonic generalized singlet state $|A_3\rangle$. Three identical bosons localized on distinct modes are subjected to arbitrary local noise (LN) and subsequently depolarized (DN). Later on, two of them are cast onto a beam splitter U_2. Two single-particle non-absorbing detectors perform a coincidence measurement on the output modes, selecting only the anti-bunched results. The three particles are then injected into a tritter U_3. Three single-particle detectors perform a final coincidence measurement on the output, collecting only the anti-bunched states. The last step can be done either with QND detectors or with absorbing detectors via postselection. Part of the scheme enclosed in a dashed box can be replaced with a heralded generation of the singlet state $|A_2\rangle$.

from the totally antisymmetric subspace is invariant under Fourier multiport U_N and coincident detection C_N. For the sake of simplicity we restrict our attention to $d = N$ (see Appendix C for the general case). The totally antisymmetric space is then spanned by $|A_N\rangle$. From Eq. (8.2) and Eq. (8.1) it follows that

$$U_N|A_N\rangle = \frac{1}{\sqrt{N!}} \det(U_N \mathsf{A})\,|0\rangle, \tag{8.10}$$

where

$$\mathsf{A} = \begin{pmatrix} a^\dagger_{1,1} & a^\dagger_{1,2} & \dots & a^\dagger_{1,N} \\ a^\dagger_{2,1} & a^\dagger_{2,2} & \dots & a^\dagger_{2,N} \\ \vdots & \vdots & \vdots & \vdots \\ a^\dagger_{N,1} & a^\dagger_{N,2} & \dots & a^\dagger_{N,N}. \end{pmatrix} \tag{8.11}$$

But as $\det(U_N\mathsf{A}) = \det U_N \det \mathsf{A} = (-1)^{N+1} \det \mathsf{A}$ we get that $U_N|A_N\rangle = (-1)^{N+1}|A_N\rangle$. Clearly the global phase shift is irrelevant, and the fact that $|A_N\rangle$ has a single particle in each mode ensures that it is not affected by the coincidence measurement C_N.

This shows that *the generalized singlet state of N identical bosons with N levels can be probabilistically distilled from an arbitrary initial state ρ_{in} with a single particle per mode by acting on it with a sequence of Fourier $2-, \dots, N$-ports and selecting only the results which anti-bunch at every step* (see Fig. 8.1 for a pictorial representation of the setup for $N = 3$). The procedure we just described can be seen as a filtering scheme where the generalized singlet component of the input state ρ_{in} is probabilistically distilled. Its success probability $p_s = \text{Tr}\left[|A_N\rangle\langle A_N|\,\rho_{\text{in}}\right]$ depends on the overlap of the initial state with the generalized singlet, in particular being null when there is none.

It should be stressed that the coincidence measurements C_j must be nondemolitive, as the particles emerging from a Fourier multiport are later cast onto the next one. Such measurements can be implemented with nonabsorbing detectors [191–193]. This requirement does not hold for the last measurement (following the Fourier N-port), which can be realized using standard single particle detectors in a postselected implementation [1, 3, 59, 60, 167].

8.6 Robust generalized singlet preparation

As previously stated, we want to distill the generalized singlet state in a way which is robust to the action of lossless local noise acting on the initial state. To do so, we start with an arbitrary state ρ_N of N identical bosons with N internal levels occupying one spatial mode each. Following the idea introduced in Ref. [3, 167], we act on each particle with local externally-activated depolarizing noise, obtaining the N-body maximally mixed state $\rho_{\text{dep}} = \bigotimes_{j=1}^{N} \rho_j$, where ρ_j is the Werner state $\rho_j = \frac{1}{N}\sum_{k=0}^{N-1} |k\rangle_j\langle k|_j$ of the particle in the j^{th} mode with internal level k. This operation has a double role: first of all, it resets the system to the known state $\rho_{\text{in}} = \rho_{\text{dep}}$, thus making the obtained result independent of the original state ρ_N, of the characteristics of the noisy environments acting on the constituents prior to the depolarization, and on the interaction time between them. Secondly, it ensures that the state ρ_{in} injected in the setup has a nonzero overlap with the generalized singlet, guaranteeing that the probability of extracting $|A_N\rangle$ is non-zero. Indeed, ρ_{dep} can always be expressed in a diagonal form on a N^N-dimensional orthonormal basis which includes $|A_N\rangle$. Therefore, the proposed preparation technique is deemed to be robust, although it succeeds with probability

$$p_s = \text{Tr}\left[|A_N\rangle\langle A_N|\,\rho_{\text{dep}}\right] = 1/N^N. \tag{8.12}$$

8.7 Alternative realizations with specific initial states

In the suggested implementation, robustness to noise is obtained in exchange for a low success rate and the requirement of QND measurements. Nonetheless, these two drawbacks can be mitigated when a free choice of the initial state is allowed. This is the case, for example, of a preparation occurring immediately after the state initialization, or when the noise affecting the system between the source and the implementation of our scheme is negligible. In these scenarios, for instance, the preparation of N spatially separated bosons in the product state $|0, 1, \ldots, N-1\rangle$ would guarantee an enhanced success probability of $p_s = 1/N!$.

The possibility to choose the initial state also allows to avoid relying on nonabsorbing detectors in specific scenarios, opening the path for realistic experimental implementations. Consider, for example, $N = 3$ qutrits in the initial state $|\psi_{\text{in}}\rangle = |A_2\rangle \otimes |2\rangle$. The implementation of the Fourier 2-port (beam splitter) can now be avoided, reducing our setup to a single tritter: indeed, it can be easily checked that $C_3U_3\,|\psi_{\text{in}}\rangle = |A_3\rangle$, so that the generalized singlet state is distilled with probability $p_s = |\langle A_3|\psi_{\text{in}}\rangle|^2 = 1/3$. Similarly, we can allow for the third qutrit to be depolarized as in the robust approach (see Figure 8.1), obtaining $\rho_{\text{in}} = |A_2\rangle\langle A_2| \otimes \frac{1}{3}\big(\sum_{k=0}^{2} |k\rangle\langle k|\big)$ and preparing $|A_3\rangle$ with probability $p_s = \text{Tr}\left[|A_3\rangle\langle A_3|\,\rho_{\text{in}}\right] = 1/9$. Crucially, the QND measurement C_3 can be substituted in both cases by a postselection carried out with standard single-particle detectors. The preparation of such initial states only requires the ability to entangle 2 qutrits in a Bell singlet-like state and to eventually depolarize a third one, a challenge which could be tackled, for example, with frequency-bin manipulation techniques [194], thus making the preparation of the bosonic generalized singlet of 3 qutrits an experimentally feasible task.

8.8 Conclusions

We have introduced a theoretical protocol to probabilistically prepare the totally antisymmetric state $|A_N\rangle$ of N distinct bosons with N internal levels. This state finds potential applications in quantum information protocols [179–181], simulating systems of fermionic indistinguishable particles [183], certifying the non-projective character of measurements [182], and in quantum metrology [184].

The scheme, which generalizes the one devised in Ref. [3, 167] to many-body systems, employs a sequence of Fourier multiports with the number of ports ranging from 2 to N, interlaced with coincidence measurements distilling the results where one constituent per mode is found. The measurements, which have to be insensitive to the internal degree of freedom, must preserve the detected particles and are thus required to be nondemolitive. This does not hold for the last coincidence count, which can be deferred and realized with standard absorbing detectors via postselection [1, 59, 60]. We stress that the emergence of the generalized singlet from the proposed setup is merely due to the interference effects between the identical constituents generated by the Fourier multiports, as discussed in Ref. [3, 167]. Therefore, our work supports the perspective of identicality as a potential quantum resource.

The success probability depends on the overlap between the initial state and the generalized singlet, as the latter has been shown to be the only state to satisfy the necessary condition to anti-bunch under the proposed setup. This property has been used to propose a feasible scheme where the N particles are initially externally depolarized, leading to a maximally mixed state which always has nonzero overlap with the generalized singlet. This strategy also allows one to ignore the previous history of the system, including the initially prepared state and the eventual local interaction of the N particles with lossless noisy environments. This feature enables our scheme to successfully prepare the generalized singlet state even when the setup is implemented far from the particles source, assuming no particle losses. In this sense, the proposed protocol is robust against local noise acting prior to the externally-induced depolarization.

With the suggested realization, the success probability is found to scale as $1/N^N$. Nonetheless, alternative initial states can be employed to provide higher success rates when the presence of noise is low enough to avoid resorting to the external depolarization. This occurs, for example, when our scheme can be applied immediately after the preparation of the initial state. Although our findings further point out the relevance QND detectors might have for quantum information protocols, we have shown that specific experimentally-achievable initial states can be used to obtain generalized singlet states without relying on nonabsorbing detectors. Looking for initial states exploitable to generate high-dimensional generalized singlet states with current technology is surely a direction which is worth of further investigation. Moreover, in Ref. [167] the proposed scheme was shown to distill pure $N = 2$ NOON states when applied to two identical fermions. It would thus be interesting to work out its generalization to multipartite fermionic systems.

A Supplemental Note I

In this section we briefly review the suppression law which led to the equation

$$\pi_{(1,2,\ldots,N)} |\varphi\rangle = (-1)^{N-1} |\varphi\rangle . \tag{A1}$$

reported in the main text.

In [189] the authors derive a general suppression law for any pure initial state $|\psi_{\text{in}}\rangle$ of identical bosons distributed over n spatial modes subjected to a unitary mode-mixing evolution. The particles are further characterized by an internal degree of freedom $|I\rangle$, with $I \in \{1, 2, \ldots, d\}$. Such a suppression law is ultimately found to be strictly related to the permutation symmetries of the initial state $|\psi_{\text{in}}\rangle$. In particular, $|\psi_{\text{in}}\rangle$ is characterized by the *mode occupation list* $\vec{r} = (r_1, \ldots, r_n)$ describing the number r_j of particles occupying the j^{th} mode. To such an input configuration is associated the *mode assignment list* $\vec{d}(\vec{r}) = (d_1(\vec{r}), \ldots, d_N(\vec{r}))$, where N is the total number of particles and $d_\alpha(\vec{r}) \in \{1, \ldots, n\}$ specifies the mode occupied by the α^{th} particle. Since the constituents are identical, the ordering in $\vec{d}(\vec{r})$ is irrelevant and here assumed to be given in increasing order of the spatial modes. Let us now consider a permutation $\mathcal{P}$ of the n spatial modes which leaves $|\psi_{\text{in}}\rangle$ invariant except for a real phase φ, that is,

$$|\psi_{\text{in}}\rangle \xrightarrow{\mathcal{P}} e^{i\varphi} |\psi_{\text{in}}\rangle . \tag{A2}$$

Notice that $\mathcal{P}$ leaves the internal degree of freedom unaffected. We proceed by computing the eigenvectors of $\mathcal{P}$ and the related eigenvalues $\lambda_1, \lambda_2, \ldots, \lambda_n$. Arranging the eigenvectors as columns, we build the matrix A and the unitary evolution matrix $U = A\Sigma$, where Σ is an arbitrary diagonal unitary matrix accounting for eventual local phase operations on the output modes. We then focus on the output distribution given by the mode occupation list $\vec{s}$ and the related mode assignment list $\vec{d}(\vec{s})$. Finally, we build the vector $\vec{\Lambda}(\vec{s}) := (\lambda_{d_1(\vec{s})}, \ldots, \lambda_{d_N(\vec{s})})$. The suppression law derived in [Phys. Rev. A 97, 062116 (2018)] states that the probability of getting the output distribution $\vec{s}$ by evolving the input distribution $\vec{r}$ via U is zero if

$$\Pi_{\alpha=1}^{N} \Lambda_\alpha(\vec{s}) \neq e^{i\varphi}. \tag{A3}$$

In particular, we notice that Eq. (A3):

1. depends on the input distribution $\vec{r}$ and the internal input configuration $\Omega_{\text{in}} = (|I_1\rangle, \ldots, |I_N\rangle)$ characterizing $|\psi_{\text{in}}\rangle$ by means of $\vec{\Lambda}(\vec{s})$, which is given by the eigenvalues of the permutation $\mathcal{P}$ which satisfies Eq. (A2);

2. depends on the output distribution $\vec{s}$ via $\vec{\Lambda}(\vec{s})$;

3. does not depend on the internal output configuration Ω_{out};

4. provides a *necessary*, but *not sufficient* condition to obtain the distribution $\vec{s}$ evolving $|\psi_{\text{in}}\rangle$ via U, that is, $\Pi_{\alpha=1}^{N}\Lambda_\alpha(\vec{s}) = e^{i\varphi}$.

Since we are interested in the suppression law for anti-bunching, we set $\vec{s} = (\underbrace{1, 1, \ldots, 1}_{N \text{ times}})$ and $\vec{d}(\vec{s}) = (1, 2, \ldots, N)$, obtaining $\vec{\Lambda}(\vec{s}) = (\lambda_1, \lambda_2, \ldots, \lambda_N)$ for which Eq. (A3) returns

$$\prod_{j=1}^{N} \lambda_j = e^{i\varphi}. \tag{A4}$$

In the main text, we consider the unitary evolution matrix

$$U_N = \frac{1}{\sqrt{N}} \begin{pmatrix} 1 & 1 & 1 & \dots & 1 \\ 1 & \omega & \omega^2 & \dots & \omega^{N-1} \\ 1 & \omega^2 & \omega^4 & \dots & \omega^{2(N-1)} \\ \vdots & \vdots & \vdots & \vdots & \vdots \\ 1 & \omega^{N-1} & \omega^{2(N-1)} & \dots & \omega^{(N-1)(N-1)} \end{pmatrix}, \tag{A5}$$

with $\omega = e^{2\pi i/N}$. Its columns are the eigenvectors of the cyclic permutation $\pi_{(1,2,\dots,N)}$, whose eigenvalues are

$$\lambda_j = \omega^{1-j} = e^{-\frac{2\pi i}{N}(1-j)}, \quad j = 1, \dots, N. \tag{A6}$$

The LHS of Eq. (A4) is equal to $\prod_{j=1}^{N} \omega^{1-j} = e^{\frac{2\pi i}{N}\sum_{k=1}^{N}(1-k)} = (-1)^{N-1}$, so that a necessary condition for a state $|\psi_{\text{in}}\rangle$ to anti-bunch under U_N is given by Eq. (A1).

B Supplemental Note II

Here we provide a proof of the relation

$$\prod_{j=N}^{2} P_{E_{((-1)^{j-1})}(\pi_{(1,\dots,j)})} = \frac{1}{N!} \sum_{\pi \in S_N} \text{sgn}(\pi)\, \pi \tag{B1}$$

reported in the main text.

Eq. (B1) holds for $N = 2$; indeed, from the definition

$$P_{E_{(-1)^{N-1}}(\pi_{(1,2,\dots,N)})} := \frac{1}{N} \sum_{k=1}^{N} \left[(-1)^{N-1}\, \pi_{(1,2,\dots,N)}\right]^k \tag{B2}$$

it follows that

$$P_{E_{-1}(\pi_{(1,2)})} = \frac{1}{2}\left(\mathbb{1} - \pi_{(1,2)}\right) = \frac{1}{2} \sum_{\pi \in S_2} \text{sgn}(\pi)\, \pi.$$

Let us now assume that Eq. (B1) also holds for all $n < N$. We have

$$\begin{aligned}
\prod_{j=N}^{2} P_{E_{((-1)^{j-1})}(\pi(1,\dots,j))} &= P_{E_{(-1)^{N-1}}(\pi_{(1,2,\dots,N)})} \left[\prod_{j=N-1}^{2} P_{E_{((-1)^{j-1})}(\pi_{(1,\dots,j)})}\right] \\
&= \frac{1}{N} \sum_{k=1}^{N} \left[(-1)^{N-1}\, \pi_{(1,2,\dots,N)}\right]^k \left[\frac{1}{(N-1)!} \sum_{\pi \in S_{N-1}} \text{sgn}(\pi)\pi\right] \\
&= \frac{1}{N!} \sum_{k=1}^{N} \Big[\underbrace{(-1)^{N-1}}_{\text{sgn}\left(\pi_{(1,2,\dots,N)}\right)}\, \pi_{(1,2,\dots,N)}\Big]^k \left[\sum_{\pi \in S_{N-1}} \text{sgn}(\pi)\pi\right] \\
&= \sum_{k=1}^{N} \sum_{\pi \in S_{N-1}} \text{sgn}\left(\pi^k_{(1,2,\dots,N)}\pi\right)\, \pi^k_{(1,2,\dots,N)}\, \pi \\
&= \frac{1}{N!} \sum_{\pi \in S_N} \text{sgn}(\pi)\, \pi.
\end{aligned}$$

The last step follows from the fact that both the symmetric group S_{N-1} and the cyclic group $\langle \pi_{(1,2,\ldots,N)} \rangle$ are subgroups of S_N and

$$\begin{aligned} |S_{N-1}\langle \pi_{(1,2,\ldots,N)} \rangle| &= \frac{|S_{N-1}||\langle \pi_{(1,2,\ldots,N)} \rangle|}{|S_{N-1} \cap \langle \pi_{(1,2,\ldots,N)} \rangle|} \\ &= (N-1)!N = |S_N|, \end{aligned}$$

where $S_{N-1} \cap \langle \pi_{(1,2,\ldots,N)} \rangle = \{1_N\}$ is the identity permutation of N elements.

C Supplemental Note III

Here we demonstrate that any state $|\Psi\rangle$ from the totally antisymmetric subspace given by the projector $P_{A_N^d} = \frac{1}{N!} \sum_{\pi \in S_N} \mathrm{sgn}(\pi)\, \pi$ with $d \geq N$ is invariant (up to a global phase) under the action of an arbitrary unitary followed by a coincidence measurement on the output modes, that is,

$$C_N U \, |\Psi\rangle = e^{i\phi} \, |\Psi\rangle \, . \tag{C1}$$

A generic state $|\Psi\rangle$ in the totally antisymmetric subspace given by $P_{A_N^d}$ can be written as

$$|\Psi\rangle = \sum_{\mathcal{S} \in \mathcal{P}_N([d])} c_{\mathcal{S}} \, |A_N^{\mathcal{S}}\rangle \, , \tag{C2}$$

where $\mathcal{P}_N([d])$ is the family of sets of cardinality N over the set $[d] = \{1, \ldots, d\}$, $|A_N^{\mathcal{S}}\rangle$ denotes an N-partite N-level singlet state corresponding to the choice $\mathcal{S} \in \mathcal{P}_N([d])$ of N out of d levels, and $c_{\mathcal{S}}$ are coefficients such that $\sum_{\mathcal{S} \in \mathcal{P}_N([d])} |c_{\mathcal{S}}|^2 = 1$. Each generalized singlet state $|A_N^S\rangle$ associated to the choice $\mathcal{S} = \{s_1, s_2, \ldots, s_N\}$ can be written in terms of the determinant of a matrix of creation operators as

$$|A_N^{\mathcal{S}}\rangle = \frac{1}{\sqrt{N!}} \det \mathsf{A}_{\mathcal{S}} \, |0\rangle \, , \tag{C3}$$

where

$$\mathsf{A}_{\mathcal{S}} = \begin{pmatrix} a^\dagger_{1,s_1} & a^\dagger_{1,s_2} & \ldots & a^\dagger_{1,s_N} \\ a^\dagger_{2,s_1} & a^\dagger_{2,s_2} & \ldots & a^\dagger_{2,s_N} \\ \vdots & \vdots & \vdots & \vdots \\ a^\dagger_{N,s_1} & a^\dagger_{N,s_2} & \ldots & a^\dagger_{N,s_N} \end{pmatrix} . \tag{C4}$$

A generic unitary operator U acting on the N spatial modes transforms the creation operators into $u^\dagger_{k,m} = \sum_{\ell=1}^N (U)_{k,\ell} \, a^\dagger_{\ell,m}$, so that

$$U|A_N^{\mathcal{S}}\rangle = \frac{1}{\sqrt{N!}} \det(U\mathsf{A}_{\mathcal{S}}) \, |0\rangle. \tag{C5}$$

Since $\det(U\mathsf{A}_{\mathcal{S}}) = \det U \det \mathsf{A}_{\mathcal{S}} = e^{i\theta} \det \mathsf{A}_{\mathcal{S}}$ for some real θ, we get that $U|A_N^{\mathcal{S}}\rangle = e^{i\theta}|A_N^{\mathcal{S}}\rangle$. Therefore, from Eq. (C2) it follows

$$U \, |\Psi\rangle = \sum_{\mathcal{S} \in \mathcal{P}_N([d])} c_{\mathcal{S}} \, U \, |A_N^{\mathcal{S}}\rangle = e^{i\phi} \, |\Psi\rangle \, . \tag{C6}$$

This means that $|\Psi\rangle$ is, up to a global phase, invariant under any unitary operator acting on the N spatial modes. Eq. (C1) follows from the fact that each $|A_N^{\mathcal{S}}\rangle$ is a state of

N particles occupying N distinct spatial modes, so that it is left invariant by a QND coincidence measurement on the output modes: $C_N|A_N^{\mathcal{S}}\rangle = |A_N^{\mathcal{S}}\rangle$.

Notice that the invariance of the totally antisymmetric state under arbitrary unitaries ensures that our scheme can use any unitary that leads to the same suppression laws as U_N. These include the unitaries U'_N resulting from the application of local phases to the input/output modes of the Fourier multiport, $U' = D\,U_N\,D'$, where D, D' are diagonal unitary matrices.

Conclusive remarks

This thesis has been dedicated to the study of identical particles and of their indistinguishability as a useful quantum resource in quantum information operational tasks. Chapters 2-4 and 6-8 report the main papers to which I collaborated during my PhD studies, whereas Chapter 1 and Chapter 5 provide original presentations, elaborations, and insights on the main topics underlying this work.

In Chapter 1, we introduced identical particles and the concept of spatial indistinguishability. In particular, the latter has been presented as a purely quantum property occurring when the wave functions of distinct identical constituents spatially overlap over a same detection region, giving rise to a scenario where both particles can individually trigger the detector. In this situation, called *ambiguous* [7, 12], the detector is not able to distinguish which constituent has actually been detected, connecting the concept of *spatial indistinguishability* to the one of *no which-particle information*, and further and relating the latter to the ones of *no which-way information* and *no which-spin information*. We have shown that the straightforward application of the symmetrization postulate to systems of identical particles within the standard, first quantization, label-based approach [4] leads to incorrect results when evaluating their entanglement with the same tools employed for nonidentical constituents [13, 21, 22]. We have highlighted how the origin of the issue resides in the labels employed to address the constituents, which can give rise to correlations which are actually unphysical. We have discussed different solutions to this problem; these include adopting a point of view focusing on operations performed in *local regions* of space rather than on individual particles, and relying on a mathematical formalism which does not involve labels. The former, called *spatially localized operations and classical communication* (sLOCC) [20], solves the issue of evaluating entanglement of identical constituents localized in distinct regions of space (distinguishable particles/unambiguous settings), whereas the latter, called *no-label approach*, allows to directly evaluate the quantum correlations of identical particles even in ambiguous scenarios, by suitably extending the standard tools employed for nonidentical ones. After that, we reported prior results showing how spatial indistinguishability can be quantified by an entropic measure [2], and used within the sLOCC framework to generate entanglement [1, 20], coherence [128], and to recover quantum correlations between identical qubits affected by local white noise [2].

In Chapter 2 we extended the indistinguishability measure to the multipartite scenario and to different degrees of freedom, and provided a theoretical generalization of the *spatial deformation* technique employed to generate no which-way information between identical constituents [23].

In Chapter 3 we introduced a theoretical protocol exploiting spatial indistinguishability within the sLOCC framework to directly measure the exchange phase of identical particles of any species [59]. The scheme has been experimentally implemented in an all-optical setup by colleagues of the University of Science and Technology of China, leading to the

direct measurement of the real bosonic exchange phase and of other simulated ones whose results are reported in the same manuscript.

In Chapter 4 we show how spatial indistinguishability of identical constituents and the sLOCC framework can be exploited to recover the quantum correlations between initially entangled qubits which have locally interacted with detrimental noisy environments [37], extending the results introduced in Ref. [2].

Chapter 5 explores some issues arising from the straightforward application of the no which-way information and the related indistinguishability measure to scenarios where interference effects can lead to the loss of particles' individuality, providing insights on the origin of the problem and proposing a solution to it.

In Chapters 6 and 7 we proposed a scheme to probabilistically distill maximally entangled states of two identical qubits regardless of their initial state, in a way which is robust to the action of local, particle-preserving noisy channels [3, 167]. The protocol works for both bosons and fermions and allows to prepare either Bell states or NOON states thanks to the introduction of *passive optical operations* and the exploitation of a polarization-insensitive, nonabsorbing parity check detector.

Finally, in Chapter 8 we extended the scheme introduced in the two previous chapters and proposed an interferometric protocol to probabilistically prepare generalized singlet states of N identical bosons with N internal levels, in a way which is robust to detrimental local noise [159].

In conclusion, this thesis provides a useful review of the techniques developed by our group to activate and exploit spatial indistinguishability of identical particles as a genuine quantum resource for quantum information processing, paving the way for future developments. The latter include, but are not limited to, a better understanding of the relationship between the measure of indistinguishability introduced and the quantum correlations present in the state resulting from the sLOCC protocol for multipartite systems, the development of more reliable interferometric schemes for the generation of many-body entangled states and their extension to the fermionic case, and the application of the sLOCC framework to obtain advantages in quantum thermodynamics.

Lastly, I highlight an ongoing collaboration with the team directed by Prof. Roberto Morandotti at Institut National de la Recherche Scientifique in Montreal, Canada, where I am currently working at the development of optical implementations of quantum algorithms based on qudits encoded within single photons, expanding my experience and knowledge in the field of quantum computing and quantum optics.

Acknowledgements

I'm immensely thankful to Prof. Rosario Lo Franco, who has been a Mentor well beyond the academic role and a person that today I can call Friend. Your support has been fundamental: I could have not asked for a better supervisor.

I sincerely thanks Prof. Andreas Winter for the hospitality and the time he dedicated to me during my visit to Universitat Autònoma de Barcelona, immediately putting me at ease.

I thank all the members of the group: Farzam, Kobra, Mashid, Samira, Vincenzo, Federico, and Alberto. Not only for the useful discussions carried out in front of a blackboard or a beer, but also and most importantly for making me feel at home.

I'm deeply thankful to my family: mum, dad, and Ale, for having always believed in me, for never giving up on me, and for the love you show me daily without asking for anything in exchange. You have been my best medicine.

Thanks from the bottom of my heart to Andre, who in nineteen years has never given up on me and has always stayed by my side as a brother. Watching you walking your way withstanding the adversities fills me with joy and pride.

How could I not thank Alice, the proof that sometimes Life is really a mysterious spiral. The relevance of our bond is written in the intricate paths that led us where we are now, an indelible symbol of the value of changing and forgiving.

Thanks to Samu, which managed to stay close to me in the right times, demonstrating that that the physical distance doesn't do justice to the mutual affection and esteem.

Thanks to Luca for always being so stimulating, an intellectual fire but also a sincere friend to rely on.

Thanks to all those who, even just by chance, have stayed close to me in that which has been one of my gloomiest times: in the indescribable darkness of those days you have been many little candles which allowed me to recover my light. I don't know how to thank you.

Lastly, I thank Life for everything it gave me and still gives me, for the marvel it continuously strikes me with, for giving me the possibility to observe the beauty which surrounds us and to study its laws, for the daily wonder of investigating, rediscovering and finding myself, and for reminding me that looking at the good in what surrounds us and allowing us to forgive usually means loving ourselves.

Ringraziamenti

Un grazie infinito al Prof. Rosario Lo Franco, che ben oltre il ruolo accademico è stato un Mentore e una persona che oggi posso chiamare Amico. Il tuo supporto è stato fondamentale: non avrei potuto chiedere un supervisore migliore.

Ringrazio sentitamente il Prof. Andreas Winter per l'ospitalità e la disponibilità dimostratemi durante il mio soggiorno all'Università Autonoma di Barcellona, facendomi subito sentire a mio agio.

Ringrazio tutti i membri del gruppo: Farzam, Kobra, Mashid, Samira, Vincenzo, Federico, e Alberto. Non solo per le utili discussioni di Fisica condotte davanti a una lavagna o a una birra, ma anche e soprattutto per avermi fatto sentire a casa.

Immensamente grazie alla mia famiglia: mamma, papà, e Ale, per aver sempre creduto in me, per non avermi mai lasciato solo, e per il bene che mi dimostrate quotidianamente senza chiedere nulla in cambio. Siete stati per me la medicina più efficace.

Grazie di cuore ad Andre, che in diciannove anni non mi ha mai abbandonato standomi accanto come un fratello. Vederti percorrere la tua strada resistendo alle intemperie mi riempie di gioia e di orgoglio.

Come non ringraziare Alice, la dimostrazione che a volte la Vita è davvero una misteriosa spirale. L'importanza del nostro legame è scritta negli intricati percorsi che ci hanno portato dove siamo ora, simbolo indelebile del valore del mutamento e del perdono.

Grazie a Samu, che ha saputo starmi accanto nei momenti giusti, dimostrandomi che la distanza fisica non rende giustizia all'affetto e alla stima reciproca.

Grazie a Luca per essere sempre così stimolante, fuoco intellettuale ma anche amico sincero su cui poter fare affidamento.

Grazie a tutti coloro che, anche solo di passaggio, mi sono stati vicino in quello che è stato uno dei miei periodi più bui: nell'indescrivibile oscurità di quei giorni siete stati tante piccole candele che mi hanno permesso di ritrovare la mia luce. Non so come ringraziarvi.

Lascio infine un ringraziamento alla Vita per tutto ciò che mi ha dato e che continua a darmi, per la meraviglia con cui mi colpisce di continuo, per avermi dato la possibilità di osservare la bellezza che ci circonda e di studiarne le leggi, per lo stupore quotidiano del ricercarmi, riscoprirmi e ritrovarmi, e per avermi ricordato che spesso guardare al buono di ciò che ci cirdonda e concedersi il perdono significa amarsi.

Bibliography

[1] K. Sun, Y. Wang, Z.-H. Liu, X.-Y. Xu, J.-S. Xu, C.-F. Li, G.-C. Guo, A. Castellini, F. Nosrati, G. Compagno, and R. Lo Franco, "Experimental quantum entanglement and teleportation by tuning remote spatial indistinguishability of independent photons," *Opt. Lett.*, vol. 45, no. 23, pp. 6410–6413, 2020.

[2] F. Nosrati, A. Castellini, G. Compagno, and R. Lo Franco, "Robust entanglement preparation against noise by controlling spatial indistinguishability," *npj Quant. Inf.*, vol. 6, no. 1, p. 39, 2020.

[3] M. Piccolini, V. Giovannetti, and R. Lo Franco, "Asymptotically deterministic robust preparation of maximally entangled bosonic states," *Phys. Rev. Res.*, vol. 6, no. 1, p. 013073, 2024.

[4] C. Cohen-Tannoudji, B. Diu, F. Laloe, and B. Dui, *Quantum Mechanics (2 vol. set)*. Wiley-Interscience, 2006.

[5] G. Ghirardi, L. Marinatto, and T. Weber, "Entanglement and properties of composite quantum systems: a conceptual and mathematical analysis," *J. Stat. Phys.*, vol. 108, no. 1, pp. 49–122, 2002.

[6] A. Peres, *Quantum Theory: Concepts and Methods*. Springer, 2002.

[7] M. C. Tichy, F. de Melo, M. Kus, F. Mintert, and A. Buchleitner, "Entanglement of identical particles and the detection process," *Fortschr. Phys.*, vol. 61, pp. 225–237, 2013.

[8] C. H. Bennett, D. P. DiVincenzo, J. A. Smolin, and W. K. Wootters, "Mixed-state entanglement and quantum error correction," *Phys. Rev. A*, vol. 54, no. 5, p. 3824, 1996.

[9] E. Chitambar, D. Leung, L. Mančinska, M. Ozols, and A. Winter, "Everything you always wanted to know about locc (but were afraid to ask)," *Commun. Math. Phys.*, vol. 328, no. 1, pp. 303–326, 2014.

[10] R. Horodecki, P. Horodecki, M. Horodecki, and K. Horodecki, "Quantum entanglement," *Rev. Mod. Phys.*, vol. 81, pp. 865–942, 2009.

[11] P. Blasiak and M. Markiewicz, "Entangling three qubits without ever touching," *Sci. Rep.*, vol. 9, no. 1, p. 20131, 2019.

[12] M. C. Tichy, F. Mintert, and A. Buchleitner, "Essential entanglement for atomic and molecular physics," *J. Phys. B: At. Mol. Opt. Phys.*, vol. 44, p. 192001, sep 2011.

[13] G. Ghirardi and L. Marinatto, "General criterion for the entanglement of two indistinguishable particles," *Phys. Rev. A*, vol. 70, p. 012109, 2004.

[14] J. Schliemann, J. I. Cirac, M. Kuś, M. Lewenstein, and D. Loss, "Quantum correlations in two-fermion systems," *Phys. Rev. A*, vol. 64, no. 2, p. 022303, 2001.

[15] K. Eckert, J. Schliemann, D. Bruß, and M. Lewenstein, "Quantum correlations in systems of indistinguishable particles," *Ann. Phys.*, vol. 299, no. 1, pp. 88–127, 2002.

[16] F. Benatti, R. Floreanini, F. Franchini, and U. Marzolino, "Entanglement in indistinguishable particle systems," *Phys. Rep.*, vol. 878, pp. 1–27, 2020.

[17] F. Benatti, R. Floreanini, F. Franchini, and U. Marzolino, "Remarks on entanglement and identical particles," *Open Syst. Inf. Dyn.*, vol. 24, no. 03, p. 1740004, 2017.

[18] H. Barnum, E. Knill, G. Ortiz, R. Somma, and L. Viola, "A subsystem-independent generalization of entanglement," *Phys. Rev. Lett.*, vol. 92, no. 10, p. 107902, 2004.

[19] P. Zanardi, "Virtual quantum subsystems," *Phys. Rev. Lett.*, vol. 87, no. 7, p. 077901, 2001.

[20] R. Lo Franco and G. Compagno, "Indistinguishability of elementary systems as a resource for quantum information processing," *Phys. Rev. Lett.*, vol. 120, no. 24, p. 240403, 2018.

[21] R. Lo Franco and G. Compagno, "Quantum entanglement of identical particles by standard information-theoretic notions," *Sci. Rep.*, vol. 6, p. 20603, 2016.

[22] G. Compagno, A. Castellini, and R. Lo Franco, "Dealing with indistinguishable particles and their entanglement," *Phil. Trans. R. Soc. A*, vol. 376, no. 2123, p. 20170317, 2018.

[23] M. Piccolini, F. Nosrati, G. Adesso, R. Morandotti, and R. Lo Franco, "Generating indistinguishability within identical particle systems: spatial deformations as quantum resource activators," *Phil. Trans. R. Soc. A*, vol. 381, no. 2255, p. 20220104, 2023.

[24] C.-K. Hong, Z.-Y. Ou, and L. Mandel, "Measurement of subpicosecond time intervals between two photons by interference," *Phys. Rev. Lett.*, vol. 59, no. 18, p. 2044, 1987.

[25] H. Lee, P. Kok, and J. P. Dowling, "A quantum rosetta stone for interferometry," *J. Mod. Opt.*, vol. 49, no. 14-15, pp. 2325–2338, 2002.

[26] E. Polino, M. Valeri, N. Spagnolo, and F. Sciarrino, "Photonic quantum metrology," *AVS Quantum Sci.*, vol. 2, no. 2, p. 024703, 2020.

[27] V. Giovannetti, S. Lloyd, and L. Maccone, "Quantum metrology," *Phys. Rev. Lett.*, vol. 96, no. 1, p. 010401, 2006.

[28] V. Giovannetti, S. Lloyd, and L. Maccone, "Advances in quantum metrology," *Nat. Photon.*, vol. 5, no. 4, pp. 222–229, 2011.

[29] A. Kaufman, B. Lester, M. Foss-Feig, M. Wall, A. Rey, and C. Regal, "Entangling two transportable neutral atoms via local spin exchange," *Nature*, vol. 527, no. 7577, pp. 208–211, 2015.

[30] A. Castellini, R. Lo Franco, L. Lami, A. Winter, G. Adesso, and G. Compagno, "Indistinguishability-enabled coherence for quantum metrology," *Phys. Rev. A*, vol. 100, p. 012308, 2019.

[31] R. F. Werner, "Quantum states with einstein-podolsky-rosen correlations admitting a hidden-variable model," *Phys. Rev. A*, vol. 40, no. 8, p. 4277, 1989.

[32] M. A. Nielsen and I. L. Chuang, *Quantum Computation and Quantum Information*. Cambridge University Press, 2010.

[33] W. K. Wootters, "Entanglement of formation of an arbitrary state of two qubits," *Phys. Rev. Lett.*, vol. 80, p. 2245–2248, Mar 1998.

[34] R. Horodecki, P. Horodecki, M. Horodecki, and K. Horodecki, "Quantum entanglement," *Rev. Mod. Phys.*, vol. 81, no. 2, p. 865, 2009.

[35] F. Herbut and M. Vujicic, "Irrelevance of the pauli principle in distant correlations between identical fermions," *J. Phys. A: Math. Gen.*, vol. 20, pp. 5555–5563, nov 1987.

[36] F. Nosrati, A. Castellini, G. Compagno, and R. Lo Franco, "Dynamics of spatially indistinguishable particles and quantum entanglement protection," *Phys. Rev. A*, vol. 102, no. 6, p. 062429, 2020.

[37] M. Piccolini, F. Nosrati, G. Compagno, P. Livreri, R. Morandotti, and R. Lo Franco, "Entanglement robustness via spatial deformation of identical particle wave functions," *Entropy*, vol. 23, p. 708, 2021.

[38] M. Piccolini, F. Nosrati, R. Morandotti, and R. Lo Franco, "Indistinguishability-enhanced entanglement recovery by spatially localized operations and classical communication," *Open Syst. Inf. Dyn.*, vol. 28, no. 04, p. 2150020, 2021.

[39] Y.-S. Li, B. Zeng, X.-S. Liu, and G.-L. Long, "Entanglement in a two-identical-particle system," *Phys. Rev. A*, vol. 64, p. 054302, 2001.

[40] R. Paskauskas and L. You, "Quantum correlations in two-boson wave functions," *Phys. Rev. A*, vol. 64, p. 042310, 2001.

[41] J. Schliemann, J. I. Cirac, M. Kus, M. Lewenstein, and D. Loss, "Quantum correlations in two-fermion systems," *Phys. Rev. A*, vol. 64, p. 022303, 2001.

[42] P. Zanardi, "Quantum entanglement in fermionic lattices," *Phys. Rev. A*, vol. 65, p. 042101, 2002.

[43] B. Morris, B. Yadin, M. Fadel, T. Zibold, P. Treutlein, and G. Adesso, "Entanglement between identical particles is a useful and consistent resource," *Phys. Rev. X*, vol. 10, p. 041012, 2020.

[44] K. Eckert, J. Schliemann, D. Bruss, and M. Lewenstein, "Quantum correlations in systems of indistinguishable particles," *Ann. Phys.*, vol. 299, no. 1, pp. 88–127, 2002.

[45] A. P. Balachandran, T. R. Govindarajan, A. R. de Queiroz, and A. F. Reyes-Lega, "Entanglement and particle identity: A unifying approach," *Phys. Rev. Lett.*, vol. 110, p. 080503, 2013.

[46] F. D. Cunden, S. Di Martino, P. Facchi, and G. Florio, "Spatial separation and entanglement of identical particles," *Int. J. Quantum Inform.*, vol. 12, p. 461001, 2014.

[47] T. Sasaki, T. Ichikawa, and I. Tsutsui, "Entanglement of indistinguishable particles," *Phys. Rev. A*, vol. 83, p. 012113, 2011.

[48] S. Bose and D. Home, "Generic entanglement generation, quantum statistics, and complementarity," *Phys. Rev. Lett.*, vol. 88, no. 5, p. 050401, 2002.

[49] S. Bose and D. Home, "Duality in entanglement enabling a test of quantum indistinguishability unaffected by interactions," *Phys. Rev. Lett.*, vol. 110, p. 140404, 2013.

[50] N. Killoran, M. Cramer, and M. B. Plenio, "Extracting entanglement from identical particles," *Phys. Rev. Lett.*, vol. 112, no. 15, p. 150501, 2014.

[51] S. Sciara, R. Lo Franco, and G. Compagno, "Universality of Schmidt decomposition and particle identity," *Sci. Rep.*, vol. 7, p. 44675, 2017.

[52] A. C. Lourenço, T. Debarba, and E. I. Duzzioni, "Entanglement of indistinguishable particles: A comparative study," *Phys. Rev. A*, vol. 99, no. 1, p. 012341, 2019.

[53] S. Chin and J. Huh, "Entanglement of identical particles and coherence in the first quantization language," *Phys. Rev. A*, vol. 99, no. 5, p. 052345, 2019.

[54] S. Chin and J. Huh, "Reduced density matrix of identical particles from three aspects: the first quantization, exterior products, and gns representation," *arXiv preprint arXiv:1906.00542*, 2019.

[55] T. Qureshi and U. Rizwan, "Hanbury brown–twiss effect with wave packets," *Quanta*, vol. 6, no. 1, pp. 61–69, 2017.

[56] H. Mani, N. Ramadas, and V. Sreedhar, "Quantum entanglement in one-dimensional anyons," *Phys. Rev. A*, vol. 101, no. 2, p. 022314, 2020.

[57] K. Tschernig, C. Müller, M. Smoor, T. Kroh, J. Wolters, O. Benson, K. Busch, and A. Pérez-Leija, "Direct observation of the particle exchange phase of photons," *Nat. Photon.*, vol. 15, pp. 671–675, 2021.

[58] R. Lo Franco, "Directly proving the bosonic nature of photons," *Nat. Photon.*, vol. 15, no. 9, pp. 638–639, 2021.

[59] Y. Wang, M. Piccolini, Z.-Y. Hao, Z.-H. Liu, K. Sun, J.-S. Xu, C.-F. Li, G.-C. Guo, R. Morandotti, G. Compagno, *et al.*, "Proof-of-principle direct measurement of particle statistical phase," *Phys. Rev. Appl.*, vol. 18, no. 6, p. 064024, 2022.

[60] K. Sun, Z.-H. Liu, Y. Wang, Z.-Y. Hao, X.-Y. Xu, J.-S. Xu, C.-F. Li, G.-C. Guo, A. Castellini, L. Lami, *et al.*, "Activation of indistinguishability-based quantum coherence for enhanced metrological applications with particle statistics imprint," *PNAS*, vol. 119, no. 21, p. e2119765119, 2022.

[61] A. Perez-Leija, D. Guzmán-Silva, R. d. J. León-Montiel, M. Gräfe, M. Heinrich, H. Moya-Cessa, K. Busch, and A. Szameit, "Endurance of quantum coherence due to particle indistinguishability in noisy quantum networks," *npj Quant. Inf.*, vol. 4, no. 1, p. 45, 2018.

[62] J. M. Leinaas and J. Myrheim, "On the theory of identical particles," *Il Nuovo Cimento B (1971-1996)*, vol. 37, no. 1, pp. 1–23, 1977.

[63] F. Wilczek, "Magnetic flux, angular momentum, and statistics," *Phys. Rev. Lett.*, vol. 48, no. 17, p. 1144, 1982.

[64] C. Nayak, S. H. Simon, A. Stern, M. Freedman, and S. D. Sarma, "Non-abelian anyons and topological quantum computation," *Rev. Mod. Phys.*, vol. 80, no. 3, p. 1083, 2008.

[65] J. Nakamura, S. Liang, G. C. Gardner, and M. J. Manfra, "Direct observation of anyonic braiding statistics," *Nat. Phys.*, vol. 16, no. 9, pp. 931–936, 2020.

[66] H. Bartolomei, M. Kumar, R. Bisognin, A. Marguerite, J.-M. Berroir, E. Bocquillon, B. Placais, A. Cavanna, Q. Dong, U. Gennser, *et al.*, "Fractional statistics in anyon collisions," *Science*, vol. 368, no. 6487, pp. 173–177, 2020.

[67] R. C. Hilborn and C. L. Yuca, "Spectroscopic test of the symmetrization postulate for spin-0 nuclei," *Phys. Rev. Lett.*, vol. 76, pp. 2844–2847, 1996.

[68] G. Modugno, M. Inguscio, and G. M. Tino, "Search for small violations of the symmetrization postulate for spin-0 particles," *Phys. Rev. Lett.*, vol. 81, pp. 4790–4793, 1998.

[69] D. English, V. V. Yashchuk, and D. Budker, "Spectroscopic test of bose-einstein statistics for photons," *Phys. Rev. Lett.*, vol. 104, p. 253604, 2010.

[70] K. Deilamian, J. D. Gillaspy, and D. E. Kelleher, "Search for small violations of the symmetrization postulate in an excited state of helium," *Phys. Rev. Lett.*, vol. 74, pp. 4787–4790, 1995.

[71] M. de Angelis, G. Gagliardi, L. Gianfrani, and G. M. Tino, "Test of the symmetrization postulate for spin-0 particles," *Phys. Rev. Lett.*, vol. 76, pp. 2840–2843, 1996.

[72] S. Ospelkaus, K.-K. Ni, D. Wang, M. H. G. de Miranda, B. Neyenhuis, G. Quéméner, P. S. Julienne, J. L. Bohn, D. S. Jin, and J. Ye, "Quantum-state controlled chemical reactions of ultracold potassium-rubidium molecules," *Science*, vol. 327, no. 5967, pp. 853–857, 2010.

[73] F. Benatti, R. Floreanini, and U. Marzolino, "Bipartite entanglement in systems of identical particles: the partial transposition criterion," *Ann. Phys.*, vol. 327, no. 5, pp. 1304–1319, 2012.

[74] M. R. Barros, S. Chin, T. Pramanik, H.-T. Lim, Y.-W. Cho, J. Huh, and Y.-S. Kim, "Entangling bosons through particle indistinguishability and spatial overlap," *Opt. Express*, vol. 28, pp. 38083–38092, Dec 2020.

[75] C. F. Roos, A. Alberti, D. Meschede, P. Hauke, and H. Häffner, "Revealing quantum statistics with a pair of distant atoms," *Phys. Rev. Lett.*, vol. 119, p. 160401, 2017.

[76] D. F. V. James, P. G. Kwiat, W. J. Munro, and A. G. White, "Measurement of qubits," *Phys. Rev. A*, vol. 64, p. 052312, 2001.

[77] J. C. Matthews, K. Poulios, J. D. Meinecke, A. Politi, A. Peruzzo, N. Ismail, K. Wörhoff, M. G. Thompson, and J. L. O'Brien, "Observing fermionic statistics with photons in arbitrary processes," *Sci. Rep.*, vol. 3, no. 1, pp. 1–7, 2013.

[78] L. Sansoni, F. Sciarrino, G. Vallone, P. Mataloni, A. Crespi, R. Ramponi, and R. Osellame, "Two-particle bosonic-fermionic quantum walk via integrated photonics," *Phys. Rev. Lett.*, vol. 108, no. 1, p. 010502, 2012.

[79] T. Krisnanda, S. Ghosh, T. Paterek, W. Laskowski, and T. C. Liew, "Phase measurement beyond the standard quantum limit using a quantum neuromorphic platform," *Phys. Rev. Appl.*, vol. 18, no. 3, p. 034011, 2022.

[80] S. Taravati and G. V. Eleftheriades, "Low-noise and linear nonmagnetic circulator by a temporal nonreciprocal phase shifter," *Phys. Rev. Appl.*, vol. 18, no. 3, p. 034082, 2022.

[81] R. Wang, S. He, and H. Luo, "Photonic spin-hall differential microscopy," *Phys. Rev. Appl.*, vol. 18, no. 4, p. 044016, 2022.

[82] C. Bäuerle, D. C. Glattli, T. Meunier, F. Portier, P. Roche, P. Roulleau, S. Takada, and X. Waintal, "Coherent control of single electrons: a review of current progress," *Rep. Prog. Phys.*, vol. 81, no. 5, p. 056503, 2018.

[83] E. Bocquillon, V. Freulon, J.-M. Berroir, P. Degiovanni, B. Plaçais, A. Cavanna, Y. Jin, and G. Fève, "Coherence and indistinguishability of single electrons emitted by independent sources," *Science*, vol. 339, no. 6123, pp. 1054–1057, 2013.

[84] G. Fève, A. Mahé, J.-M. Berroir, T. Kontos, B. Placais, D. Glattli, A. Cavanna, B. Etienne, and Y. Jin, "An on-demand coherent single-electron source," *Science*, vol. 316, no. 5828, pp. 1169–1172, 2007.

[85] D. Press, T. D. Ladd, B. Zhang, and Y. Yamamoto, "Complete quantum control of a single quantum dot spin using ultrafast optical pulses," *Nature*, vol. 456, no. 7219, pp. 218–221, 2008.

[86] J. R. Petta, A. C. Johnson, J. M. Taylor, E. A. Laird, A. Yacoby, M. D. Lukin, C. M. Marcus, M. P. Hanson, and A. C. Gossard, "Coherent manipulation of coupled electron spins in semiconductor quantum dots," *Science*, vol. 309, no. 5744, pp. 2180–2184, 2005.

[87] R. Hanson, L. P. Kouwenhoven, J. R. Petta, S. Tarucha, and L. M. Vandersypen, "Spins in few-electron quantum dots," *Rev. Mod. Phys.*, vol. 79, no. 4, p. 1217, 2007.

[88] A. Y. Kitaev, "Fault-tolerant quantum computation by anyons," *Ann. Phys.*, vol. 303, no. 1, pp. 2–30, 2003.

[89] B. Field and T. Simula, "Introduction to topological quantum computation with non-abelian anyons," *Quantum Sci. Technol.*, vol. 3, no. 4, p. 045004, 2018.

[90] M. Hiekkamäki, R. F. Barros, M. Ornigotti, and R. Fickler, "Observation of the quantum gouy phase," *Nat. Photon.*, vol. 16, no. 12, pp. 828–833, 2022.

[91] S. Hong, J. Ur Rehman, Y.-S. Kim, Y.-W. Cho, S.-W. Lee, H. Jung, S. Moon, S.-W. Han, and H.-T. Lim, "Quantum enhanced multiple-phase estimation with multi-mode n 00 n states," *Nat. Commun.*, vol. 12, no. 1, p. 5211, 2021.

[92] J. Preskill, "Quantum computing in the nisq era and beyond," *Quantum*, vol. 2, p. 79, 2018.

[93] I. Rotter and J. Bird, "A review of progress in the physics of open quantum systems: theory and experiment," *Rep. Prog. Phys.*, vol. 78, no. 11, p. 114001, 2015.

[94] J. Preskill, "Reliable quantum computers," *Proc. Math. Phys. Eng. Sci.*, vol. 454, no. 1969, pp. 385–410, 1998.

[95] E. Knill, "Quantum computing with realistically noisy devices," *Nature*, vol. 434, no. 7029, p. 39, 2005.

[96] P. W. Shor, "Scheme for reducing decoherence in quantum computer memory," *Phys. Rev. A*, vol. 52, no. 4, p. R2493, 1995.

[97] A. M. Steane, "Error correcting codes in quantum theory," *Phys. Rev. Lett.*, vol. 77, no. 5, p. 793, 1996.

[98] L. Mazzola, S. Maniscalco, J. Piilo, K.-A. Suominen, and B. M. Garraway, "Sudden death and sudden birth of entanglement in common structured reservoirs," *Phys. Rev. A*, vol. 79, no. 4, p. 042302, 2009.

[99] B. Bellomo, R. Lo Franco, S. Maniscalco, and G. Compagno, "Entanglement trapping in structured environments," *Phys. Rev. A*, vol. 78, no. 6, p. 060302, 2008.

[100] R. Lo Franco, B. Bellomo, S. Maniscalco, and G. Compagno, "Dynamics of quantum correlations in two-qubit systems within non-markovian environments," *Int. J. Mod. Phys. B*, vol. 27, no. 01n03, p. 1345053, 2013.

[101] L. Aolita, F. De Melo, and L. Davidovich, "Open-system dynamics of entanglement: a key issues review," *Rep. Prog. Phys.*, vol. 78, no. 4, p. 042001, 2015.

[102] J.-S. Xu, C.-F. Li, M. Gong, X.-B. Zou, C.-H. Shi, G. Chen, and G.-C. Guo, "Experimental demonstration of photonic entanglement collapse and revival," *Phys. Rev. Lett.*, vol. 104, no. 10, p. 100502, 2010.

[103] B. Bylicka, D. Chruściński, and S. Maniscalco, "Non-markovianity and reservoir memory of quantum channels: a quantum information theory perspective," *Sci. Rep.*, vol. 4, no. 1, pp. 1–7, 2014.

[104] Z.-X. Man, Y.-J. Xia, and R. Lo Franco, "Cavity-based architecture to preserve quantum coherence and entanglement," *Sci. Rep.*, vol. 5, no. 1, pp. 1–13, 2015.

[105] J. Tan, T. H. Kyaw, and Y. Yeo, "Non-markovian environments and entanglement preservation," *Phys. Rev. A*, vol. 81, no. 6, p. 062119, 2010.

[106] Q.-J. Tong, J.-H. An, H.-G. Luo, and C. Oh, "Mechanism of entanglement preservation," *Phys. Rev. A*, vol. 81, no. 5, p. 052330, 2010.

[107] H.-P. Breuer, E.-M. Laine, J. Piilo, and B. Vacchini, "Colloquium: Non-markovian dynamics in open quantum systems," *Rev. Mod. Phys.*, vol. 88, no. 2, p. 021002, 2016.

[108] Z.-X. Man, Y.-J. Xia, and R. Lo Franco, "Harnessing non-markovian quantum memory by environmental coupling," *Phys. Rev. A*, vol. 92, no. 1, p. 012315, 2015.

[109] C. H. Bennett, G. Brassard, S. Popescu, B. Schumacher, J. A. Smolin, and W. K. Wootters, "Purification of noisy entanglement and faithful teleportation via noisy channels," *Phys. Rev. Lett.*, vol. 76, no. 5, p. 722, 1996.

[110] P. G. Kwiat, S. Barraza-Lopez, A. Stefanov, and N. Gisin, "Experimental entanglement distillation and hidden non-locality," *Nature*, vol. 409, no. 6823, pp. 1014–1017, 2001.

[111] R. Dong, M. Lassen, J. Heersink, C. Marquardt, R. Filip, G. Leuchs, and U. L. Andersen, "Experimental entanglement distillation of mesoscopic quantum states," *Nat. Phys.*, vol. 4, no. 12, pp. 919–923, 2008.

[112] P. Zanardi and M. Rasetti, "Noiseless quantum codes," *Phys. Rev. Lett.*, vol. 79, no. 17, p. 3306, 1997.

[113] D. A. Lidar, I. L. Chuang, and K. B. Whaley, "Decoherence-free subspaces for quantum computation," *Phys. Rev. Lett.*, vol. 81, no. 12, p. 2594, 1998.

[114] L. Viola and S. Lloyd, "Dynamical suppression of decoherence in two-state quantum systems," *Phys. Rev. A*, vol. 58, pp. 2733–2744, 1998.

[115] L. Viola and E. Knill, "Random decoupling schemes for quantum dynamical control and error suppression," *Phys. Rev. Lett.*, vol. 94, no. 6, p. 060502, 2005.

[116] A. D'Arrigo, R. Lo Franco, G. Benenti, E. Paladino, and G. Falci, "Recovering entanglement by local operations," *Ann. Phys.*, vol. 350, pp. 211–224, 2014.

[117] R. Lo Franco, A. D'Arrigo, G. Falci, G. Compagno, and E. Paladino, "Preserving entanglement and nonlocality in solid-state qubits by dynamical decoupling," *Phys. Rev. B*, vol. 90, no. 5, p. 054304, 2014.

[118] A. Orieux, A. D'Arrigo, G. Ferranti, R. Lo Franco, G. Benenti, E. Paladino, G. Falci, F. Sciarrino, and P. Mataloni, "Experimental on-demand recovery of entanglement by local operations within non-markovian dynamics," *Sci. Rep.*, vol. 5, no. 1, pp. 1–8, 2015.

[119] P. Facchi, D. Lidar, and S. Pascazio, "Unification of dynamical decoupling and the quantum zeno effect," *Phys. Rev. A*, vol. 69, no. 3, p. 032314, 2004.

[120] R. Lo Franco, B. Bellomo, E. Andersson, and G. Compagno, "Revival of quantum correlations without system-environment back-action," *Phys. Rev. A*, vol. 85, no. 3, p. 032318, 2012.

[121] J.-S. Xu, K. Sun, C.-F. Li, X.-Y. Xu, G.-C. Guo, E. Andersson, R. Lo Franco, and G. Compagno, "Experimental recovery of quantum correlations in absence of system-environment back-action," *Nat. Commun.*, vol. 4, no. 1, pp. 1–7, 2013.

[122] S. Damodarakurup, M. Lucamarini, G. Di Giuseppe, D. Vitali, and P. Tombesi, "Experimental inhibition of decoherence on flying qubits via "bang-bang" control," *Phys. Rev. Lett.*, vol. 103, no. 4, p. 040502, 2009.

[123] Á. Cuevas, A. Mari, A. De Pasquale, A. Orieux, M. Massaro, F. Sciarrino, P. Mataloni, and V. Giovannetti, "Cut-and-paste restoration of entanglement transmission," *Phys. Rev. A*, vol. 96, no. 1, p. 012314, 2017.

[124] T. D. Ladd, F. Jelezko, R. Laflamme, Y. Nakamura, C. Monroe, and J. L. O'Brien, "Quantum computers," *Nature*, vol. 464, p. 45, 2010.

[125] E. Altman *et al.*, "Quantum simulators: Architectures and opportunities," *PRX Quantum*, vol. 2, p. 017003, 2021.

[126] G. Benenti, S. Siccardi, and G. Strini, "Entanglement in helium," *Eur. Phys. J. D*, vol. 67, p. 83, 2013.

[127] N. Killoran, M. Cramer, and M. B. Plenio, "Extracting entanglement from identical particles," *Phys. Rev. Lett.*, vol. 112, p. 150501, 2014.

[128] A. Castellini, B. Bellomo, G. Compagno, and R. Lo Franco, "Activating remote entanglement in a quantum network by local counting of identical particles," *Phys. Rev. A*, vol. 99, no. 6, p. 062322, 2019.

[129] K. Berrada, M. El Baz, H. Eleuch, and Y. Hassouni, "A comparative study of negativity and concurrence based on spin coherent states," *Int. J. Mod. Phys. C*, vol. 21, no. 03, pp. 291–305, 2010.

[130] A.-B. A. Mohamed and H. Eleuch, "Generation and robustness of bipartite nonclassical correlations in two nonlinear microcavities coupled by an optical fiber," *J. Opt. Soc. Am. B*, vol. 35, pp. 47–53, 2018.

[131] H. Breuer and F. Petruccione, *The Theory of Open Quantum Systems*. Clarendon, 2002.

[132] P. Haikka and S. Maniscalco, "Non-Markovian dynamics of a damped driven two-state system," *Phys. Rev. A*, vol. 81, May 2010.

[133] B. Bellomo, R. Lo Franco, and G. Compagno, "Non-markovian effects on the dynamics of entanglement," *Phys. Rev. Lett.*, vol. 99, no. 16, p. 160502, 2007.

[134] C. Bruzewicz, J. Chiaverini, R. McConnell, and J. Sage, "Trapped-ion quantum computing: Progress and challenges," *Appl. Phys. Rev.*, vol. 6, p. 021314, 06 2019.

[135] C. J. Myatt, B. E. King, Q. A. Turchette, C. A. Sackett, D. Kielpinski, W. M. Itano, C. Monroe, and D. J. Wineland, "Decoherence of quantum superpositions through coupling to engineered reservoirs," *Nature*, vol. 403, no. 6767, pp. 269–273, 2000.

[136] P. Schindler, D. Nigg, T. Monz, J. T. Barreiro, E. Martinez, S. X. Wang, S. Quint, M. F. Brandl, V. Nebendahl, C. F. Roos, M. Chwalla, M. Hennrich, and R. Blatt, "A quantum information processor with trapped ions," *New J. Phys.*, vol. 15, p. 123012, dec 2013.

[137] V. Giovannetti and R. Fazio, "Information-capacity description of spin-chain correlations," *Phys. Rev. A*, vol. 71, p. 032314, 2005.

[138] A. Blais, J. Gambetta, A. Wallraff, D. I. Schuster, S. M. Girvin, M. H. Devoret, and R. J. Schoelkopf, "Quantum-information processing with circuit quantum electrodynamics," *Phys. Rev. A*, vol. 75, p. 032329, 2007.

[139] A. Blais, S. M. Girvin, and W. D. Oliver, "Quantum information processing and quantum optics with circuit quantum electrodynamics," *Nat. Phys.*, vol. 16, no. 3, pp. 247–256, 2020.

[140] D. Zhou, A. Lang, and R. Joynt, "Disentanglement and decoherence from classical non-markovian noise: random telegraph noise," *Quantum Inf. Process.*, vol. 9, no. 6, pp. 727–747, 2010.

[141] R. Lo Franco, A. D'Arrigo, G. Falci, G. Compagno, and E. Paladino, "Entanglement dynamics in superconducting qubits affected by local bistable impurities," *Phys. Scr.*, vol. 2012, no. T147, p. 014019, 2012.

[142] P. Bordone, F. Buscemi, and C. Benedetti, "Effect of markov and non-markov classical noise on entanglement dynamics," *Fluct. Noise Lett.*, vol. 11, no. 03, p. 1242003, 2012.

[143] B. Bellomo, R. Lo Franco, E. Andersson, J. D. Cresser, and G. Compagno, "Dynamics of correlations due to a phase-noisy laser," *Phys. Scr.*, vol. 2012, no. T147, p. 014004, 2012.

[144] X. Cai, "Quantum dephasing induced by non-markovian random telegraph noise," *Sci. Rep.*, vol. 10, no. 1, pp. 1–11, 2020.

[145] H. J. Wold, H. Brox, Y. M. Galperin, and J. Bergli, "Decoherence of a qubit due to either a quantum fluctuator, or classical telegraph noise," *Phys. Rev. B*, vol. 86, p. 205404, 2012.

[146] M. G. Paris, "Quantum estimation for quantum technology," *Int. J. Quantum Inf.*, vol. 7, no. supp01, pp. 125–137, 2009.

[147] T. D. Ladd, F. Jelezko, R. Laflamme, Y. Nakamura, C. Monroe, and J. L. O'Brien, "Quantum computers," *Nature*, vol. 464, no. 7285, pp. 45–53, 2010.

[148] S. Pirandola, U. L. Andersen, L. Banchi, M. Berta, D. Bunandar, R. Colbeck, D. Englund, T. Gehring, C. Lupo, C. Ottaviani, *et al.*, "Advances in quantum cryptography," *Adv. Opt. Photonics*, vol. 12, no. 4, pp. 1012–1236, 2020.

[149] M. Horodecki, P. Horodecki, and R. Horodecki, "Inseparable two spin-1 2 density matrices can be distilled to a singlet form," *Phys. Rev. Lett.*, vol. 78, no. 4, p. 574, 1997.

[150] M. Horodecki, P. Horodecki, and R. Horodecki, "Mixed-state entanglement and distillation: Is there a "bound" entanglement in nature?," *Phys. Rev. Lett.*, vol. 80, no. 24, p. 5239, 1998.

[151] P. Horodecki and R. Horodecki, "Distillation and bound entanglement.," *Quantum Inf. Comput.*, vol. 1, no. 1, pp. 45–75, 2001.

[152] A. Mortezapour, M. A. Borji, and R. Lo Franco, "Protecting entanglement by adjusting the velocities of moving qubits inside non-markovian environments," *Laser Phys. Lett.*, vol. 14, no. 5, p. 055201, 2017.

[153] A. Mortezapour and R. Lo Franco, "Protecting quantum resources via frequency modulation of qubits in leaky cavities," *Sci. Rep.*, vol. 8, no. 1, p. 14304, 2018.

[154] Y. Wang, Z.-Y. Hao, Z.-H. Liu, K. Sun, J.-S. Xu, C.-F. Li, G.-C. Guo, A. Castellini, B. Bellomo, G. Compagno, *et al.*, "Remote entanglement distribution in a quantum network via multinode indistinguishability of photons," *Phys. Rev. A*, vol. 106, no. 3, p. 032609, 2022.

[155] F. Nosrati, B. Bellomo, G. De Chiara, G. Compagno, R. Morandotti, and R. Lo Franco, "Indistinguishability-assisted two-qubit entanglement distillation," *Quantum Sci. Technol.*, vol. 9, p. 015027, 2024.

[156] C. H. Bennett, H. J. Bernstein, S. Popescu, and B. Schumacher, "Concentrating partial entanglement by local operations," *Phys. Rev. A*, vol. 53, no. 4, p. 2046, 1996.

[157] T. Pittman, D. Strekalov, A. Migdall, M. Rubin, A. Sergienko, and Y. Shih, "Can two-photon interference be considered the interference of two photons?," *Phys. Rev. Lett.*, vol. 77, no. 10, p. 1917, 1996.

[158] O. Siltanen, T. Kuusela, and J. Piilo, "Engineering of hong-ou-mandel interference with effective noise," *Phys. Rev. A*, vol. 104, no. 4, p. 042201, 2021.

[159] M. Piccolini, M. Karczewski, A. Winter, and R. Lo Franco, "Robust generation of N-partite N-level singlet states by identical particle interferometry," *arXiv preprint arXiv:2312.17184*, 2023.

[160] W. Dür, G. Vidal, and J. I. Cirac, "Three qubits can be entangled in two inequivalent ways," *Phys. Rev. A*, vol. 62, no. 6, p. 062314, 2000.

[161] D. M. Greenberger, M. A. Horne, and A. Zeilinger, "Going beyond bell's theorem," in *Bell's theorem, quantum theory and conceptions of the universe*, pp. 69–72, Springer, 1989.

[162] N. D. Mermin, "Quantum mysteries revisited," *Am. J. Phys*, vol. 58, no. 8, pp. 731–734, 1990.

[163] R. H. Dicke, "Coherence in spontaneous radiation processes," *Phys. Rev.*, vol. 93, no. 1, p. 99, 1954.

[164] H.-J. Briegel, W. Dür, J. I. Cirac, and P. Zoller, "Quantum repeaters: the role of imperfect local operations in quantum communication," *Phys. Rev. Lett.*, vol. 81, no. 26, p. 5932, 1998.

[165] L.-M. Duan, M. D. Lukin, J. I. Cirac, and P. Zoller, "Long-distance quantum communication with atomic ensembles and linear optics," *Nature*, vol. 414, no. 6862, pp. 413–418, 2001.

[166] W. J. Munro, K. Azuma, K. Tamaki, and K. Nemoto, "Inside quantum repeaters," *IEEE J. Sel. Top. Quantum Electron*, vol. 21, no. 3, pp. 78–90, 2015.

[167] M. Piccolini, V. Giovannetti, and R. Lo Franco, "Robust engineering of maximally entangled states by identical particle interferometry," *Adv. Quantum Technol.*, vol. 6, no. 9, p. 2300146, 2023.

[168] N. Gisin and R. Thew, "Quantum communication," *Nat. Photonics*, vol. 1, no. 3, pp. 165–171, 2007.

[169] F. Xu, X. Ma, Q. Zhang, H.-K. Lo, and J.-W. Pan, "Secure quantum key distribution with realistic devices," *Rev. Mod. Phys.*, vol. 92, no. 2, p. 025002, 2020.

[170] P. G. Kwiat, K. Mattle, H. Weinfurter, A. Zeilinger, A. V. Sergienko, and Y. Shih, "New high-intensity source of polarization-entangled photon pairs," *Phys. Rev. Lett.*, vol. 75, no. 24, p. 4337, 1995.

[171] X. Li, P. L. Voss, J. E. Sharping, and P. Kumar, "Optical-fiber source of polarization-entangled photons in the 1550 nm telecom band," *Phys. Rev. Lett.*, vol. 94, no. 5, p. 053601, 2005.

[172] H. Takesue and K. Inoue, "Generation of polarization-entangled photon pairs and violation of bell's inequality using spontaneous four-wave mixing in a fiber loop," *Phys. Rev. A*, vol. 70, no. 3, p. 031802, 2004.

[173] E. Knill, R. Laflamme, and G. J. Milburn, "A scheme for efficient quantum computation with linear optics," *Nature*, vol. 409, no. 6816, pp. 46–52, 2001.

[174] Q. Zhang, X.-H. Bao, C.-Y. Lu, X.-Q. Zhou, T. Yang, T. Rudolph, and J.-W. Pan, "Demonstration of a scheme for the generation of "event-ready" entangled photon pairs from a single-photon source," *Phys. Rev. A*, vol. 77, no. 6, p. 062316, 2008.

[175] M. Varnava, D. E. Browne, and T. Rudolph, "How good must single photon sources and detectors be for efficient linear optical quantum computation?," *Phys. Rev. Lett.*, vol. 100, no. 6, p. 060502, 2008.

[176] F. Gubarev, I. Dyakonov, M. Y. Saygin, G. Struchalin, S. Straupe, and S. Kulik, "Improved heralded schemes to generate entangled states from single photons," *Phys. Rev. A*, vol. 102, no. 1, p. 012604, 2020.

[177] S. Chin, Y.-S. Kim, and M. Karczewski, "Shortcut to multipartite entanglement generation: A graph approach to boson subtractions," *arXiv preprint arXiv:2211.04042*, 2022.

[178] S. Chin, M. Karczewski, and Y.-S. Kim, "From graphs to circuits: Optical heralded generation of n-partite ghz and w states," *arXiv preprint arXiv:2310.10291*, 2023.

[179] A. Cabello, "N-particle n-level singlet states: some properties and applications," *Phys. Rev. Lett.*, vol. 89, no. 10, p. 100402, 2002.

[180] A. Cabello, "Solving the liar detection problem using the four-qubit singlet state," *Phys. Rev. A*, vol. 68, no. 1, p. 012304, 2003.

[181] A. Cabello, "Supersinglets," *J. Mod. Opt.*, vol. 50, no. 6-7, pp. 1049–1061, 2003.

[182] Z. Ma, M. Rambach, K. Goswami, S. S. Bhattacharya, M. Banik, and J. Romero, "Randomness-free test of nonclassicality: A proof of concept," *Phys. Rev. Lett.*, vol. 131, no. 13, p. 130201, 2023.

[183] M. Karczewski, D. Kaszlikowski, and P. Kurzyński, "Monogamy of particle statistics in tripartite systems simulating bosons and fermions," *Phys. Rev. Lett.*, vol. 121, no. 9, p. 090403, 2018.

[184] I. Urizar-Lanz, P. Hyllus, I. L. Egusquiza, M. W. Mitchell, and G. Tóth, "Macroscopic singlet states for gradient magnetometry," *Phys. Rev. A*, vol. 88, no. 1, p. 013626, 2013.

[185] G. Tóth and M. W. Mitchell, "Generation of macroscopic singlet states in atomic ensembles," *New J. Phys.*, vol. 12, no. 5, p. 053007, 2010.

[186] N. Behbood, F. M. Ciurana, G. Colangelo, M. Napolitano, G. Tóth, R. Sewell, and M. Mitchell, "Generation of macroscopic singlet states in a cold atomic ensemble," *Phys. Rev. Lett.*, vol. 113, no. 9, p. 093601, 2014.

[187] J. Kong, R. Jiménez-Martínez, C. Troullinou, V. G. Lucivero, G. Tóth, and M. W. Mitchell, "Measurement-induced, spatially-extended entanglement in a hot, strongly-interacting atomic system," *Nat. Commun.*, vol. 11, no. 1, p. 2415, 2020.

[188] N. Behbood, G. Colangelo, F. M. Ciurana, M. Napolitano, R. Sewell, and M. Mitchell, "Feedback cooling of an atomic spin ensemble," *Phys. Rev. Lett.*, vol. 111, no. 10, p. 103601, 2013.

[189] C. Dittel, G. Dufour, M. Walschaers, G. Weihs, A. Buchleitner, and R. Keil, "Totally destructive interference for permutation-symmetric many-particle states," *Phys. Rev. A*, vol. 97, no. 6, p. 062116, 2018.

[190] W. Fulton, *Young tableaux: with applications to representation theory and geometry*. No. 35, Cambridge University Press, 1997.

[191] V. B. Braginsky and F. Y. Khalili, "Quantum nondemolition measurements: the route from toys to tools," *Rev. Mod. Phys.*, vol. 68, no. 1, p. 1, 1996.

[192] J.-F. Roch, G. Roger, P. Grangier, J.-M. Courty, and S. Reynaud, "Quantum nondemolition measurements in optics: a review and some recent experimental results," *Appl. Phys. B*, vol. 55, pp. 291–297, 1992.

[193] C. Unnikrishnan, "Quantum non-demolition measurements: concepts, theory and practice," *Curr. Sci.*, pp. 2052–2060, 2015.

[194] M. Clementi, F. A. Sabattoli, M. Borghi, L. Gianini, N. Tagliavacche, H. El Dirani, L. Youssef, N. Bergamasco, C. Petit-Etienne, E. Pargon, *et al.*, "Programmable frequency-bin quantum states in a nano-engineered silicon device," *Nat. Commun.*, vol. 14, no. 1, p. 176, 2023.